

STUDIES IN THE GEOMETRY OF FOLDING
AND ITS
MECHANICAL INTERPRETATION

by

CHRISTOPHER McAULAY POWELL, B. Sc. (Hons).
(University of Queensland)

A thesis submitted in partial fulfilment of the
requirements for the degree of

Doctor of Philosophy

UNIVERSITY OF TASMANIA

HOBART

July 1967

This thesis contains no material which has been accepted for the award of any other degree or diploma in any university and to the best of my knowledge and belief contains no copy or paraphrase of material previously published or written by another person except where due reference is made in the text of the thesis.

C. M^cA. Powell

CHRISTOPHER McA. POWELL

University of Tasmania

Hobart

July 1967

ABSTRACT

Analysis of thickness variation of folded layers in terms of apparent flattening indicates the relative "viscosities" of the layers, and hence modes of deformation. Orthogonal-thickness ratios, which are unique for each percentage of flattening, are convenient indicators of the equivalent flattening of an initially concentric profile. Axial-thickness ratios, intrinsically more sensitive, are less useful because there is a spread of values for each percentage of flattening.

Measurements of fold profiles from diverse sedimentary, diagenetic and low-grade metamorphic environments show that the higher the temperature and pressure at which the rocks were deformed the smaller the range of fold style. At Port Moresby, Papua, progressive syntaphral sliding has folded Eocene cherts and less competent argillite in a complex polyclinal style. Individual layers, then groups of layers up to one metre thick, and finally slip sheets tens of metres thick slid towards the west-southwest.

Structural analysis of linear and planar fold elements in diagenetic or low-grade metamorphic environments in Tasmania leads to the conclusion that cleavage developed contemporaneously in both sandstone and slate as a planar feature. The cleavage

in the slate is penetrative to the scale of detrital grains, but non-penetrative in the sandstone where pelitic ribbons anastomose through the rock enclosing non-cleaved lenses of normal greywacke fabric. The most satisfactory hypothesis to account for the observed mesoscopic configurations is that the cleavage formed during deformation as pelitic deposits in channels along which excessive water was forced out of the rock at very high pore pressures.

The ratio between pore pressure and confining pressure is a significant parameter determining fold style. Heterogeneities necessary for concentric folding are effective where the pore pressure is relatively low, and the fold style is similar where the pore pressure approaches the pressure on the grain fabric. Pore-pressure ratios are most readily varied in superficial deposits, and many different fold styles occur in the intrastratal contortions in the terrestrial, Pleistocene, proglacial deposits in Tasmania, and in the intraformational slumps of the Pleistocene Lisan Formation in Israel. Irregular "flow" folds in the contact aureoles of two intrusive bodies in Tasmania grade outwards into more regular, concentric and disjunctive folds. Both the folding and the variation in fold style may have been caused by water pressures approaching the lithostatic load in the intrusions, and decreasing outwards.

CONTENTS

	Page <i>pages prec.</i>
ABSTRACT	
LIST OF ILLUSTRATIONS	i
INTRODUCTION	vii
CHAPTER 1 THICKNESS MEASUREMENTS	1
1. INTRODUCTION	1
2. RELATIONSHIP OF FOLD PARAMETERS IN IDEAL PROFILES	4
(a) VARIATION OF AXIAL THICKNESS, $T\alpha$, WITH RESPECT TO α , THE ANGLE BETWEEN THE NORMAL TO THE LAYER AND THE AXIAL PLANE, IN CONCENTRIC FOLDS	4
(b) TYPES OF FLATTENING	5
(c) RECOGNITION OF DIFFERENTIAL FLATTENING	7
(d) RECOGNITION OF NONUNIFORM FLATTENING	8
(e) NON-AXIAL-PLANE FLATTENING	8
(f) EFFECTS OF FLATTENING ON A CONCENTRIC PROFILE	9
(g) DIFFICULTIES IN THE MEASUREMENT OF ORTHOGONAL THICKNESS IN FLATTENED CONCENTRIC FOLDS	11
(h) EFFECT OF THE R-RATIO ON THE AXIAL- RATIO PLOT FOR FLATTENED CONCENTRIC FOLDS	13
(i) USE OF AXIAL-RATIO PLOTS FOR FLATTENED CONCENTRIC FOLDS	14
(j) DIFFICULTIES IN LOCATING THE CENTRE OF CURVATURE IN FLATTENED CONCENTRIC PROFILES	15
(k) EFFECTS OF SIMPLE AND PURE SHEAR OF A CONCENTRIC PROFILE	16

	Page
(l) DISTINCTION BETWEEN SIMPLE AND PURE SHEAR	17
(m) DEFORMATION OF ANGLES DURING FLATTENING	19
(n) OTHER METHODS OF ESTIMATING FLATTENING IN FOLDS	20
(o) CONCLUSIONS	21
3. DILATATIONAL STRAIN AND FOLDING	23
(a) GENERAL REMARKS	23
(b) RELATIONSHIP BETWEEN DECREASE IN POROSITY AND VOLUME CHANGE	24
(c) RELATIONSHIP BETWEEN VOLUME CHANGE AND FLATTENING	24
(d) EFFECTS OF DIFFERENTIAL COMPACTION ON FOLD STRUCTURES	25
(e) RELATIONSHIP BETWEEN COMPACTION AND THE PLANE OF APPARENT FLATTENING	26
CHAPTER 2 SYNTAPHRAL FOLDING IN EOCENE CHERTS, PORT MORESBY	29
1. INTRODUCTION	29
2. PETROLOGY	29
(a) GENERAL STATEMENT	29
(b) FAUNA	30
(c) PETROGRAPHY	31
(d) CHERT AND FLINT NODULES	35
(e) NON-TECTONIC, SEDIMENTARY STRUCTURES	35
(f) ENVIRONMENT OF DEPOSITION	37
(g) CONCLUSIONS	38

	Page
3. STRUCTURE	
(a) GENERALIZED SECTION	39
(b) FLAP FOLDS	40
(c) SMALL-SCALE GLIDES	46
(d) SLIP SHEETS AND SLIP ZONES	46
(e) BROAD SYNCLINES AND TIGHT ANTICLINES	48
(f) ZONE OF GENERAL INVOLUTION	48
(g) RECUMBENT FOLDS	49
(h) FAULTING	49
4. ORIGIN OF THE FOLDING	50
(a) THE LACK OF CLEAVAGE	50
(b) THE LACK OF ANY METAMORPHISM	51
(c) THE SEQUENCE OF OVERFOLDING	51
(d) GEOMETRY OF THE FOLDING	52
(e) ORIENTATION OF AXIAL SURFACES	52
5. CONCLUSIONS	53
CHAPTER 3 TECTONIC DIAGENETIC FOLDS AT SULPHUR CREEK, NORTHERN COAST OF TASMANIA	54
1. INTRODUCTION	54
2. STRUCTURAL DESCRIPTIONS	56
(a) GENERAL DESCRIPTION	56
(b) DISJUNCTIVE FOLD IN AREA A	58
(c) AREA B	60
(d) AREA C	64

	Page
(e) AREA D	74
(f) AREA E	76
(g) INDIVIDUAL FOLD DESCRIPTIONS	78
3. DESCRIPTION OF CLEAVAGE	98
(a) GENERAL STATEMENT	98
(b) MESOSCOPIC DESCRIPTION	99
(c) THIN-SECTION DESCRIPTION	102
(d) CONCLUSIONS	103
4. ORIGIN OF CLEAVAGE	104
(a) GENERAL STATEMENT	104
(b) DETAILED CONSIDERATIONS	106
5. REFRACTION OF CLEAVAGE	114
(a) GENERAL DESCRIPTION	114
(b) ORIGIN	115
(c) CONCLUSIONS	119
6. THE NATURE OF THE P1 DEFORMATION AT SULPHUR CREEK	119
(a) THE EARLY DIAGENETIC PHASE	120
(b) THE EARLY P1 PHASE	120
(c) THE CLEAVAGE FORMATION	121
(d) THE LATE P1 PHASE	122
CHAPTER 4 FOLDING IN INTERBEDDED SANDSTONES AND SLATES AT TULLOCHGORUM, NORTHEASTERN TASMANIA	123

	Page
1. INTRODUCTION	123
2. STRUCTURAL DESCRIPTIONS	125
(a) ANTICLINE 1 AND SYNCLINE 1	125
(b) ANTICLINE 2	127
(c) SYNCLINE 2	128
(d) ANTICLINE 3	129
(e) SYNCLINE 3	130
(f) SYNCLINE 4	132
(g) FOLDED SLATE-CLEAVAGE	133
(h) JOINTING	137
3. FLATTENING	138
4. CLEAVAGE	142
(a) GENERAL DESCRIPTION	142
(b) THIN-SECTION DESCRIPTION	144
(c) ORIGIN OF CLEAVAGE	147
5. HISTORY OF STRUCTURAL EVOLUTION	161
(a) SEDIMENTARY AND EARLY DIAGENETIC STAGE	161
(b) EARLY FOLDING STAGE	161
(c) CLEAVAGE FORMATION	162
(d) LATE FOLDING STAGE	163

	Page
CHAPTER 5 INTRAFORMATIONAL STRUCTURES IN THE PLEISTOCENE GLACIAL MORaine AT GORMANSTON, WEST COAST OF TASMANIA	164
1. INTRODUCTION	164
2. STRUCTURAL DESCRIPTIONS	167
(a) GENERAL DESCRIPTION	167
(b) COMPACTION STRUCTURES	168
(c) DIAPIRIC FOLDS	170
(d) CONVOLUTE FOLDS	174
(e) MISCELLANEOUS STRUCTURES	177
3. INTERPRETATION	183
(a) ORIGIN OF THE CONTORTIONS	183
(b) CONCLUSIONS	186
CHAPTER 6 EARLY-DIAGENETIC, INTRAFORMATIONAL FOLDING IN THE PLEISTOCENE LISAN FORMATION, ISRAEL	187
1. INTRODUCTION	187
2. PETROLOGY	188
3. STRUCTURAL DESCRIPTIONS	190
4. ORIGIN OF THE INTRASTRATAL CONTORTIONS	196
5. CONCLUSIONS	200
CHAPTER 7 FOLDING IN THE CONTACT AUREOLE OF A QUARTZ-DIORITE DYKE, NORTHEASTERN TASMANIA	201
1. INTRODUCTION	201

	Page
2. STRUCTURE	202
(a) GENERAL	202
(b) FOLDING	203
3. PETROGRAPHY	206
(a) QUARTZ DIORITE	206
(b) HORNFELS	207
(c) GRANODIORITIC VEINS	210
(d) HORNFELS CONTACT ZONE	210
(e) ZONED PLAGIOCLASE CRYSTALS	211
4. STRUCTURAL INTERPRETATION	213
(a) INTRUSIVE NATURE OF THE QUARTZ DIORITE	213
(b) ORIGIN OF THE QUARTZ-DIORITE LOBES	213
(c) ORIGIN OF THE FOLDING	215
(d) NATURE OF THE QUARTZ DIORITE DURING INTRUSION	216
(e) INTERPRETATION OF THE HISTORY OF INTRUSION	222
CHAPTER 8 FOLDING IN A HORNFELS ADJACENT TO A DOLERITE CONTACT, REMARKABLE CAVE, S. E. TASMANIA	225
1. INTRODUCTION	225
2. PETROGRAPHY	226
3. FOLDING	230
(a) GENERAL STATEMENT	230
(b) DETAILED DESCRIPTIONS	232

	Page
4. INTERPRETATION	237
CHAPTER 9 MISCELLANEOUS FOLDS	240
1. A SMALL-SCALE INTRAFORMATIONAL FOLD FROM ARM RIVER, NORTHERN TASMANIA	240
(a) INTRODUCTION	240
(b) STRUCTURAL DESCRIPTIONS	241
(c) INTERPRETATION	248
(d) CONCLUSION	252
2. FOLDS IN THE MARTINSBURG SLATE, PENNSYLVANIA	252
3. RECUMBENT, ZIG-ZAG FOLDS IN THE FRANCISCAN CHERTS, CALIFORNIA	256
CHAPTER 10 VARIATION IN FOLD STYLE	261
1. INTRODUCTION	261
2. GEOMETRICAL ANALYSIS OF FOLDS	262
(a) THE BEHAVIOUR OF GEOLOGIC MATERIALS IN DIFFERENT ENVIRONMENTS	262
(b) VARIATION OF STYLE IN A SINGLE FOLD	264
(c) VARIATION OF STYLE IN DIFFERENT ENVIRONMENTS	266
3. MECHANICAL ANALYSIS OF FOLDS	267
(a) GENERAL STATEMENT	267
(b) SCALE IN MECHANICAL INTERPRETATIONS	269
(c) THE ROLE OF LAYERING IN DEFORMATION	269
(d) POSSIBLE MECHANICAL CAUSES OF VARIATION IN FOLD STYLE	270

	Page
REFERENCES	274
APPENDIX I DEFINITION OF TERMS	14 pages
APPENDIX 2 THE TERMS <i>SEDIMENTARY</i> AND <i>TECTONIC</i> AS APPLIED TO ROCK STRUCTURES	7 pages
APPENDIX 3 CRITIQUE OF SOME ASPECTS OF MODERN STRUCTURAL ANALYSIS	11 pages

LIST OF ILLUSTRATIONS

FIGURE	Following Page
1-1 Fold Parameters	4
1-2 Types of flattening	6
1-3 Effects of flattening and simple shear on a concentric profile	10
1-4 Relationship between fold parameters	12
1-5 Axial ratios in flattened concentric folds	14
1-6 Angular deformation during flattening	19
1-7 Effects of differential compaction	25
1-8 Effects of compaction on slaty cleavage	27
2-1 Location map of Paga Point sections	29
2-2 Photomicrographs (a) Angular grains in calcarenite (b) Well-rounded grain of labradorite	33
2-3 (a) Photomicrograph. Spherulites of chalcedonic quartz (b) Photograph. Large, irregular nodules in chert	34
2-4 Photographs (a) Small, spherical concretion in chert (b) Flinty nodules stretched into boudins	35
2-5 (a) Photomicrograph. Fine-grained, chalcedonic quartz in flinty nodule (b) Photograph. Convolute folds	36
2-6 Diagrammatic section through syntaphral folding, Paga Point	39
2-7 Accurate sections A-B and B-C along Paga Point cliff face	40

FIGURE

Following Page

2-8	Accurate sections C-D and E-F along Paga Point cliff face	40
2-9	Cross-section below sea-level, Paga Point	40
2-10	Photographs (a) Flap fold (b) Contorted slip zone	40
2-11	Formation of flap folds	43
2-12	Some profile sketches and a block diagram of a refolded fold	47
2-13	Photographs (a) Folded recumbent fold (b) Folded isoclinal fold	49
3-1	Location map, Sulphur Creek area	56
3-2	Area A, and structural elements of area B	58
3-3	Area B	60
3-4	Area C, with linear structural elements	64
3-5	Variation in fold-hinges in Area C	69
3-6	Planar elements, area C	72
3-7	Area D	74
3-8	Structural elements, area D	75
3-9	Area E, with structural elements	76
3-10	Photographs (a) P1 fold core (b) Tight P1 fold core	78
3-11	Photographs (a) Isoclinal, early P1 fold core (b) Complexly folded nose of early P1 fold core	80
3-12	Photographs (a) Sinistral fold couple (b) Disjunctive fold	81
3-13	Photographs (a) Concentric fold (b) Tight, small-amplitude crenulations in pelite	83
3-14	Photographs (a) Large parasitic fold (b) Small parasitic fold	85
3-15	Photographs (a) Refolded, slipped-off nose of fold (b) Intraformational, open-cast slump folds	87
3-16	Photographs (a) Detached core of early P1 fold (b) Late P1 fold	89

FIGURE	Following Page
3-17 Multilith half-tone. Asymmetrical syncline and orthogonal-thickness-ratio graph	90
3-18 Multilith half-tone. Small, flattened concentric fold in a thick slate band, and orthogonal-thickness-ratio graph	91
3-19 Photographs (a) Asymmetrical similar fold (b) Concentric fold in a thin sandstone bed	93
3-20 Multilith half-tone. Asymmetrical anticline and orthogonal-thickness-ratio graph	95
3-21 Multilith half-tone. Similar fold in slate and orthogonal-thickness-ratio graph	95
3-22 Photographs (a) Anticline with non-penetrative cleavage in the sandstone (b) Close-up view of the non-penetrative cleavage	99
3-23 Photographs (a) Cleavage blocks in sandstone (b) Refraction of cleavage from sandstone into slate	100
3-24 Photomicrographs (a) Non-penetrative sandstone cleavage (b) Penetrative slaty cleavage	102
3-25 Multilith half-tone. Fold couple in slate with oblique, transecting cleavage. Orthogonal-thickness-ratio graph	108
3-26 Photographs (a) Refraction of cleavage in a thin slate band between thick sandstone beds (b) Refraction of cleavage in graded beds	115
4-1 Block-diagram of Tullochgorum road section, and field-tracings of synclines 2 and 3	123
4-2 Fold elements and joints	124
4-3 Cross-section through folded zone, Tullochgorum	124
4-4 Structural elements, anticline 1	125
4-5 Structural elements, syncline 1	126
4-6 Profile drawings of anticline 2 and synclines 2 and 3.	127
4-7 Structural elements, anticline 2	128

FIGURE	Following Page
4-8 Structural elements, syncline 2	129
4-9 Structural elements, anticline 3	130
4-10 Structural elements, syncline 3	131
4-11 Effects of rotation on β -lineation during folding	131
4-12 Structural elements, syncline 4	132
4-13 Concertina-style folding of interlayered sandstones and slates	134
4-14 Non-coaxial folded cleavage	135
4-15 Differential flattening in a quartzite layer	139
4-16 Generalised fold-style at Tullochgorum	140
4-17 Composite plots of cleavage	143
4-18 Reconstruction of folded zone, Tullochgorum	150
5-1 Glacial moraine at Gormanston	164
5-2 Compaction structures and lobate synclines	168
5-3 Diapiric folds	170
5-4 Photographs (a) Broad, concentric synclines and tight, similar anticlines in a clay band (b) Unusual, mushroom-shaped folds	172
5-5 Photographs (a) Bulbous-shaped, convolute folds (b) Convolute folds in a silty layer above a box fold in brown clay	175
5-6 Photographs (a) Close-up view of convolute folds (b) Less intense folding in brown clays	176
5-7 Miscellaneous fold structures	177
6-1 Multilith half-tone. Lateral slip on fold zone	190
6-2 Distorted concentric fold	191
6-3 Multilith half-tone. Small-scale, nappe-like folds	193
6-4 Multilith half-tone. Intraformational box-folds	195

FIGURE		Following Page
7-1	Geological sketch-map, Diana's Basin	201
7-2	Igneous contact zone, Diana's Basin	202
7-3	Photographs (a) Quartz-diorite lobes (b) Essentially concentric style of folding	204
7-4	Folds caused by quartzdiorite magma, and formation of quartzdiorite lobes	204
7-5	Structural elements, Diana's Basin	205
7-6	(a) Photomicrograph. Quartz diorite (b) Photograph. Plastic folding in contact hornfels	206
7-7	Photomicrographs (a) Cement-like texture in hornfels remote from quartz-diorite contact (b) Hornfels texture immediately adjacent to the quartz-diorite contact	209
7-8	Photomicrographs (a) Zoned plagioclase crystal in hornfels contact zone (b) zoned plagioclase crystal in hornfels contact zone	210
7-9	Zoning in plagioclase	211
7-10	Photographs (a) Disoriented xenoliths in a quartz-diorite dyke (b) Terminated beds in a quartz-diorite dyke	213
7-11	Photographs (a) Quartz-diorite lobe in early stage of formation (b) Folds caused by lateral push of a quartz-diorite lobe	214
7-12	Photographs (a) Oblique section of plastic folds in quartz-diorite contact zone (b) Autointrusion of mobilized sediment into quartz diorite	223
8-1	Photographs (a) View of northeastern side of Remarkable Cave (b) Irregular "flow" folding in the lower hornfels, Remarkable Cave	225
8-2	Photomicrographs (a) Zeolite patch with intricate twinning of stilbite (b) Euhedral quartz crystal and chlorite spherulite surrounded by zeolite	227
8-3	Photomicrographs (a) Heavily embayed quartz in hornfels (b) Re-entrant, rational, crystallographic faces in quartz caused by growth	230

FIGURE		Following Page
8-4	Fold elements, Remarkable Cave	231
8-5	Rheomorphic fold profiles	232
8-6	Multilith half-tone. Intraformational profiles	234
8-7	Large photograph of disjunctive folding caused by intrusion of coarse-grained, zeolite-bearing hornfels	236
9-1	Intraformational fold traced from photographs of thin-section, Arm River	240
9-2	Fold-out photographs of thin-section, Arm River	240
9-3	Orthogonal-thickness ratios, thick psammitic band, Arm River	243
9-4	Photomicrographs (a) Cleavage ribbons which transect a fold core in a thin psammitic layer (b) Intense development of cleavage ribbons in a fold core	244
9-5	Photomicrographs (a) Ptygmatic folding of a thin psammitic layer in a thicker pelite band (b) Sigmoidals developed in a thin psammitic layer	246
9-6	Fold profiles in the Martinsburg Slate	253
9-7	Recumbent, zig-zag folds in the Franciscan Cherts, California	256
9-8	Flattened concentric profile	257

INTRODUCTION

This thesis is based on an intensive study of a number of small, widely scattered areas. I have carried out a routine, geometrical structural analysis of each of these areas, and outlined possible mechanical models to account for the deformation.

SCOPE OF STUDY

The mechanics of folding can be approached in two main ways *viz.* theoretically and empirically. I have used the empirical approach, and the folds I have considered come from seven main localities, with a few miscellaneous examples from other places. The seven main areas have been plane-tabled and/or photographed in sections perpendicular to the mean fold-axis. Within each area all structurally significant surfaces (bedding, cleavage, faults and axial surfaces) have been measured, and fold-hinges were either measured directly in the field, or calculated stereographically by taking the normal to the bedding poles (the π - method). The geometry of individual

fold profiles together with standard structural analysis, is the basis on which I have made my interpretation of the mechanics of folding.

One of the main problems in mechanical analysis is to eliminate some of the variables, and to this end I have restricted my study in both scale and environment. The scale of mapping is between 1:10 and 1:100, although some considerations of fold profiles have been made on smaller scales. Thin-sections have been cut mainly for petrology and the study of cleavage. The detailed relationship between microscopic structures and mesoscopic folds is outside the scope of this thesis, although where possible I have checked out any obvious mechanical implications of my hypotheses.

The environments to which I have restricted my work are all sedimentary, diagenetic or low-grade metamorphic, with the exception of two folded aureoles around intrusive bodies. Even in these two contact zones there is no evidence of high metamorphic grade, and the style of folding has many similarities with some of the other areas.

PRESENTATION

The first chapter is a theoretical analysis in which I have outlined the properties of the orthogonal- and axial-thickness ratios, and their use in determining apparent flattening of

concentric profiles. This work is somewhat negative since in most cases there is no advantage in using the axial-thickness ratios in preference to the orthogonal-thickness ratios, but I have included it in case some of the difficulties are overcome in the future.

Chapters 2 to 9 (inclusive) deal with the individual areas, and contain descriptions followed by particular, and then generalized interpretations. Chapters 2, 3 and 4 are considerably longer than Chapters 5 to 9 partly because most time was spent on this work, and partly because detailed interpretations outlined in these chapters are used by means of reference in the succeeding chapters. Chapter 10 is the final chapter in which I have outlined both the geometrical and mechanical causes of variation in fold style.

There are three appendices: Appendix 1 lists the main definitions I have used; Appendix 2 outlines my use of the terms *sedimentary* and *tectonic*; and Appendix 3 is a review of the status of some aspects of modern structural analysis. All rock numbers quoted are Departmental catalogue numbers referring to specimens located in the University of Tasmania rock store.

ACKNOWLEDGEMENTS

This thesis has been prepared under the supervision of Professor S. W. Carey whose encouragement has enabled me to develop many of the ideas expressed. I have consulted most

members of the staff of the Geology Department of Tasmania, and in particular I would like to thank Mr. M. R. Banks (for advice on sedimentation), Mr. R. J. Ford (X-rays), Mr. P. G. Quilty (micropalaeontology), Dr. M. Solomon (general criticism) and Dr. A. H. Spry (petrology). Thanks are due to Professor J. G. Ramsay (Imperial College, London) who read the manuscript, and Dr. E. Williams and Mr. R. D. Gee (both of Mines Department, Tasmania) who have provided stimulating discussion. I am grateful to Professor L. Picard (Hebrew University, Jerusalem) and Mr. Y. Langozky (Geological Survey of Israel) who provided references and samples of the Lisan Formation of Israel. Throughout this work I have been supported by a Commonwealth Postgraduate Scholarship.

CHAPTER 1

THICKNESS MEASUREMENTS

1. INTRODUCTION

The measurement of variations in the thickness of a layer in specified directions in a fold is an important determination in the description of the style of folding. Ramsay (1962) examined several folds to determine how closely they resembled ideal concentric and similar folds. He concluded that many natural folds have been modified by flattening and described a method whereby the amount of flattening in any fold which was originally concentric can be calculated. The method which Ramsay used was designed for folds of hand-specimen scale; folds which could be polished and measured in the laboratory, or for profile photographs. The method, while quite practical for laboratory use, can not be extended to field application without a full realization of its limitations.

For various reasons it is generally impractical to transport a fold back to the laboratory. It therefore remains that to use Ramsay's

method without restrictions, photographs be taken of the fold profile. While this enables many more folds to be studied in detail there are certain difficulties which render the use of photographs of otherwise excellent examples of folding unsuitable for quantitative work. Some of these difficulties are listed:-

- (1) The scale varies radially from the centre of any photograph. Fields of wide angle must not be used.
- (2) The cross-section available is usually not a planar surface and this gives irregular variations in scale on the photograph. Stereographic pairs help to minimise this effect.
- (3) The cross-section exposed may not be perpendicular to the fold-axis. Geometrical corrections can be made, but they are tedious.
- (4) It may not be possible to take the photograph directly down the fold-axis. A portable step ladder can help to overcome this difficulty.
- (5) The fold may be too large to be conveniently photographed.

The combination of all these factors is commonly sufficient to render many excellent folds unsuitable for photographic work. What is required is a method of direct measurement in the field which enables calculation of the parameters on all well-exposed folds irrespective of the section available and the scale of folding, the only restriction being that one layer may be traced around the fold.

The first essential in these calculations is to know the position of the axial plane or the best approximation to it for the layer involved, as this is the datum direction used in further calculations. The axial plane

can be estimated to a reasonable degree of accuracy in the hinge region, but it is difficult to transfer this direction into the limbs as required by Ramsay's method for measuring the axial thickness, T_α , the thickness of the layer measured in the direction of the axial plane to which the layer is inclined at an angle $\pi/2 - \alpha$. Particularly when the limbs are at a small angle to the axial surface, any small deviation in the estimation of this measurement will incur significant errors in T_α .

There is no problem in concentric or slightly flattened concentric folds with the measurement of orthogonal thickness, t_α , the distance between two parallel tangents to the layer. In a concentrically folded layer a perpendicular to the upper surface will intersect the lower surface at the point of contact of the parallel tangent to the lower surface. However, when the fold has been flattened to any considerable degree and R (the ratio of the radius of curvature, r , to the apical thickness, t_0) is less than 8:1, there is an uncertainty about the position of the tangents. An easier measurement which can be taken in the field is the distance, p_α , between the bounding surfaces of the layer along the normal to the outer surface [See Fig. 1-3(c)]. Calculations of the difference between this measurement and Ramsay's t_α have been made for various combinations of flattening, the ratio, R , and angle, α .

2. RELATIONSHIP OF FOLD PARAMETERS IN IDEAL PROFILES

(a) VARIATION OF AXIAL THICKNESS, T_α , WITH RESPECT TO α , THE ANGLE BETWEEN THE NORMAL TO THE LAYER AND THE AXIAL PLANE, IN CONCENTRIC FOLDS

The relationship between T_α and t_α is shown in Fig. 1-1(a). Ramsay (1967) states,

$$t_\alpha = T_\alpha \cos \alpha \dots \text{(Eqn. 7-5)}$$

which can be written,

$$T_\alpha = t_\alpha / \cos \alpha \dots \quad (1)$$

However the measurement, T_α , indicated in this equation and in Ramsay's Fig. 7-18 is not the axial thickness that Ramsay defined as

"... the distance between the bounding surfaces measured in a direction parallel to the axial surface of the fold".

This latter measurement, T_α , which is the measurement potentially useful for field measurements, has the relation

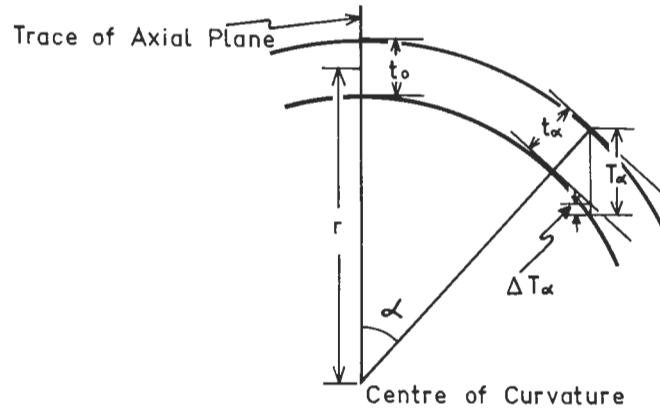
$$T_\alpha = t_\alpha / \cos \alpha + \Delta T_\alpha \dots \quad (2),$$

where ΔT_α is an increment, generally small, depending on α and R [Fig. 1-1(a)].

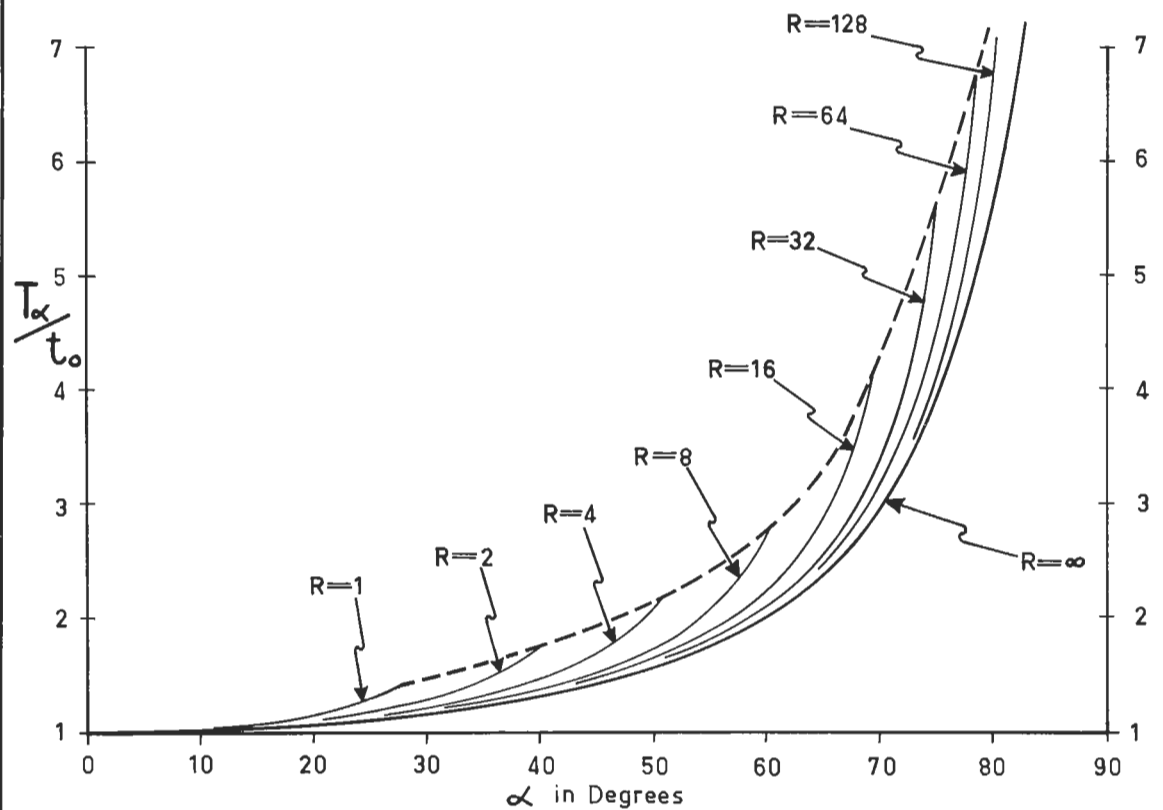
The variation of T_α/t_0 with respect to α for different R is shown in Fig. 1-1(b). There are several important features displayed in this graph, and they must be taken into account in the measurement of T_α in any layer.

(1) Measurements of T_α in an ideal concentric fold plot on slightly different curves depending on R for the layer. Hence the plots from different layers in an ideal concentric fold may not correspond, and if all the plots are placed on one graph they form a curved band.

FOLD PARAMETERS



(a) RELATIONSHIP BETWEEN ORTHOGONAL THICKNESS, t_α AND AXIAL THICKNESS, T_α



(b) AXIAL-RATIO GRAPH FOR CONCENTRIC FOLDS WITH VARIABLE RATIO, R

(2) The lower limit of this band is a curve of the form

$$Y = 1.0/\cos\alpha \dots \quad (3).$$

This limit is approached as successively thinner layers are selected for measurement.

(3) There is a limit in any layer to the angle, α , at which measurements of T_α can be made. This is shown on the graph by the intersection of the T_α/t_0 plots for different R with the dotted upper bounding curve. The limiting angle is the highest value of α on the outer surface of the layer such that a line parallel to the trace of the axial plane will intersect the inner curve. It is lowest for low R and approaches 90° for infinitesimally thin layers. For layers with R greater than 100, 80° is usually the practical limit of α for measurement of T_α .

(b) TYPES OF FLATTENING

Flattening as defined by De Sitter (1958, p.283) is a process whereby a rock is deformed plastically such that there is no change in volume and the principal directions remain orthogonal. In all the calculations made of flattening hitherto, it has been assumed that the flattening is statistically homogeneous in the region under consideration. Furthermore, in applying flattening to folds, the direction of maximum shortening has been equated to the direction perpendicular to the axial plane of a fold. These assumptions are not justified in all cases, and indeed, it is important to recognize the variations from

these ideal conditions when trying to evaluate amounts of flattening. In order to consider these features it is necessary to define some reference directions.

Direction of flattening. The direction in which the greatest amount of shortening occurs.

Surface of flattening. The surface perpendicular to the direction of flattening.

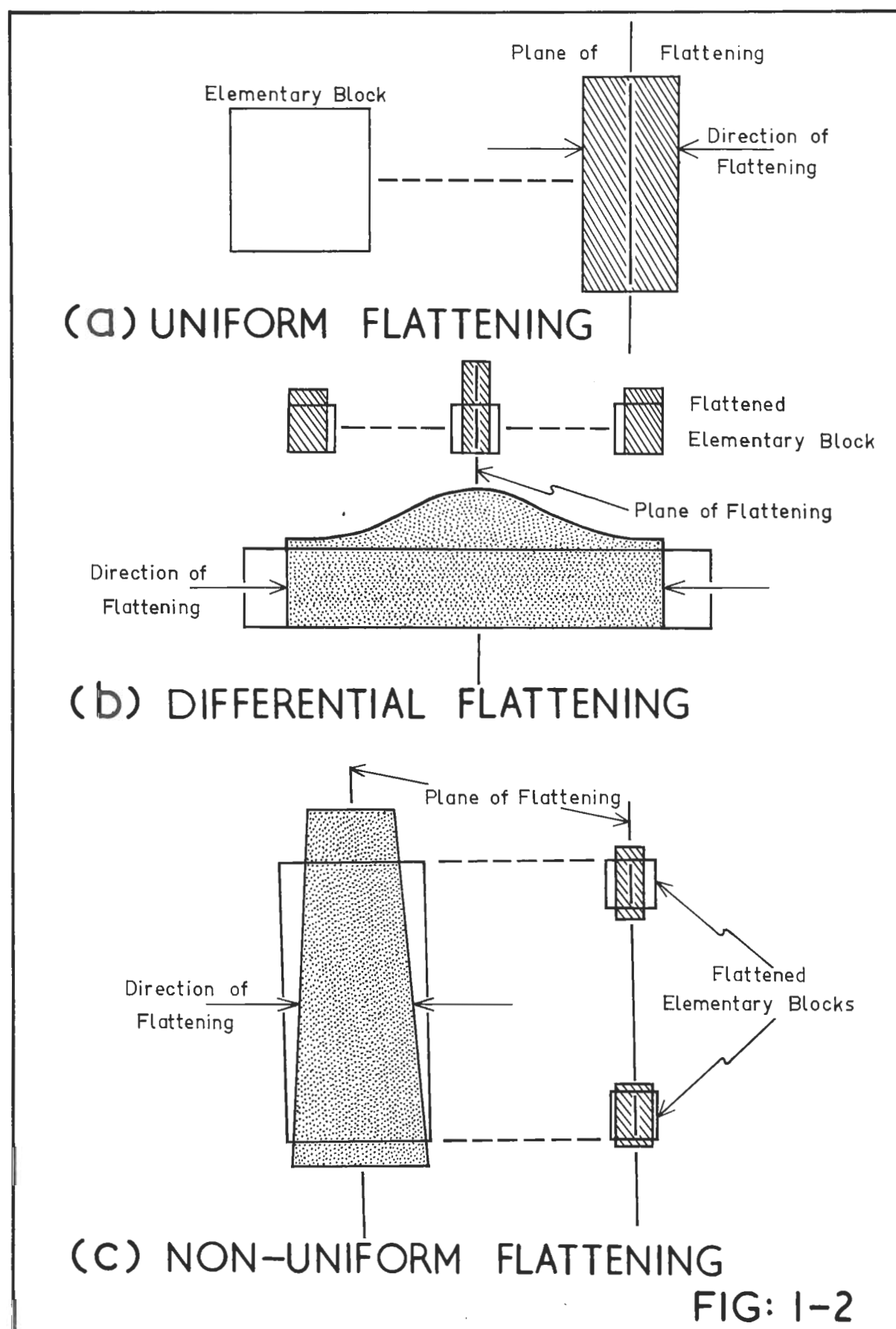
Plane of flattening. The plane which is tangential to the surface of flattening at a given point.

Uniform flattening. Flattening in which all elementary blocks undergo the same amount of deformation.

Differential flattening. Flattening in which the elementary blocks in a line along the direction of flattening undergo different amounts of deformation.

Nonuniform flattening. Flattening in which the elementary blocks in the surface of flattening undergo different amounts of deformation.

Flattening is a three-dimensional process. However, for simplicity it is usually considered in a two-dimensional *ac*-profile, although if there is a significant amount of extension or contraction along the fold-axis there will be an increase or decrease in profile area. The directions and types of flattening regarded in a plane are shown in Fig. 1-2. The amount of flattening, x , is expressed as the percentage shortening of a unit length along the direction of flattening. Thus,



if a length, a , is transformed to $X \times a$, the percentage of flattening is given by

$$x = (1 - X)100.$$

(c) RECOGNITION OF DIFFERENTIAL FLATTENING.

Differential flattening can most easily be detected in the axial-thickness-ratio graph. The plot of T'_α with respect to α may be a smooth curve, but it cuts across the standard curves for uniform flattening. In particular, in very low-grade metamorphic rocks, it is found that flattening is greatest close to the axial surface of a fold and decreases away from it. Thus the apical thickness, t_0 , is increased comparatively more than the axial thicknesses away from the hinge. As a result the T'_α values appear too low in the limbs, and the minimum T'_α value may occur when $\alpha \neq 0$. The difference in amount of flattening in the hinge and the limbs can be calculated directly by comparing the minimum axial thickness and the apical thickness. If the axial ratios are recalculated using the minimum axial thickness instead of the apical thickness, and the differential flattening is removed from the hinge, the axial-ratio curve should approximate to one of the ideal flattening curves. This process of removing differential flattening can be repeated progressively further away from the hinge until the adjusted ratios do approximate to one of the ideal flattening curves.

(d) RECOGNITION OF NONUNIFORM FLATTENING

Nonuniform flattening becomes apparent when different percentages of flattening are obtained for different layers in a fold. Commonly the layers with smallest curvature in concentric folds have little or no flattening while the layers on the concave side of the cusp may be quite highly flattened. Particularly in folded sequences of interbedded competent and incompetent layers where there is an irregular spacing of the competent horizons, a considerable variation in flattening may occur from layer to layer. It is essential in such cases to measure many layers before attempting to estimate the overall amount of flattening in any region, and even then such estimates are of doubtful significance. To make any reasonably accurate estimate of the overall amount of flattening a map should be constructed of the region, and the areal distribution of the flattening considered.

(e) NON-AXIAL-PLANE FLATTENING

It is often assumed that the axial surface of a fold is the surface of flattening. This is a reasonable assumption if the folds are caused by deformation in which none of the principal directions are rotated. In practice, however, individual folds may become disoriented out of the direction of flattening, either by rotational strain or by change in the direction of flattening. Where this occurs it is important to recognize the local plane of flattening and to *use the plane of flattening and not necessarily the axial plane of the fold when calculating amounts of flattening.*

Recognition of the plane of flattening is not easy. There is no geological feature which is universally accepted as having a constant orientation with respect to the surface of flattening although slaty cleavage in low-grade metamorphic rocks is probably parallel to the surface of flattening. Even so the direction of flattening may be variable from one part of the fold to another owing to local reorientation of the cleavage-forming stresses. Deformed bodies elongated in the plane of cleavage in slates are thought to be evidence of flattening perpendicular to the cleavage, and in general, the plane of flattening in folded competent and incompetent layers is assumed to be parallel to the slaty cleavage in the hinge region. This assumption may not be justified as shown in the diagenetic folds at Sulphur Creek where most flattening has occurred in the axial surface rather than in the cleavage plane.

(f) EFFECT OF FLATTENING ON A CONCENTRIC PROFILE

(i) Orthogonal-thickness ratios Consider a pair of continuous curves of the form $y = f(x)$ that are related in a manner such that the distance between their parallel tangents is constant. Let these curves also be of a form such that $f'(x)$ is continuous and $f''(x) \neq 0$ [i.e. at any point (x,y) , $f'(x-\Delta x) > f'(x) > f'(x + \Delta x)$, where Δx is a small increment in x]. Such a pair of curves represents a "concentric" fold profile.

Let these curves undergo a linear transformation such that $y = f(x)$ becomes $v = f(u)$, where

$$u = Kx \text{ and } v = y/K.$$

Then $dv/du = (dv/dy) \times (dy/dx) \times (dx/du) = (1/K^2) dy/dx$.

Therefore the parallel tangents in the original field will be parallel lines in the transformation, and since $f'(x-\Delta x) > f'(x) > f'(x+\Delta x)$, then $F'(u-\Delta u) > F'(u) > F'(u+\Delta u)$ in the transformed field showing that the transformed tangents are still tangents to the transformed curves. Hence, since the orthogonal thickness is defined as the perpendicular distance between the tangents, it can be seen that irrespective of the shape of the original curves there is a unique set of t_α/t_0 ratios for each percentage of flattening.

(ii) Axial ratios Consider a layer of uniform thickness which is folded concentrically. Take an elementary block as in Fig. 1-3(a) where the layer is inclined so that the normal to the layer makes an angle, α , with the axial plane. Let the block be flattened uniformly by $x\%$ perpendicular to the axial plane as shown in Fig. 1-3(b).

Then,

$$A'B' = X \times AB = t_{\alpha'}/\cos \alpha',$$

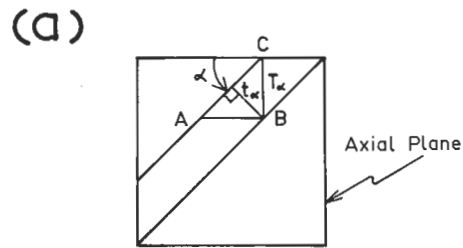
and

$$B'C' = (1.0/X) \times BC = t_{\alpha'}/\sin \alpha',$$

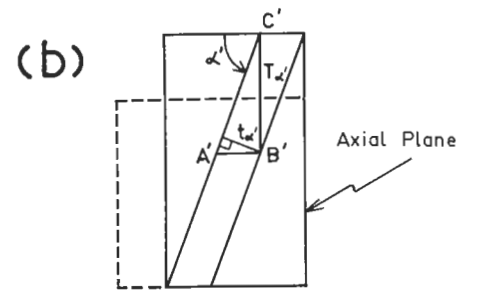
whence

$$\tan \alpha' = (1.0/X^2) \tan \alpha \dots, \quad (4).$$

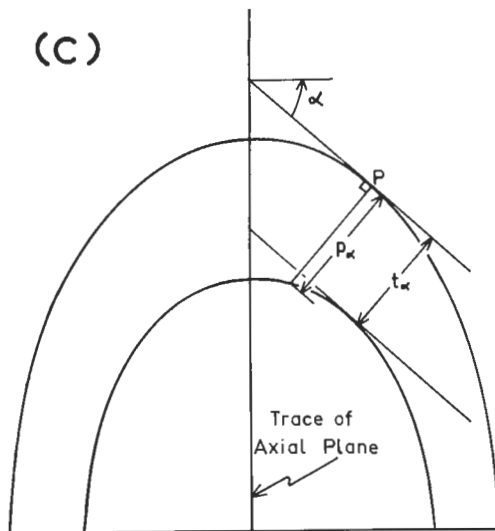
EFFECTS OF FLATTENING AND SIMPLE SHEAR ON A CONCENTRIC PROFILE



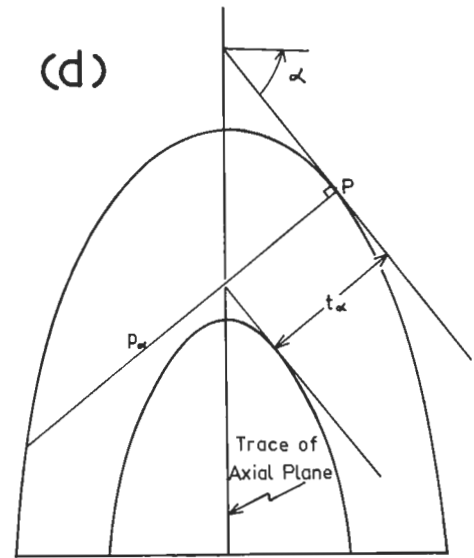
ELEMENTARY BLOCK OF A
NORMAL CONCENTRIC PROFILE



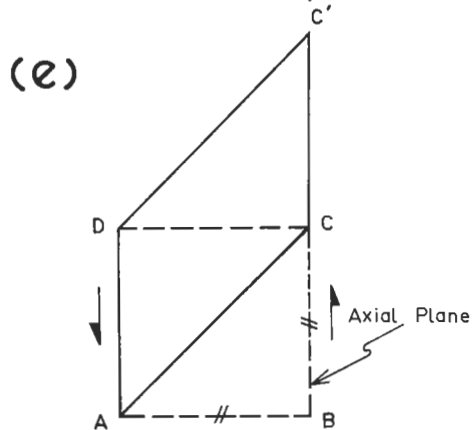
FLATTENED ELEMENTARY BLOCK



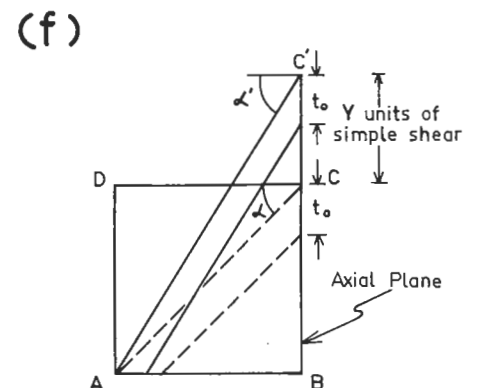
RELATION BETWEEN p_α AND t_α



PERPENDICULAR TO OUTER CURVE, p_α ,
DOES NOT INTERSECT INNER CURVE



1 UNIT OF SIMPLE SHEAR
ABCD becomes A'B'C'D'



SIMPLE SHEAR OF A FOLDED LAYER

Therefore during uniform flattening perpendicular to the axial plane, the ratio T_α/t_0 remains constant for any region of the layer and the angle α is increased to α' such that $\tan \alpha' = (1.0/X^2)\tan \alpha$.

(g) DIFFICULTIES IN THE MEASUREMENT OF ORTHOGONAL THICKNESS IN FLATTENED CONCENTRIC FOLDS

Flattening of a concentric fold transforms concentric circles, or parts thereof, into concentric ellipses, or parts thereof. In a concentric fold the points of contact of the parallel tangents lie on a common perpendicular to the layer so that there is little problem in measuring the orthogonal thickness at any point on the profile. However, in flattened concentric profiles the points of contact of the parallel tangents do not lie on a common perpendicular, and they may be considerably displaced. It may even become difficult in the field to determine accurately the location of the tangents, and the problem becomes acute in layers with a low R-value or a large amount of flattening. This error in estimating t_α may introduce inaccuracy equivalent to $\pm 10\%$ of flattening.

An easier measurement to make is p_α which is the distance between the bounding surfaces of the layer along the normal to the outer surface [Fig. 1-3(c)]. However, this measurement is not always possible as can be seen in Fig. 1-3(d) where the perpendicular to the outer surface does not intersect the inner surface. It would be useful to know within which limits of flattening and ratio, R, the difference between t_α and

p_α can be neglected, and a computer programme examining these two measurements was made to determine

- (1) the region in which p_α does not intersect the inner surface, and
- (2) the percentage error involved in measuring p_α instead of t_α in the region in which both measurements are possible.

The generalized results are shown in Fig. 1-4(a). The maximum percentage deviation of p_α from t_α is plotted for various R and amounts of flattening. p_α is always larger than t_α and the maximum deviation for any particular combination of R and x generally occurs when α is approximately 45° . A zone can be drawn dividing the results into two groups. On one side of the zone there is no significant difference between t_α and p_α , while on the other side either,

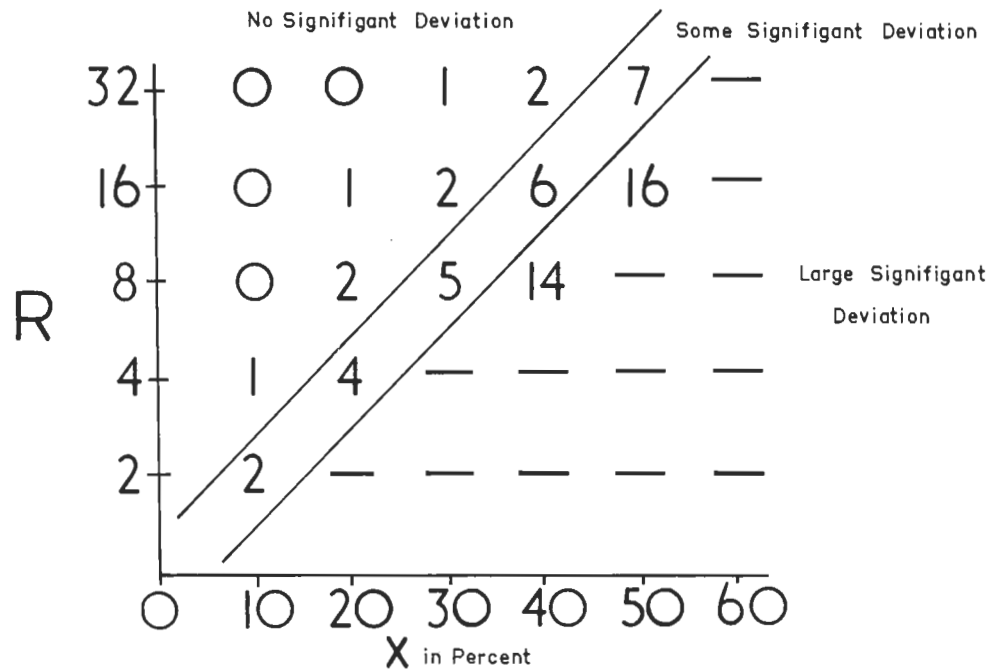
- (1) there are marked deviations of p_α from t_α , or
- (2) p_α does not intersect the inner curve.

In the zone itself there is some deviation but for most α the percentage deviation is within the accuracy of the field measurements. It is shown in this diagram that in dealing with orthogonal-thickness ratios in flattened concentric profiles

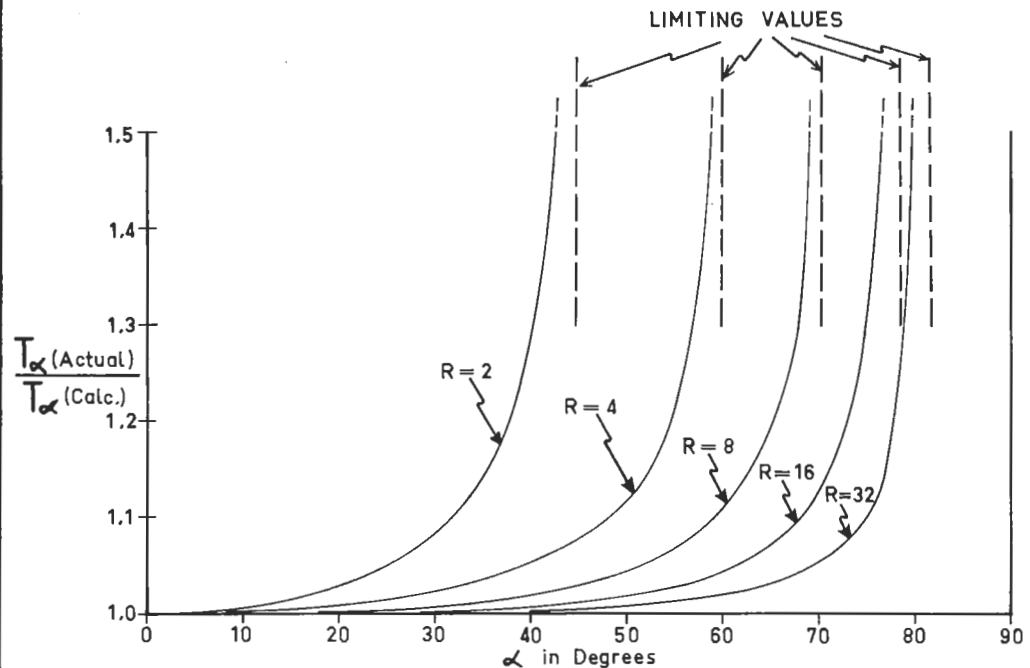
- (1) the thinner the layer (i.e. the larger R) the smaller the possible error in the measurements, and
- (2) the higher the percentage of flattening the thinner the layer on which accurate measurements are possible.

It is important to remember that only the maximum deviation of p_α from t_α is shown in this diagram. There are many values of α for

RELATIONSHIP BETWEEN FOLD PARAMETERS



(a) MAXIMUM PERCENTAGE DEVIATION OF p_α FROM t_α FOR DIFFERENT VALUES OF R and X



(b) RELATIONSHIP BETWEEN $T_\alpha(\text{Actual})/T_\alpha(\text{Calc.})$ and α FOR $X=20\%$ and VARIOUS R .

which p_α can almost always be measured, and a set of correction tables could be constructed to give accurate t_α . However this is unweildy and the justification for measuring p_α instead of t_α , which was that p_α could be more easily measured in the field than t_α , is seriously outweighed by the limitations to p_α . Thus it appears that despite the uncertainties about the position of the tangents, t_α is more useful than p_α .

(h) EFFECT OF THE R-RATIO ON THE AXIAL-RATIO PLOT FOR FLATTENED CONCENTRIC FOLDS

The effect of the R-ratio on the T_α/T_0 plot of a layer in a concentric fold has been shown in Fig. 1-1(b). which shows that whereas there is a unique t'_α plot for a concentrically folded layer, there are a multiplicity of possible T'_α plots. This effect also occurs in flattened concentric profiles and a comparison can be made between the actual T_α and the curve, $y = 1.0/\cos \alpha$, which T_α approaches as R approaches ∞ . Fig. 1-4(b) shows the relationship between $T_\alpha(\text{Actual})/T_\alpha(\text{Calculated})$ and α for 20% flattening and various R.

Each plot for a particular R is asymptotic towards a vertical line which represents the limiting angle, α , above which value the line parallel to the axial plane from a point on the outer surface does not intersect the inner surface of the profile. The higher the R-ratio the higher the angle, α , which can be used, and given any particular R-value, as angle, α , is increased, so is the ratio of the actual T_α

to the calculated T_α . A series of graphs could be constructed to allow corrections to T_α (Calc.), but their use would be tedious and unwarranted.

(i) USE OF AXIAL-RATIO PLOTS FOR FLATTENED CONCENTRIC FOLDS

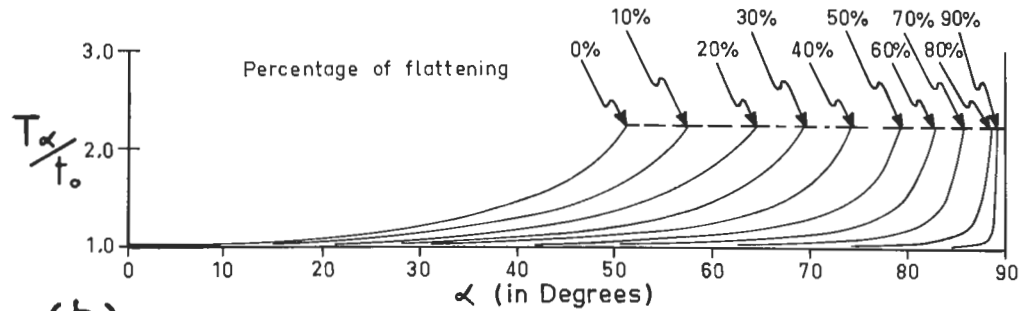
In a concentric profile $t_\alpha/t_0 = 1$ and there is no dependence of the plot on the R-ratio. Therefore in uniform flattening there is a unique set of t_α/t_0 values for each percentage of flattening, and this renders t_α measurements far more readily applicable to a graphical solution for flattening than T_α measurements; the graph constructed by Ramsay (1962, p.315, Fig. 7) is the one used. Nevertheless, this graph, while excellent for estimating the lower percentages of flattening, is not sensitive for amounts of flattening in excess of 40%.

From equation (4) a series of graphs may be constructed showing the T_α/t_0 ratio for any flattened concentric profile. It was shown in Fig. 1-4(b) that the influence of the R-ratio is very important in consideration of T_α/t_0 ratios for flattened concentric profiles. The relations between T_α/t_0 and α for given R ratios of 4, 32, and ∞ with varying amounts of flattening are shown in Fig. 1-5. There are several important features which can be seen by comparing these graphs.

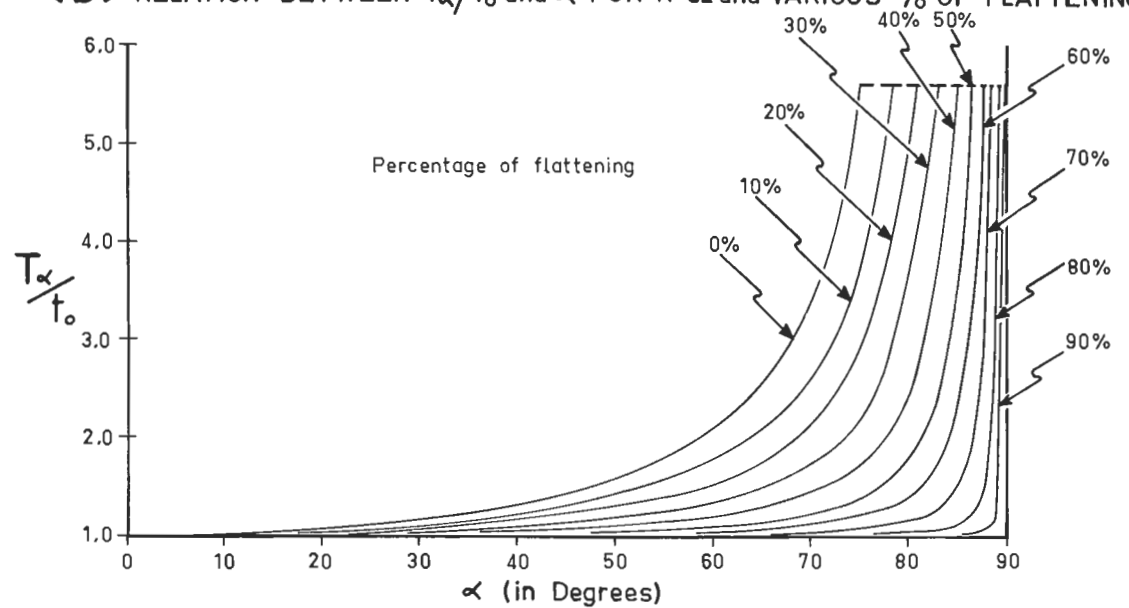
(1) The graph for $R = \infty$ represents a uniform flattening of the curve $y = 1.0/\cos \alpha$ which is the relation Ramsay has used for T'_α (Calc.). This plot has the same sensitivity as the t'_α graph as it is constructed from the same data.

AXIAL RATIOS IN FLATTENED CONCENTRIC FOLDS

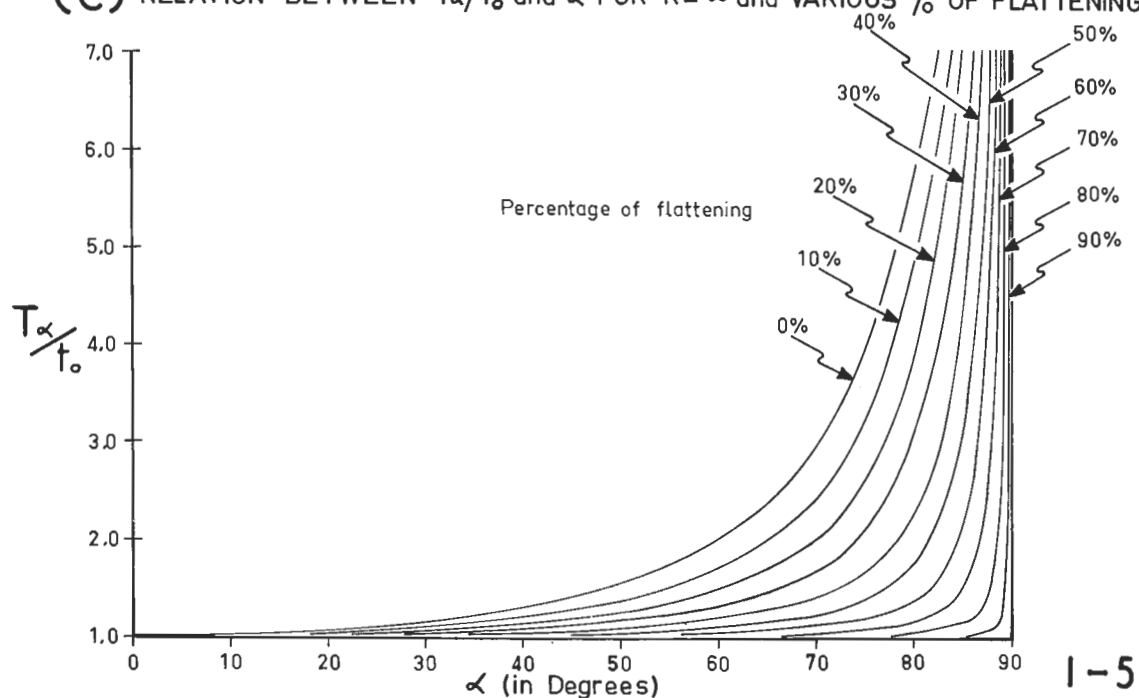
(A) RELATION BETWEEN T_{α}/T_0 and α FOR $R=4$ and VARIOUS % OF FLATTENING



(b) RELATION BETWEEN T_{α}/T_0 and α FOR $R=32$ and VARIOUS % OF FLATTENING



(C) RELATION BETWEEN T_{α}/T_0 and α FOR $R=\infty$ and VARIOUS % OF FLATTENING



(2) When α is less than 40° none of the curves is sensitive enough to permit an estimation of flattening. Uncertainty in measurement of α and T_α , as well as primary variations in layer thickness render the use of this part of the T'_α graph impractical.

(3) Although the higher the R-ratio the higher the limiting α which can be used for T_α measurements, the lower the R-ratio the more sensitive the graph. Thus there is a greater spread of α over which a T_α/t_0 ratio of 1.5 occurs for low R rather than for high R. A balance has to be attained between the upper limit of α and the sensitivity required, bearing in mind the restrictions already outlined. In general any R-ratio less than 4 is not very useful, but with an increasing amount of flattening, the closer this limit can be approached the more reliable the results.

(j) DIFFICULTIES IN LOCATING THE CENTRE OF CURVATURE IN FLATTENED CONCENTRIC PROFILES

In all the considerations of axial-ratio graphs the location of the centre of curvature has to be known with some degree of certainty. With concentric profiles the centre of curvature of any part of the folded layer which corresponds to an arc of a circle may be found at the intersection of two normals to the surface of the layer. If the whole profile is part of one circle then the centre of curvature for all parts of the fold is a unique point. However, particularly in folds with narrow angular hinges and long straight limbs, it is commonly found that different parts of a fold have different centres of curvature. Thus,

if measured T'_α values are compared with standard graphs, allowances must be made for the different R-ratios in different parts of the fold.

The problem is aggravated by flattening as it is not valid to project perpendiculars to the surface of the folded layer to determine the centre of curvature even though the unflattened profile corresponded to an arc of a circle. In those parts of the fold where the layers make a low angle with the direction of flattening, the curvature is increased and thus R decreased; where the layers make a high angle with the direction of flattening, the curvature is decreased and R increased. It is therefore necessary in the use of axial-ratio diagrams firstly to make a rough estimate of the flattening and to obtain an approximation to the true curvature from which the desired R-ratio can be calculated. Then the measured T_α/t_0 values can be compared accurately with the ideal flattening curves. Fortunately there is not much error involved in calculations of flattening from the axial-ratio graphs by a 20% error in the estimation of R as long as R is not less than 4.

(k) EFFECTS OF SIMPLE AND PURE SHEAR OF A CONCENTRIC PROFILE

In all the considerations of flattening it must not be forgotten that the similar geometry may not be caused by flattening (i.e. pure shear) but by simple shear parallel to a given direction. Flattening produces changes in thickness both parallel and perpendicular to the direction of application, whereas simple shear produces no change in thickness parallel to the shearing direction. However, neither of

these deformations produce changes in the axial-thickness ratios, and unless there is additional information about the nature of the strain involved, the gross geometry of the deformed layer will not indicate whether pure or simple strain is involved.

Let us define a unit of simple shear as the displacement of a particle by a unit distance in a plane unit distance from the origin [Fig. 1-3(e)]. Consider an elementary block of a concentrically folded layer undergoing Y units of simple shear [Fig. 1-3(f)].

Then α becomes α' , and $\tan \alpha / \tan \alpha' = BC / (BC + Y \times AB)$,

whence $Y = \tan \alpha' - \tan \alpha$.

Thus the amount of simple shear of a concentric profile can be calculated directly from the axial-ratio plot by considering the increase in α to α' for a given T'_α value.

(1) DISTINCTION BETWEEN SIMPLE AND PURE SHEAR

The geometrical similarity of simple and pure shear makes it impossible to distinguish which type of deformation is present merely by considering the gross geometry of the profile. However there are a number of methods whereby the type of strain involved may be inferred, and these may be classified into two categories:-

- (1) Knowledge of the original thickness of the layer, and
- (2) Knowledge of the original shape of deformed bodies within the layer.

Knowledge of the original thickness of the layer is a direct criterion which can be used to determine the type of strain. If it is possible to say that a layer originally had a certain thickness, then it can be found whether the layer has been thickened (pure shear), or whether it maintains its original thickness (simple shear) in the hinge of the fold. In this way the similar geometry impressed on a concentric profile can be divided into amounts of simple and pure shear.

It is also possible, by averaging the apical thicknesses of a group of layers in a folded zone to compare this average with the same, or similar layers in a nonfolded zone. If the similar profile is caused by simple shear then the average apical thickness of a particular group of folded layers should be the same as the average thickness of a comparable group of layers outside the folded zone.

In practice, it is never certain that the thickness represented in an apparently undeformed zone is the original thickness, and in any case primary variations are usually present. Methods more indirect usually have to be employed. The change in shape of a body during deformation is the best index available, and although accurate calculation of the amount of either type of strain has probably never been made satisfactorily, some conclusions about the type of strain have been drawn from both the geometry and the symmetry of the deformed bodies. O'Driscoll (1964 and other papers) has made extensive studies of the change in shapes by both simple and pure shear. Some of the simple geological structures which are most useful are current cross-bedding, oolites or clay pellets,

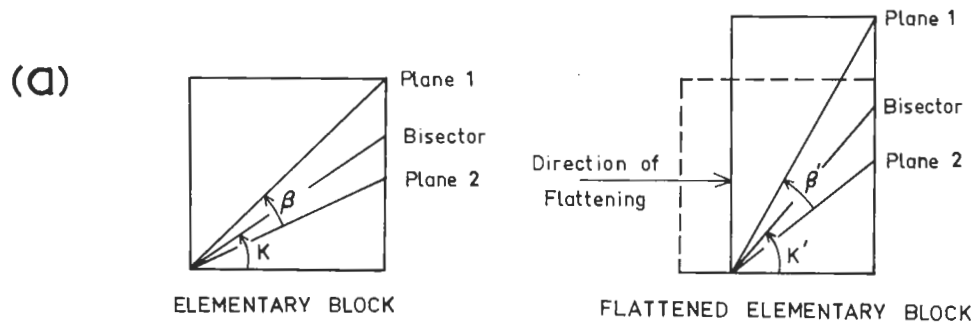
fossils and in general anything about which reasonable predictions can be made regarding their original shape. The change in angular rather than linear measurements is the most commonly used criterion, and perhaps the most reliable.

(m) DEFORMATION OF ANGLES DURING FLATTENING

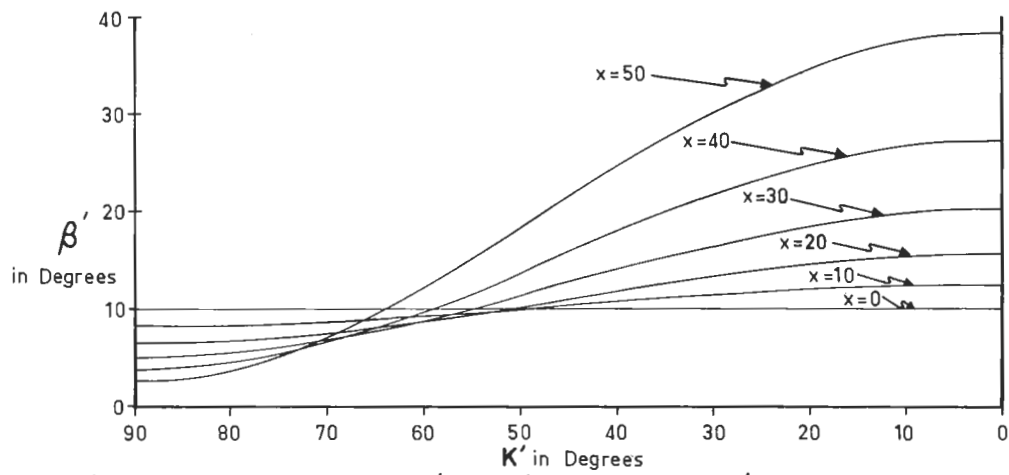
Consider two planes at an angle, β , apart which are in a layer undergoing flattening. Let the body be flattened by $x\%$ in a direction making an angle, K , with the bisector of the angle between the two planes [Fig. 1-6(a)]. Then β becomes β' and K becomes K' . In the field β' and K' can be measured and from the knowledge of the original β , percentage of flattening can be calculated. Fig. 1-6(b) shows the variation of β' with K' for various amounts of flattening, the original β having been 10° . Accuracy in measuring β' controls the sensitivity of the method, and the larger the original β , the more tolerance in measurement of β' for an acceptable accuracy in the estimation of flattening. Although Fig. 1-6(b) is constructed for $\beta = 10^\circ$ and similar graphs could be constructed for any desired angle. However for $0^\circ < \beta < 20^\circ$ the results may be scaled up or down by a factor so that the original β is made to equal 10° , and the graphs in Fig. 1-6(b) can be used.

The best estimation of flattening is obtained when K is lowest, i.e. when β is in such a position that it is opened by the flattening rather than closed. Because of the uncertainty of the value of the original β estimations of flattening should not be made from readings

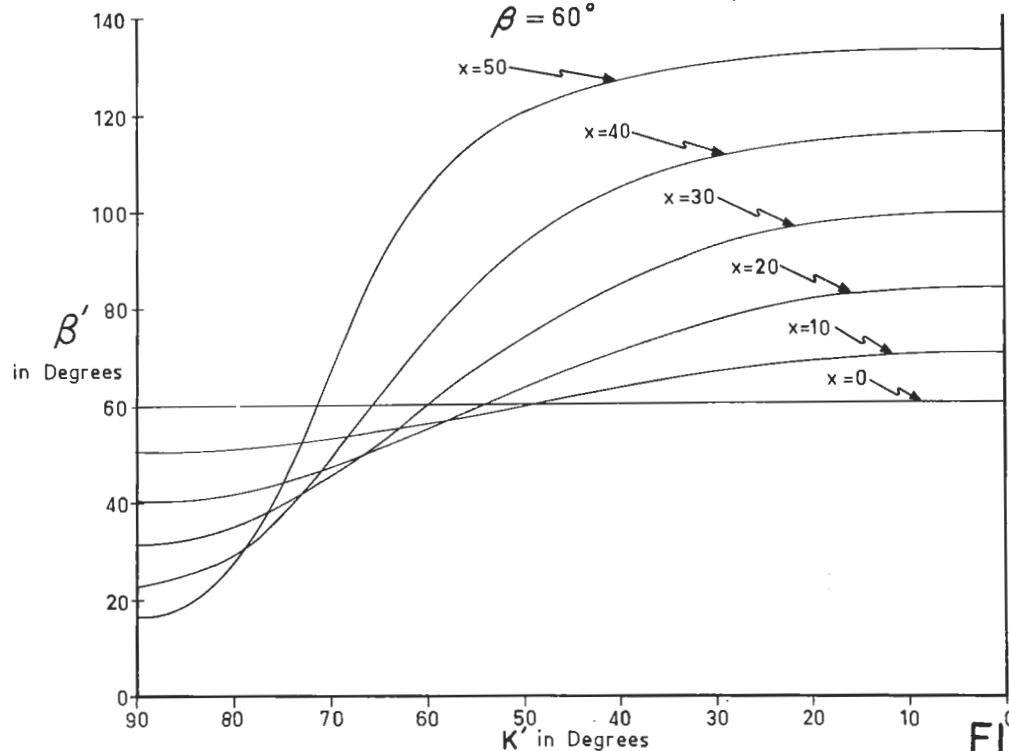
ANGULAR DEFORMATION DURING FLATTENING



(b) RELATION BETWEEN β' and K' FOR VARIOUS % OF FLATTENING, X
 $\beta = 10^\circ$



(c) RELATION BETWEEN β' and K' FOR VARIOUS % OF FLATTENING, X
 $\beta = 60^\circ$



over a small range of K' . If possible, β' should be measured over the whole range of K' , and the curve compared with standards.

The results for $\beta = 60^\circ$ are shown in Fig. 1-6(c). It is important to note that although the maximum angle between any two planes is 90° , values of β' greater than 90° have been quoted. This effect is caused by the orientation of the planes in the flattening field, where the acute angle has been transformed into an obtuse angle. It is therefore necessary to note the orientation of the planes in the flattening field and to measure β' in the same sense of rotation from one plane to the other.

(n) OTHER METHODS OF ESTIMATING FLATTENING IN FOLDS

Williams (1965) has developed a simple method for estimating flattening in folds which is particularly useful in the field where fold hinges are well exposed and correspond closely to flattened arcs of circles. The folds Williams was concerned with have long straight limbs and tight angular hinges. Often the layers have a sharp cusp on their inner surfaces which gives good control on the location of the centre of curvature. If the centre of curvature is well known, and if the shape of the folded layer represents a flattened arc of a circle good estimations of flattening can be made. However, when the location of the centre of curvature is not well known and the shape of the outer curve is not necessarily a flattened arc of a circle, estimations of flattening may become subject to considerable error. The method is further restricted in scale to a range of folds in which

(1) the whole fold is visible in the outcrop, and

(2) the observer can stand in a position such that he can look directly down the fold-axis.

In practice the use of Williams' method for estimating flattening is restricted to folds with tight angular hinges between the scale of a decimetre and a couple of metres.

One of the problems affecting calculations of flattening is primary variation in the thickness of the layer. This variation may be of two types:

(1) continuous variation such as a regular increase or decrease in thickness due to lensing, or

(2) irregular variation due to sedimentary structures.

Folds in which there has been primary variation can not be easily dealt with by either orthogonal- or axial-ratio plots, and the method of recording thickness at various distances along the bedding plane as indicated by Ramsay (1962, p.311) is the most suitable to estimate variations which might have been caused by flattening. There is the added problem that sedimentary irregularities tend to localize fold hinges (De Sitter, 1939 and 1957). Estimations of flattening in folds in which the layering was not originally of uniform thickness are usually best avoided.

(o) CONCLUSIONS

Although the basis of the axial-ratio diagram has been shown to be much more complicated than the basis of the orthogonal-thickness diagram, with due consideration of the restrictions the axial-ratio diagram can be used more successfully for the determination of amounts of apparent flattening than can the orthogonal-thickness diagram. The following conclusions can be drawn about the two different plots.

(1) The axial-ratio plot is not suitable for field use because,

(a) T_{α} can not be measured satisfactorily in the field, and

(b) α can not be measured with sufficient accuracy to allow successful application of the corrections to t_{α} , with regard to the R-ratio, to enable an axial ratio to be calculated.

(2) The ratio of the radius of curvature to the apical thickness, R, has an important effect on axial-ratio diagrams giving,

(a) a multiplicity of different T_{α}/t_0 values for any given percentage of flattening depending on the R-ratio, and

(b) an upper limit of α for which measurements of T_{α} can be made, this limit being highest for large R.

(3) In the field the difficulty in determining t_{α} because of the position of the tangents can be neglected for thin beds or small percentages of flattening.

(4) For percentages of flattening up to 40% the orthogonal-thickness diagram is most readily usable. However, the axial-thickness ratio plots are more sensitive for higher amounts of flattening. Layers with R not less than, but approaching 4 give the highest sensitivity.

3. DILATATIONAL STRAIN AND FOLDING

(a) GENERAL REMARKS

The effects which volume change during or after deformation have on the geometry of folds are rarely considered by structural geologists. Most deformations are related to non-dilatational strains, and Turner and Weiss (1963, p.274) in discussing types of strain, reflect this attitude by stating,

"... by no means are all the strain types ... likely to have statistically defined counter parts in natural strains as exemplified by tectonites. We can omit types ... in which the sole or principal component of strain is dilatation ..."

This attitude is due principally to two factors. Firstly, most geologists concerned with strain in rocks consider that they are dealing with consolidated, compacted rocks in which there is no significant loss or gain of void space or material such as water. Most structures attributed to swelling or contraction are considered superficial and not extensive enough to be important in conventional structural analyses. Secondly, in rocks which are consolidated the volume changes caused by metamorphism accompanying deformation are not usually considered large enough to be significant. The volume change involved in the change from anhydrite to gypsum is one exception. In this section I propose to consider briefly the geometry of strains caused by loss of water during compaction and the possible implications of this volume change with respect to tectonic folding in partially consolidated rocks.

(b) RELATIONSHIP BETWEEN DECREASE IN POROSITY AND VOLUME CHANGE

Porosity is defined as the percentage of pore space in the total volume of the rock. The porosity of a newly deposited mud may be as high as 80%, and there is a complete gradation from this value to shales with porosities less than 10%. If porosity is expressed as a percentage,

$$\text{decrease in volume} = \text{decrease in porosity} / (100 - \text{present porosity}).$$

This is not a linear function, as noted by Weller (1959, p.302). A 20% decrease in porosity in a rock having an original porosity of 50% produces a decrease of approximately 29% in volume, while the same decrease in porosity in a rock having an original porosity of 40% produces a decrease in volume of 25%.

(c) RELATIONSHIP BETWEEN VOLUME CHANGE AND FLATTENING

Up to this point flattening has been assumed to be a non-dilatational transformation, and the deformation has been considered in terms of change of shape rather than change in finite dimensions. Although the change in volume of a sediment during compaction is a three-dimensional process, it can be approximated to a linear function since the surface area of the sediments remains approximately constant, and a change in volume is directly proportional to a change in thickness of the unit. Thus a sediment which decreases in volume by 20% also decreases in thickness by approximately 20%, and the apparent uniform flattening caused by compaction is given by the equation

$$\% \text{ Uniform Flattening} = 100[1 - (1 - \text{Reduction in Volume})^{\frac{1}{3}}].$$

A 20% decrease in volume produces a uniform flattening of just over 10% parallel to the bedding.

(d) EFFECTS OF DIFFERENTIAL COMPACTION ON FOLD STRUCTURES

The loss of volume in an argillite during compaction is much greater than the loss of volume in a sand. Thus the amount of apparent flattening is greater in a pelite than in a psammite. If the mud compacts from an original porosity of 50% at the time of deformation to 10% after burial, and the sandstone compacts from an original porosity of 40% at the time of deformation to 30% after burial, then the uniform flattening of layers in the shale is approximately 25%, while in the sandstone it is only 7%. In cases where the sandstone and shale are interbedded, and the folds involve more than one unit of each, the case is a little more complicated. The style of folding in such sandstone-shale sequences is commonly such that the sandstone beds act as competent layers roughly maintaining their orthogonal thickness while the shale acts incompetently filling the interspaces. Differential compaction after deformation has two main effects.

(1) Planar features oblique to the bedding become non-planar if they pass through different rock types, and

(2) The volume of shale in fold cores is reduced thereby producing fold limbs convex towards the axial surface.

These effects are shown diagrammatically in Fig. 1-7. In Fig. 1-7(a) the elementary case of normal compaction of interbedded

EFFECTS OF DIFFERENTIAL COMPACTION

Plane of Compaction is horizontal

UNCOMPACTED STRUCTURES—COMPACTED STRUCTURES

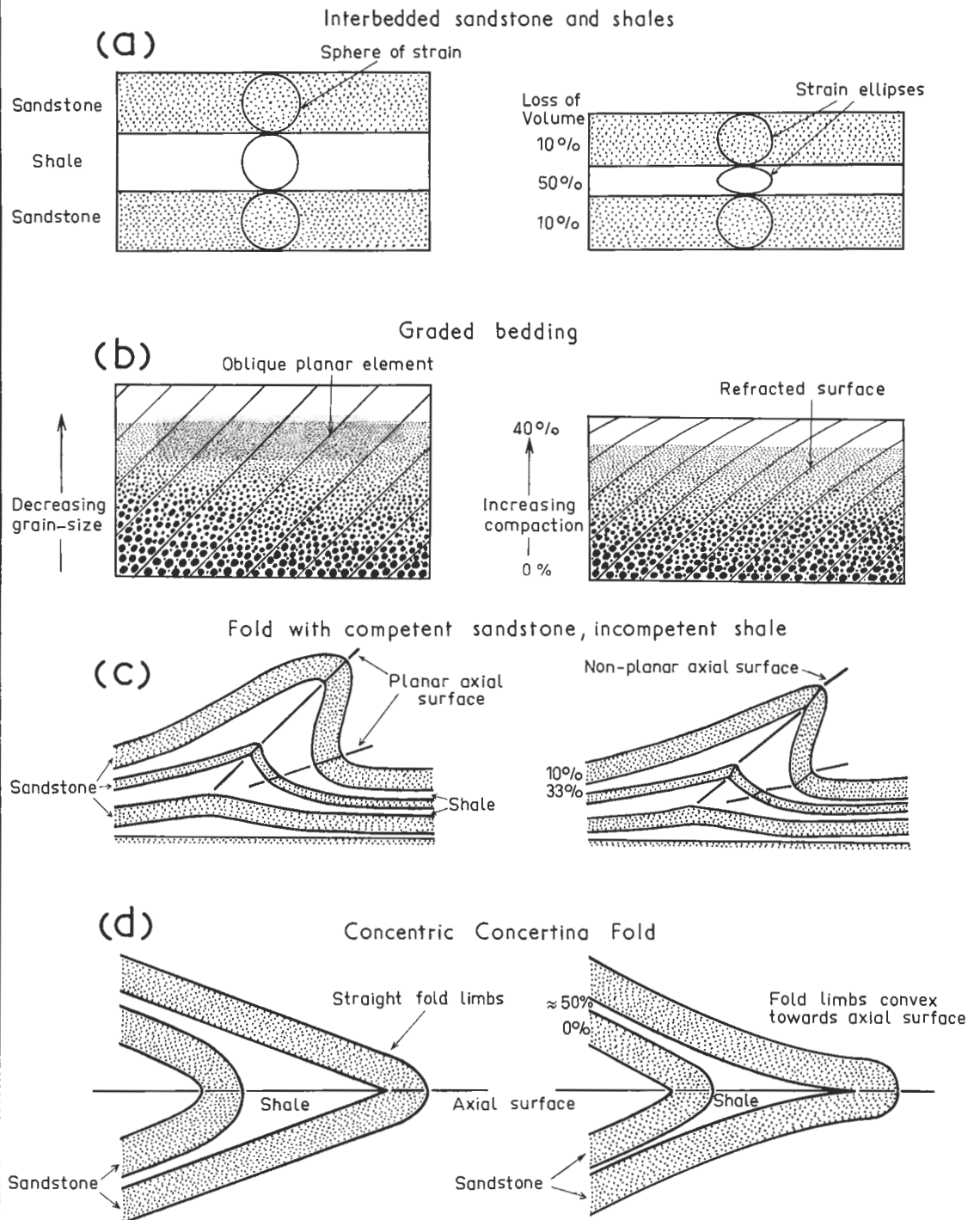


FIG: I-7

sandstone and shale is shown. If reference spheres are inscribed in the different rock types at any time during compaction the spheres in the shale are flattened more than the spheres in the sandstone. In Fig. 1-7(b) the effect of differential compaction on an oblique planar feature in graded bedding is shown. The original plane becomes bent or "refracted" with the part in the pelitic material being rotated furthest towards the plane of flattening. In Fig. 1-7(c) the effect of differential compaction on a fold with competent sandstone layers and incompetent shale is shown. The axial plane becomes "kinked" as it passes from the sandstone into the shale, and the volume of the shaly core is reduced. The effect of the reduction in volume of the shaly core is shown in Fig. 1-7(d) where the originally straight planar limbs become convex towards the axial surface.

(e) RELATIONSHIP BETWEEN COMPACTION AND THE PLANE OF APPARENT FLATTENING

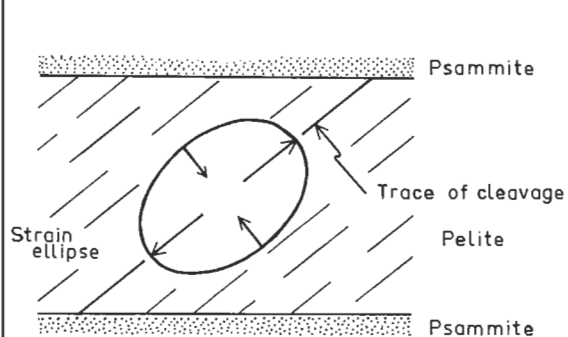
One of the problems in the use of Ramsay's graphs to calculate percentage of flattening is how to determine the plane of flattening. In simple cases the axial plane may be assumed to be the plane of flattening. However, in structures which undergo apparent flattening by compaction after their formation the axial plane is not necessarily the plane of flattening. The problem can be discussed with respect to the two dominant rock types, viz. pelites and psammites.

(i) The plane of flattening in pelites.

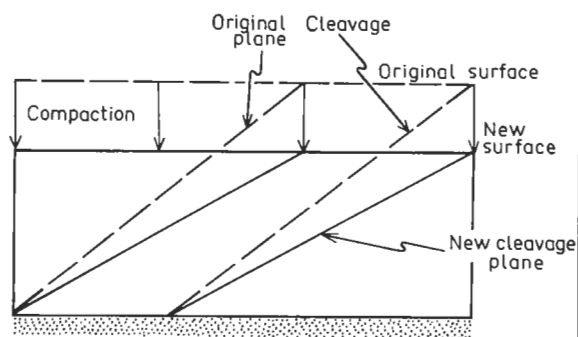
Consider the formation of a planar structure (e.g. cleavage) in a pelite interbedded with psammities [Fig. 1-8(a)]. There are two ways in which the pelite might compact. In the first model no account is taken of the structure of the pelite, or the way in which it is dehydrated. Compaction occurs perpendicular to the bounding psammities thereby shortening all dimensions in the pelite except those parallel to the bedding to which the plane of apparent flattening is thus parallel [Fig. 1-8(b)].

In the second model cognizance is taken of the type of structure that exists in the pelite. If the planar structure is a cleavage of the slaty type such as exists at Sulphur Creek and Tullochgorum, most of the platy minerals are oriented parallel to it. This type of cleavage appears to have formed perpendicular to the maximum applied stress, and any excess water in the rock will have been forced out along the cleavage surfaces. Under these conditions it is reasonable to assume that the area of the cleavage surfaces did not decrease, and may, in fact, have increased. Likewise the area of the bedding surfaces of the psammities did not decrease, so that there were two non-parallel directions in the rock which did not shorten during tectonic compaction. Fig. 1-8(c) illustrates the postulated mechanism for compaction in which the cleavage slices maintain constant length, but decrease in thickness due to loss of water as they rotate towards the bedding surface during compaction. The plane of apparent flattening is located half-way between the bedding and the cleavage, as is shown in Fig. 1-8(d).

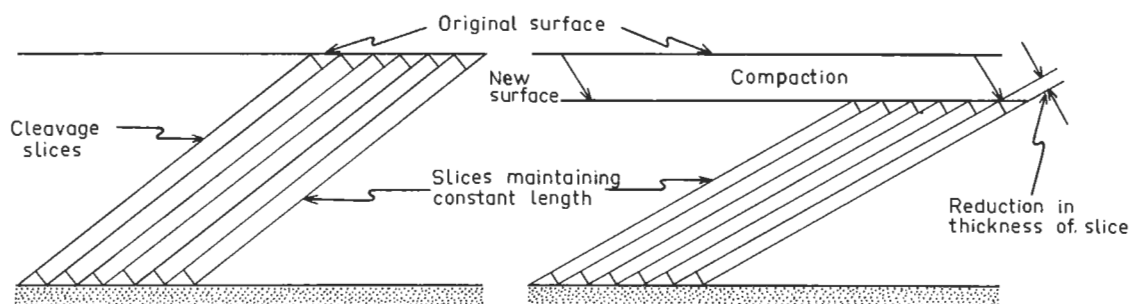
EFFECTS OF COMPACTION ON SLATY CLEAVAGE



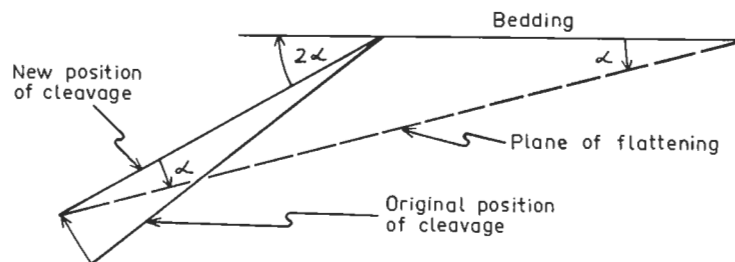
(a) Initial flattening perpendicular to the cleavage in the pelite



(b) Rotation of cleavage by normal compaction



(c) Rotation of constant-length cleavage slices by reducing thickness



(d) Relationship between cleavage, bedding and plane of flattening

Which, if either, of these two models of compaction is operative in any particular case is not easily determined. In the first model the strain may be related to two planes of flattening; initially, deformation associated with the cleavage formation may cause flattening in the cleavage plane and subsequent flattening caused by compaction is perpendicular to the bedding. In the second model there may be initial flattening in the cleavage plane and subsequent flattening perpendicular to the bisector between the cleavage and the bedding. Nevertheless, both models involve strain which can be related to a plane of flattening that is not parallel to either the bedding or the cleavage.

(ii) The plane of flattening in psammites.

The problem is far simpler in psammites. Because of the equidimensional shape of the grains there is little loss of volume during compaction, and the amount of apparent flattening is negligible. Thus in psammites the plane of flattening determined from the symmetry of the thickness ratios is the true plane of flattening related to the flattening deformation. In practice, the plane of flattening in individual psammite layers is generally parallel to the axial plane for each layer, and thus in folds in interbedded psammites and pelites where the axial surface becomes kinked by oblique compaction, the trace of the plane of flattening can be found by joining the points of maximum curvature on the bounding surfaces of the layer.

CHAPTER 2

SYNTAPHRAL FOLDING IN EOCENE CHERTS, PORT MORESBY

1. INTRODUCTION

The southern cliff of Paga Point, Port Moresby (Fig. 2-1) exposes a 400-metre-long section of highly contorted cherts, argillites and calcarenites. An intensive study, during which the cliff face was scaled-off into 5-metre sections and then photographed, was undertaken in January and February, 1965. Using these photographs as a base, structures and attitudes were recorded, and accurate sections have been made. An extension ladder forty feet long was used to reach the top of the cliff.

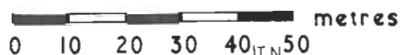
2. PETROLOGY

(a) GENERAL STATEMENT

The rocks involved in the folding at Paga Point, Port Moresby are calcarenites, argillites, and spherulitic cherts. The section

LOCATION MAP OF PAGA POINT SECTIONS

SCALE



Stereographic nets contoured for
1-3-6-10-14 pts per 1% area

TRUE
NORTH

6°

Magn.

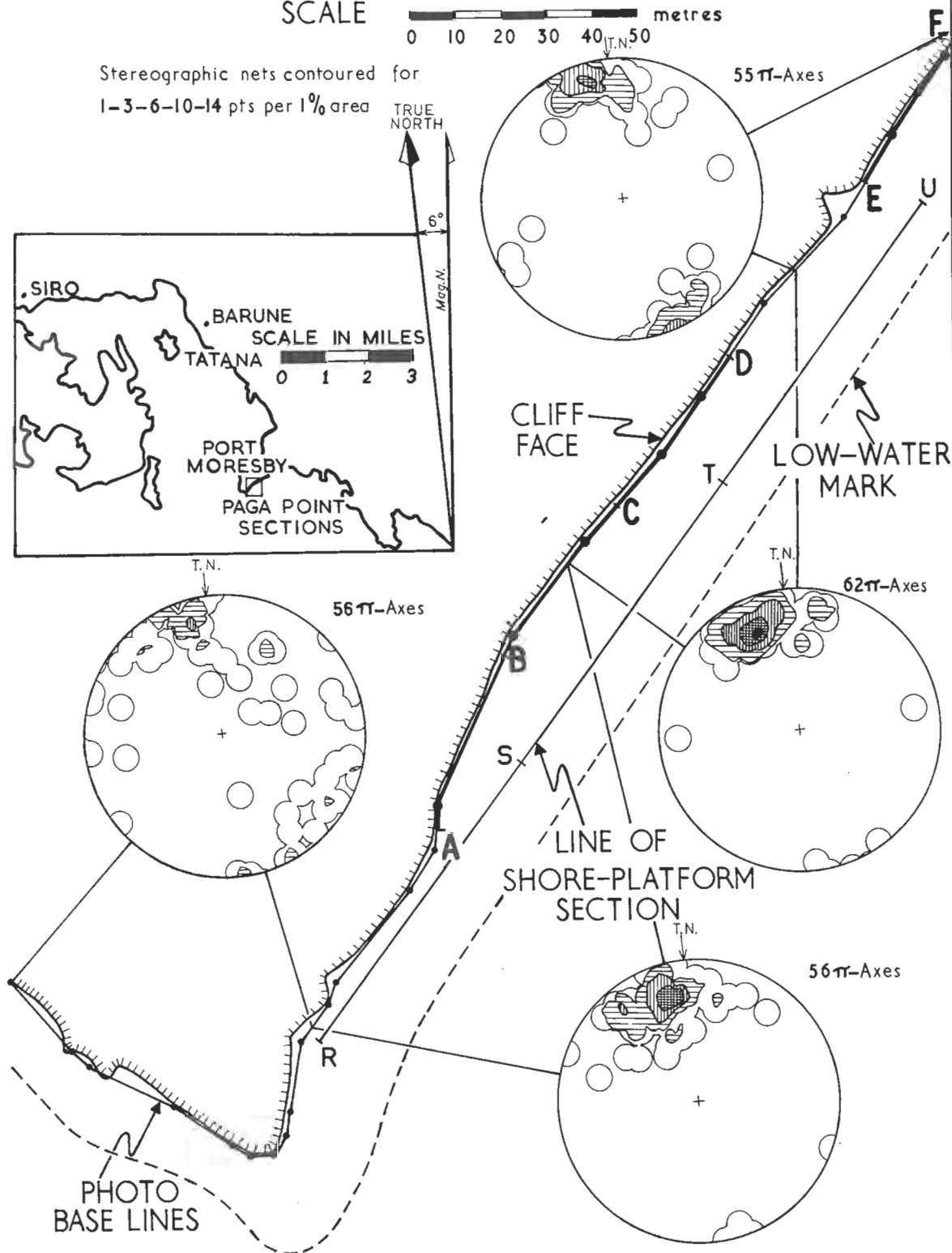
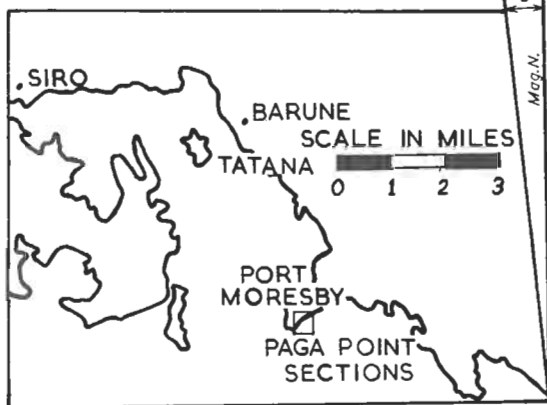


FIG:2-1

exposed includes about 100 metres of the Port Moresby Group (Glaessner, 1952). Competent beds are generally 10 to 20 cms. thick with the intervening incompetent beds 5 to 10 cms. thick. The beds were originally well defined in their mechanical behaviour, but owing to the growth of siliceous nodules, boudinage during folding, and induration of the exposed section, individual beds are hard to follow for any distance along a profile. In places they have been lensed-out completely, and in general, any bed pinches out laterally.

The rock type varies through the section, tending to become coarse-grained towards the top. The lower part consists entirely of spherulitic cherts and argillites with some thin bands of fine-grained calcarenite 2 to 3 cms. thick. The only difference between the competent and incompetent cherts in the lower part of the section appears to be the darker colour and more numerous fractures in the incompetent chert. This incompetent material is thought to have been argillite originally. In the upper part of the cliff section the rocks are medium-grained calcarenites with interbedded argillites. There is no cleavage despite the intense folding.

(b) FAUNA

There is an abundant fauna of predominantly planktonic foraminifera in the calcarenites, with radiolaria, bryozoans and sponge spicules also present. However, because of the likelihood that many of these calcarenites are formed of reworked material, the fauna from the cherts was used to date the sequence.

The cherts contain a poorer fauna than the calcarenites, and it consists predominantly of planktonic foraminifera and sponge spicules. Mr. P. G. Quilty (University of Tasmania, *pers. comm.*), has identified the following, *Globigerina yeguaensis*, *G. boweri*, *G. soldadoensis*, *Globorotalia bullbrooki*, *G. cf. renzi*, *Globoconusa cf. echinatus*, which indicate an age in the lower part of the Middle Eocene. Glaessner (1952, p. 72) has suggested "... an upper Eocene age of the Port Moresby Group seems therefore likely" mainly on the basis of large foraminifera in the calcarenites. The foraminifera identified from the cherts at Paga Point indicate that the Port Moresby Group may have extended at least through both Middle and Upper Eocene.

(c) PETROGRAPHY

(i) Spherulitic cherts (34918) These are very fine-grained rocks with some bedding variations, and they may well have been precipitated chemically as suggested by Montgomery (1930).

35% to 40% Sponge spicules and a few foraminifera. The sponge spicules are up to 1 mm. long and 0.1 mm. in diameter.

10% Spherulites of fibrous chalcedonic quartz, up to 0.1 mm. in diameter.

5% Clastic quartz, mica, plagioclase and opaque iron minerals. These are angular and up to 0.05 mm. in diameter.

40% to 50% Unidentified clay with some quartz and calcite. Individual particles are too fine to distinguish optically.

10% Calcite, in veins and also distributed throughout the matrix. In the veins the calcite has recrystallized up to 1 mm. across, but remains finely disseminated in the matrix.

(ii) Fine-grained Argillite Individual particles can not be distinguished optically, but probably consist of clay, chalcedonic quartz and calcite. The chalcedonic quartz also occurs in sponge spicules, which are very numerous and compose up to half the rock. Spherulites of fibrous chalcedonic quartz are usually less than 0.05 mm. in diameter, but a few larger spherulites reach 0.15 mm. across.

(iii) Fine-grained Calcarenite (34922) This rock type occurs as beds or lenses, usually less than 3 cms. thick where associated with the spherulitic chert and fine-grained argillite, and it forms only a minor proportion of whole chert sequence.

20% to 30% Clastic quartz, very angular and poorly sorted, low sphericity, unstrained extinction.

10% Plagioclase, An_{32} , remarkably fresh, angular and poorly sorted, medium sphericity.

Both the plagioclase and clastic quartz have a maximum diameter of 0.15 mm.

2% to 3% Glauconite, in very fine-grained, granular particles up to 0.15 mm. diameter. It appears moderately well rounded and in some examples is located in tests of foraminifera.

30% to 40% Foraminiferal tests and sponge spicules. The grain-size is similar to that of the larger clastic minerals.

less than 2% Chlorite, biotite and opaque iron minerals.

30% Matrix, consisting of quartz and calcite. The quartz is of several types,

(a) Opaline quartz, often in sponge spicules,

(b) Microcrystalline chalcedonic quartz which dominates the matrix, and replaced or infills fossil tests,

(c) Spherulites of radiating chalcedonic quartz, up to 0.5 mm. in diameter, and

(d) Thin rims of chalcedonic quartz encasing foraminifera and, in some places, clastic grains.

The calcite occurs either as a very fine-grained matrix throughout the rock or as coarse crystals in veins.

(iv) Medium-grained Calcarenites [Fig.2-2(a),34917] This is the dominant rock type in the upper part of the section and is usually well bedded with alternating green and grey beds, the green layers having been incompetent with respect to the grey ones.

15% to 25% Detrital quartz. There are two types:-

(a) Subrounded to rounded grains up to 1 mm. in diameter. These grains have a sphericity of 0.6, good extinction, numerous small inclusions of apatite, zircon and sericite, and are interpreted as plutonic quartz.

(b) Smaller angular quartz with lower sphericity. The maximum size is 0.5 mm. in diameter, but they are very poorly sorted down to fine-silt size. The grains have numerous curved cracks and indented margins, and a few have strained extinction with small biaxially positive interference figures. They are interpreted as volcanic quartz.

10% to 15% Plagioclase. There are two types:-

(a) Subrounded to rounded grains up to 0.7 mm. in diameter. They show good cleavage, moderate relief with n greater than that of Canada balsam, low birefringence and some polysynthetic twinning. The angle $2V$ is approximately 90° and the maximum extinction angle parallel to the faster ray is 27° . The composition is believed to be approximately An_{60} . [Fig. 2-2(b)]

(b) Smaller, fresh angular grains showing very strong polysynthetic twinning. The size varies up to 0.5 mm. in diameter with irregular and re-entrant shapes, and they are poorly sorted. Some weak compositional zoning can be seen, and these zones indicate that the present grains were once part of crystals 1 to 2 mms. in diameter. Several grains also appear to be deformed and cracked. They are biaxially negative with a maximum extinction angle of 15° parallel to the faster ray. The composition is believed to be approximately An_{30} .

less than 5% Potassic feldspar. Grains are subrounded, sphericity 0.7, size up to 0.5 mm. in diameter, and they are commonly altered with sericite inclusions. Perthite and microcline fragments are also present.

less than 5% Other clastic minerals and rock fragments. Biotite flakes up to 1 mm. in maximum diameter are commonly bent around detrital grains, and in some cases have been distorted by calcite crystallizing along the cleavage surfaces. Glauconite, which comprises an average of 1% to 2% of the sediment, occurs in rounded, fine-grained granular particles up to 0.5 mm. in maximum diameter. The glauconite is often located in foraminiferal tests, but the average size is approximately equal to that of the larger clastic grains in the rock. Pyroxene, opaque iron minerals,

chlorite and possibly lava fragments are present in small amounts and make up the remainder of the clastic particles apart from fossil fragments.

40% to 50% Calcite matrix (including 30% to 40% fossil fragments). The calcite occurs as (a) fine-grained matrix, disseminated throughout the rock, and (b) coarse crystals up to 1 mm. diameter in dilatant veins. The fossil fragments are 30% to 40% of the volume of the rock. They are foraminiferal and radiolarian tests and sponge spicules of the same grain-size as the larger detrital minerals. They are, however, completely replaced by quartz, or in some cases calcite, and while initially they may have acted mechanically as grains they are now part of the recrystallized matrix.

20% to 30% Quartz cement. The proportion of quartz cement in the specimens examined varies markedly, but is generally one of four main types:-

- (a) Spherulites of fine-grained, chalcedonic quartz crystallographically oriented radially. These spherulites [Fig. 2-3(a)] are commonly up to 0.5 mm. in diameter and many have formed in foraminiferal tests, although this locale is not essential. The spherulites have developed by radial growth outwards from a nucleus, and appear to have pushed the calcite matrix and all impurities outwards. In many places they have interfered with one another and have completely surrounded areas of calcite in thin-section. Coarsely crystallized calcite veins cut the spherulites.
- (b) Irregular patches of very fine-grained, microcrystalline quartz which is finely disseminated throughout the matrix. This fine-grained quartz has replaced some of the fossil fragments.
- (c) Encrusting rims of chalcedonic quartz, commonly formed around fossils and rarely around clastic minerals. The rim is usually 0.01 mm. wide with quartz *c*-axes arranged perpendicular to the margins.
- (d) Opaline quartz in sponge spicules.

(v) Dilatant Calcite-filled Veins In all rock types dilatant veins filled with recrystallized calcite have formed. These veins fracture matrix, spherulites and clastic grains alike, and have formed when the rocks were strongly cemented. This brittle behaviour post-dates the folding.



Fig. 2 - 3 (a). (34914) Crossed polaroids X 45. Spherulites of chalcedonic quartz in a matrix of fine granular quartz and calcite.

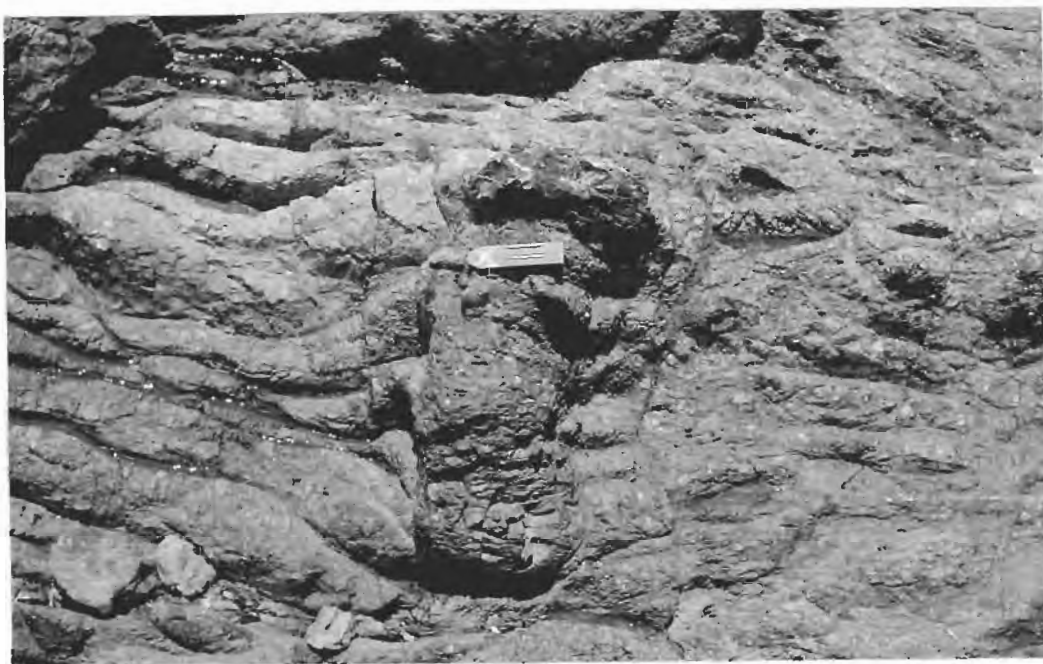


Fig. 2 - 3 (b). Large, irregular nodule which is composed of dark, flint-like chalcedony and extends across several beds. Differential flattening during deformation has caused the encompassing layers to bow around the nodule. Six-inch rule shown.

(d) CHERT AND FLINT NODULES

Siliceous nodules are very common in the chert beds, and vary in size up to 2 metres across. The nodules have a variety of forms. Some are irregularly shaped, flint-like bodies which encompass several beds [Fig. 2-3(b)]. Others are light-coloured and almost spherical with concentric banding. These quasi-spherical nodules are often confined to a single layer. Most of the nodules have been stretched into boudins during folding, and are elongate parallel to the bedding, but there are some which appear undeformed [Fig. 2-4(a)].

In thin-section the dark, flint-like nodules (34920) appear to be composed almost entirely of microcrystalline quartz less than 0.02 mm. in diameter. There are less than 5% of included detrital grains, and these are mainly opaque iron minerals less than 0.05 mm. in diameter. The lighter coloured, concentrically laminated nodules (34919) contain up to 20% of silicified foraminifera, sponge spicules and spherulites of radiating chalcedonic quartz up to 0.05 mm. diameter. The remainder of the rock is very fine-grained clay and quartz, with some calcite forming a compact matrix. Dilatant calcite veins transect the nodules.

(e) NON-TECTONIC, SEDIMENTARY STRUCTURES

There are several internal structures which are considered to have formed penecontemporaneously with deposition.



Fig. 2 - 4 (a). A small spherical concretion composed of chert. There are some concentric laminations. Six-inch rule shown.



Fig. 2 - 4 (b). Flinty nodules belonging to the same type as the large irregular nodules, stretched to boudins by folding. Six-inch rule shown.

(i) **Cross-Bedding** Small-scale cross-bedding is common in the medium- to fine-grained calcarenites, but is not present in the cherts. The units are usually 1 cm. to 2 cms. thick, and always less than 5 cms. Truncations are visible in most examples and have been used to determine direction of younging.

(ii) **Folded Cross-Bedding** These structures are different from convolute folds in that their geometry is essentially similar with axial surfaces oriented parallel to the bedding. They are probably caused by current-drag shearing of cross-bedded lenses (McKee, 1962).

(iii) **Convolute Folds** Several examples were seen, mainly in the medium- to fine-grained calcarenite in the upper part of the cliff section. Often they are truncated at their upper margins [Fig. 2-5(b)].

(iv) **Terminated Faults** These are structures in which small normal faults affect one bed only, and the beds above and below show no evidence of displacement. This could be because the upper bed is deposited after the faulting or because the interbedded incompetent material was mobile enough to take up all the strain.

(v) **Load casting** Load casting can be seen in some of the medium-grained calcarenites where the incompetent, greenish calcarenite intrudes the competent white layers.

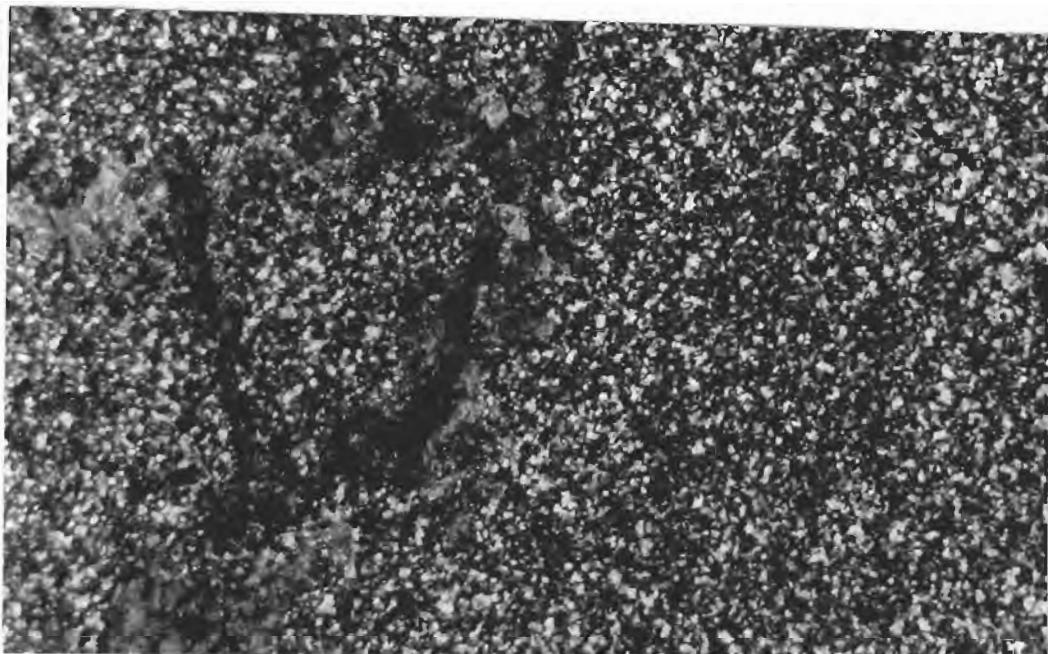


Fig. 2 - 5 (a). (34921). Crossed polaroids. X 60. Very fine-grained chalcedonic quartz in one of the large irregular nodules.



Fig. 2 - 5 (b). Convolute folds in medium to fine-grained calcarenite. Six-inch rule shown.

(f) ENVIRONMENT OF DEPOSITION

There are several criteria which are important in interpretation of the environment of deposition of the Paga Point rocks.

(i) Fauna The bulk of the fauna is Lower Middle Eocene planktonic foraminifera. Although exact correlation of the fauna to depth by reference to recent distributions must be undertaken with reservation, it is likely that the arenaceous bands accumulated in a water depth as great as, or greater than, the deeper limits of Norton's (1930) Zone B. The depth of accumulation was thus probably at least 100 metres.

(ii) Two Clastic Fractions In the medium-grained calcarenites there are two distinct clastic fractions. The first fraction consists of medium-grained sand-sized particles of well-rounded quartz, plagioclase An_{60} , potassium feldspar and glauconite. The well-rounded nature indicates that the particles were derived from an active environment, but the freshness of the feldspars indicates that weathering was mechanical and transport to this active environment rapid. The minor biotite and pyroxene could also belong to this fraction. The terrain from which this composition could be derived is plutonic igneous.

The second fraction consists of fine-grained, angular quartz, and plagioclase An_{30} . Commonly the quartz is fractured and strained. This fraction is believed to be of tuffaceous origin and to have suffered little or no abrasion during transport to the site of final deposition. Both Montgomery (1930) and Glaessner (1952, p. 66) have recorded abundant tuffs nearby in the Port Moresby Beds. The vulcanism was acid.

(iii) **Sponge-Spicule Chert** The high proportion of sponge spicules present in the chert indicates an environment protected from normal supplies of clastic particles, although the calcarenite bands throughout the sequence indicate an occasional influx of detritus.

(iv) **Non-Tectonic Structures** The penecontemporaneous structures described indicate intermittent bottom currents. Apart from small-scale cross-bedding which is present in the fine-grained calcarenites throughout the sequence, these structures are confined to the medium-grained calcarenite in the uppermost part of the section.

(v) **Maximum Size of the Clastics** The maximum size of the clastic particles in the calcarenites is approximately equal to the mean size of the foraminifera. This indicates that the foraminifera, which have an effective specific gravity less than that of the clastics, were transported by the same currents as were the clastic particles. Since the foraminifera indicate a depth of at least 100 metres, the depth of accumulation of these calcarenites may have been still deeper.

(vi) **Glaucinite** The presence of rounded glauconite grains indicates that at least some of the particles are reworked from an active shallow-water regime.

(g) CONCLUSIONS

The environment of deposition was a protected one at least 100 metres deep. It was not close to the strand line, but in a basin

or on the edge of the continental shelf where there were occasional influxes of clastic particles from shallower regions. The medium- to coarse-grained calcarenite towards the top of the section indicates a somewhat different environment from that of the cherts, although there are no data on relative depths. The change in environment could have been caused by an increase in supply of detritus from shallower zones, or it is conceivable that the calcarenites have slid under gravity from a shallower region.

3.

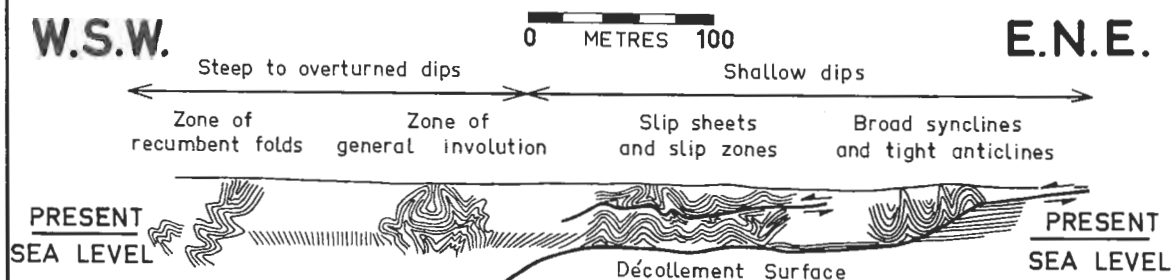
STRUCTURE

(a) GENERALIZED SECTION

Fig. 2-6(a) is a generalized diagram of the syntaphral folding at Paga Point. It shows that four structural zones have been distinguished although it is possible that more zones could be identified if the section were complete. The orientation of bedding surfaces and fold-axes is more ordered towards the northeast than towards the southwest, and in general the intensity of folding decreases towards the northeast.

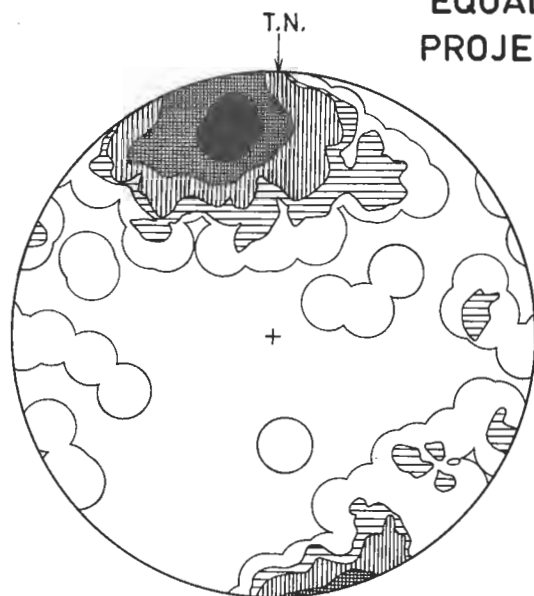
Individual fold-axes were calculated by taking the pole of the great circle through the bedding-poles (the π -method), and the distribution is shown in Fig. 2-6(b). The concentration of fold-axes at $21^{\circ}/347^{\circ}$ may have been tilted from the horizontal by later regional folding, but it is essentially horizontal and the cliff face is a

DIAGRAMMATIC SECTION THROUGH SYNTAPHRAL FOLDING, PAGA POINT



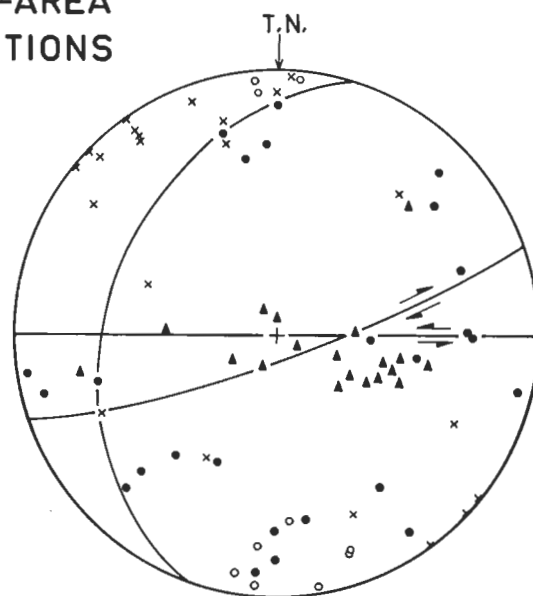
(a)

EQUAL-AREA PROJECTIONS



(b) 231 π -AXES

(TOTAL COLLECTED FROM WHOLE SECTION)
CONTOURS 1,3,5,11,23 Points per 1% area
Maximum $21^\circ/347^\circ$



(c) 71 POLES

(FAULT PLANES)

- × Dextral movement (19 pts)
- Sinistral movement (10 pts)
- ▲ Thrust movement (19 pts)
- Unknown movement (24 pts)

TRACES of planes of Dextral, Sinistral
and Thrust movement shown

FIG: 2-6

section at approximately 60° to the mean fold-axis. Variations in thickness appearing in the cross-sections Figs. 2-7 and 2-8 can not be attributed solely to the oblique and varying profiles. Nevertheless, many variations of local importance are caused by the sinuous nature of the fold-hinges which are variable in orientation both in an individual bed and from one bed to another in any particular fold. The cross-sections show the polyclinal nature of many of the folds. The section (Fig. 2-9) along the shore platform has been constructed on the Buskian principle, which may not be justified in the region of steep to overturned dips in the southwestern part, but the gradual overturning of the beds towards the southwest is apparent. The total thickness of beds calculated from this section is thus a minimum one, because of the likelihood of thinning perpendicular to the bedding surfaces.

(b) FLAP FOLDS

(i) Description The earliest recognizable fold form in the section is one which is termed a flap fold [Fig. 2-10(a)]. A *flap fold* is a parallel isoclinal fold, the maintenance of orthogonal thickness and parallelism of limbs being the two most important characteristics. Flap folds usually involve only one layer, and at most two or three. All the examples observed are restricted to the chert, and this lithic criterion may be important in mechanical interpretations. Spherulites of chalcedonic quartz, which form 10% of this chert, appear undeformed.

ACCURATE SECTIONS A-B and B-C ALONG PAGA POINT CLIFF FACE EACH DIVISION IS A 5-METRE-WIDE VERTICAL SECTION

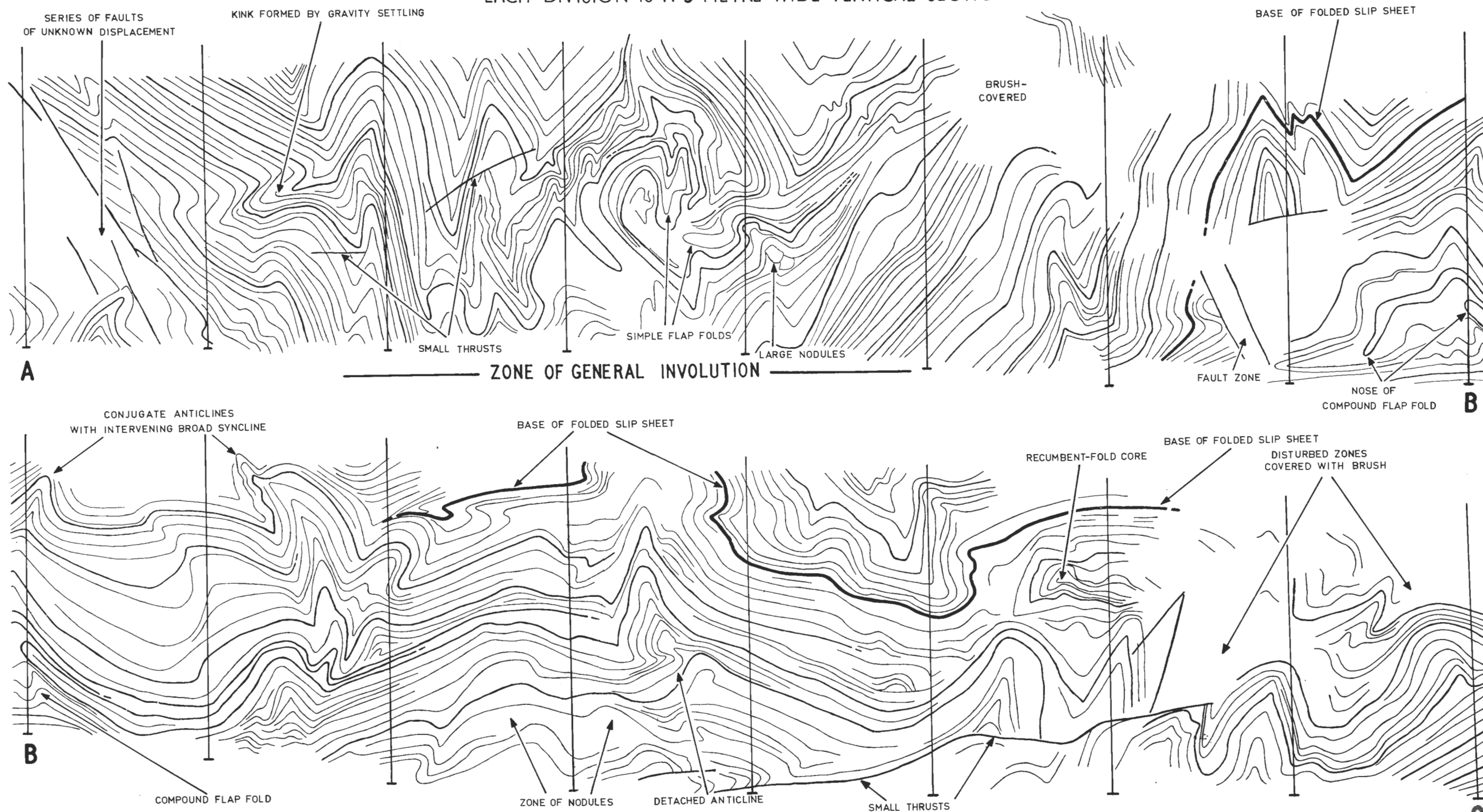


FIG: 2-7 C

ACCURATE SECTIONS C-D and E-F ALONG PAGA POINT CLIFF FACE

EACH DIVISION IS A 5-METRE-WIDE VERTICAL SECTION

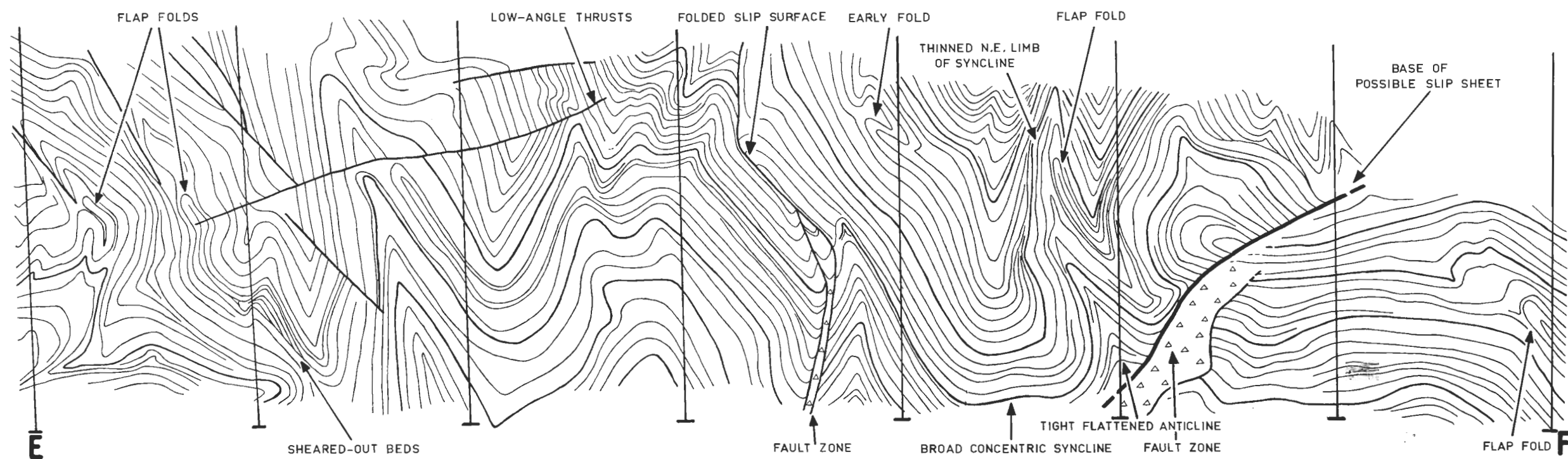
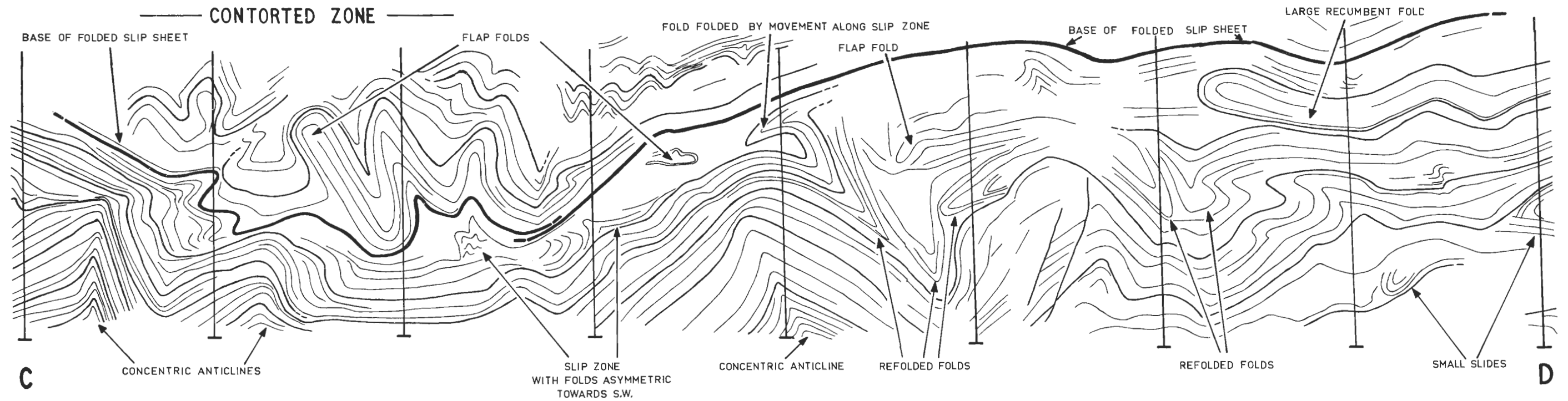


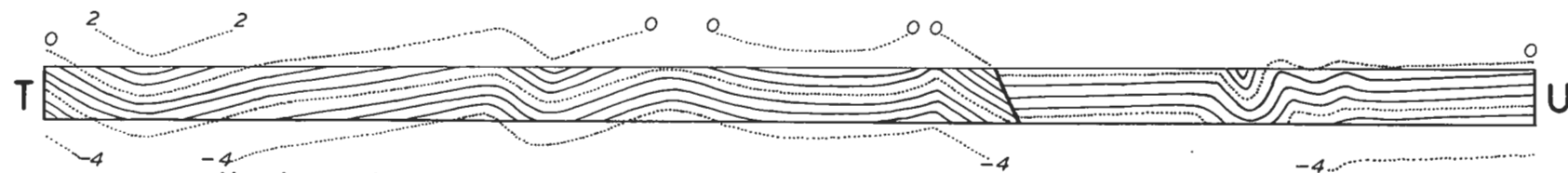
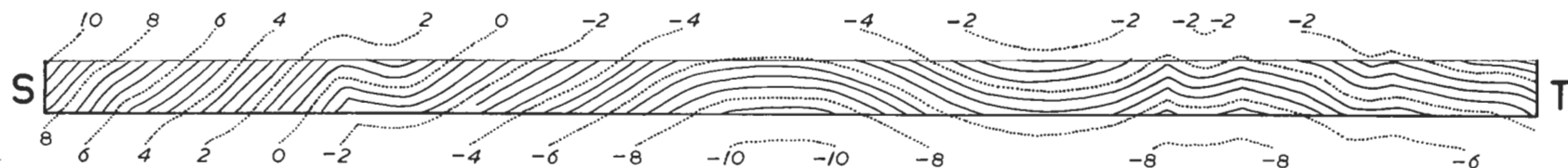
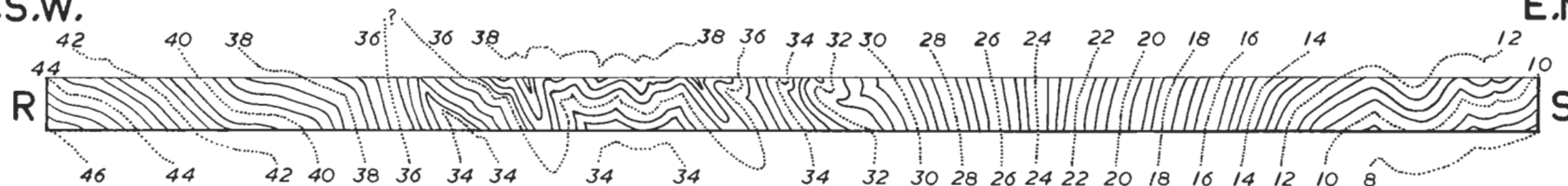
FIG:2-8

CROSS-SECTION BELOW SEA-LEVEL, PAGA PT.

RECONSTRUCTED ON BUSKIAN PRINCIPLE

W.S.W.

E.N.E.



Numbers show stratigraphic thicknesses in metres above and below an arbitrary level

SCALE 0 2 4 6 8 10 METRES

FIG: 2-9



Fig. 2 - 10 (a). A flap fold, showing the maintenance of orthogonal thickness around the hinge, and the isoclinal nature of long limbs. Six-inch rule shown.

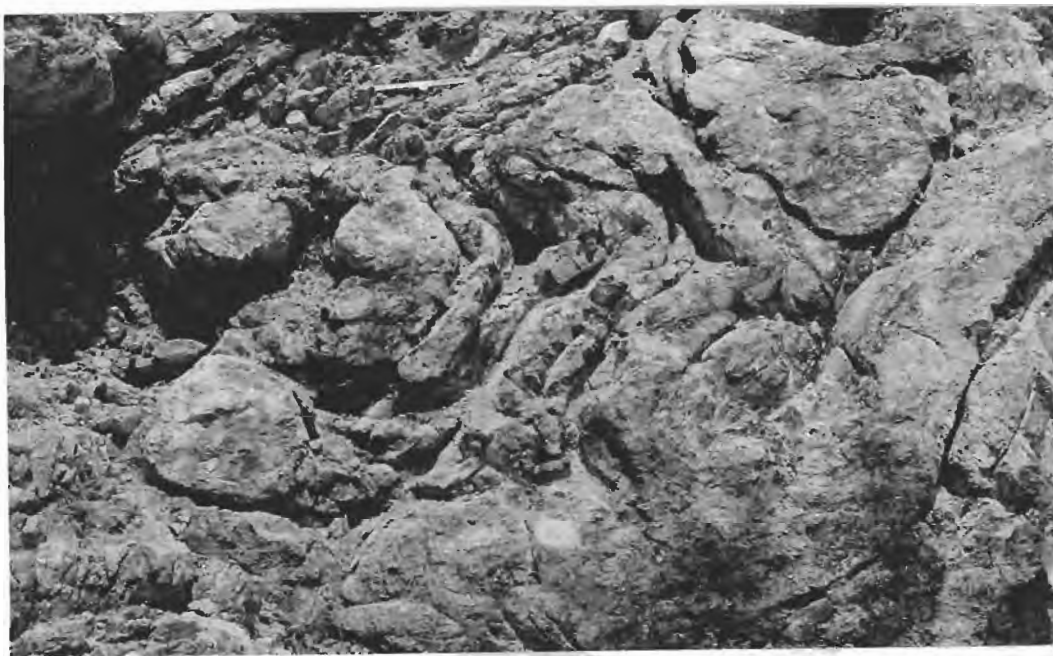


Fig. 2 - 10 (b). A contorted region in a slip zone separating two slip sheets. The large concretions are usually confined to one bed and appear to have been involved in the deformation. One-foot rule in the background.

Nodules, silicification and induration of layers, and boudinage during later deformations prevent accurate study of the geometry and possible folding mechanisms in the field. However, these folds do not appear to have affected either the deposition of succeeding layers or the deformation of these layers in later episodes of movement. The layers forming the flap folds are competent white cherts, and the total width of a fold perpendicular to its axial surface is usually less than 50 cms. and always less than 2 metres. The ratio of width to length in a profile-section is less than 1:10, and examination of the encompassing layers reveals that there is no possibility that these folds are part of larger structures analogous to the structure in the core of a parallelloid fold (Waterhouse and Bradley, 1957, Fig. 3, p. 535).

(ii) Origin of flap folds Attempts to explain the origin of flap folds in terms of more commonly accepted processes have failed. No theory of flow in viscous material will account for the approximate retention of orthogonal thickness around the hinge zones of the folds. Nor is it likely that the flap structure has developed by a bed rising vertically off the sea floor under tangential compression, and then reclining under gravity.

Flap folds on a larger scale from Persia have been described by Harrison and Falcon (1936), and in these structures a block of limestone has folded back on itself forming a recumbent fold. It is from these phenomena that the name flap fold has been borrowed. Waterhouse and Bradley (1957) have also described structures from New Zealand which resemble flap folds.

Fairbridge (1946, p.85) illustrates a diagram [Fig. 3(b)] showing "Sealing-Wax or Flow Structure" which strongly resembles the flap folds described. No locality or reference is given but it may be that the term originated from Brown (1938, p.360) who states

"... fine sands will flow like a very viscous fluid, such as sealing wax, forming small-scale contortions and lenses."

Fairbridge's structures bear no resemblance to Brown's structures which are convolute folds.

Fairbridge (1947, p.104) writing on the possible causes of intraformational disturbances in the Carboniferous varve rocks of Australia refers to

"... ribbon-like overfolds, grading into overthrusts and imbrications, or 'schuppen' and miniature 'nappes'. Generally one annual layer is involved, often a fairly thick and competent one. The layer involved would belong to the year preceding the movement. This layer appears to have come 'unstuck' and become folded over and piled up together, while the soft mud of the contemporary year fills in the loops and cracks. Folds and 'schuppen' will range in this way up to about six inches in height."

Plate III, Fig. 2 of Fairbridge's paper shows one of these folds which has a style very similar to the flap folds described, although it is somewhat thickened in the hinge region by flattening, perhaps caused by compaction.

Rigby (1958) writing on slump folds in Permian rocks states that:-

"... The bedding is well preserved in complex recumbent folds and is not appreciably modified by pinching and swelling ... (p. 311)"

"... the sediments were not lithified at the time of deformation ... (p. 312)

"... the black fine-grained beds were relatively plastic during deformation ... (p. 311)

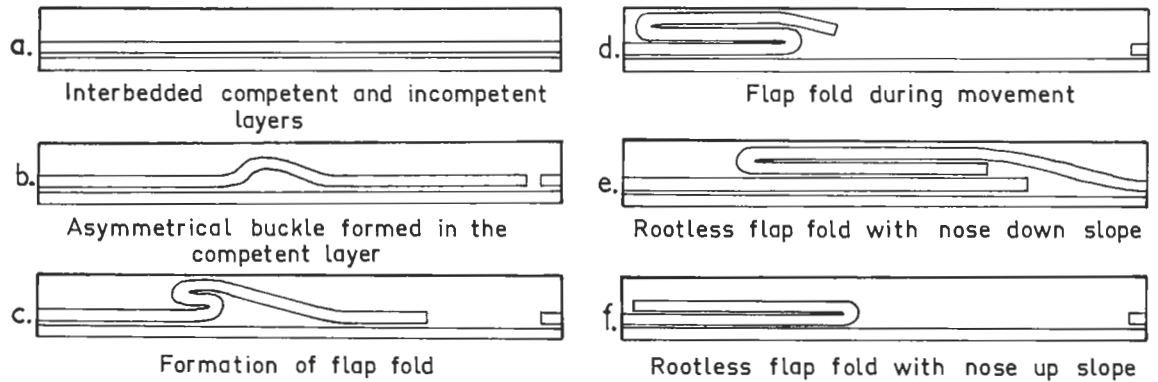
"... individual folds die out vertically within a few feet. They were probably formed in plastic calcareous muds beneath a light cover of sediment ... (p. 313)

"... sandstone and siltstone with minor beds of calcarenite are complexly folded and broken. Shale and siltstone beds behave as incompetent units, swelling and pinching, but very rarely fracturing. Interbedded calcareous sandstone and silty calcarenites are competent and fracture easily." (p. 315)

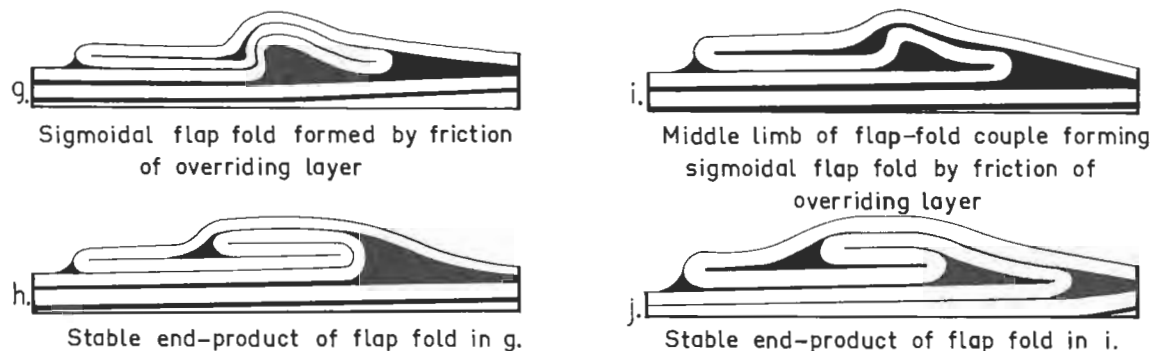
These descriptions serve to show that certain layers in slump deposits have acted as competent layers forming concentric-style folds. These beds have often acted independently of the rest of the sediment moving through the mud slurry with little friction. Both the Persian and New Zealand examples are explained by a mechanism of caterpillar-track action during folding of the layers, and in the other examples such a mechanism has been hinted at. Caterpillar-track action, with migration of the bed around the fold-hinge causing folding and unfolding, is the basis of the explanation of the Paga Point flap folds.

Figs. 2-11(a) to (f) show the proposed development of simple flap folds by caterpillar-track action. Bands of chert are chemically precipitated on a sea floor which is gradually tilted. The bands of chert are interbedded with more argillaceous material, which at or near the sediment-water interface would be a waterlogged clay of low specific gravity. A zone of instability is thought to develop in the chert band under the changing gravity field caused by the continuous tilting

FORMATION OF SIMPLE FLAP FOLDS



FORMATION OF COMPLEX FLAP FOLDS



FORMATION OF COMPOUND FLAP FOLDS

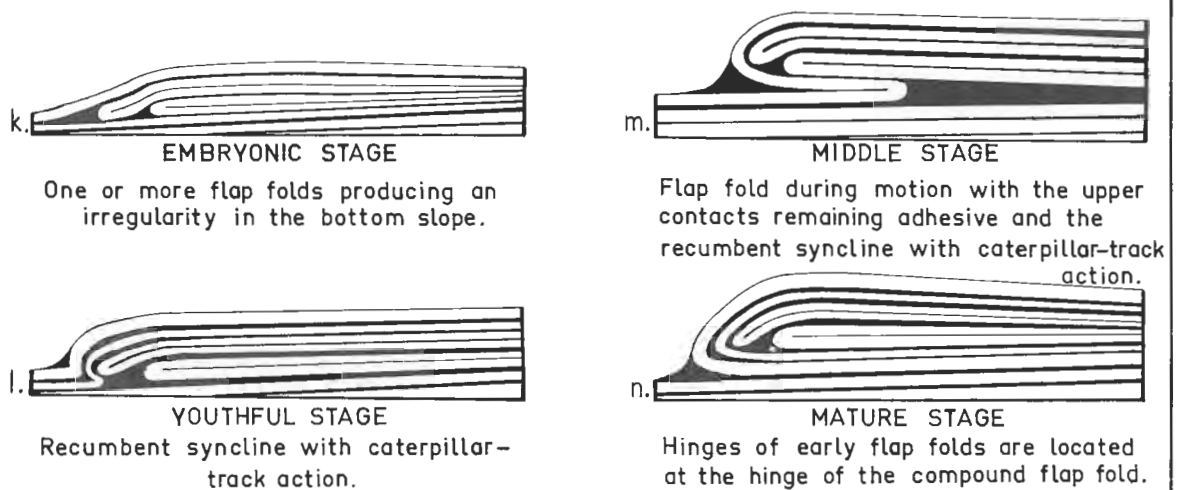


FIG:2-11

[differential compaction(?)], and a small, overturned, anticline-syncline couple forms as in Fig. 2-11(c). This fold form then migrates down slope with a caterpillar-track action, each part of the bed moving up one limb of the fold, around the nose and down the other limb. The uppermost layer travels twice as fast as the nose of the fold.

It should be noted that these figures are drawings of the flap folds *in motion*, and they are not likely to be preserved in these stages. The stable endform of the flap fold is shown in Figs. 2-11(e) and (f) with the nose facing up slope or down slope depending on whether the break in the bedding occurred up slope or down slope from the fold hinge.

Compound and complex flap folds are formed when more than one chert band becomes involved. Figs. 2-11(g) to (m) show some of the possible sophistications of this mechanism. Not all of these forms has been found, and compound flap folds are much less common than simple flap folds.

(iii) Depth of formation There is no definite criterion to indicate at what depth the flap folds formed, except that they are the earliest recognizable folds in section. No erosional truncations have been seen, but erosion of a structure forming at the sediment-water interface is unlikely in the depositional environment of the cherts. Two factors do, however, seem relevant.

(a) Considerable volume changes are required of the incompetent material to fill the spaces between the folding layer and the undisturbed basal layer. This is unlikely to be able to occur unless there

is a highly mobile interlayer material such as a clay slurry. Under any considerable cover of sediment the argillaceous layers would have lost much of their water and mobility, and the difference in viscosity between the competent and incompetent layers would be much less than it would be close to the sediment-water interface.

(b) Spherulites of chalcedonic quartz in the competent cherts are undeformed, indicating either that they were much stronger than the enclosing matrix at the time of deformation, or that they were formed after the movement. However, the large chert nodules to which the spherulites are probably genetically related were deformed during later movements.

It is suggested that the flap folds formed at, or near, the sediment-water interface.

(iv) The Problem of Cohesion The immediate problem which arises from the suggested mechanism of folding is one of cohesion. The chert layers must be strongly cohesive to undergo the bending and unbending required by caterpillar-track action, and must also be ductile enough to resist fracture. Cohesion due to interatomic forces acting between clay particles will not provide the cohesion required, as the incompetent material has a higher proportion of clay. It has been noted that the flap folds are restricted to the cherts, and it may well be that colloidal silica, either in spherulites or distributed throughout the matrix, provided the necessary cohesion. Taliaferro (1934) has suggested such a mechanism in the Franciscan cherts, California.

(c) SMALL-SCALE GLIDES

There are several examples of small-scale glides as drawn in Fig. 2-12(c). These glides are characterized by a number of beds being flexed into a small anticline and ending abruptly against an undisturbed basal bedding surface. The beds above follow the form of the anticline and continue laterally parallel to the lower bedding. The glides may have originated in two ways:-

- (1) By fracturing of a fold in the early stages of its formation, and subsequent gliding down slope, or
- (2) By drag of strata on a low-angle thrust fault.

No evidence was seen in the outcrops examined to favour either one of these hypotheses, but since the encompassing beds remained parallel for a considerable distance either side of the structure, there must have been considerable movement between the upper and lower beds. These glides appear to have been formed either when the cherts were more brittle (and therefore more consolidated), or when the strain rate was higher than when the flap folds were formed.

(d) SLIP SHEETS AND SLIP ZONES

(i) Description A *slip sheet* is an essentially horizontal group of strata which has glided as a unit under gravity, and it is separated by a slip zone from other slip sheets or the undisturbed basal strata. A slip sheet is characterized by the disharmonic nature of the folding within the sheet when it is compared with the strata above and below,

both the amplitude of folds and the position of fold-hinges showing no relation to those in adjacent slip sheets. The amplitude of folds in a slip sheet appears to be dependent on the thickness of the sheet.

A *slip zone* is the highly disturbed zone which separates either successive slip sheets, or a slip sheet from the undisturbed strata below. Slip zones may vary in thickness from a few centimetres where all the movement is concentrated along one bedding unit, to a metre or two in which several competent layers are highly contorted. The slip zone usually contains a higher proportion of argillaceous material than the intervening slip sheets. Commonly, rolled structures and involuted folds are found, and the strata are not traceable laterally for any considerable distance. The orientation of structure in a slip zone may give the direction of movement of a slip sheet. Figs. 2-7, 2-8 and 2-12(a) show the base of a slip sheet and a slip zone. Movement has been from east-northeast to west-southwest.

(ii) *Origin* The nodules appear to have acted as rigid bodies in the deformations associated with the slip zones and slip sheets. Beds adjacent to the concretions are frequently thinned against them and the concretions themselves may be elongated in the bedding in a manner resembling boudins [Figs. 2-4(b) and 2-10(b)].

It is unlikely that the concretions were present in beds undergoing flap folding, but they had developed before the slip sheets formed. Compaction and resultant loss of water would cause increased friction between the competent and incompetent layers, and this would

SOME PROFILE-SKETCHES

BLACK IS INCOMPETENT CHERT , DIRECTION OF TRANSPORT ←

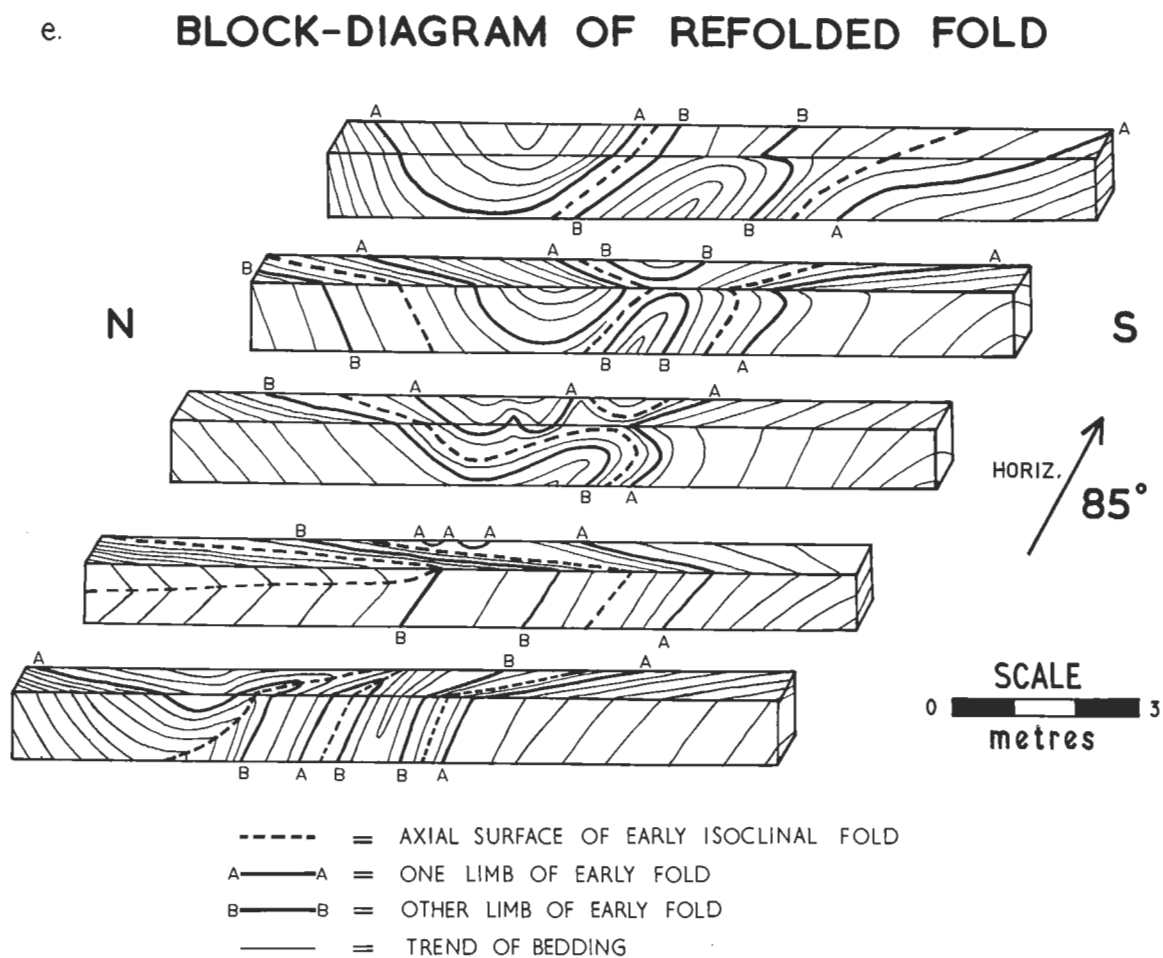
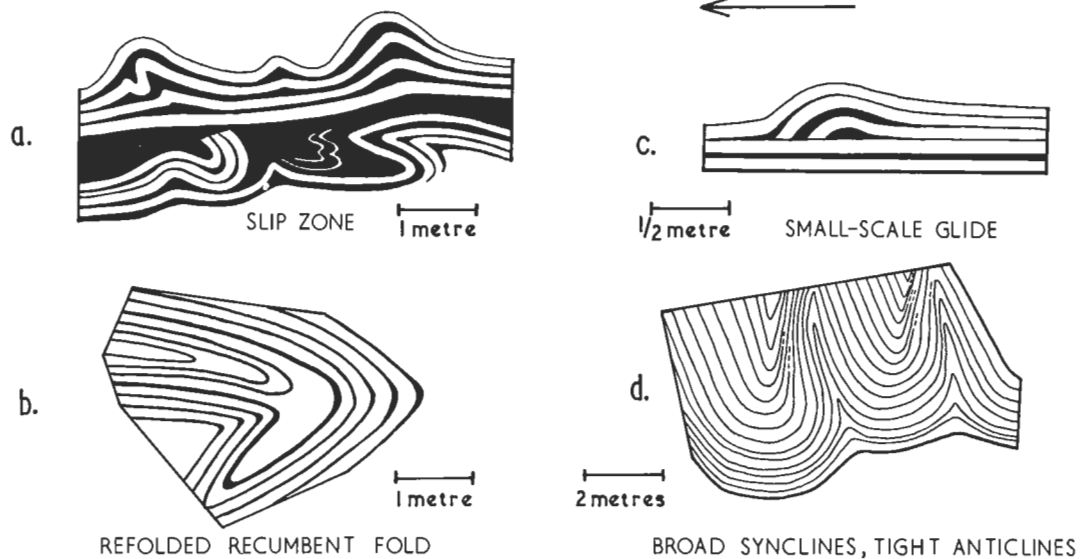


FIG: 2-12

enable the slip sheets to act as cohesive units separated by zones of lower viscosity. The depth of burial at the time of slip can not be estimated from the data available.

(e) BROAD SYNCLINES AND TIGHT ANTICLINES

A series of broad, open synclines and tight anticlines folds the slip sheets in the northeastern part of the section. The sedimentary facings are generally right-way up [Figs. 2-8 and 2-12(d)]. Measurements of orthogonal thickness show that the synclines have nearly perfect concentric geometry, but the anticlines have been differentially flattened, the maximum flattening occurring along the axial surface. Some flap folds have been identified, and these have acted as part of the bedding during the folding. The cusp-like synclines and anticlines have steep limbs and are generally overturned towards the southwest. Many of the southwestern limbs of the anticlines have been thinned by boudinage and internal flowage. A décollement separates the synclines and anticlines from the relatively undisturbed shore platform.

(f) ZONE OF GENERAL INVOLUTION

Between the zone of slip sheets and slip zones, and the zone of recumbent folds, there is a zone of general involution (Fig. 2-6). The folds are polyclinal and have been refolded into complicated shapes. Some of the folds can be recognized as earlier than others by overfolding relationships, and others which have their axial surfaces

oriented subhorizontally appear to have been formed by gravity settling after the main folding. Although the shape of the folds is very complicated, the competent layers have maintained their orthogonal thickness. Regions of more complicated contortion occur within the zone of general involution, but the extent of the zone appears to be limited by the coarser-grained calcarenite in the southwestern part of the section.

(g) RECUMBENT FOLDS

Recumbent folds are typical of the southwestern part of the Paga Point Section where they overfold all structures hitherto described. They have essentially horizontal axial surfaces, but fold-hinges are very variable in direction, many curving through 90°-azimuth in a distance of a few metres. In several cases a recumbent fold has been refolded by a slightly later fold as shown in Figs. 2-12(b) and 2-13(a) and (b). The axial surfaces of early recumbent folds in such cases are folded into new recumbent folds. The style tends towards concentric although in the hinge regions there is a considerable amount of flattening in the axial surface. In the middle part of the section, several of these folds are arranged in conjugate sets which seem to have formed by gravitational settling of the strata under their own load during or near the completion of the large-scale sliding.

(h) FAULTING

Apart from one or two slip zones along which there may have been considerable movement, there are no faults with a displacement greater



Fig. 2 - 13 (a). Folded recumbent fold. White marks on the rock belong to a single bed. One-foot rule in centre of photo.



Fig. 2 - 13 (b). Folded isoclinal fold immediately above Fig. 2 - 13 (a). The isoclinal fold was originally recumbent and has been rotated to vertical. Width of photo is approximately 5 metres.

than a few metres. However, there are many minor fault surfaces, often with observable displacement direction. These fractures are in contrast to the general behaviour of the rocks during the folding deformation which was characterized by lack of fracture. Calcite commonly lines the fault surfaces some of which are slickenslided. The faults are later than any fold structure in the cliff face. Fig. 2-6(c) shows 71 poles of fault planes, and the distribution of the various types of fault movement. The pattern is consistent with having been caused by the regional folding on a northwest-southeast axis. The vertical faults are thought to be dextral and sinistral shear faults, and the thrusts (which are reversed to the direction of movement during the soft-sediment sliding) are possibly concentric shears developed in the mass of contorted bedding which during later folding had lost the facility for easy movement parallel to the original bedding surfaces.

4.

ORIGIN OF THE FOLDING

There are six characteristics which seem important in a consideration of the state of consolidation and the causal forces of the folding.

(a) THE LACK OF CLEAVAGE

Most folds which have formed under some load with an appreciable stress difference have developed a cleavage of one type or another.

Folding as intense as that at Paga Point generally has a strongly developed cleavage associated, even in the lowest greenschist facies, and some folds in superficial deposits such as the South Mountain fold of Cloos (1947) have developed a strong axial-surface cleavage. The only known examples of intense folding in low-grade rocks with no associated cleavage have been ascribed to soft-sediment folding. On the basis of this reasoning, the lack of any cleavage may be regarded as indicating little or no load on the sediment at the time of deformation.

(b) THE LACK OF ANY METAMORPHISM

Although this may seem a trivial criterion it is important in that the depth of burial was never great and the complicated sequence of overfolding can not be attributed to a plastic zone at depth.

(c) THE SEQUENCE OF OVERFOLDING

If the techniques of structural geometry had been applied to this section at least four distinct "phases" of coaxial folding would have been determined. It was not necessary to use such techniques as overfolding relationships are plainly visible in the cliff face.

The sequence of folding follows a distinctive pattern:--

- (1) Flap folds - involving one bed.
- (2) Recumbent folds - involving several beds.
- (3) Slip sheets - involving up to 10 metres of sediment.
- (4) Broad synclines and anticlines involving some tens of metres.

Each successive folding involves a greater thickness of sediment. Even some of these phases can be subdivided, for there are excellent examples of refolding of recumbent folds by other recumbent folds. Similar sequences of multiple deformation in superficial sediments have all been ascribed to soft-sediment folding.

(d) GEOMETRY OF THE FOLDING

The style of all phases of folding is essentially concentric with some minor flattening in the axial surface in the hinge regions of the later-developed folds. This concentric geometry indicates that there was a large viscosity difference between the competent and incompetent rocks, but yet the overall viscosity of the rocks must have been low to have permitted the intense contortion in the cherts without fracture. Such conditions would only prevail very soon after deposition when compaction and diagenesis had not seriously reduced the high water content of the pelite.

(e) ORIENTATION OF AXIAL SURFACES

Except for the last phase of folding (the development of broad synclines and tight anticlines) the axial surfaces are always parallel to the bedding which when unfolded is essentially horizontal. This indicates that the maximum shortening (assumed to be normal to the axial surface) was vertical, and the folding was caused by sliding under gravity.

5.

CONCLUSIONS

- (a) The folding at Port Moresby is believed to have been initiated during sedimentation of the cherts with the formation of flap folds.
- (b) Folding continued involving successively thicker units of bedding with the formation of recumbent folds, some of which were slightly later than others and refolded the early ones.
- (c) After the recumbent folding whole sheets of sediments acting as coherent units slid under gravity.
- (d) Eventually the whole slump series involving several sheets moved laterally towards the west-southwest into the Eocene trough.
- (e) The folding is probably an example of syntaphral tectonics.

CHAPTER 3

TECTONIC DIAGENETIC FOLDS AT SULPHUR CREEK, NORTHERN COAST OF TASMANIA

1.

INTRODUCTION

The Sulphur Creek area was originally selected for study because of the excellent exposures of individual folds on the mesoscopic scale. The method of study was to select a small area in which there is one or more well-developed folds and to plane-table the immediate vicinity so that the fold can be placed in its spatial environment. The plane-table maps were constructed mainly on a scale of 1:80, a scale which enabled most minor details to be adequately represented. Five main areas were mapped in this manner and have been termed areas A to E for ease of reference.

Although originally the main purpose of the study was to describe and document the fold style of the Sulphur Creek folds which have been collectively classified as P1 (Phase 1) by Gee (*pers. comm.*, 1966), it was soon found that the detailed mapping provided excellent data on a variety of important problems including some of the basic concepts of deformation. For this reason the scope of the study has been extended

from its initial intention to include problems concerning development of cleavage, progressive deformation, the definition and recognition of "phases" in deformation as well as the mechanical characteristics of the particular style of folding.

To discuss these questions adequately it is necessary to separate clearly fact from opinion, since the very nature of the problems involves much interpretation. It has been considered convenient to limit verbal description to a minimum because if any debate arises, such description is usually the first data to be questioned. Therefore I have presented as much data as possible in the form of diagrams, and in the descriptive passages have limited any logical operations on the data to those deductions which can be made easily, and which have no immediate bearing on the discussions to follow. In the interpretation of the results it may be unavoidable to refer frequently to some diagrams, and occasionally to some data which may have been already described.

The fact that my experience in the area is limited to one month's field work, wholly on the shore platform, has caused me to rely considerably on the work of Gee (*op. cit.*) for the local and regional settings. I have checked the section in the field with Mr. Gee and we have no disagreements on what is present. The main difference between Gee's work and mine is the scale on which mapping was carried out. If there is any difference in our interpretation this should be judged on its merits, remembering that the final solution to any particular problem should account for all the evidence.

2. STRUCTURAL DESCRIPTIONS

(a) GENERAL DESCRIPTION

The rocks which outcrop along the shore platform at Sulphur Creek belong to the comparatively unmetamorphosed Burnie Quartzite and Slate which are tentatively thought to belong to the younger Precambrian (Spry, 1962). K. L. Burns (1964) measured the structure in the region immediately east of Sulphur Creek, and the Sulphur Creek region is the eastward extent of the area R. D. Gee has examined for a doctoral thesis.

The rocks have been described in detail by Gee (unpub. Ph.D. thesis, 1967), and it is sufficient for the purposes of this thesis to describe the rocks as an alternation of sandstones and slates. The cleavage in the slate varies in intensity and in some specimens where it is absent, the rocks appear to be almost unmetamorphosed shales. The sandstones are variable in composition from some ill-sorted greywackes to fairly clean quartzites. Spilitic pillow lavas occur in parts of the section, and there is some dolerite which in parts shows concordant, and in other parts discordant relations with the surrounding sediments. The rock type changes westward from Sulphur Creek as the proportion of pelitic material decreases and more massive sandstone beds occur, often up to ten feet thick. There is a variety of primary sedimentary structures including cross-bedding, graded bedding, load casts, flames, flute marks, intraformational slumping etc., all of which are described in detail by Gee (*op. cit.*).

LOCATION MAP

Sulphur Creek Area
(Geology by R.D. Gee, unpublished Ph.D. thesis 1967)

LEGEND

- Conspicuous Sandstones
- Concordant Dolomite
- Pillow layers
- Interbedded mudstones and slates with thin sandstone layers
- Clump of trees
- Bedding trace
- Cleavage trace
- Fault
- Traces of main fold axial surfaces shown

SCALE IN METRES
0 20 50 100 200 300

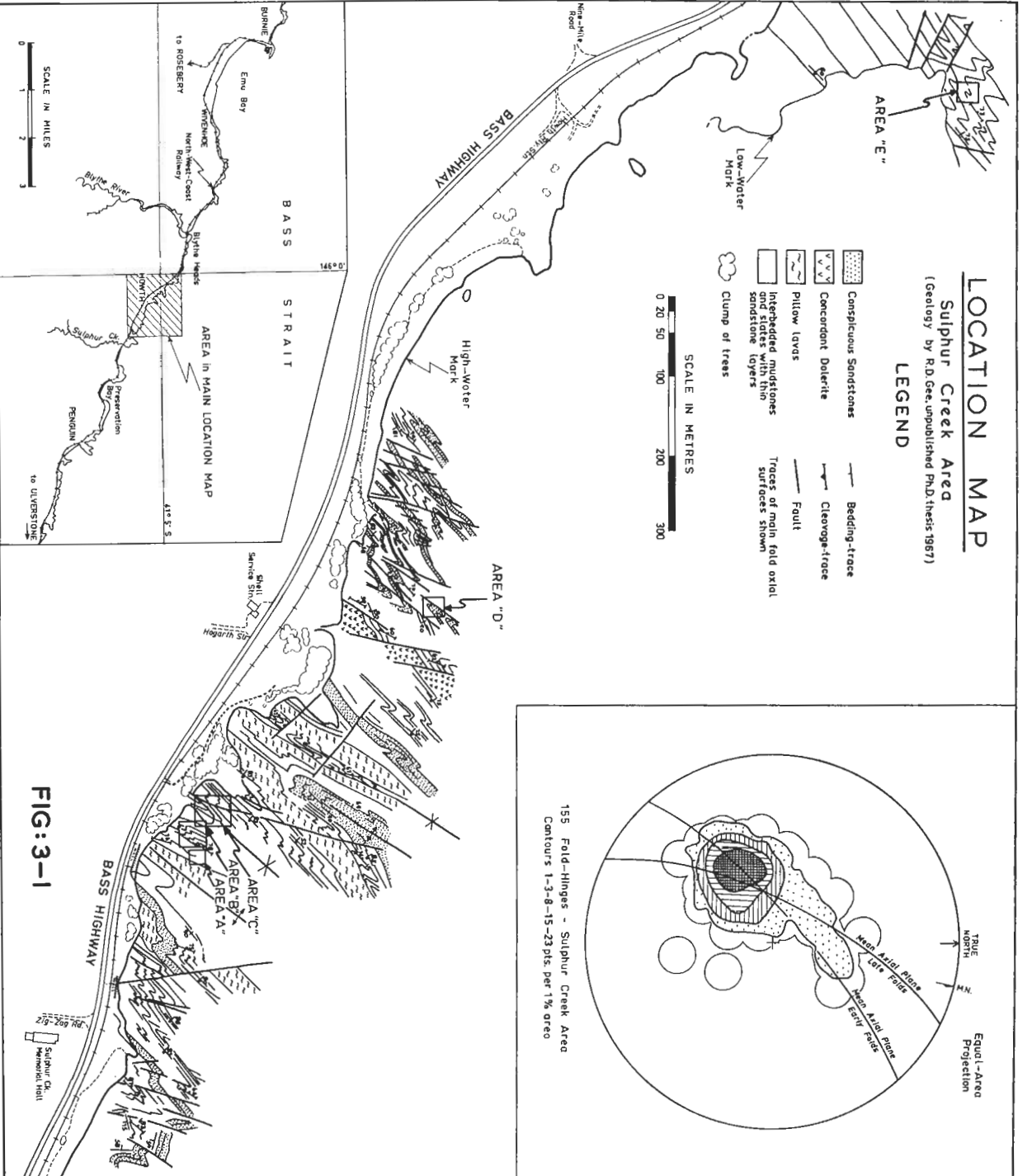


FIG:3-1

Fig. 3-1 shows the location of the various areas A to E, and is copied directly from the maps of Gee. There are only a few salient features which should be treated here, as the detailed analysis of this, and other similar maps, is the basis of Gee's dissertation.

Firstly, all the folds present are part of a group of folds which Gee has named the P1 phase. In this region the P1 phase, which is the earliest recognizable fold form after the intraformational disturbances, is characterized by isoclinal coupled folds with a dextral vergence. The sandstone layers in general tend to be folded in a concentric fashion, although they have been flattened in parts, while the pelite has acted in an extremely incompetent manner undergoing extreme flowage and dislocation.

Secondly, the sandstone layers are discontinuous. There are a number of contributory causes:-

- (a) The sandstone beds are lenses.
- (b) There has been strong faulting with a general sinistral displacement.
- (c) There has been extension in the general axial-surface direction which causes the fold limbs to be sheared out or stretched into boudins. The folded sandstone lenses exist in the form of tectonic "fish" in a slaty matrix.

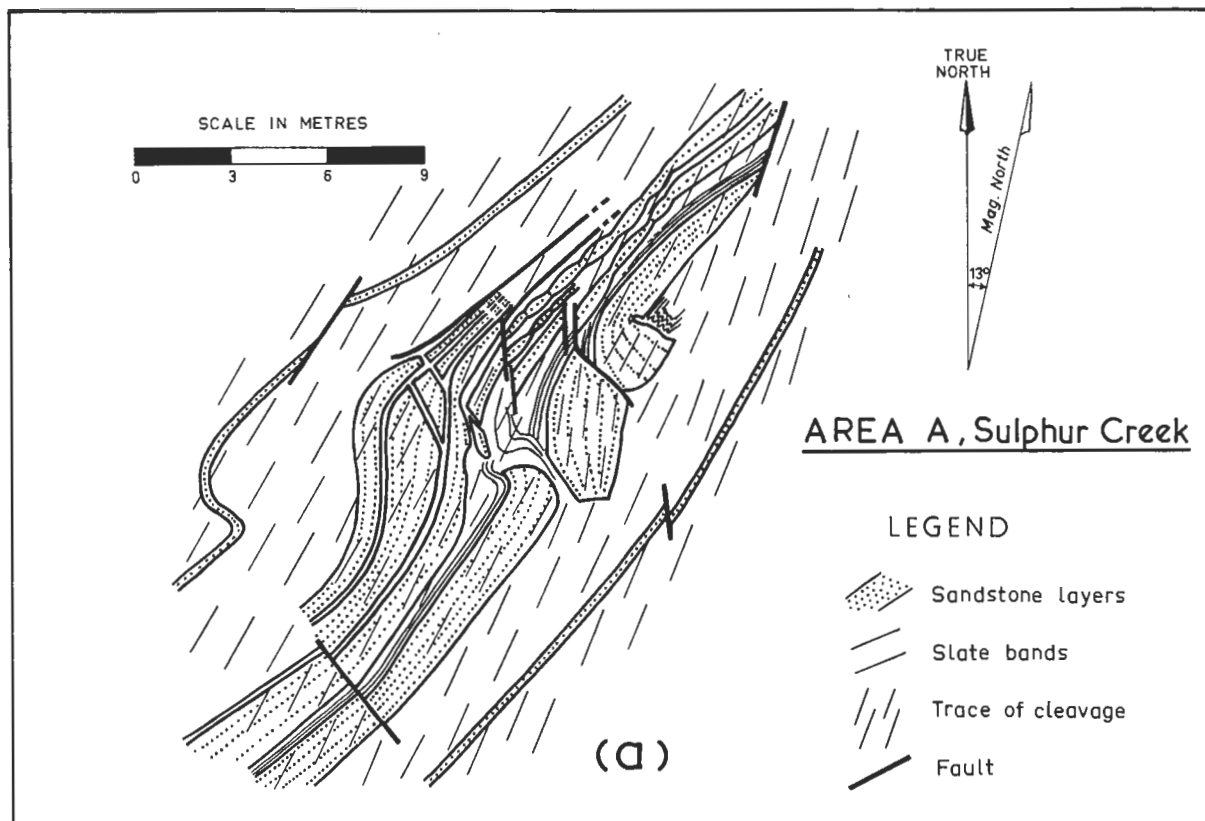
Thirdly, between Sulphur Creek and Burnie, folding appears to be confined to certain zones, a hundred metres or so in width, which are separated by several hundred metres of relatively undeformed straight-bedded strata. In the deformed zones the folds have a

constant dextral vergence which is typical of drag folding. At Sulphur Creek, however, the whole section appears to have been folded. While the overall pattern of folds is reasonably regular to follow, in detail there is great disruption and confusion. Certainly stress differences can not have been transmitted far laterally along the sandstone layers during folding, and it is probable that the deforming force was either viscous drag caused by movement between the bounding zones, or a body force of the moving rock itself.

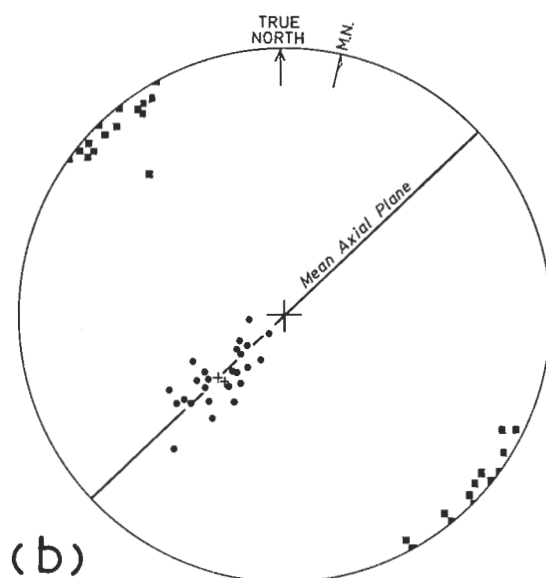
(b) DISJUNCTIVE FOLD IN AREA A

Fig. 3-2(a) is a plane-table sketch of a fold couple on the eastern limb of a syncline at Sulphur Creek. The dotted layers are sandstone blocks with the lines of dots parallel to the original bedding surfaces. The unshaded regions are predominantly slate although there are some pillow lavas to the southeast. The axis of folding plunges $80^{\circ}/293^{\circ}$ with an approximately vertical axial surface, so that this sketch, made on the horizontal shore platform, is an almost perfect axial profile.

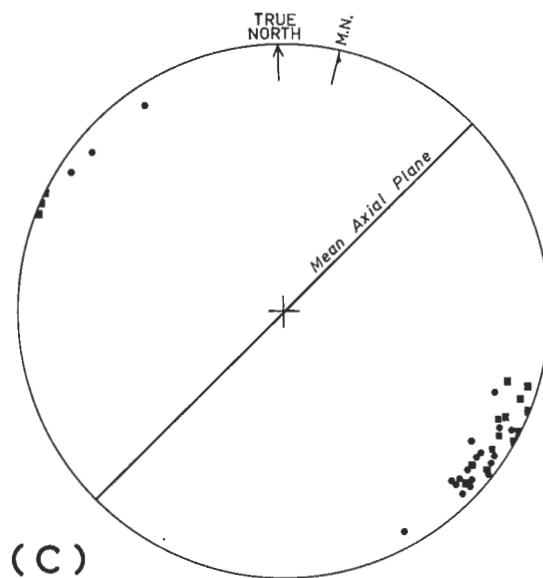
The most striking feature is the disruption of the sandstone layers into blocks, usually lens-shaped, which are generally bounded by blunt ends. These blocks maintain an overall pattern suggesting a fold couple with a sinistral vergence. However, in detail the structure is quite complex with the sandstone blocks surrounded by pelite that has penetrated along the fractures separating individual blocks of a once-continuous layer. Many of the lenses are hard to trace along their



STRUCTURAL ELEMENTS, AREA B



- Early Fold-Hinges 25 pts.
- + Late Fold-Hinges 2 pts.
- Pole of Axial Planes 24 pts.



- Pole of Cleavage in slate 20 pts.
- Pole of Cleavage in sandstone 13 pts.

FIG: 3-2

strike as they have been severely boudined, and sometimes pinched right out. This style of folding is disjunctive, and although the whole fold couple has not lost its cohesion, there can have been no stress differences transmitted along individual sandstone layers.

The structure of the slate cannot be satisfactorily represented on a diagram, and is extremely hard to determine in the field because the slate mass contains few sandy bands which can be followed. It is, however, intensely fractured and disrupted on the scale of decimetres. The fractures show no striations or polish, and may have formed when there was sufficient water to "heal" the pelitic mass and allow it to become essentially structurally homogeneous.

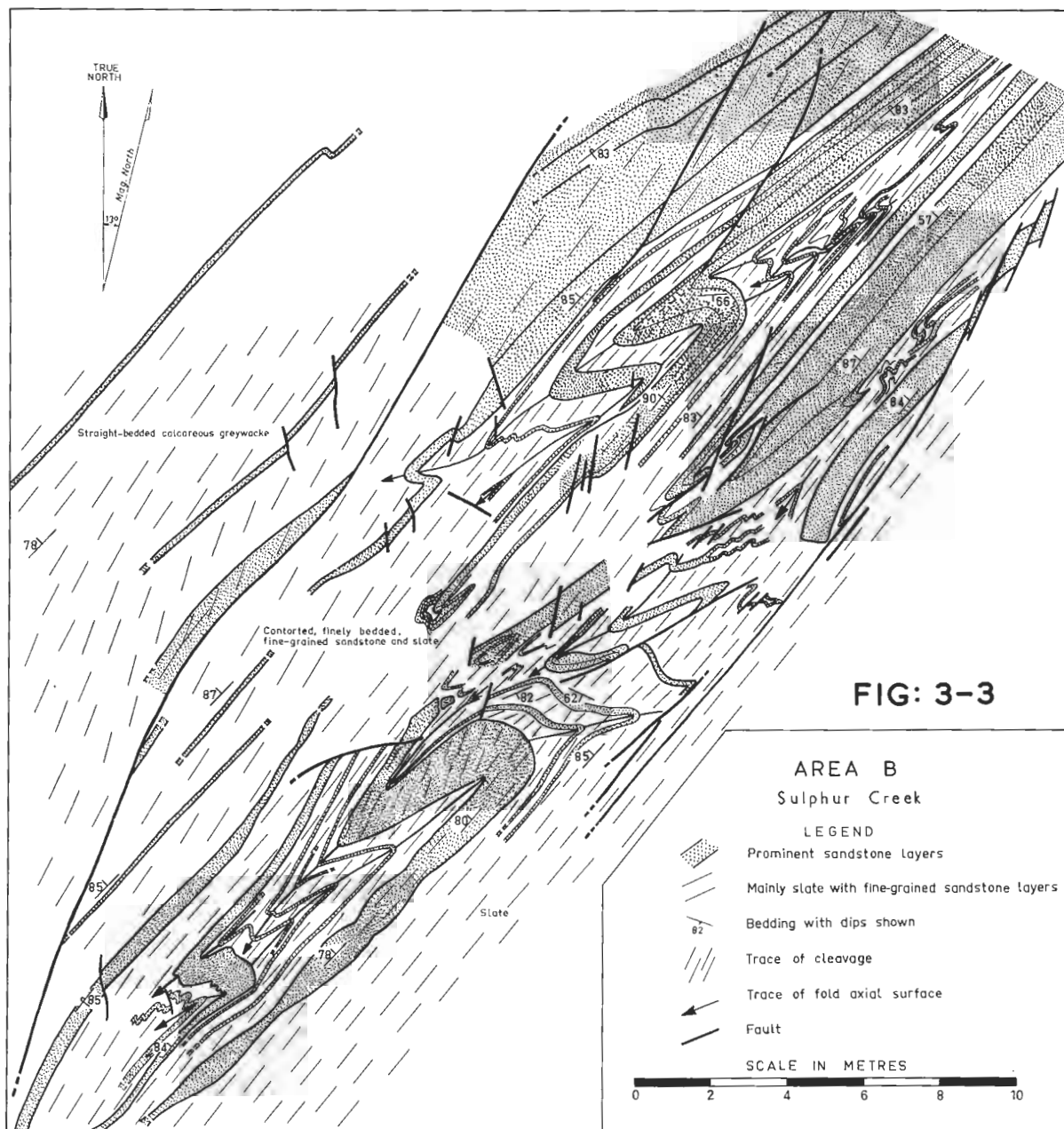
In the core regions of the folds there has been quite intense folding of the pelite which has moved into the fractures separating the sandstone blocks. The traces of the cleavage are shown by the light dashes and are distinctly not parallel to the axial surface of the fold. The cleavage is most prominently developed in the slate where it is a good penetrative cleavage, but is also moderately well developed in the sandstone blocks. It cuts straight across the whole fold couple and shows no regard for local perturbations of the bedding. In particular, in many places the cleavage cuts across a small parasitic fold in the pelite forming a transected core (i.e. one cleavage surface will cut both limbs of a small fold). The only block in which the cleavage seems disoriented is the block in the middle of the sketch of the fold core. This block has been rotated from its original position with respect to

the layer from which it formed, and the rotation of the cleavage indicates that this particular rotation occurred after the cleavage in the sandstone formed.

(c) AREA B

(i) General Description Area B is located on the southeastern flank of one of the larger synclines in the Sulphur Creek area. The plane-table map is presented as Fig. 3-3, and the most notable feature of the folding is the departure from the normal dextral vergence. Almost all the folds, except a few minor, late flexures, have a sinistral sense of coupling. This sinistral coupling is not anomalous if the folds are considered as parasitic folds on a larger syncline the axis of which is just to the west of Area B.

The sandstone layers are noticeably lensoid in shape and this is well shown by the thick band in the southern part of the sketch. The northern part of the area shows relatively undisturbed, thick sandstone beds containing a more pelitic band. There has been considerable movement in the slate band forming several folds which increase in amplitude towards the southwest and culminate by folding the confining sandstones. The folds have a detachment surface (*décollement*) adjacent to the straight-bedded sandstone layers on the southeastern margin of the slate zone. Between the northern and southern parts there is a zone of almost undecipherable contortion. The layers are fragmentary, boudined, rolled-up and dislocated by faults. No one layer can be traced through the whole zone.



The folded zone in Area B consists of sandstone lenses in slate, and both rock types are present in approximately equal proportions. As a whole the folded zone has the form of a lens bounded by faults. On the southeastern side all the sandstone layers are terminated against a thick band of slate, and the contact is parallel to the cleavage. The structure of the slate could not be mapped as there are no traceable markers. However, where some banding is present it can be seen that the slate band is very intensely dislocated by a set of anastomosing fractures usually decimetres apart. These fractures which now have welded contacts, dissect the slate band into a set of lensoid fragments elongate in the general cleavage plane.

On the northwestern side there is another contact which is sub-parallel to the cleavage. This contact is concordant with the cleavage in some parts but discordant in others, and it separates the folded sandstone band from relatively unfolded, calcareous greywacke and slate to the west. The bedding in this greywacke and slate band is uniform and planar, and although the individual rock types are massive, there are no distinct bedding surfaces which have acted as mechanical discontinuities. The bedding is not parallel to the faulted contact with the folded sandstone band, and in one place there is a small basin in the outcrop plan of the contact. This basin effect indicates that there was probably some vertical component of movement along the fault.

The overall style of folding is not regular enough to enable a general term to be applied to it. There are some bands which have been folded on a strictly concentric principle; others which have undergone

irregular thickening and thinning, and yet others which are completely "balled-up" resembling structures that have been described from regions deformed when the sediments were unconsolidated. In the more regular folds the sandstone beds form flattened concentric folds (Ramsay's Class 1C), and the common limb of adjacent coupled folds (which is usually at a high angle to the cleavage) is markedly thickened.

The cleavage is penetrative in the slate and is moderately well developed. It extends through the sandstones in parts, and is planar throughout the whole deformed band except adjacent to the hinge regions of folds in the sandstone lenses where some local deviations occur. The cleavage is distinctly not parallel to the axial plane from which it diverges by striking more northerly. Good examples of transected cores can be found in the middle and northern part of the field-sketch. In places the cleavage transects some of the early, balled-up folds and it shows no congruous relationship to the curved axial surfaces. In the greywacke to the northwest of the folded sandstone band, there are some shale fragments which are elongated in the plane of the cleavage.

The extensive fracturing falls into two categories. One set of faults is oriented parallel to the cleavage and has a constant sinistral sense of displacement. The largest displacements occur along these faults. The other set is a conjugate set of faults with a small dihedral angle bisected by the cleavage plane. The effect of these faults is to extend the rock mass parallel to the cleavage. Boudinage

in sandstone lenses is common, and often the lenses are thinned out completely, as in the southern part of the area.

(ii) Distribution of Fold Elements Fig. 3-2(b) shows the orientation of the fold-hinges and axial planes from Area B. Twenty-seven fold-hinges were measured, and the folds have all formed earlier than the cleavage, except for 2 folds which have a dextral vergence and which are associated with the refolding of the thin sandstone layers at the nose of the fold in the middle of the field-sketch. These two folds are marked by crosses. The distribution shows that the average fold-axis for the area is $62^{\circ}/228^{\circ}$, and thus the plane-table map is an oblique profile-projection at 62° to the fold-axis. Although accurate measurements can not be made on such a profile, the obliquity is not sufficient to cause any serious errors in qualitative interpretation. Moreover, the orientation of fold-hinges is quite consistent throughout the area, and shows that despite the contorted nature of the profile, most of the deformation can be considered to have occurred about a constant kinematic axis. The axial planes have an average orientation $90^{\circ}/\text{str. } 47^{\circ}$ and the bedding in the straight-bedded zones averages $85^{\circ}/308^{\circ}$.

Fig. 3-2(c) shows the cleavage in the slate as circular dots and that in the sandstone as squares. The orientation of the cleavage in the slate averages $80^{\circ}/311^{\circ}$, whereas the cleavage in the sandstone has an average orientation, $83^{\circ}/301^{\circ}$. This 10° -divergence between the cleavage in the sandstone and in the slate is interpreted as caused by

the rotation of the common limbs of coupled folds after the formation of an all-pervading planar cleavage, since most of the cleavage in the sandstones was measured on this common limb.

(d) AREA C

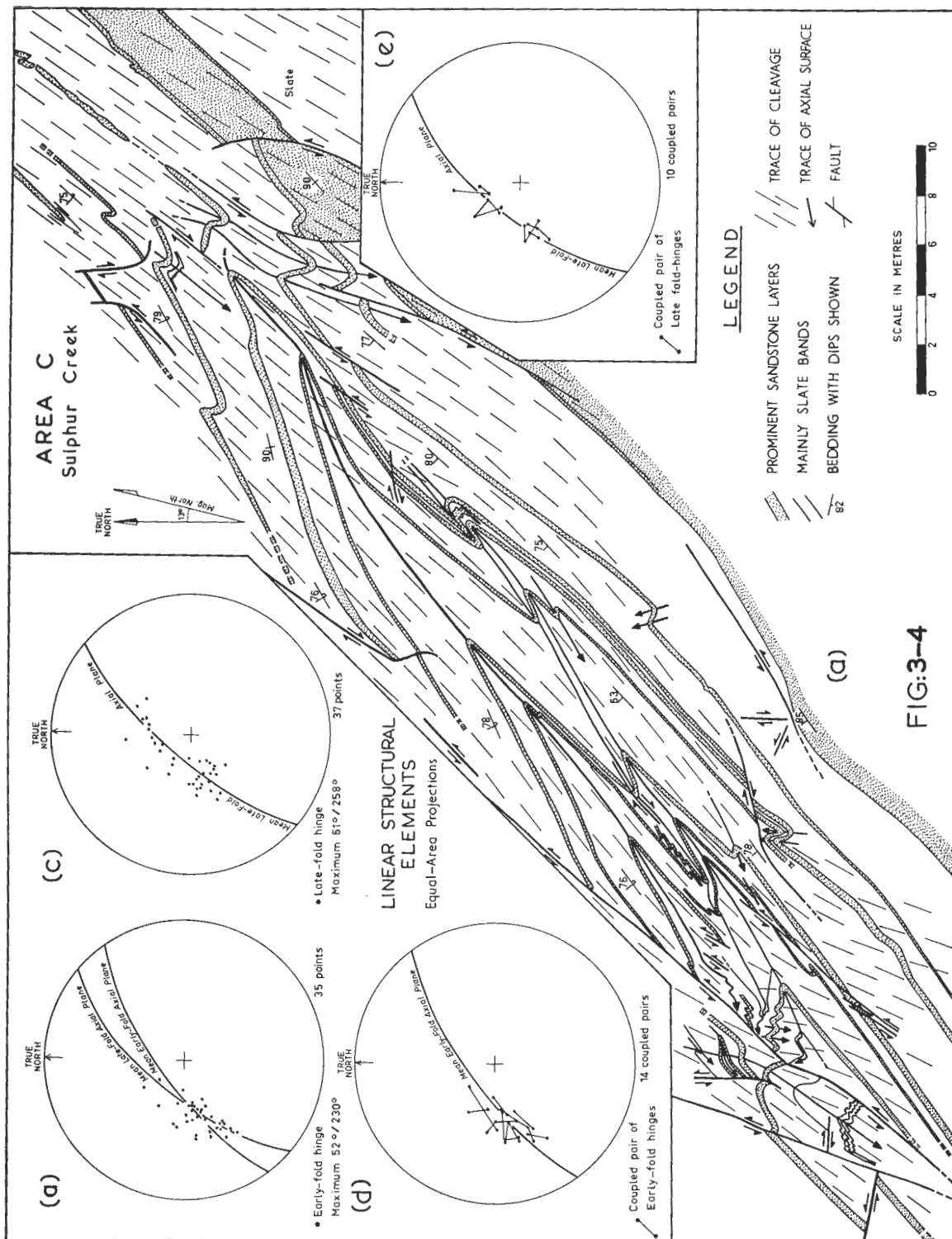
(1) General Description Area C covers the core region of one of the larger synclines in the Sulphur Creek section. It is shown in Fig. 3-4(a), which is a horizontal plan and represents a cross-section 60° to 70° oblique to the average fold-axis. The ratio of sandstone to slate is very low, and the pelitic matrix can be considered the dominant rock type. Indeed, on the northwestern and southeastern flanks of the fold immediately adjacent to the plane-table area there are thick bands of slate with no markers at all. The core may thus be considered to be "floating" in a mass of slate. There are several important features to be noted.

(1) The isoclinal nature of the main fold.

This syncline is probably one of the tightest folds in the P1 group. The dihedral angle is very small, less than 10° , so that the limbs on either side of the hinge are essentially parallel. In fact, the only way that a major fold-axis can be easily recognized in parts of the shore platform is by the reversal of the direction of sedimentary younging.

(2) The refolding in parts of the fold.

The refolding can be seen in this sketch in the southwestern part and



in the northeast around the nose of the main syncline. Later folds with a constant dextral vergence have folded both the limbs and the apical regions of the main syncline. In places the axial surfaces of the early folds have been rotated to a position almost perpendicular to the general trend of the fold axial surfaces.

(3) The discordant cleavage.

Throughout most of the Sulphur Creek region the cleavage approximates to an axial-surface cleavage, although it lies distinctly closer to the common limb of a pair of dextrally coupled folds than to the outer limbs. It is only in places of refolding such as Area C that the cleavage can be seen distinctly cutting from one limb across to the other, thereby producing a transected core. The cleavage itself may be bent slightly indicating that some movement continued after cleavage formation. As a general rule the cleavage approximates more closely to a plane than do the axial surfaces of the early folds.

(4) There are numerous faults parallel to the cleavage, and these have a predominantly sinistral displacement.

These faults have formed late in the movement sequence, and are reverse to the sense of displacement indicated by the general, dextral fold couple. They may indicate an overall extension slightly oblique to the plane of the cleavage, or even be related to a later phase of deformation.

(5) There has been an overall extension of the region.

There are many sets of faults all of which extend the rock mass in a direction approximately parallel to the cleavage. Boudinage, such as in the northeastern part of Area C, is common, and the long axes of boudins

appear to be parallel to the fold-axes. It was not possible to determine whether there was also extension in the direction of the fold-axes.

(6) The sandstone lenses exist as sheared-off blocks surrounded by slate.

In Area C the strip along the axial surface of a large syncline has been mapped, and the beds around the hinge are terminated before they pass out of the diagram. This is because they could not be traced further, and they disappear into a mass of dislocated pelite through which there are no traceable markers. It seems that there are zones of intense shearing bounding the core region and giving it the form of a tectonic lens. Reference to the location map shows that this dissection into slices is typical of the whole Sulphur Creek region.

(ii) Distribution of Linear Fold Elements Seventy-three fold-hinges were measured in Area C. The outcrop is excellent and the sandstone beds are easily excavated to permit direct measurement with a clino-rule, of pitch of the hinge on the axial plane. The style of folding varies considerably from the overall shape of the main syncline, which is an isoclinal similar fold in profile, to the individual parasitic folds which tend to be concentric. Nevertheless, two classes of folds can be recognized. Folds on which the cleavage has been superposed are termed early P1 folds, and folds which have cleavage parallel to the axial surface, or which fold the cleavage, are grouped as late P1 folds. In general, the early folds are isoclinal and similar in

broad profile although sandstone layers maintain their orthogonal thickness. The later folds seem to be associated with, or slightly later than the development of cleavage in the pelite. They are more open than the early folds, and although the overall profile is more or less similar, the sandstone layers tend to maintain their orthogonal thickness.

Fig. 3-4(b) shows the distribution of the early fold-hinges. The equal-density contours of orientation are slightly elongate along the mean early-fold axial plane, $75^{\circ}/323^{\circ}$. The main concentration of late folds [Fig. 3-4(c)] is slightly steeper in the mean late-fold axial plane, $70^{\circ}/307^{\circ}$, than are the early folds, and shows quite a prominent asymmetrical distribution along the axial plane. Considering that some of the folding has occurred before the cleavage formed, and some after, it is remarkable that the early fold-hinges show less scatter than the hinges of the later folds. The explanation is thought to lie in the concept of heterogeneous "stiffening" of the slate during cleavage formation. It is important to remember that all these folds are measured in sandy layers which are usually surrounded by a considerably larger volume of slate. The hinges of the early folds show a much more regular distribution than those of the late folds, and are thought to have developed in an essentially homogeneous stress system. After cleavage formation, which seems to have occurred as a definite episode, the folding movement still continued along more or less the same kinematic axes, but the slate seems to have become much "stiffer"

or more viscous than before, and movement seems to have been concentrated along certain zones between more rigid blocks.

Heterogeneous folding caused by drag between these blocks is believed to have caused the asymmetrical tail to the late fold-hinge distribution. Certainly superposed similar folding could not have caused this smearing out of hinges because the late folds are more concentric than the early folds. Furthermore, there can have been little rotation between the blocks as this would have disoriented the early fold-hinges.

To consider the possible effects of rotation during folding within a single bed pairs of adjacent fold-hinges have been plotted on stereograms in Fig. 3-4(d) and (e). Tie-lines connect coupled pairs. The maximum divergence of any coupled pair is 30° , and this is in an early-fold couple. The average of all coupled pairs measured is 13° , although this value has little real significance. Nevertheless, it can be seen that the early-fold couples show a somewhat larger divergence than the later ones.

De Sitter (1939) noted that there was a relation between the amplitude of folds and the thickness of the layers involved. Currie *et al.* (1962) found that in areas of very open, concentric-style folding there appears to be a constant relationship between the wavelength of the fold and the thickness of the effective layers. It is not necessary at this juncture to consider whether or not concentric folds are elastically induced, but the empirical evidence of Currie *et al.* that there is some constant relationship between the thickness

of the layer and the amplitude of induced folds may be accepted for the purpose of logical extrapolation. It can readily be seen that a layer with a variable thickness (i.e. a lens) will have folds of variable wavelength induced in it.

Consider a wedge [Fig. 3-5(a)] which is rectangular in one section but lenses in a direction at right angles to this profile. Let the thickness, t , at one end of the wedge become λt at a distance, d , from the rectangular profile. Let the ratio of the wavelength of an induced concentric fold to the thickness of the layer be K . Then the wavelength will be Kt at one end of the lens and λKt at the other end.

Suppose that these folds become very tight or even isoclinal, but still maintain a constant arc length between their respective hinges. Such a model corresponds closely to the folds at Sulphur Creek where the overall style is almost isoclinal, and the sandstone layers maintain their orthogonal thickness.

Thus, in Fig. 3-5(b), $AB = Kt$ and $A'B' = \lambda Kt$.

As a first approximation, since the profile shapes at both ends of the lens are likely to be comparable, it may be assumed that the amplitudes of the folds are proportional to the distance between the adjacent hinges, and in very tight folds are approximately equal to this distance.

Therefore, $a \approx Kt$, and $a' \approx \lambda Kt$.

The problem may now be considered in an axial-plane projection where the trapezium, $ABB'A'$ [Fig. 3-5(c)], represents the geometry of

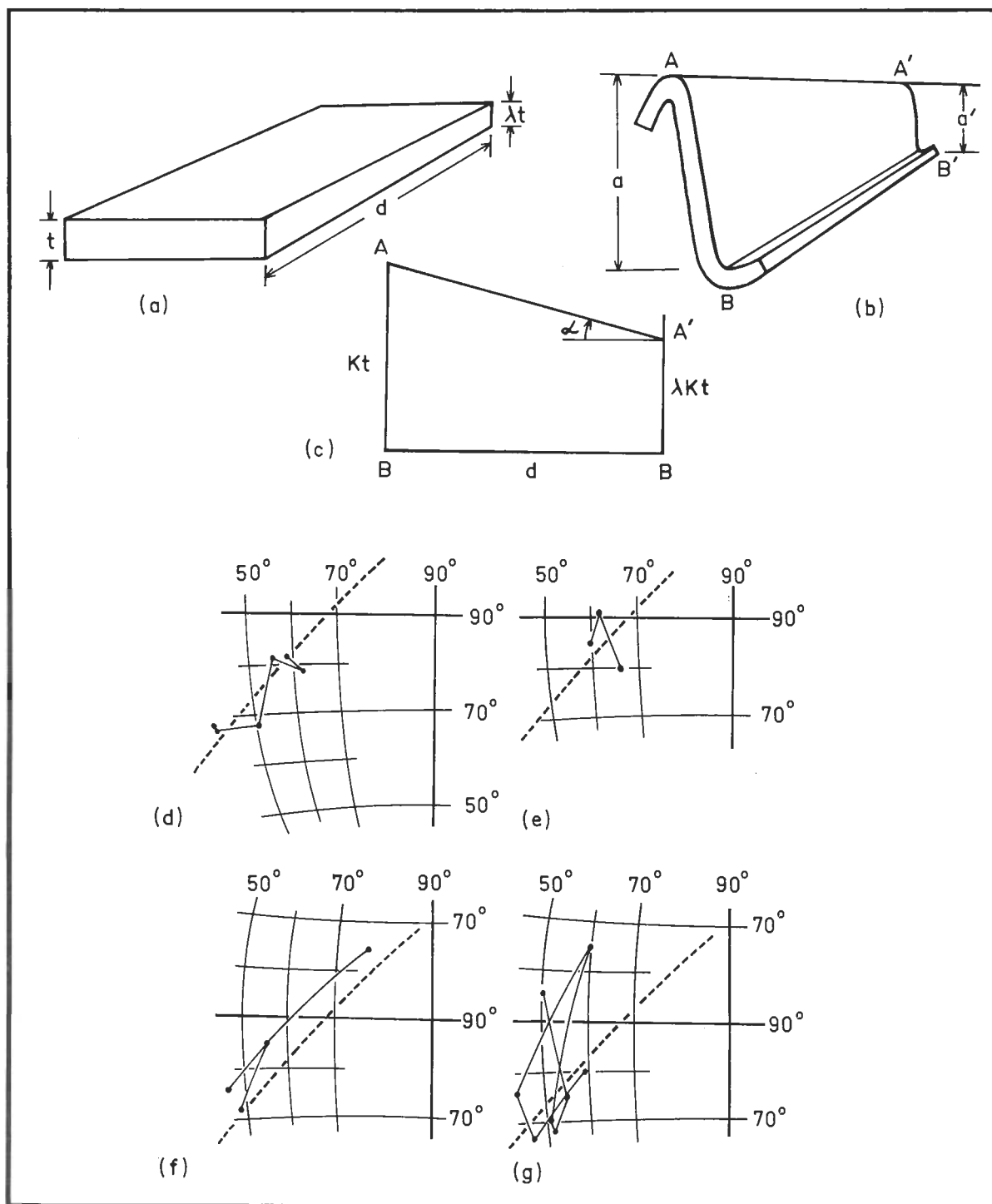


FIG: 3-5. (a) Lens with a rectangular end-section. (b) Folded lens with folds of different amplitude dependent on the lens thickness. (c) Axial-surface profile of divergent fold-hinges. (d) to (g) Distribution of fold-hinges from Area C measured for one fold form in different beds. Hinges in adjacent beds are connected by light lines, 20°-sectors of equal-area stereograms are shown. The heavy dotted line is the mean early-fold axial plane. (d) is a syncline; (e) a syncline; (f) the main syncline; (g) an anticline.

the divergent fold hinges. AB and A'B' are proportional to the amplitudes of the folds and d is the distance separating the two profiles. The angle, α , is the angle of divergence.

$$\text{Hence, } \alpha = \tan^{-1}(1-\lambda) Kt/d.$$

In the area considered (and indeed in most cases) the maximum slope between the upper and lower boundaries of a lens is likely to be less than 1:10.

Therefore, $(1-\lambda) t/d$ is less than or equal to 0.1,

$$\text{whence } \alpha \text{ is less than or equal to } \tan^{-1} (K/10).$$

K, as determined by Currie *et al.* is 27. Whether this value is valid is debatable, but it is probable at least that the order is right. This permits a maximum possible divergence of adjacent coupled fold-hinges of up to 60° , a value which seems unduly high. Probably the model in which adjacent fold-hinges at the thick end of the wedge become adjacent fold-hinges at the thin end of the wedge is not valid. Subsidiary folds develop in the thin end of the wedge between the main fold-hinges, taking up the strain and greatly reducing the divergence. It is apparent, however, that quite considerable divergence of adjacent coupled fold-hinges can be accounted for on the basis of primary lensing.

In Area C the maximum divergence between adjacent fold couples is 30° . It was not possible to determine whether there was lensing of the bed along the axis. There are, nevertheless, at least two other explanations which can account for this divergence.

Firstly, a fold couple which formed early in folding of the sandstone-mudstone sequence would be a heterogeneity in the surrounding pelite so that later movements might cause some rotation increasing any divergence already present.

Secondly, if the sandstone-mudstone sequence had a considerably higher water content during the early folding, the difference in viscosity between the sandstone and mudstone would have been much larger than it was during the later folding. The heterogeneity caused by divergent hinges in a fold couple would be far more easily accommodated during the early folding than in the late folding where the sandstone beds would be confined by stiffer surroundings.

The syntaphral folding at Port Moresby (Chapter 2) which has occurred under very low confining pressures with high water content shows very large divergences between coupled folds. It is not possible from available data to favour one or other of the hypotheses and it is quite possible that any or all of these three mechanisms may have been operative in any particular case.

Figs. 3-5(d) to (g) show the variation in the orientation of the hinges of individual fold forms along the trace of the axial surface in the profile-projection. The hinges from adjacent sandstone layers are connected by light tie-lines. 20°-sectors of an equal-area net are shown and the thick dotted line is the mean early-fold axial plane for Area C. Figs. 3-5(d) and (e) are synclines; Fig. 3-5(f) represents the main syncline and Fig. 3-5(g) is an anticline. It can

be seen that quite large variations, up to 40° , can be expected for one fold form as it passes into different layers. This indicates,

(a) that the folds are not ideally cylindrical, and

(b) that there must be quite a large amount of differential movement between the adjacent sandstone beds in the direction of the fold-axis.

Any one layer may have a curvilinear hinge, and the slate between this layer and the next has been able to take up the strain apparently without affecting the orientation of the fold-hinge in the adjacent layer. It was not possible to excavate along the fold-hinges so that these diagrams are prepared from a random profile-plane.

(iii) Distribution of Planar Fold Elements Figs. 3-6(a), (b) and (c) show the orientations of the early- and late-fold axial planes, and the cleavage in the slate. Fig. 3-4(d) is a composite diagram with the 8% contours of the early- and late-fold axial surfaces being shown as well as the 20% contour for the cleavage planes. The overall distribution of these planar elements is markedly elongate along a partial girdle perpendicular to the mean late-fold axis. Furthermore, the three different planar elements are arranged in a progression along this girdle the order of which correlates with the succession of events deduced from field relationships.

If it is assumed that the axial surfaces of the early and late folds, and the cleavage, represent a certain orientation in the

PLANAR ELEMENTS AREA C Equal-Area Projections

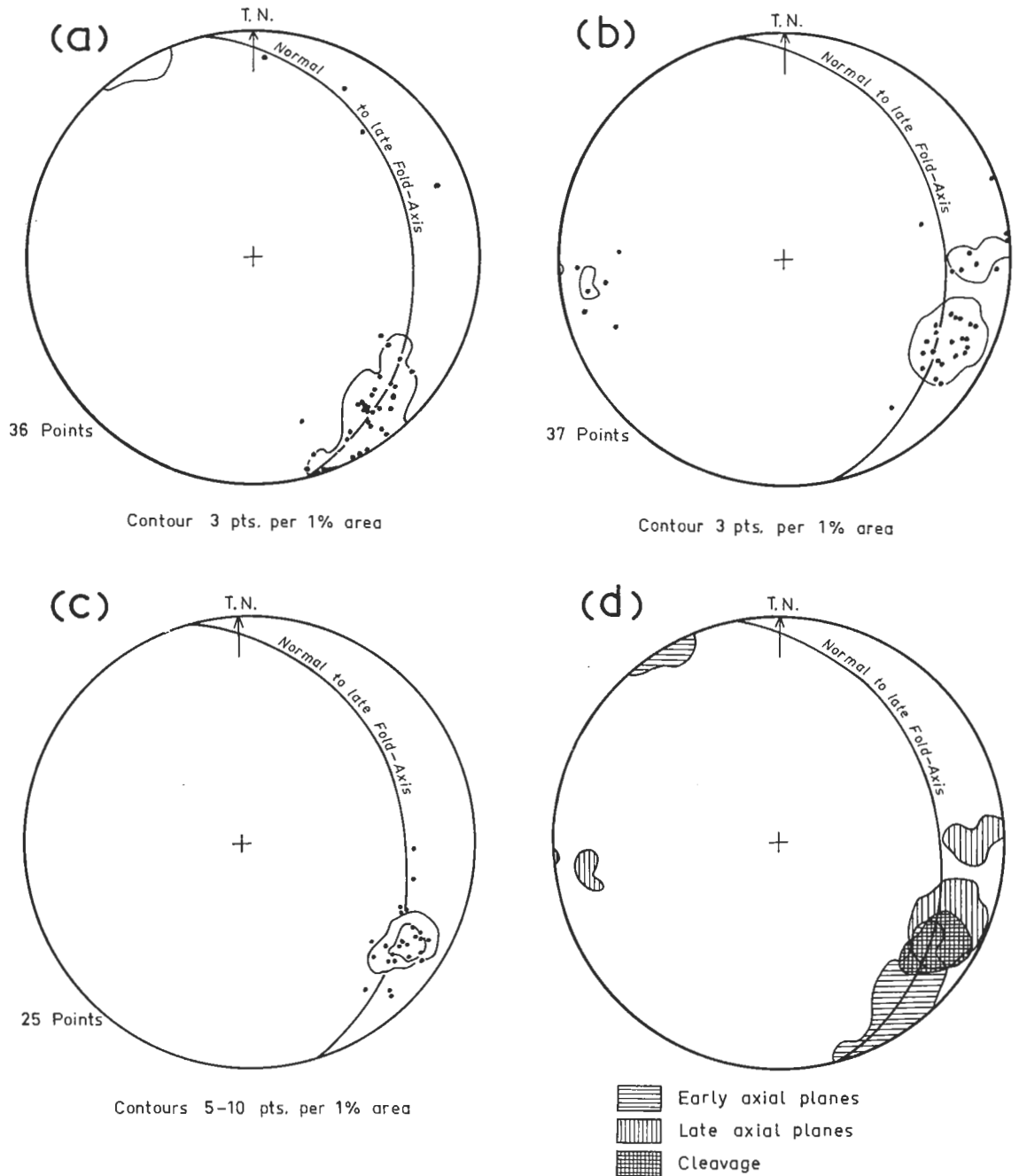


FIG: 3-6. (a) Poles of Early Fold Axial Planes
 (b) Poles of Late Fold Axial Planes
 (c) Poles of Cleavage (Mainly in Slate)
 (d) Composite Diagram showing 8% Contour from (a) and (b), and 20% contour from (c)

instantaneous stress field (viz. the plane of flattening perpendicular to the maximum stress), then it can be seen

(a) that the early fold elements have been rotated about the late fold-axes, and

(b) that the rotation has been in a clockwise or dextral sense, the early planar elements having been rotated furthest from the position of the late-fold axial surfaces.

Such a pattern of rotation could be caused by either a continuous variation of the stress field or continuous deformation about a constantly oriented couple.

On the basis of larger-scale mapping up to regional-map scale Gee (*pers. comm.*, 1966) has recognized that all these fold elements are part of one "phase" of folding, Pl. Although this small area shows many excellent examples of refolding and cross-cutting relations, the refolding does not continue on the larger scales. Profiles on scales greater than 1,000:1 show little, if any, evidence of the refolding that occurs on smaller scales. This suggests that the external stress system maintained a constant orientation throughout the duration of deformation, and that continuing strain on a constantly oriented couple has caused the axial surfaces to become disoriented. The sense of rotation, as deduced from both the field-sketches and the stereograms, is a clockwise or dextral movement.

(e) AREA D

(i) General Description Area D is dominated by a thick sandstone lens which is folded by a dextral couple (Fig. 3-7). There are some thinner sandstone beds immediately above and below this sandstone lens, and the whole band is bounded by thick blocks of slate on the northwestern and southeastern margins. In the northeastern part of the area the sandstone band has been faulted along the cleavage, and the sandstone blocks are completely surrounded by pelite.

The folding has the characteristic dextral vergence of the P1 phase, and there is refolding in the southwestern part where the sandstone layers have lensed-out to a few thin beds. Folds which have formed before, and others which have formed after the slaty cleavage can be distinguished, and at the hinge of the main anticline there is a thin sandstone bed which has been rolled off the nose and refolded. The style of folding in the sandstone layers is essentially concentric with a variable amount of flattening, but similar folds occur in the slate where slight textural variations can be used as markers.

The cleavage is quite intensely developed and penetrative in the slate, and also penetrative to the scale of centimetres in the sandstone. It is planar in the slate bands except in the southwestern portion where there has been folding after cleavage formation. The cleavage in the sandstone shows a small fan, since the cleavage in the common limb between coupled folds is essentially parallel to the cleavage in the slate, whereas the cleavage in the outer limbs has

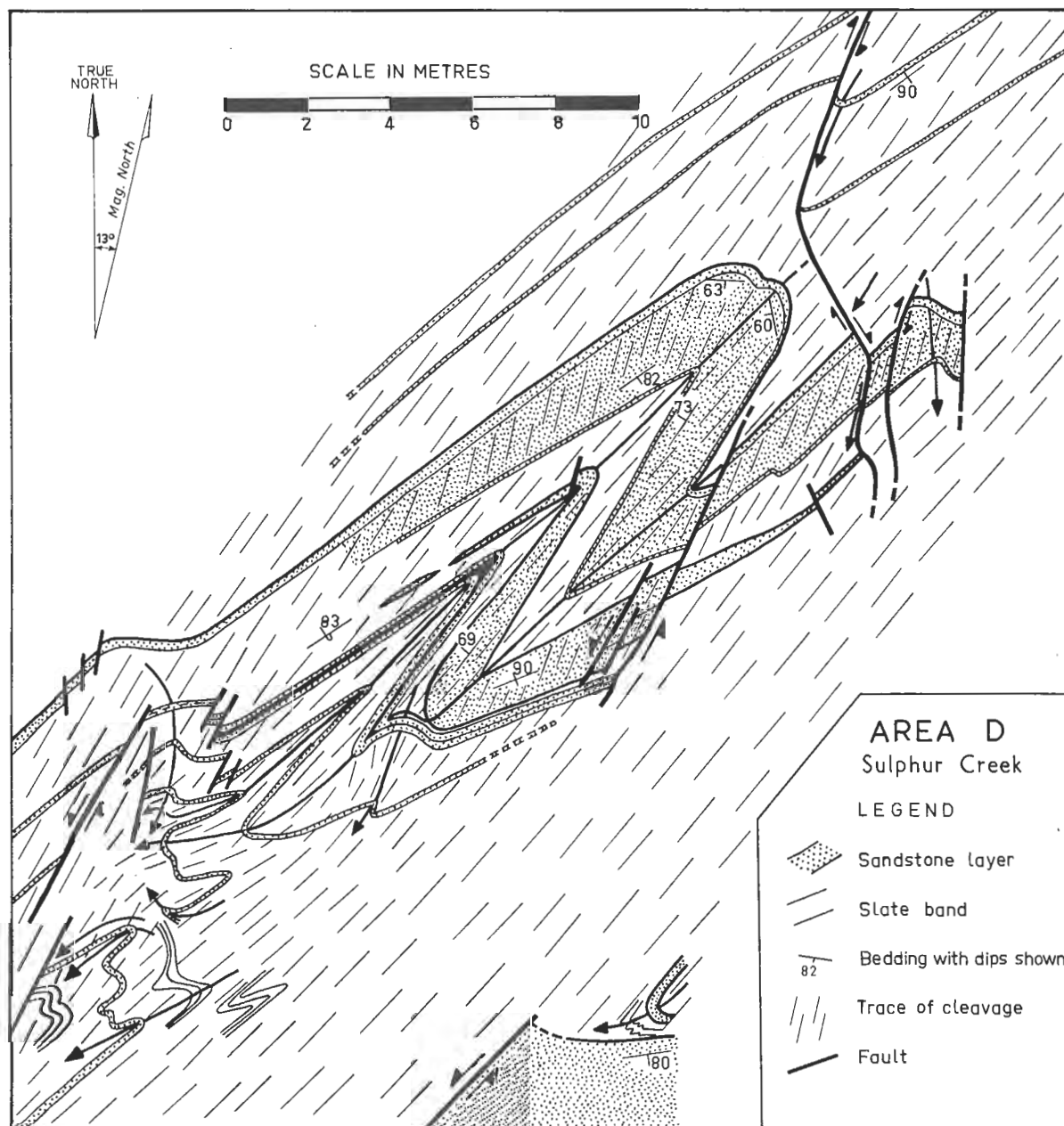


FIG: 3-7

a divergence of about 20° . The common limb itself appears to be thinned, and in the nose of the syncline where the bedding is at a high angle to the cleavage, there is oversteepened cross-bedding which suggests that there has been some flattening in the axial plane.

(ii) Distribution of Fold Elements Fig. 3-8(a) shows the distribution of fold-hinges which have been divided into early and late categories on field evidence depending on whether they formed before or after the cleavage. Twenty-five early fold-hinges and 7 late fold-hinges were recorded, and there does not appear to be any significant difference in orientation between the two groups. However, when the axial planes are plotted in Fig. 3-8(b) it can be seen that there is a divergence of 25° between the orientations of the average early-fold and late-fold axial planes.

Twenty-four cleavage planes, mostly from the slate, are recorded in Fig. 3-8(c) and the mean cleavage plane is $79^{\circ}/312^{\circ}$. Fig. 3-8(d) is a composite diagram showing the approximate 20% contours for the early- and late-fold axial planes, and the cleavage, and these lie along a great circle perpendicular to the average fold-axis, $53^{\circ}/237^{\circ}$. The order of progression along this great circle correlates with the succession of events deduced in the field and is interpreted, as in Area C, as indicating rotation caused by continuing strain about a constantly oriented dextral couple.



Fig. 5 - 5 (a). Highly contorted layer of bulbous-shaped, convolute folds in a silty-clay band between more regularly folded, bounding layers of brown clay. Six-inch rule shown.

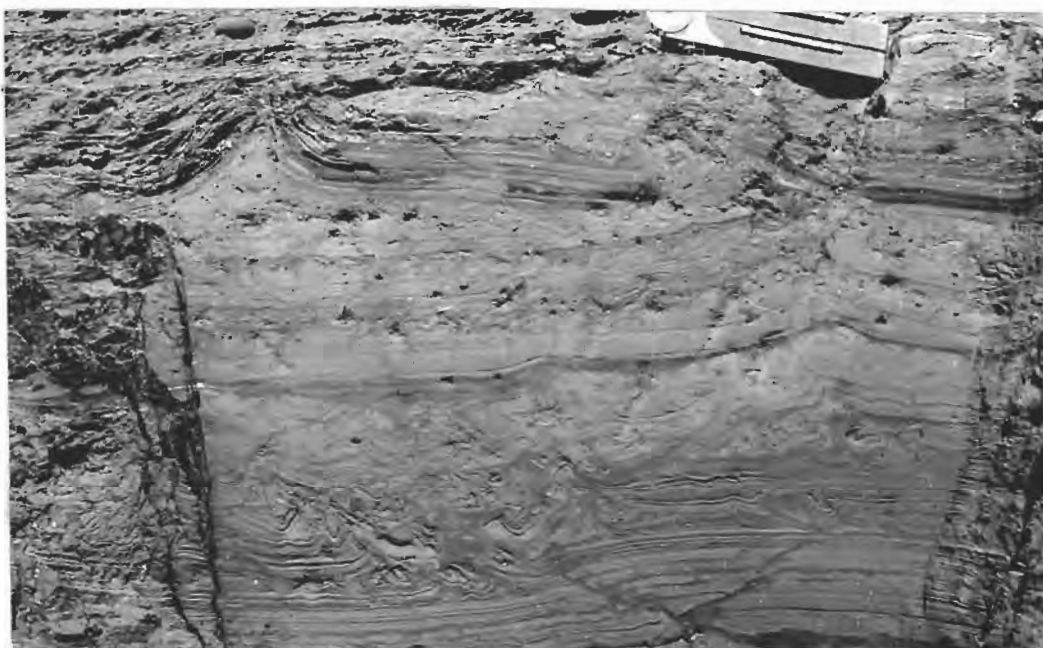


Fig. 5 - 5 (b). Convolute folds in a silty layer above a box fold in brown clay. The disturbed layers pass laterally into undeformed strata. Six-inch rule shown.

STRUCTURAL ELEMENTS, AREA D

Equal-Area Projections

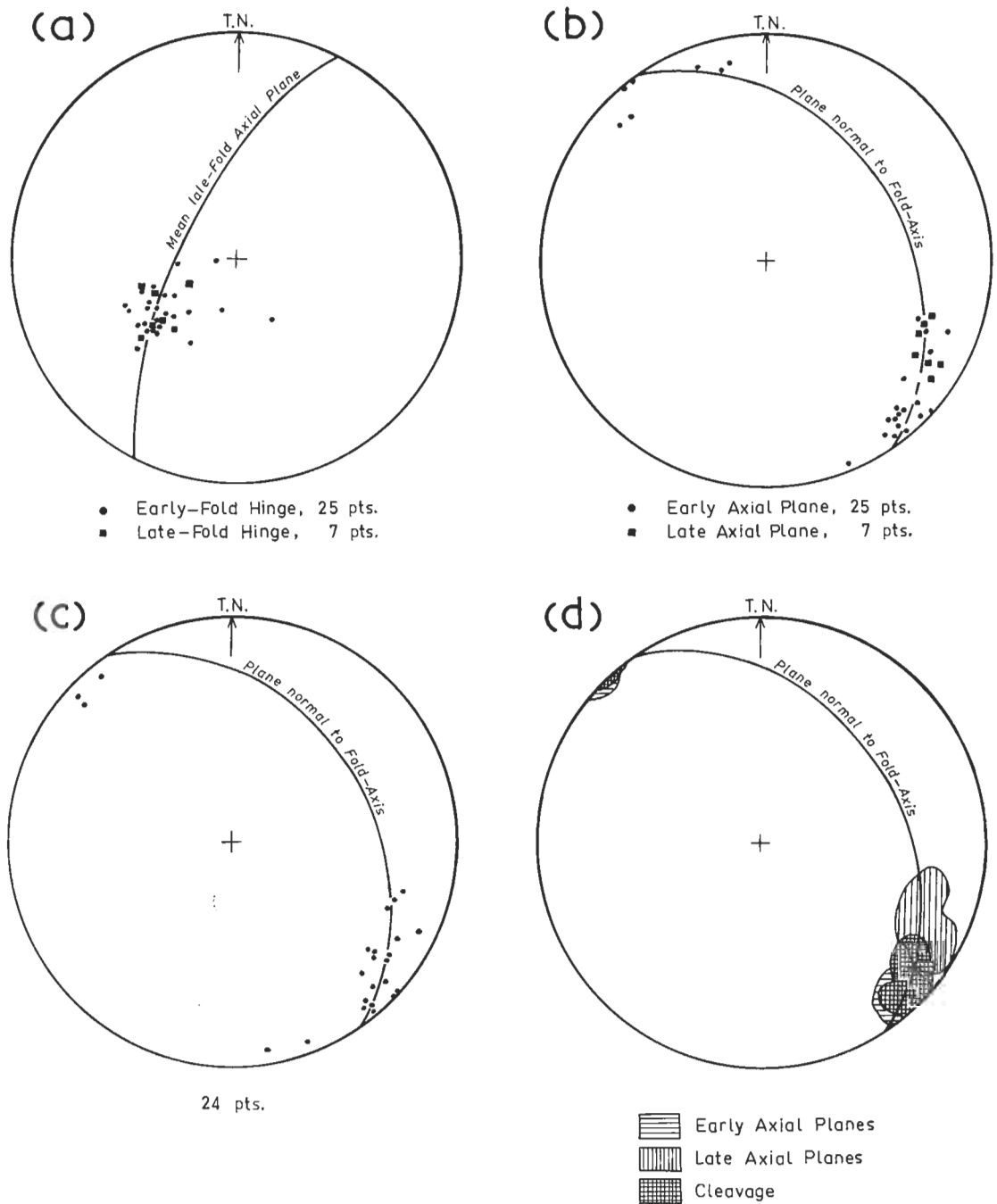
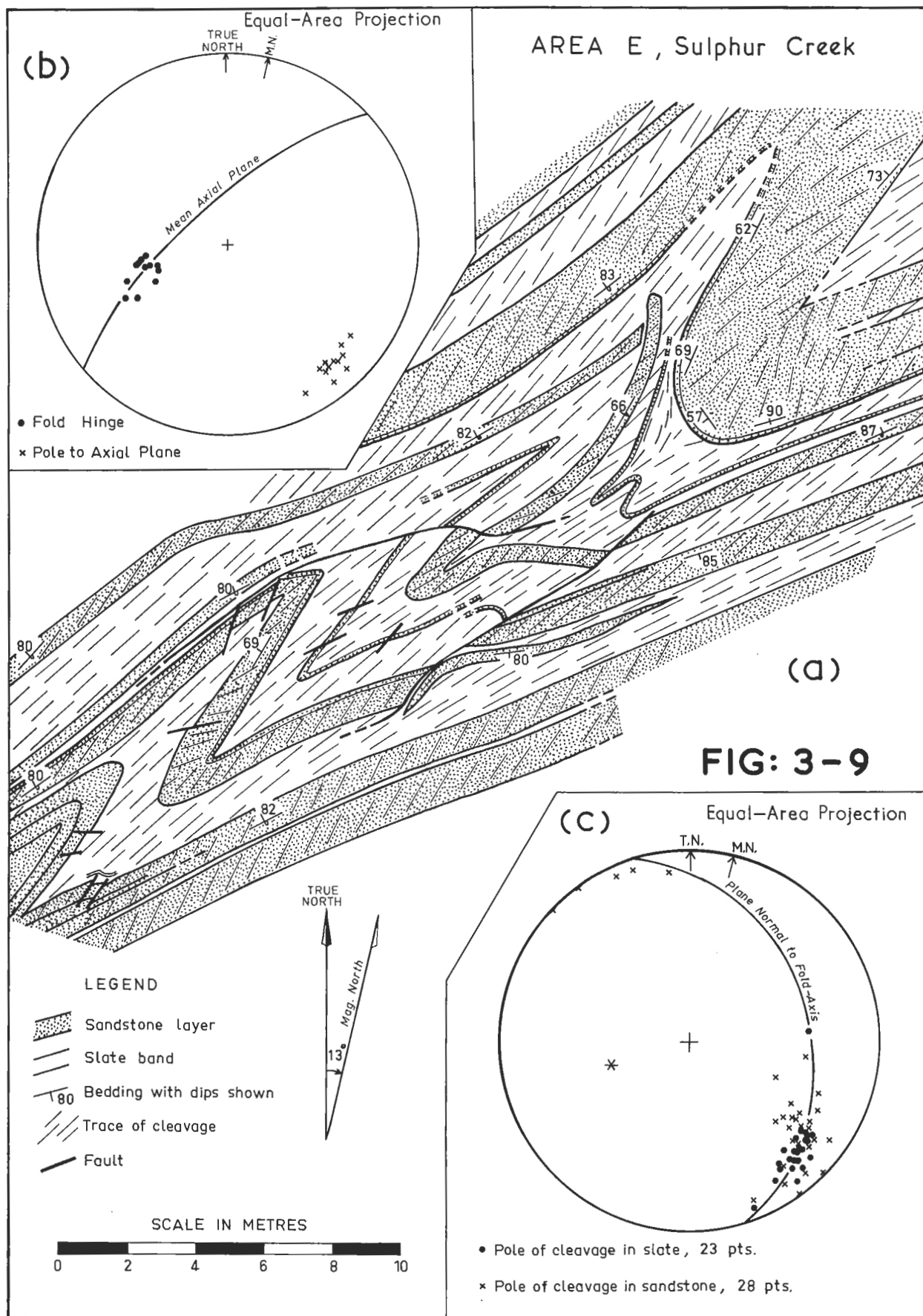


FIG: 3-8. (a) Poles of Fold-Hinges
 (b) Poles of Axial Planes
 (c) Poles of Cleavage
 (d) Composite Diagram showing approximate 20% per 1% area concentration of Axial Planes and Cleavage

(f) AREA E

(i) General Description Area E, north of Howth railway station, is in a zone of interbedded sandstones and mudstones which are sandwiched between a series of more massive, straight-bedded sandstones (Fig. 3-9). The rock type is considerably different from the rocks at Sulphur Creek where there is a larger proportion of slate. Sandstones varying from greywackes to coarse-grained quartz-wackes are the predominant lithic types, with less than 30% interbedded pelite, and some of the individual sandstone beds are up to 4 metres thick. The whole zone is less than 100 metres wide, and relatively undeformed, straight-bedded rocks on either side are several hundred metres thick. It appears that the folded zone was less competent than the surrounding rocks, and that stress on the surrounding area was relieved by strain in this zone. This style of deformation, where folded zones separate much thicker, relatively undeformed, straight-bedded sequences, is typical of the Burnie Quartzite and Slate from Sulphur Creek to Burnie.

The folds are part of the P1 phase, and the sense of coupling is dextral. In the sandstones the folds are concentric with variable amounts of flattening. Cleavage is quite intensely developed, and is mesoscopically penetrative in both sandstone and slate, but whereas it is essentially planar in the slate, it forms fans with divergences up to 40° in the sandstone. In contrast to some of the areas further east at Sulphur Creek, the cleavage in Area E is essentially parallel to the fold axial surfaces, and there are no zones of refolding.



The whole folded zone appears to have been extended in the plane of the cleavage. Pairs of conjugate faults with small dihedral angle and opposite sense of displacement, cut the limbs of individual folds and extend the sandstone layers along the axial surface. In the northeastern part of the sketch the thin sandstone layers around the nose of the thick folded lens are concave towards the axial surface. The cleavage in the slate around the nose of this fold is also strongly convergent.

(ii) Distribution of Fold Elements Twelve fold-hinges with the same number of axial planes were measured in Area E and their orientation is shown in Fig. 3-9(b). The average fold-axis is $54^{\circ}/252^{\circ}$ and the average axial plane is $74^{\circ}/319^{\circ}$. The orientation of the cleavage is shown in Fig. 3-9(c) where cleavage in the slate is represented as round dots, and that in the sandstone as crosses. As has already been noted, the cleavage in the slate corresponds closely with the orientation of the axial surfaces. The sandstone-cleavage, on the other hand, is rotated up to 20° from the slaty cleavage in a clockwise manner about the mean fold-axis. One of the problems is whether the sandstone-cleavage has been rotated out of the axial-plane direction, or whether the axial surfaces themselves have been rotated. Since the cleavage in the sandstone is essentially planar throughout the relatively undeformed straight-bedded zones, and has the same orientation as in the folded zone, it is likely that either,

(a) the cleavage in the slate had an initially different orientation from the cleavage in the sandstone, or

(b) the orientation of the cleavage in the slate has been modified subsequent to its formation.

It is not likely that the orientation of cleavage in the bounding straight-bedded sandstones has been changed by rotation because of the relative scales of the two structural domains. The problem will be discussed more fully in a section on cleavage, and it is sufficient to note here that the refraction of cleavage from the sandstone to the slate is adequately explained by differential compaction.

(g) INDIVIDUAL FOLD DESCRIPTIONS

(i) Fig. 3-10 Fig. 3-10(a) is a profile photograph of a P1 fold core in a sandstone layer just west of Area D. The sandstone layer is 20 to 30 cms. thick and surrounded by thicker bands of slate. The steep, westward-dipping cleavage in the slate is moderately well developed and is 10° more steeply inclined than the axial surface of the fold. The poorly developed cleavage in the sandstone forms a fan of 40° , and in the field appears to be non-penetrative. Analysis of the orthogonal thicknesses of the outer half of the sandstone band indicates a uniform flattening of 15% perpendicular to the axial plane, with an additional 15% differential flattening in the hinge region.

Fig. 3-10(b) is a profile photograph of a tighter P1 core in a sandstone layer just west of Area D. The sandstone layer is thinner



Fig. 3 - 10 (a). Profile photograph of a P1 fold core in a sandstone layer just west of Area D. Six-inch rule shown. Section is oriented southeast-northwest looking towards the southwest.



Fig. 3 - 10 (b). Profile photograph of a tight P1 fold core just west of Area D. Six-inch rule shown. Section is oriented southeast - northwest looking towards the southwest.

than the sandstone layer in Fig. 3-10(a), and is surrounded by a thick band of well-cleaved slate. The orthogonal thicknesses of two bands within the sandstone layer were measured to determine the percentage of flattening. The outer band (i.e. the band on the convex side of the folded layer) shows 5% to 10% uniform flattening in the core region with greatly increased flattening in the limbs. The southeastern limb, which is the common limb with an adjacent coupled anticline, shows uniform flattening greater than 40% while the northwestern limb is uniformly flattened by about 20%. The inner layer approaches a uniform flattening of 35% for all parts of the fold.

It appears that different parts of the folded layer have suffered different amounts of strain. The outer part of the layer in the core region could be interpreted as having been thinned slightly by stretching on the convex side of a buckled elasto-viscous body before having been flattened. The inner part of the layer has been more tightly compressed and flattened, and the apparently increased flattening in the limbs, in particular in the common limb between two coupled pairs, may be caused by stretching in the sandstone layer between two fold cores which have a fixed position relative to the slate. The cleavage in the common limb is generally parallel to the bedding, and this provides a mechanical surface which may have facilitated stretching of the sandstone layers as the distance between the adjacent coupled fold cores was increased by flattening in the slate.

(ii) Fig. 3-11 Fig. 3-11(a) shows a folded isoclinal fold from Area C, and this fold which is one of the earliest-formed folds of the P1 group, has been folded by a late P1 fold. There is no cleavage associated with the early fold, and a weak cleavage has developed in the slate parallel to the axial surface of the late fold (lower part of the photograph). Although the fold is isoclinal, and when unfolded is similar in overall profile, there has been no thickening of the sandy layers at the hinge of the fold. The thicker sandy band adjacent to the six-inch rule is continuous although there is incipient boudinage, but some of the thinner sandy layers have been completely dislocated and exist as discontinuous rods in a pelitic matrix. The mudstone has been almost completely squeezed out of the core and this movement has probably caused the disjunction of the thin sandstone layers. There can have been little, if any, stress difference transmitted along any of these sandy layers, and this type of folding may have occurred when the sediments were only partially consolidated and had a high water content which imparted a low viscosity to the pelite.

Fig. 3-11(b) shows the complexly folded nose of a sinistral fold couple of the early P1 group, and is located on the southeastern limb of the main syncline in Area C. The fold form is marked out by thin sandstone bands which are interlayered with mudstones. There is no cleavage in the mudstone in the core although there is a moderately well-developed cleavage near the six-inch rule. The sandstone bands, particularly the layers less than 1 cm. thick, are disjunctive, and



Fig. 3 - 11 (a). An isoclinal, early P1 fold folded by a late P1 fold in Area C. Six-inch rule shown.



Fig. 3 - 11 (b). A complexly folded nose of an early P1 fold in Area C. Six-inch rule shown.

exist as rods or tablets in the mudstone. The common limb between the fold hinge shown and the adjacent hinge (just off the lower part of the photograph), is much thicker than the straight-bedded limbs, and there is a strongly developed movement zone near the hinge of the rule, this zone being marked by a very finely laminated slate.

The complex fold structure is interpreted as having been formed by a continuing sinistral couple acting on partially consolidated sediments. The water in the rocks imparted a much lower viscosity to the pelite than to the psammite, and this permitted the intricate flowage of the mudstone during the continuing refolding of the structure. The fold core appears to have acted as a somewhat stronger block compared with the surrounding slate, and the refolding may have been caused by the drag of the faster-moving slate around the thinly bedded, more sandy core.

(iii) Fig. 3-12 The sinistral fold couple in Fig. 3-12(a) in a finely banded sandstone lens is one of the early P1 folds from Area B. It shows the typical characteristics of sinistrally coupled, early P1 folds with thin straight limbs and a thickened common limb between the adjacent fold cores. Dextrally coupled, later P1 folds tend to have a thinned common limb. The style of folding is markedly disharmonic, and thin sandstone layers on the convex side of the nose of the fold in the thick sandstone lens have been "slipped-off" and commonly refolded. The fold profile as a whole has been considerably flattened, and this accounts for most of the thickening in the common limb which is at a high angle to the regional plane of flattening.

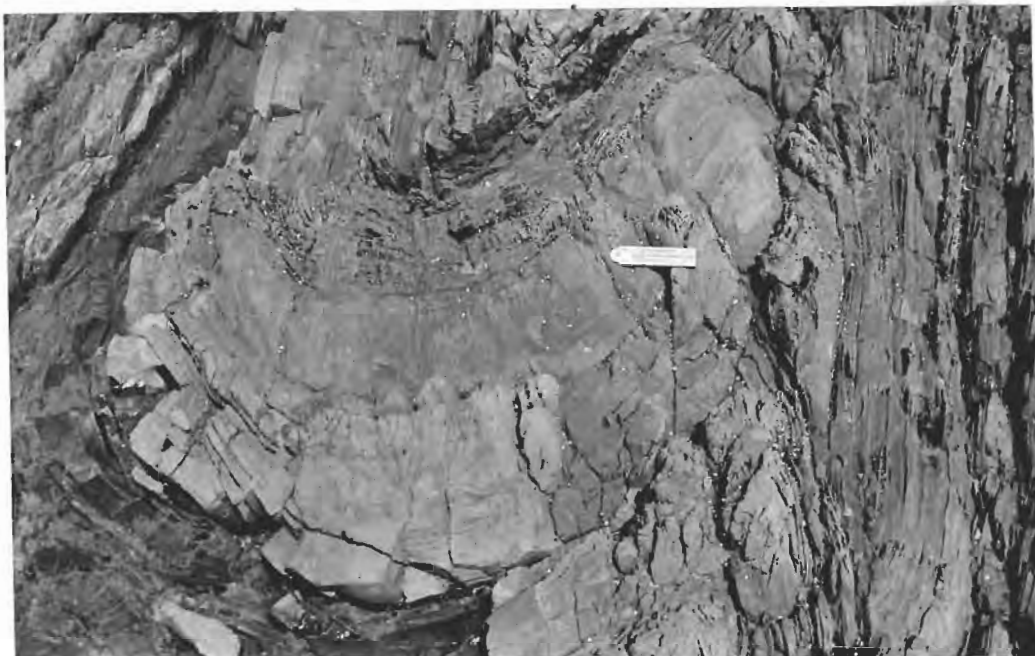


Fig. 3 - 12 (a). Sinistral fold couple in a finely banded sandstone lens, Area B. The folds belong to the early P1 movement and have a superimposed planar cleavage. Six-inch rule shown.



Fig. 3 - 12 (b). Disjunctive fold in a thin sandstone band which has slipped off the more massive fold core in Fig. 3 - 12 (a). Six-inch rule shown.

The cleavage in the sandstone lens is planar and penetrative to the scale of centimetres, but it deviates up to 20° from the axial surface which has a more variable orientation. This planar cross-cutting cleavage indicates that the present fold profile was formed before the cleavage, and that the cleavage has only an incidental relationship to the fold. In other examples it can be shown that rotation of the outer limbs towards the axial surface after cleavage formation has probably caused the cleavage fan, but it is quite apparent that all such rotation was completed in this fold before the cleavage was formed, and the sandstone acted merely as a very viscous block in the pelite.

The fold core in Fig. 3-12(b) is located on the nose of the fold couple in Fig. 3-12(a). It shows the disjunctive style of folding often associated with these thin pinched-off layers. The sandstone beds are lensoid in lateral extent, as shown by the inner lens which pinches out near the hinge of the six-inch rule. The layers maintain their orthogonal thickness but consist of disconnected blocks or rods between which the pelite has intruded. Some of the blocks have been displaced across the trend of the bedding and are welded into the pelitic matrix. There is no cleavage associated with the early folding, but there is an incipient cleavage in the mudstone parallel to the axial surface of the later fold. This late P1 fold is very open but it has a dextral vergence which is opposed to the sinistral couples in this part of the section. Nevertheless, the sinistral coupling is congruous with the general dextral couple for the entire P1 deformation

because the early folds are parasitic folds, probably induced by layer-parallel slip on the eastern limb of a larger syncline which is part of the overall dextral couple. When the later folds were formed the early structures were incorporated in the bedding, so that the manifestation of the later deformation is one of many minor folds with dextral vergence transecting the whole area. The pattern of large coupled synclines and anticlines typical of the early folding, is not developed in the late P1 folding.

(iv) Fig. 3-13 Fig. 3-13(a) is a profile photograph of a late P1 fold in one of the cleaner sandstone beds in Area C, near the nose of the main syncline. The sandstone bed is relatively uniform in thickness, but is boudined along strike and terminates in a series of rods of elliptical cross-section, the long axis of the rods being parallel to the general fold-axis.

There is no cleavage visible mesoscopically in the sandstone layer, but there is a series of non-penetrative joints which fan outwards. Some displacement of the blocks has occurred along these fractures which are most intensely developed on the concave side of the bed. These fractures are not the same as the cleavage in Fig. 3-12(a), and are probably conjugate shears developed by interlayer slip. In the slate there is a weakly developed, penetrative cleavage which is approximately parallel to the axial surface of the fold.

The essential style of this fold is concentric, with uniform flattening of 20% on the lower limb but only 10% to 15% on the



Fig. 3 - 13 (a). An essentially concentric fold in a quartzose sandstone bed in Area C. Six-inch rule shown.



Fig. 3 - 13 (b). Tight, small-amplitude crenulations which occur in the pelitic bands on the concave side of concentrically folded, thick sandstone beds as in Fig. 3 - 13 (a). Location:- Area C. Six-inch rule shown.

upper limb. This fold core belongs to a coupled pair with dextral vergence, and the lower limb is the common limb. Calculations made on subdivisions of the sandstone layer (i.e. by dividing the layer into three units - the concave, neutral and convex bands) were not satisfactory as there appears to have been primary lensing of individual sublayers, although the whole layer was of uniform thickness. However, there is an indication that the sublayer on the concave side of the bed has been flattened more than the sublayer on the convex side.

The thick sandstone layer appears to have been the controlling layer in the formation of the fold. The layers of thinly bedded, fine-grained sandstone and mudstone on the convex side are folded in an almost perfectly concentric manner, and may have been stretched slightly. Such stretching is not large because the increased distance around the outer perimeter of this fold is almost wholly compensated for by the decreased distance on the concave side of the adjacent fold core.

Nevertheless, there is some local flattening on the concave side of the sandstone bed. Fig. 3-13(b) shows the tight, small-amplitude crenulations that occur in the predominantly pelitic band on the concave side of such a fold. The folding in this photo is not located on the concave side of the fold in Fig. 3-13(a), but in a comparable position with respect to another fold from Area C. The rock is composed of very thin, fine-grained sandstone bands in a slaty matrix.

Folding is almost perfectly similar in style, and there is a well-developed slaty cleavage along which displacement has occurred during the folding. The shape of the fold curve is not sinusoidal, but it resembles a distorted square wave. If a model of movement parallel to the cleavage on a set of uniformly thick slices is used to account for the shape of the folds, there are two types of movement involved:-

(a) Minor displacements between adjacent slices producing a continuous quasi-sinusoidal curve, and

(b) Larger displacements between groups of slices.

The width of the blocks involved in (a) is finer than can be observed in hand specimen so that it can be considered penetrative flow. The width of the blocks taking part in (b) is 1 cm. to 2 cms. They may be thus considered as "macrolithons".

(v) Fig. 3-14 The fold couple in Fig. 3-14(a) is located in Area C. It is one of the larger parasitic folds on the eastern limb of the main syncline, and has a sinistral vergence. The pair of folds belong to the early P1 group, and there is no cleavage in the sandstone, the only fractures being some irregular joints shown in the photograph. Cleavage in the mudstone is very weak and was superimposed on the fold.

The sandstone layers are lensoid in shape as may be seen in the sketch (Fig. 3-4) and in the photograph. The layer in the centre of the photo thins very rapidly to the left-hand side, and likewise the thick layer on which the hinge of the ruler rests, also lenses towards the upper fold.



Fig. 3 - 14 (a). Profile photograph of one of the larger parasitic folds in Area C on the eastern limb of the main syncline. Six-inch rule shown.

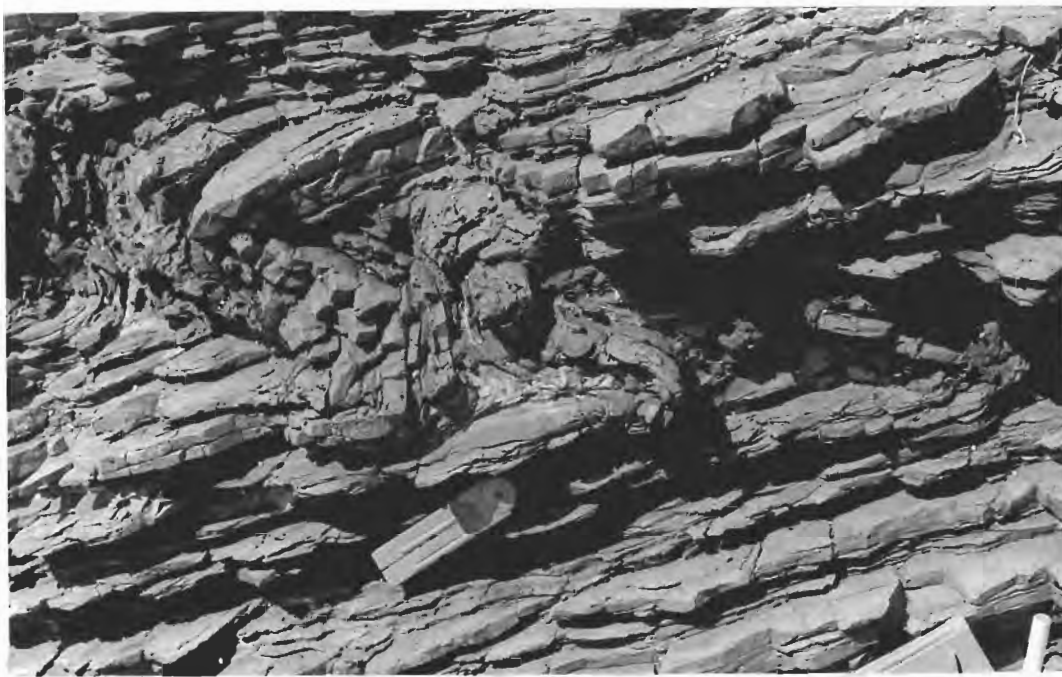


Fig. 3 - 14 (b). An oblique profile-photograph of one of the more common parasitic folds in the regions of thinly bedded sandstones and slates. Location:- Area C. Six-inch rule shown.

The style of folding is markedly different between the upper and lower folds. The upper fold is very tight with a narrow, well-defined hinge area which has been flattened. The sandstone beds in the upper straight limb are much thinner than they are in the lower fold, and the mudstone between the two limbs of the upper fold has been squeezed right out of the core. The lower fold is more open, and essentially concentric in the sandstone band on the right-hand side of the photo. Orthogonal thicknesses show that any flattening parallel to the axial plane is less than 5% in this thick layer. The sandstone layers on its concave side, however, appear to have been considerably flattened. Such variation in fold style from bed to bed is a necessary consequence of concentric folding.

Fig. 3-14(b) is a somewhat oblique photograph of one of the more common parasitic folds in the finely interbedded, sandstone-slate regions. The fold is located in Area C and belongs to the early P1 phase. The style of folding is disharmonic although the profile is projected along the axial surface to successive layers. The fine-grained sandstone layers maintain their orthogonal thicknesses and the spaces in between are occupied by slate. There is no cleavage in the sandstones but a weak penetrative cleavage, not parallel to the axial surface, is developed in the slate.

The "slipping-off" of thin sandstone beds on the convex side of a fairly open fold to form a tight, or even isoclinal nose is typical of the early P1 folds. Later P1 folds such as in Fig. 3-13(a)

do not show the same characteristics, and this is interpreted as indicating that there was only a small amount of friction between adjacent sandstone beds in the early stages of the P1 movement. The difference in viscosity between the psammites and pelites decreased during the deformation, so that in the late stages disharmonic and disjunctive folds did not form.

(vi) Fig. 3-15 Fig. 3-15(a) is a somewhat oblique photograph of the nose of the anticline in the middle of Area D. The fold limb in the upper part of the photo is the common limb of the main dextral couple in Fig. 3-7. The main sandstone lens is just to the right of the photograph and the sandstone layers depicted are thin in comparison with it. They have been "slipped-off" or "rolled-off" the nose of the main fold in such a manner that the orthogonal thicknesses have been maintained except on the common limb where there has been stretching and boudinage.

The isoclinal nose is regarded as an early P1 fold and the more open fold which folds the nose of the early fold is one of the late P1 group. There is no cleavage in either the slate or the sandstone that can be recognized as related to the early fold, but a quite prominent penetrative slaty cleavage has developed with the later fold. This cleavage shows a small fan but is essentially parallel to the axial surface of the fold.

The refolding is one of the many structures indicating continuing movement in a heterogeneous rock body. The main sandstone lens



Fig. 3 - 15 (a). Oblique photograph of the refolded, slipped-off nose of the main anticline in Area D. Six-inch rule shown.

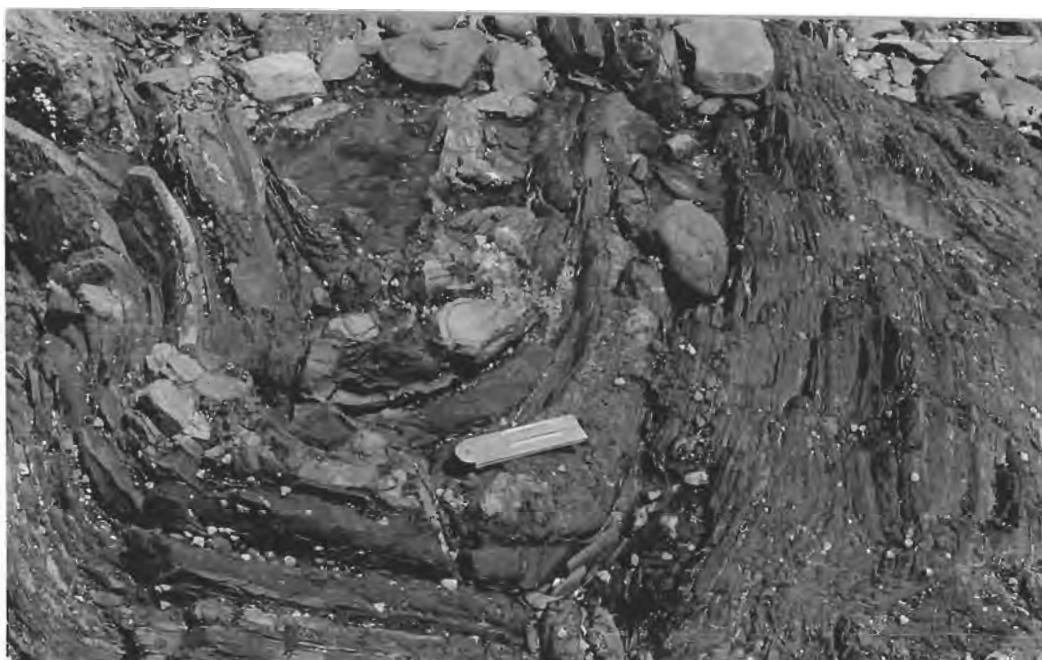


Fig. 3 - 15 (b). Intraformational, open-cast slump folds folded by an early P1 fold. Location:- Area D. Six-inch rule shown.

has remained relatively simply folded in its thickest parts (Fig. 3-7), but at the thin margins of the lens there is complicated refolding. All the structures can be accounted for by dextral movement about a constant fold-axis. In the early stages folding seems to have developed with equal intensity in all parts of the rock. Thus the early P1 folding is distributed evenly throughout the whole mass. Later, probably at about the time of cleavage formation, movement became localized in certain zones where the sandstone lenses were thinnest. The amount of deformation and refolding of early structures in these zones appears to be proportional to the extent of the adjacent relatively stronger sandstone lenses. This situation is what would be expected if there was a homogeneous stress distribution over the rock body considered on a broad scale. Each small area would tend to deform by a certain constant amount. If, at some time during the deformation, some parts of the rock body resisted deformation more strongly than others, then the strain, homogeneous on the broad scale, would become heterogeneous on a smaller scale, and the resistant bodies would be encompassed by zones of increased local strain. The larger the resistant block the greater the strain around its margins.

In Fig. 3-15(a) the isoclinal nose of the anticline in the thin sandstone layers is believed to have achieved, at some time during the deformation, a fixed location both in the sandstone layers and in the slate. Continuing dextral movement caused the lower ("straight") limb of the fold to be rolled around the nose of the thick sandstone lens

and to be refolded by the late P1 fold. On the upper limb (common with the adjacent syncline) there has been stretching associated with flattening in the slate.

Fig. 3-15(b) is located southwest of Fig. 3-15(a) in Area D in one of the zones or more concentrated late P1 movement. The fold shown is one of the early P1 folds, and in one of the sandstone layers there are many minor folds. These folds are erosionally truncated, intraformational slump folds and predate the P1 folding. They are quite common throughout the region and are always layer-delimited. The beds in which they occur are usually fine-grained sandstones less than 10 cms. thick, with the folding extending along strike for hundreds of metres. It seems that these folds, some of which show erosional truncations at the upper surface, had been formed, and were reasonably well consolidated before the P1 folding. Certainly the layers in which they occur have acted in every way as normal sandstone layers during the P1 folding.

(vii) Fig. 3-16 The fold in Fig. 3-16(a) is the detached core of the fold in the northeastern part of Area B. There is a surface along which considerable movement may have occurred between the folded layers and the straight-bedded zone in the lower part of the photograph. The fold is one of the early P1 folds, as is indicated by the transecting cleavage, the sinistral vergence and disjunctive style in the fold core, and it is a parasitic fold on the eastern limb of the main syncline, the hinge of which is in Area C. The sandy layers are folded in



Fig. 3 - 15 (a). The detached core of a fold in the northeastern part of Area B. A surface along which there may have been considerable movement separates the fold core and the straight-bedded strata in the lower part of the photograph. Six-inch rule shown.



Fig. 3 - 15 (b). A late P1 fold in the southwestern part of Area C. Six-inch rule shown.

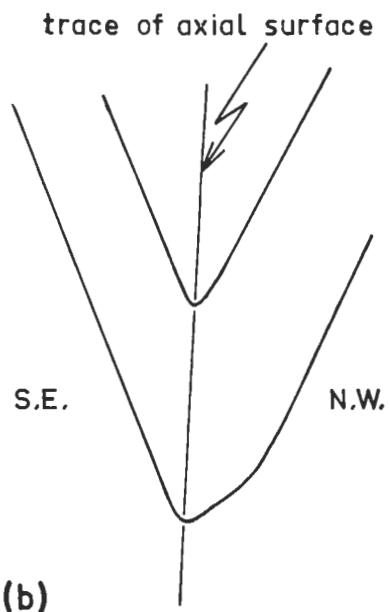
an essentially concentric manner, and in parts are broken into fragments. The superimposed planar cleavage in the slate is poorly developed but penetrative, and it diverges by 20° from the axial surface of the fold.

Fig. 3-16(b) is one of the late P1 folds in the southwestern part of Area C and shows the characteristic similar style. The hinge region has a small area, and the fold shape is angular with long straight limbs. Late P1 folds are not as tight as the early P1 folds, and although both early and late folds are broadly similar in geometry, the late P1 folds are not disharmonic. The similar-fold profile in the early P1 folds is established by a series of concentrically folded sandstone layers interbedded with slate which takes up the strain. Thus a combination of two fold styles, Class 1B and Class 3 (Ramsay, 1967, Fig. 7-26) produces a fold of Class 2. In the late P1 folds this alternation of fold styles is much less marked. Orthogonal-thickness measurements from the sandy layer adjacent to the hinge of the ruler indicate uniform flattening of 40% perpendicular to the axial plane. There is a moderately well-developed penetrative cleavage in the slate, and this cleavage is parallel to the axial surface of the late P1 fold.

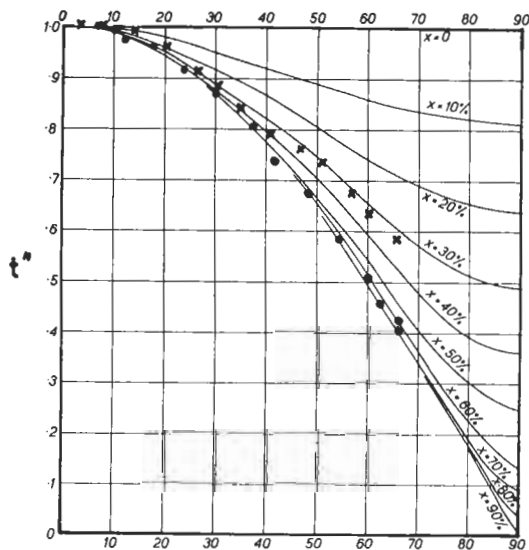
(viii) Fig. 3-17 Fig. 3-17 is a profile photograph of the main syncline in Fig. 3-7, Area D. The profile presented is from the concave side of the thick sandstone lens so that the left-hand limb is the common limb with the adjacent anticline. The rocks are composed of finely bedded, fine-grained sandstones separated by thin slate bands. There are commonly small festooned cross-beds in the sandstone layers,



(a)



(b)



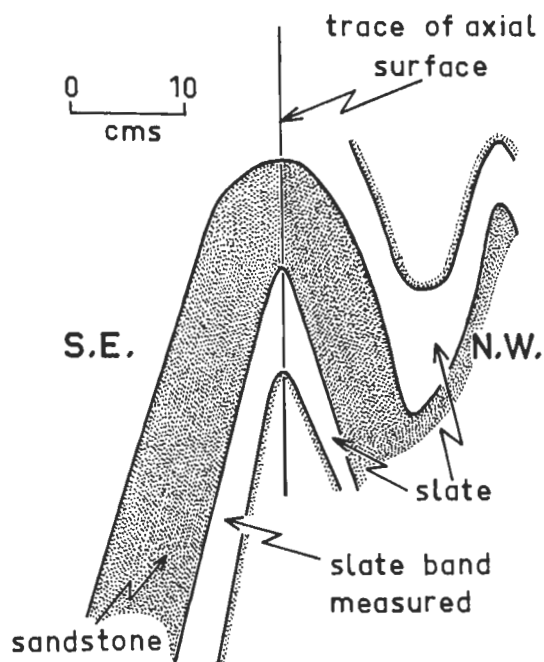
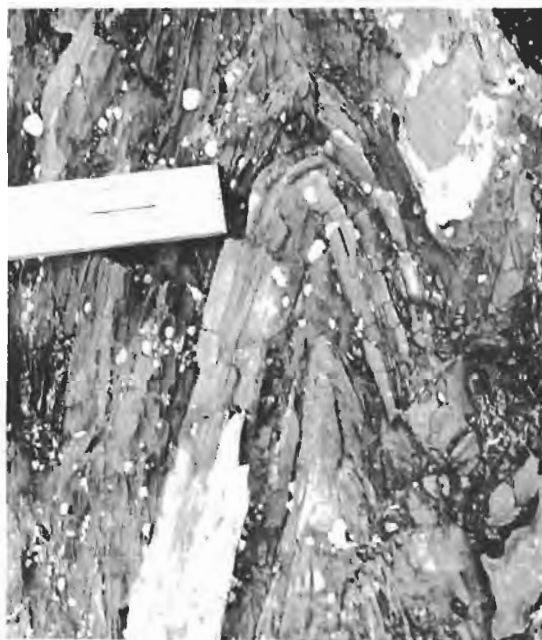
(c) • S.E.Limb \angle' \times N.W.Limb

FIG. 3-17. (a) Profile-photograph of an asymmetrical syncline in Area D. Six-inch rule shown. (b) Tracing of the profile used to measure orthogonal thicknesses. (c) Orthogonal-thickness ratio diagram.

and these are locally oversteepened in the vicinity of the fold-hinge.

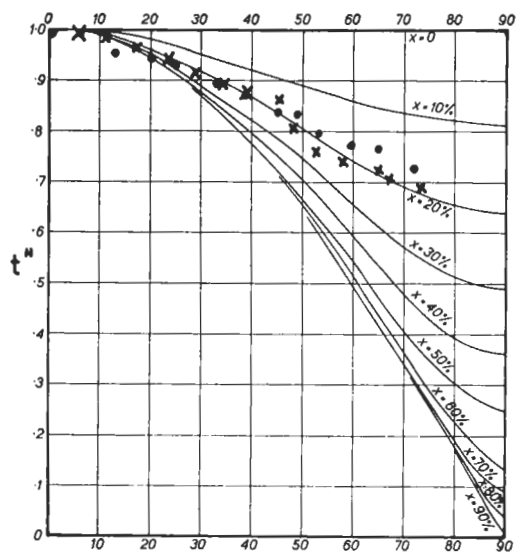
Analysis of the orthogonal-thickness ratios shows different amounts of flattening on either limb. The thickness ratios for the right-hand limb, which is the straight-bedded northwestern limb, correspond to uniform flattening of 30% perpendicular to the axial plane. The southeastern limb, however, indicates uniform flattening in excess of 60%, and the thickness ratios correspond closely to a similar geometry. This differential flattening is probably not caused by inherently different mechanical properties of the two limbs, but rather by stretching in the common limb as the two coupled fold cores moved apart during flattening in the slate.

There is a cleavage, characterized mesoscopically by anastomosing fractures and penetrative to the scale of centimetres, which is parallel to the common limb of the fold couple but which makes an angle of 40° to 50° with the bedding in the straight-bedded outer limb. This cleavage has facilitated extension in the common limb, and represents a situation typical of many of the P1 folds elsewhere in the Sulphur Creek area. The cleavage is not parallel to the axial surface of the fold from which direction it diverges by up to 15° but it is noticeable that the axial plane rather than the cleavage plane is the plane of flattening.



(a)

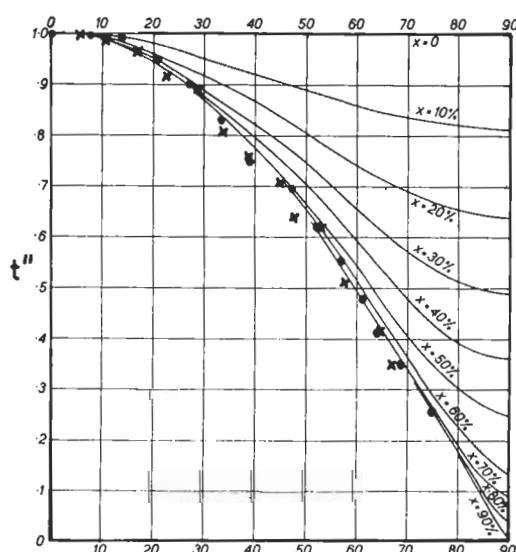
(b)



(c)

Sandstone

• S.E.Limb
x N.W.Limb



(d)

Slate

FIG. 3-18. (a) Profile-photograph of a small, flattened concentric fold in the thick slate band, Area D. Six-inch rule shown. (b) Tracing of the profile used to measure orthogonal thicknesses. (c) and (d) Orthogonal-thickness ratio diagrams.

(ix) Fig. 3-18 Fig. 3-18 is a profile photograph of a small fold in the thick slate band to the north of the main sandstone lens in Fig. 3-7. It is outlined by one of the few thin, fine-grained sandstone layers which can be recognized in the generally highly dislocated slate. The fold style is typical of the P1 group with a narrow rounded hinge and long straight limbs. In broad outline the style could be regarded as similar, since the same fold curve is projected up and down the trace of the axial surface. However, the sketch of the fold from the photo in Fig. 3-18(b) shows that the similar profile is composed of alternating folds of Classes 1C and 3 in the sandstone and slate, respectively.

The orthogonal-thickness ratios for the sandstone and slate bands are shown in Fig. 3-18(c) and (d). The sandstone band shows a fairly uniform flattening of 20% parallel to the axial plane, while the slate band approximates closely to a perfectly similar profile. Because the proportion of sandy layers in the slate is low, it is not necessary for the slate bands to show thickness ratios far into the region of Class 3 for the overall similar profile to be propagated.

There is no cleavage visible in the sandstone, but a moderately intense, penetrative cleavage exists in the slate where it is parallel to the axial surface of the fold. It was noted before that the slate in these thick bands is very highly dislocated by anastomosing faults statistically parallel to the cleavage plane. The geometry of this fold and the implied plasticity of the slate during deformation indicates that the folding occurred when either the strain rate or the

viscosity was lower than during the formation of the faults. There is no reason to propose a large increase in strain rate to account for the transition from deformation by folding to deformation by fracture. The largest amount of deformation (as measured by the early P1 structures) was accomplished by flow, so that if the change in mode of deformation was caused by an increased rate of strain, the later P1 folding must have been accomplished in a relatively very short period of time. Furthermore, the end of deformation must have been sudden, with no gradual decrease in the rate of strain. A more satisfactory solution to the problem may be that the viscosity of the rocks was increasing during the deformation so that a strain rate that was accommodated by flow early in the movement, produced fracture later. The fold style lends some support to this hypothesis, as there appears to have been a convergence of viscosities in the psammites and pelites such as would occur if the rock mass lost much of its excess water during the deformation.

(x) Fig. 3-19 Fig. 3-19(a) is a profile photograph of a fold in the thick slate band 200 metres east of Area A. The rock is dominantly slate through which a few thin, fine-grained sandstone bands can be traced. These bands often contain small-scale, festooned cross-bedding.

The characteristic style of folding is asymmetrical and similar, with the thin steeper limb usually a common limb with an adjacent fold-hinge. The hinges of individual folds are more random



Fig. 3 - 19 (a). Profile photograph of an asymmetrical similar fold in the thick slate band east of Area A. Six-inch rule shown.

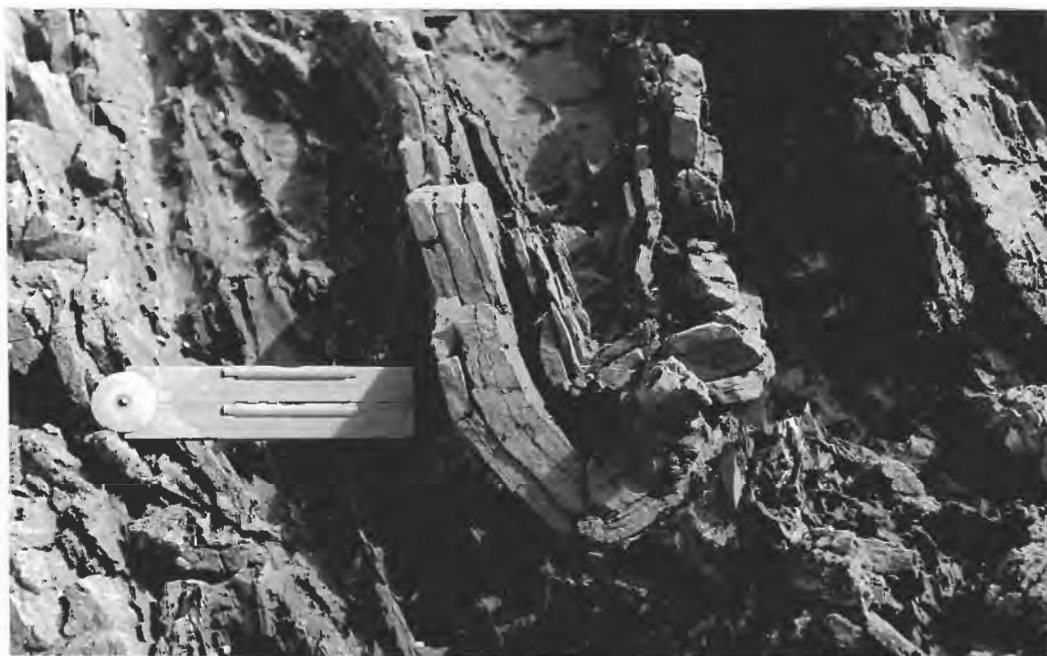


Fig. 3 - 19 (b). Concentric fold in a thin sandstone bed at the hinge of the main syncline in Area C. Six-inch rule shown.

in orientation in this region than further west, and the strong slaty cleavage diverges up to 25° from the axial surfaces. In Fig. 3-19(a) the cleavage in the profile section is almost parallel to the trace of the axial plane, but it is oblique to the strike of the axial plane.

Orthogonal thicknesses were measured on the two slate bands marked out by the thin sandstone beds, and the ratios show that both slate bands correspond closely to ideal similar profiles. Another fold in the slate, just west of Area C, has an even more asymmetrical profile. Orthogonal thicknesses were measured to determine whether there was any increase in flattening on the thinned limb, but the curves show that the profile is essentially similar and corresponds to an apparent uniform flattening of between 50% and 60%. There are no thicker sandstone bands immediately adjacent which could have controlled the movements in the slate. These similar folds in the thick slate bands were probably caused by small differential movements in the slate accompanied by considerable flattening perpendicular to the axial surface during tectonic compaction. Similar folds can also be produced by simple shear parallel to the axial surface, but in the folds at Sulphur Creek the thin sandstone beds tend to maintain their orthogonal thickness, a condition which precludes simple shear as the dominant mechanism. Nevertheless, both simple-shear and pure-shear mechanisms of fold formation would account for the large spread of fold-hinges in the slate bands in a girdle which is the mean axial plane.

Fig. 3-19(b) is one of the thin sandstone beds in Area C at the hinge of the main syncline. The overall geometry of the main syncline is isoclinal and similar, but the thin sandstone bands are folded in an essentially concentric manner. Orthogonal-thickness measurements show little uniform flattening parallel to the axial plane and the outer limbs have been rotated towards the axial surface without any increase in flattening. This rotation may have been caused by flattening in the slate without any appreciable flattening in the sandstone layer. There is a moderately well-developed cleavage in the slate, and at this location it is more or less parallel to the axial surface of the fold. There is no mesoscopic cleavage visible in the sandstone.

(xi) Fig. 3-20 Fig. 3-20(a) is a profile photograph of an asymmetrical anticline from Area E. This asymmetrical, angular style with a strong penetrative cleavage in the sandstone parallel to the thin limb and making a variable angle with the thicker limb, is typical of many of the P1 folds between Sulphur Creek and Burnie.

The reconstructed profile used for orthogonal-thickness measurements is shown in Fig. 3-20(b). The thin limb is the common limb with an adjacent syncline, the two folds forming a dextral couple. Thickness measurements indicate little more than 10% uniform flattening parallel to the axial plane on the thick limb, with almost 40% uniform flattening on the thin limb. The increased flattening on the common limb is interpreted as caused by stretching between the coupled fold cores during flattening in the surrounding slate. Another core, part

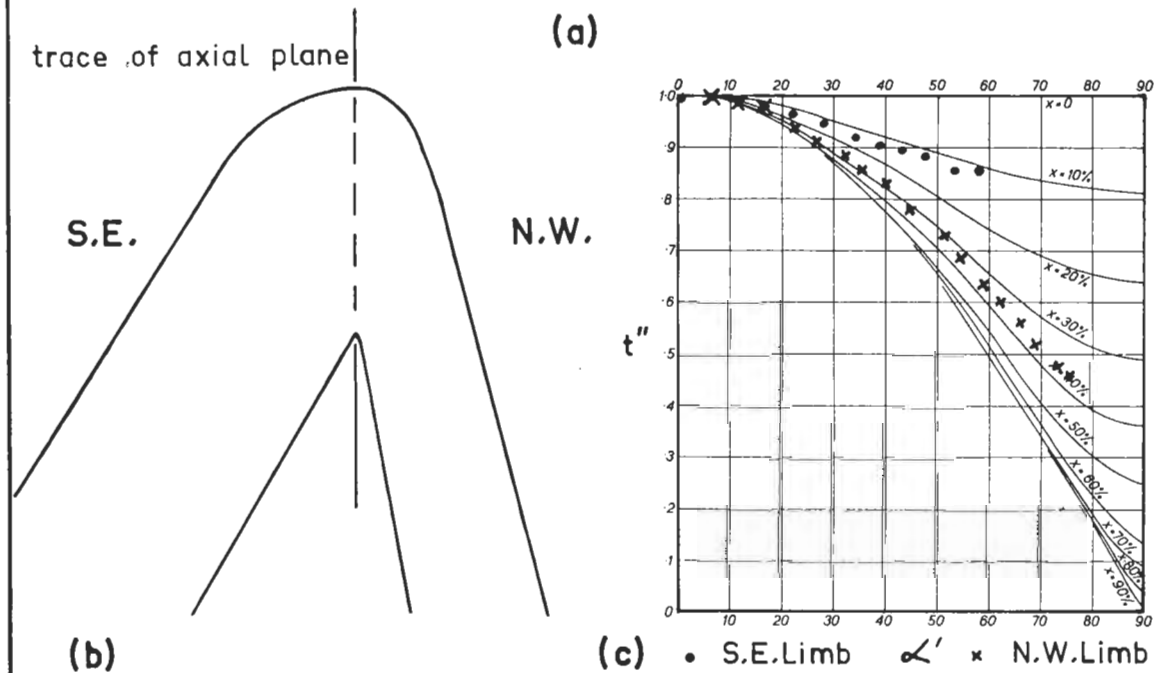


FIG: 3 - 20. (a) Profile photograph of an asymmetrical anticline from Area E. Six-inch rule shown. (b) Tracing of profile used to measure orthogonal thicknesses. (c) Orthogonal-thickness-ratio diagram.

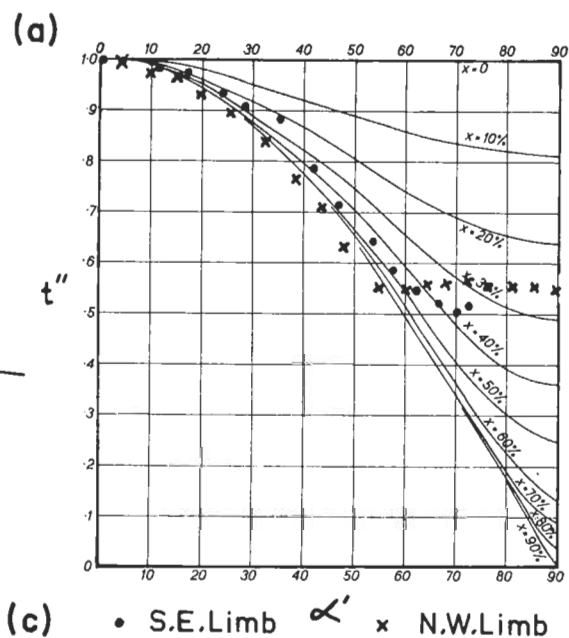
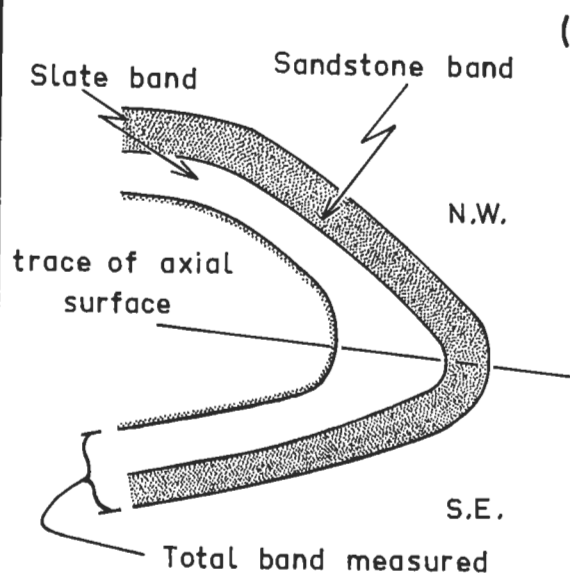
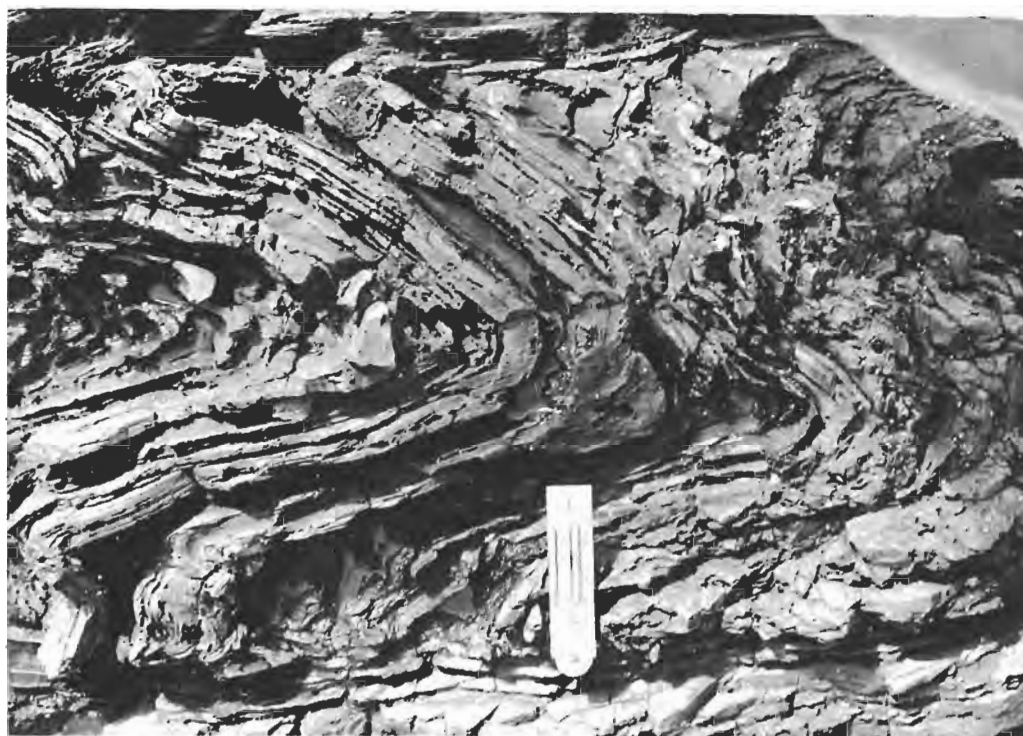


FIG. 3-21. (a) Profile-photograph showing similar folding in the slate, Area C. Six-inch rule shown. (b) Tracing of the profile used to measure orthogonal thicknesses. (c) Orthogonal-thickness ratio diagram.

of the same fold but further along the trace of the axial surface, appears to be uniformly flattened by 15% with increased flattening to 25% on the common limb.

(xii) Fig. 3-21 Fig. 3-21(a) is a profile photograph showing similar folding in the slate in Area C, Sulphur Creek. The fold form is the same as the parasitic fold in Fig. 3-14(a) which exists as a slightly flattened concentric fold in the sandstone bands. The rock is not strictly homogeneous slate but consists of thin bands of fine-grained sandstone embedded in a slaty matrix. Fig. 3-21(b) outlines both a sandy and a slaty layer traced from the photograph, and this profile has been used to calculate amounts of flattening.

The sandstone layer is folded in an essentially concentric fashion, and there is no flattening parallel to the axial plane. The slaty band has acted incompetently and belongs to Class 3. Fig. 3-21(c) depicts the orthogonal-thickness ratios for the combined thickness of the sandstone and slate layers, and the distribution corresponds closely to an ideal similar fold up to a certain point on the limbs where the thickness curve changes abruptly, and the orthogonal thickness remains constant for increasing angle. This is interpreted as indicating that although the main profile is ideally similar, the outer limbs have been bodily rotated towards the axial plane without decrease in the orthogonal thickness. Physically this interpretation implies that there has been either slipping-off of the outer layers from the nose of a fold, or a decrease in the volume of the core.

Since there is no reason to suppose that the volume of the slate in the core should decrease more than the volume of the slate in the layers outlined, it seems likely that there has been slipping-off of the outer layers of the fold, with concomitant rotation of the outer limbs towards the axial surface.

There is an important contact parallel to the lower part of the photograph near the hinge of the rule. This contact is a "welded" contact along which considerable movement may have taken place. There are no slickenslides or complementary fractures, and the layers which run obliquely into the contact are firmly stuck to it. The welded contact in its present state is as strong as the main slate mass, and a poorly developed, superimposed cleavage in the slate transects the fold core and the welded contact at an angle of 25° to the axial surface. Such welded contacts are interpreted as evidence that the slate was initially much different in character from its present state, since it was capable firstly of lubricating the slip surface so that no striations or complementary fractures were formed, and later welding the sides together so that the structural weakness no longer existed. A relatively high water content in a partially compacted pelite could provide the necessary conditions.

3.

DESCRIPTION OF CLEAVAGE

(a) GENERAL STATEMENT

The two dominant rock types from a behavioural point of view are sandstone and slate; the sandstones being competent layers, the slates incompetent. Cleavage occurs in both rock types but varies in its nature, intensity and distribution. The cleavage in the slate is everywhere penetrative to the naked eye and the intensity of its development generally increases westward; at Sulphur Creek there are places where there is no cleavage in the slate. The slaty cleavage is more planar than the axial surfaces of the major folds and tends to be parallel to the common limb of dextral fold couples, although in places a cleavage surface cuts both limbs producing a transected core. In isolated outcrops rock fragments are oriented with their long axes parallel to the cleavage.

In the sandstone the cleavage is poorly developed in parts of the Sulphur Creek region, and in places (e.g. Area B) there is no cleavage mesoscopically visible. As with the slate-cleavage, the intensity of development of the sandstone-cleavage increases westward. It is penetrative to the scale of a centimetre, and below this scale there appear to be narrow zones of more strongly developed cleavage separated by weakly cleaved, or non-cleaved blocks. The cleavage in the sandstone is relatively planar, and shows no constant geometric relationship to the bedding in the fold-hinges. In many folds it is parallel to the common limbs of dextral fold couples, and makes an

angle up to 40° with the straight-bedded outer limbs, but in other folds this relationship does not hold. There have been displacements along cleavage surfaces in some folds, but these movements do not occur generally, and are considered to be displacements subsequent to the cleavage formation.

(b) MESOSCOPIC DESCRIPTION

Figs. 3-22 and 3-23 are photographs taken from Area E which is about 1 kilometre west of the main areas considered in this study. Nevertheless, the cleavage is congruous between Area E and Sulphur Creek, the only difference being that it is more intensely developed in the sandstones in Area E than at Sulphur Creek.

Fig. 3-22(a) is a profile photograph of an anticline near Area E, and there is a six-inch rule in the foreground. The cleavage in the sandstone is quite strongly developed, and the rock is characteristically divided into blocks of non-cleaved material separated by thin zones with intensely developed cleavage. The cleavage is essentially planar and parallel to the axial plane of the fold, although there is some refraction of the cleavage surfaces as they pass through the dark zone near the top of the sandstone bed. This dark band is more pelitic than the rest of the bed and has been a zone of bedding-plane slip during the folding.

Fig. 3-22(b) is a close-up view of the right-hand limb of the anticline in Fig. 3-22(a), and shows a number of important features:-

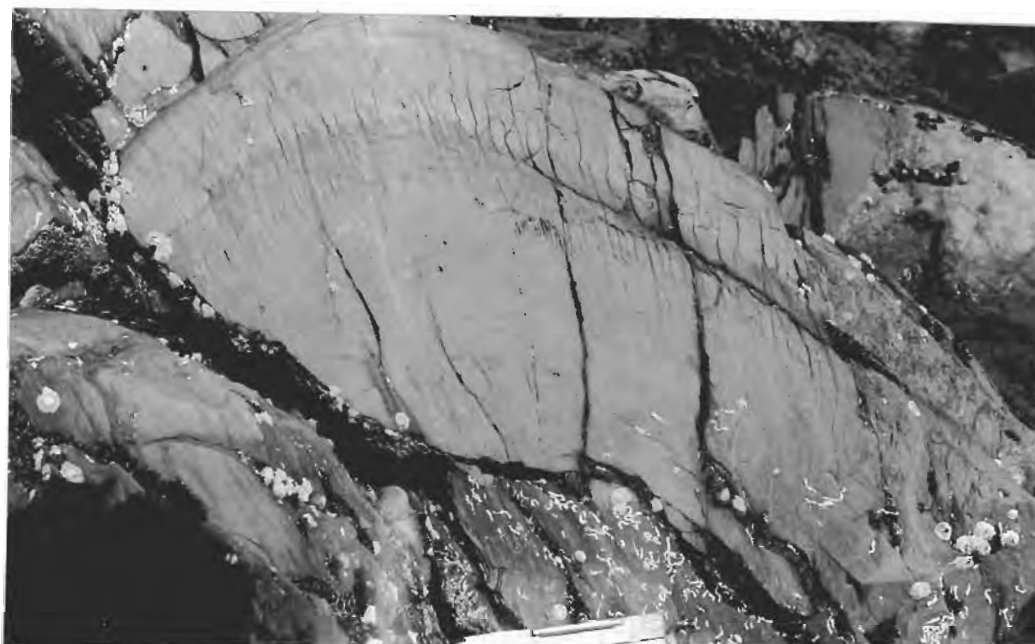


Fig. 3 - 22 (a). Profile photograph of an anticline near Area E, showing non-penetrative cleavage in the sandstone. There is a six-inch rule in the foreground.



Fig. 3 - 22 (b). Close-up of the right-hand limb of the anticline in Fig. 3 - 22 (a). Width of the photograph is approximately 15 cms.

(a) The main cleavage zones are darker in colour than the sandstone bed. This is because the cleavage zones contain pelitic material which has a penetrative slaty cleavage parallel to the boundaries. The pelitic material is thought to have been introduced from adjacent slate bands.

(b) The first-order cleavage blocks themselves are subdivided by smaller cleavage zones, usually into 3 or 4 sub-blocks. These cleavage zones have the same character as the major cleavage zones but do not penetrate as far into the sandstone.

(c) The cleavage zones tend to decrease in width and branch out as they pass from the pelitic material into the sandstone. Thus a few sharply defined cleavage zones at the lower contact with the pelitic zone branch out and reticulate through the upper part of the sandstone bed.

(d) There have been displacements along the cleavage zones with the sense of displacement always such that the block nearest the axial surface moves transverse to the fold-axis towards the convex surface of the fold.

(e) The irregularities in the lower surface of the sandstone layer along which the cleavage zones enter the sandstone were probably originally sedimentary load casts. However, their plane of symmetry commonly remains parallel to the cleavage from one limb to the other, so that they must have been reoriented during cleavage formation.

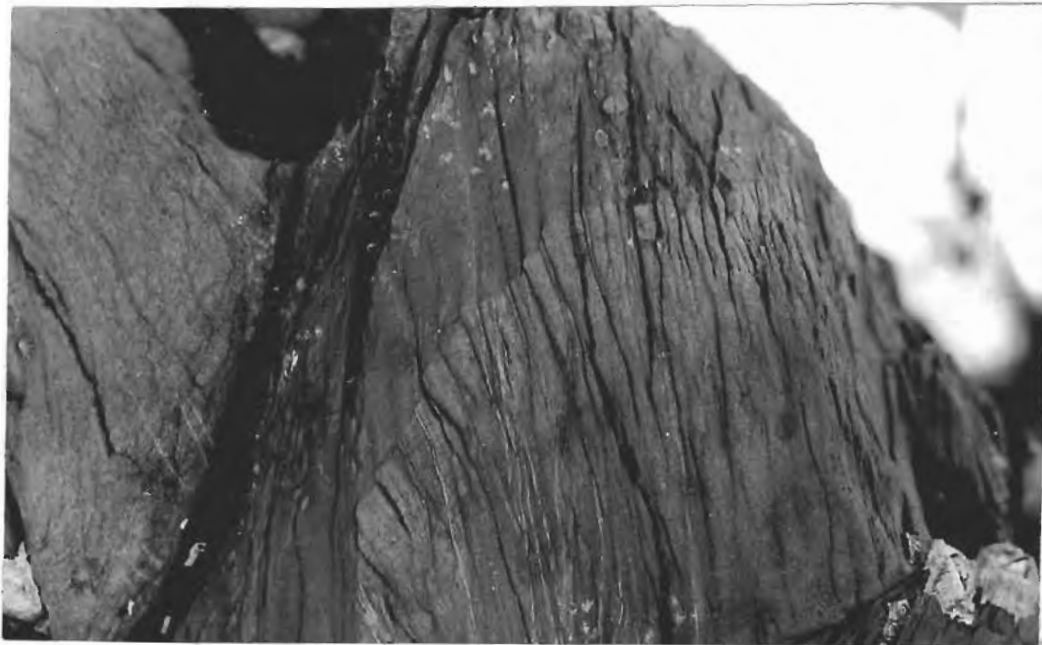


Fig. 3 - 23 (a). Left-hand limb of the anticline in Fig. 3 - 22 (a). Width of the photograph is approximately 15 cms.



Fig. 3 - 23 (b). A slate band immediately below Fig. 3 - 23 (a). Approximately 1 inch of rule is shown in the lower right-hand corner.

Fig. 3-23(a) is located on the left-hand limb of the anticline in Fig. 3-22(a). It shows the strong development of cleavage zones in the sandstone separating relatively non-cleaved blocks which in this example are less than 1 cm. wide. Discrete congruous displacements have occurred along the cleavage blocks. In the slate the spacing of the cleavage zones is much smaller and the cleavage appears penetrative to the naked eye.

Fig. 3-23(b) is located immediately below Fig. 3-23(a). It shows the cleavage extending from one sandstone bed through a thin slate layer into another sandstone bed. Individual cleavage zones can be traced right through, and although there is a refraction of about 25° from the light-coloured part of the upper sandstone bed to the slate there is no doubt that the cleavage is the same phenomenon in both rock types. Displacement of blocks along these cleavage zones can be seen in this light-coloured band, and in the slate there are many more, smaller displacements shown on thin sandy laminations. It is noteworthy that the cleavage transects a relatively undistorted flame structure in the middle of the photograph showing that,

- (1) the cleavage formed after load casting, and
- (2) the cleavage can not have formed as a layer-confined, shear cleavage induced by bedding-plane slip.

(c) THIN-SECTION DESCRIPTION

In thin-section the cleavage can be divided morphologically into two types.

(a) A non-penetrative cleavage resembling anastomosing veins, which occurs in the sandstones, and

(b) A cleavage which is penetrative to the scale of grains and which occurs in the slates.

This division corresponds broadly to the distinction between fracture and flow cleavage. However, both cleavages are intimately related in mode and place of occurrence, and in layers exhibiting refracted cleavage one type may grade into another.

The non-penetrative cleavage forms in those beds in which there is a predominance of roughly equidimensional grains, although these grains may be angular and extremely poorly sorted. The grain-size varies from medium-grained sand to fine siltstones, and the grains are mostly quartz. Particularly in the coarser sandstone sorting is extremely poor, and the cleavage is formed of ribbons of dark pelitic material up to 0.1 mm. thick. These ribbons wend their way through the matrix around the larger quartz grains, and are the surfaces along which the rock cleaves. Individual ribbons are spaced at intervals of 2 to 4 mms. apart, and smaller branches spread through the matrix which is weakly recrystallized and shows no marked reorientation of particles parallel to the cleavage surfaces. The rock as a whole may be described as non-cleaved blocks of sandstone separated by thin ribbons of pelitic material.

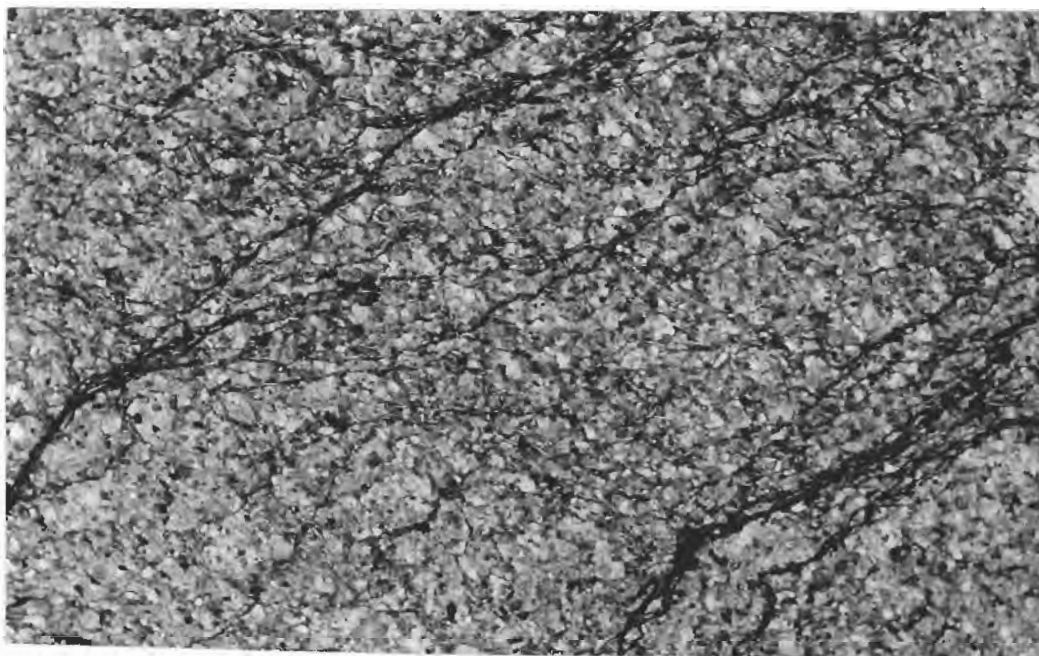


Fig. 3 - 24 (a). (33341) Non-penetrative sandstone-cleavage. Ribbons of dark pelitic material anastomose through the sandstone producing a fracture cleavage. The width of the field of the photo is approximately 4 mms.

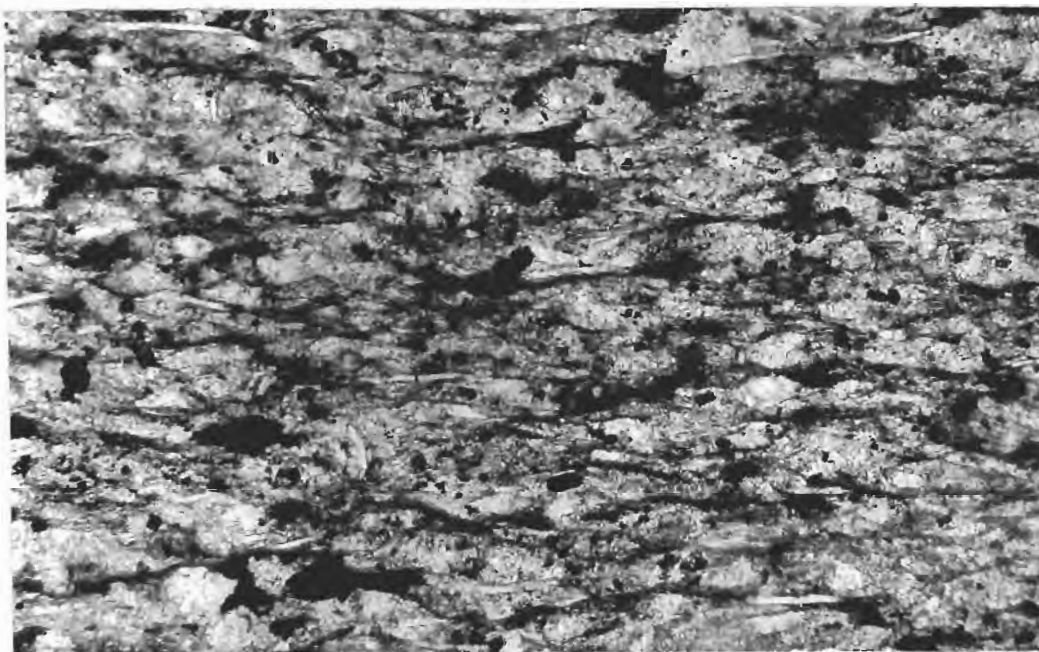


Fig. 3 - 24 (b). (33342) Penetrative slaty cleavage. Cleavage ribbons spaced on the scale of the larger clastic grains produce a strong planar cleavage in which most platy particles are oriented. The width of the field of the photo is approximately 0.8 mms.

Discrete displacements along the cleavage surfaces can be recognized. Bedding, marked by mineralogical banding, and quartz veins which cut the bedding, are displaced by movements along the cleavage. These displacements are in a congruous sense such that the block nearest the axial surface moves towards the convex surface of the fold. In most sections showing this non-penetrative type of cleavage the large quartz grains are quite severely fractured.

The penetrative cleavage forms in those beds where there is a predominance of platy particles, and these are the fine-grained rocks. The cleavage in the slate is distinctly different from the non-penetrative type in that the spacing of cleavage surfaces is on the scale of the clastic quartz grains. The diameter of the detrital muscovite flakes is slightly larger than the diameter of the quartz grains with which they are associated, and almost all the mica flakes are oriented parallel to the cleavage surfaces which are marked by dark pelitic material. However, the cleavage ribbons in the pelitic rocks are neither as wide or as widely spaced with respect to the scale of the detrital grains, as the ribbons in granular rocks. There has been some recrystallization of the finest material but this is too fine to be examined by normal microscopic methods.

(d) CONCLUSIONS

(1) The type of cleavage which forms in a rock depends not so much on grain-size as on the shape of the grains. If the rock is

composed predominantly of equidimensional grains a non-penetrative cleavage is formed, whereas if the rock has a preponderance of platy minerals a penetrative cleavage results. In this particular area the coarser rocks happen to be composed of equidimensional grains, the finer rocks of platy particles.

(2) Although there are discrete congruous displacements along the cleavage they are thought to be incidental to, and to have occurred after the formation of the cleavage. The overall mesoscopic geometry does not support a shear origin for the cleavage, and all mesoscopic displacements can be related to rotations associated with the tightening of local fold-hinges.

4. ORIGIN OF CLEAVAGE

(a) GENERAL STATEMENT

In broad terms there are four mechanisms commonly suggested whereby a flow cleavage can be developed in phyllosilicates in very low-grade rocks.

- (a) Physical rotation by flattening.
- (b) Physical rotation by simple shear.
- (c) Mimetic recrystallization.
- (d) Crystallization of new phyllosilicates.

To consider the applicability of these hypotheses in detail to the Sulphur Creek rocks it is convenient firstly to draw several

generalized conclusions about the nature of the cleavage based on the foregoing descriptions.

(1) The cleavage in both the sandstone and the slate has formed at the same time. The detailed mechanism of formation may not be the same for both cleavages, but the intimate spatial relationships throughout the whole region support this contention.

(2) Both cleavages are planar and probably formed in the plane of flattening, although there may not have been any appreciable flattening during cleavage formation. Such fanning and refraction as exists in some folds is localized, and not general in comparable positions throughout the region. The disorientations from a planar orientation are therefore thought to be caused by continuing deformation after cleavage formation.

(3) The cleavage was formed after the main P1 folding at Sulphur Creek and has only an incidental relationship to individual folds. On a larger scale it is parallel to the common limb of the regional dextral fold couple.

(4) There was only a small amount of deformation about the dextral couple during cleavage formation, and this may indicate a relatively short time of formation.

(5) Displacements along the cleavage are later than, and incidental to its formation. They are either movements geometrically related to the position in a fold which has continued to develop after cleavage formation, or late-stage sinistral movements along the cleavage.

(6) The general style of folding and flattening indicates that there may have been a considerable amount of water present in the rocks.

(b) DETAILED CONSIDERATIONS

(i) Physical rotation by flattening Consider an element of rock with a random orientation of platy particles. Let it be subjected to uniform flattening as defined earlier. It is simple to calculate the percentage of particles that lie between the plane of flattening and any chosen angle; for 50% flattening just under 40% of all particles will lie with their basal planes oriented within 10° of the plane of flattening, while for 75% flattening the figure is 80%.

The amount of flattening generally associated with folding in sandstones and slates is less than this, being of the order of 30% to 40% in the sandstones and slightly higher in the slate. If a muddy sediment is assumed to have an initial water content of 70% (Weller, 1959), then compaction to a shale with less than 10% water will correspond to a flattening of between 40% and 50%. Yet there is usually no cleavage produced by normal compaction, and when a cleavage does occur it is only a rudimentary parting parallel to the bedding. The fissility of slaty cleavage associated with folds is much more pronounced than the bedding-plane fissility of shales, indicating that there is a different type or degree of orientation of the platy particles. Hence the orientation of platy particles that produces slaty cleavage can not be accounted for simply by homogeneous flattening.

Nevertheless, numerous writers (Sorby, Sharpe, Leith, Cloos and many more recent workers) have arrived at the conclusion that slaty cleavage is formed in the plane of flattening, and the formation of slaty cleavage is usually loosely ascribed to the phenomenon of "flattening". If flattening, whether or not homogeneous, is considered as a necessary, and perhaps dominant process in the formation of slaty cleavage, there are at least two anomalous features which must be explained.

(a) The effect of preferred orientation of platy fragments before cleavage formation.

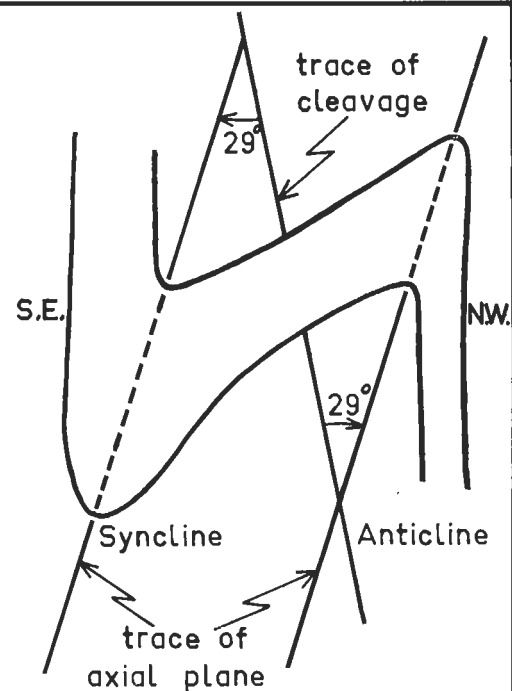
Collette (1958, p.121) noted that there is no reason why a random orientation of platy particles could be expected in a mudstone. Settling during sedimentation would tend to orient the basal plates of the micas and clays parallel to the bedding, and this would enhance the considerable orientation caused by compaction. This initial preferred orientation is perpendicular to the plane of flattening in the hinge region of the fold and tends towards parallelism in the limbs. Thus slaty cleavage should be more strongly developed in the limbs than in the hinge region, and immediately adjacent to the axial surface there should be a narrow zone of poorly developed cleavage where the initial preferred orientation is perpendicular to the plane of flattening. Homogeneous flattening would not change this orientation. In point of fact, the cleavage in the hinge zone is generally the most intensely developed cleavage.

(b) The flattening perpendicular to the cleavage may be very small.

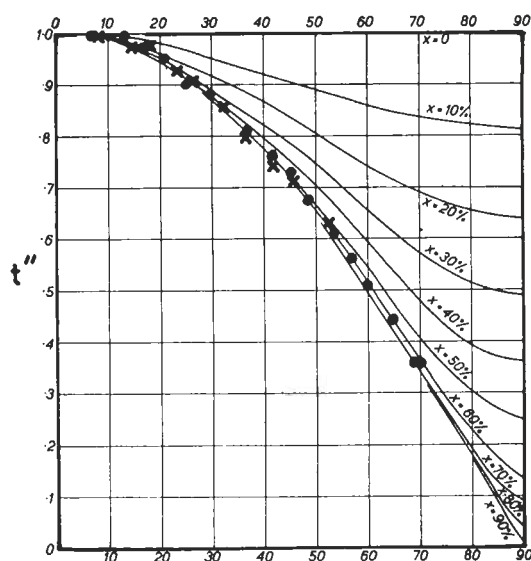
It has been argued up to this point that the overall amount of flattening in the cleavage plane is generally less than 40%, which in turn is less than the flattening involved in normal compaction. Notwithstanding this, in the Sulphur Creek folds it seems that the amount of flattening in the cleavage plane may be much less. Consider the fold in Fig. 3-25(a), which is a profile photograph of a fold couple in a thick slate band near the main syncline in Area C. The very thin sandy bands have acted only as markers, and the orthogonal-thickness ratios were calculated using the axial plane of the fold as the t_0 position. It was initially thought that the cleavage would be the plane of flattening, and that the angle for a particular ratio would have to be corrected by adding 29° on one limb and subtracting 29° on the other in order to give a symmetrical distribution of thickness ratios. Such is not the case. Figs. 3-25(c) and (d) show the orthogonal-thickness ratios for the anticline and syncline, respectively, using the axial plane as the plane of flattening. The anticline indicates uniform flattening of 50%, and the syncline uniform flattening of at least 60%. If there had been any appreciable flattening in the cleavage this would have distorted these curves. This phenomenon is not restricted to this one example as in all the folds on which flattening has been calculated, the axial plane was found to divide the orthogonal-thickness ratios symmetrically, whereas the cleavage plane did not.



(a)



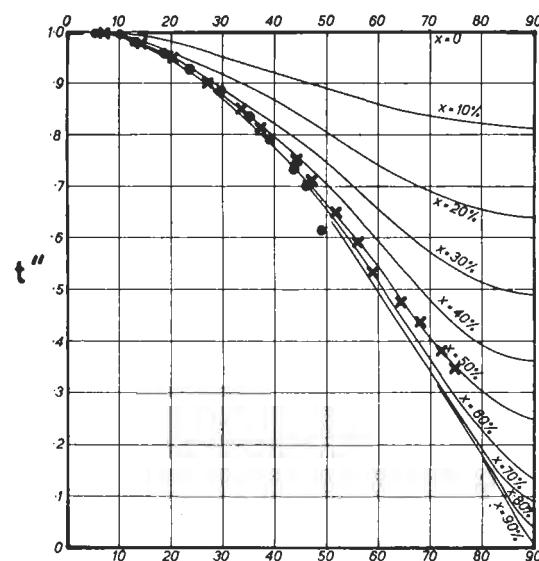
(b)



(c)

Anticline

× S.E.Limb
• N.W.Limb



(d)

Syncline

FIG. 3 - 25. (a) Profile photograph of a fold couple with oblique slaty cleavage, Area C. Six-inch rule shown. (b) Tracing of profile used to measure orthogonal thickness. (c) and (d) Orthogonal-thickness-ratio diagrams.

It can only be concluded that there is less than 10% uniform flattening in the cleavage plane.

(ii) Physical rotation by simple shear Physical rotation of platy particles by simple shear can not have produced the preferred orientation of phyllosilicates in the slates of Sulphur Creek. As O'Driscoll (1964) noted, the long axis of an originally spherical body distorted by simple shear is oblique to the shear surfaces, and its orientation depends on the amount and sense of displacement. If such shear planes exist, they must necessarily be parallel to the axial surfaces of the folds with opposed sense of rotation in either limb. Hence the cleavage in the slate should form a fan convergent towards the axial surface on the convex side of the layer. These fans do not exist at Sulphur Creek as the cleavage in the slate is essentially planar. Furthermore, in the transected cores the cleavage cuts from one limb to the other without distorting the profile of the fold.

It may be argued that large amounts of simple shear will bring the long axes of the strain ellipses almost parallel to the shear surfaces, and that the divergence would not be detected. This has not been the case at Sulphur Creek, for the bedding acts as a marker indicating the possible strain transverse to it, and there is no relation between either the intensity of the cleavage development, or the possible fanning, and the amount of simple shear indicated. In point of fact, there is no cleavage associated with the early P1 folds in which the amount of simple shear would have been greatest. The cleavage is more

closely related to the late P1 folds, and some of the best development of cleavage is in the most open folds.

(iii) *Mimetic Crystallization* Mimetic crystallization under differential stress during diagenesis could be invoked to explain the formation of cleavage in the slate. Ionic migrations in accordance with Reicke's Principle and dissolution of minerals metastable in the sedimentary environment would cause clays and micas in favourable directions to grow at the expense of minerals in other orientations. However, it is important to note that mimetic crystallization will not change the orientation of the basal plates of a micaceous mineral, since any overgrowth must either increase the size of the basal plate or add further layers to the already existing sheet structure. Thus, if there is only weak recrystallization it will not affect the overall distribution of crystallographic directions, and any method of measuring particle orientation equally weighting each particle will not detect the increased bulk heterogeneity. On the other hand, if the recrystallization is strong whole particles may disappear to form overgrowths on others with more favourable orientations. This mechanism becomes increasingly important with increasing temperature, pressure and time, and is probably one of the most common mechanisms of cleavage formation in metamorphic rocks. However, in the Sulphur Creek rocks recrystallization is weak, and many of the larger micas which facilitate the penetrative cleavage in the pelites can be recognized as detrital particles by their cloudiness and iron-stained margins.

(iv) Crystallization of new phyllosilicates Quite distinct from mimetic crystallization is the development of new phyllosilicates. It is frequently quoted that any new platy minerals will crystallize with their flat faces perpendicular to the greatest principal-stress axis (e.g. Billings, 1954, p.341). New minerals develop during metamorphism and the relationship between temperature, confining pressure and the new minerals is reasonably well known. However, much less is known of crystallization during diagenesis and in the lower grades of metamorphism, and whether there are any distinct mineral facies similar to the facies in the high-grade rocks, is not certain.

Maxwell (1962) claimed that the phyllosilicate facilitating cleavage in the Martinsburg slates was illite rather than sericite, and that overgrowths could be recognized on the detrital illites. I have attempted to treat the problem of whether sericite or illite would develop in diagenetic and low-grade metamorphic conditions in terms of the free energies of formation, but the results are not very satisfactory. Reesman and Keller (1965) have calculated the apparent free energies of formation of various minerals from experimentally determined solubility data. Calculations of the apparent free energy of formation of illite using their figures do not agree with the experimentally determined free energy from Beaver Bend quoted by the same authors (*ibid.*, p.1732), and it appears that the effects of colloidal suspension and surface reactions may be very important in any particular environment.

Nevertheless, although the dark material in the cleavage at Sulphur Creek has not been identified, it does not appear to be the same as either the large detrital micas or the small, newly crystallized sericites. The detrital micas are cloudy and commonly iron-stained around their margins or along their basal cleavage. The size of the flakes is a little larger than that of the detrital quartz grains, and they have commonly been bent by intergranular movements. The small, newly crystallized micas are clear, almost colourless flakes, an order of size smaller than the detrital mica flakes. They are evenly distributed throughout the sandstones, and do not appear to have a strongly preferred orientation. From these considerations I have concluded that the crystallization of new phyllosilicates has not caused the cleavage.

(v) Water-movement hypothesis I consider that explanation of the formation of cleavage at Sulphur Creek in terms of any of the four previously mentioned hypotheses, or any combination of them, is not satisfactory. Apart from the points already discussed, none of the hypotheses explains the formation of the narrow cleavage zones in the sandstone separating relatively non-cleaved blocks. This phenomenon, and all the others observed, can be explained by considering the cleavage to have formed by the movement of water out of the sediments under the influence of differential stress.

It has been shown through consideration of the style of folding that the Sulphur Creek rocks may have been only partially compacted at the time of deformation. A muddy sediment, if it is composed

predominantly of clay-sized platy particles, may be considered as a gel with a cardhouse or network pack, i.e. it has an open-framework structure with a low yield point which when exceeded, permits large amounts of flow (Kruyt, 1952 and van Olphen, 1963). The weight of the overburden is borne by the framework structure, and during normal compaction the rate of application of load is slow enough to allow the excess water to escape through the open voids to the surface. The pressure on the water is approximately hydrostatic, while the total pressure on the sediment is lithostatic, and in effect the open framework must bear the excess load. Thus, as the sediment is buried more deeply the pressure on the framework increases, and the chances of disrupting it are reduced.

However, if the rate of application of load is so rapid that the water can not escape, whether this be caused by sealing-off of the formation or the action of tectonic forces, the pressure of the water will increase rapidly until the whole load is borne by the water. The friction between the platy particles will be removed, and any small deformation will cause the gel to become unstable. If the mass is squeezed slightly the water in the card-house structure of platy particles will tend to move perpendicular to the maximum compressive stress. Since the platy particles are hinged to one another by electrostatic forces, the movement of the water out of the muddy mass will cause them to become strongly oriented parallel to its motion, irrespective of their original orientation.

The layers composed chiefly of equidimensional grains, the sandstones, behave differently. They do not develop a card-house structure, and hence when the card-house structure in the pelite collapses, the water pressure in the sandstones is not nearly as high. The water, escaping along the newly developed cleavage surfaces in the pelites, enters the sandstones along channels which branch out and anastomose in the general plane perpendicular to the maximum stress. Residual fluids from the pelite, bearing argillaceous material, move along these channels thereby equalizing the water pressure. As the water migrates out of the sediments along these newly formed cleavage ribbons, overgrowth and recrystallization occur thereby enhancing the cleavage. This mechanism is the same as the mechanism proposed by Maxwell (1962), with an extension to account for the cleavage in the sandstones.

5. REFRACTION OF CLEAVAGE

(a) GENERAL DESCRIPTION

Refraction of cleavage is the change in attitude of cleavage as it is traced through beds of different physical properties (Hills, 1963, p.297). Refraction does not occur in the hinges of folds, and the amount of refraction increases as the limbs approach parallelism with the axial surface. The cleavage in the pelitic bands is always more closely parallel to the axial surface than is the cleavage in the psammitic layers, and in graded beds the cleavage may form a continuous curve through almost a right-angle.

Fig. 3-26(a) shows refracted cleavage on the limb of a fold in Area E, as the cleavage surfaces pass from a thick sandstone layer into a slate band. The angle of refraction is 30° , but whereas the cleavage in the sandstone forms a small fan divergent outwards from the core of the fold, the cleavage in the slate is slightly convergent. In the slaty band itself there is some grading from very fine sandstone to argillite and the cleavage is continuously curved.

Fig. 3-26(b) illustrates refraction on the limb of an adjacent fold where there is an alternation of fine-grained sandstone layers and graded beds. The cleavage is planar in the beds of uniform composition but curves in the graded beds. The spacing of the main cleavage surfaces along which there has been some displacement in the sandstone, is fairly regular, and the blocks are about 0.2 to 0.5 cms. wide. In the pelitic bands the spacing decreases, and movements are taken up by smaller displacements on an increased number of surfaces so that non-penetrative movements along discrete surfaces can not be distinguished mesoscopically from penetrative flow.

(b) ORIGIN

The origin of refracted cleavage has not received much attention in the literature, but there are a number of ways in which it can possibly be formed.

(1) By varying the angle of internal friction depending on the rock type.

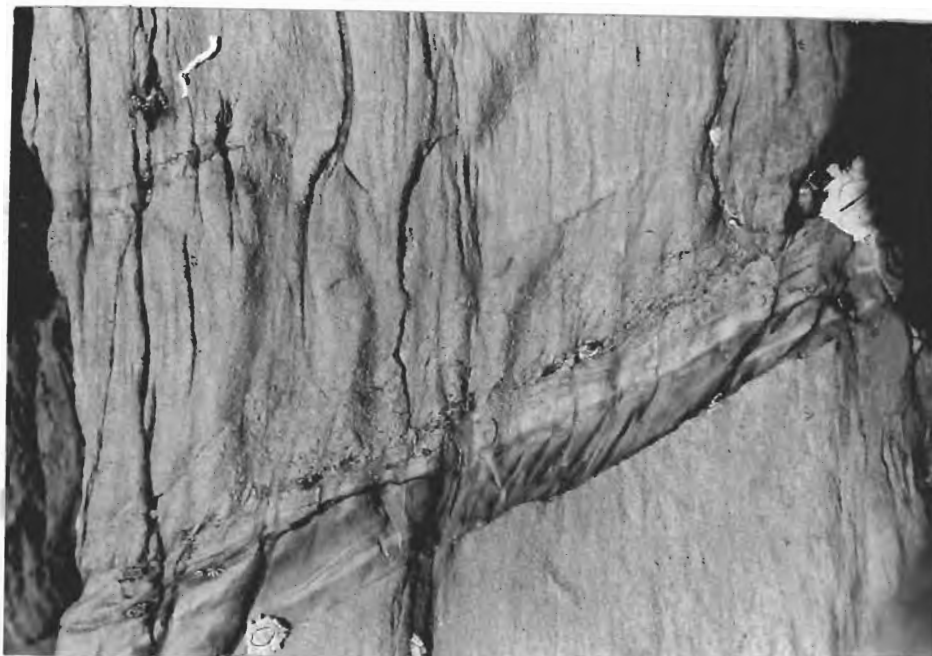


Fig. 3 - 26 (a). Refraction of cleavage in a thin slate band between two thick sandstone beds, Area E. The width of the photograph is approximately 15 cms.

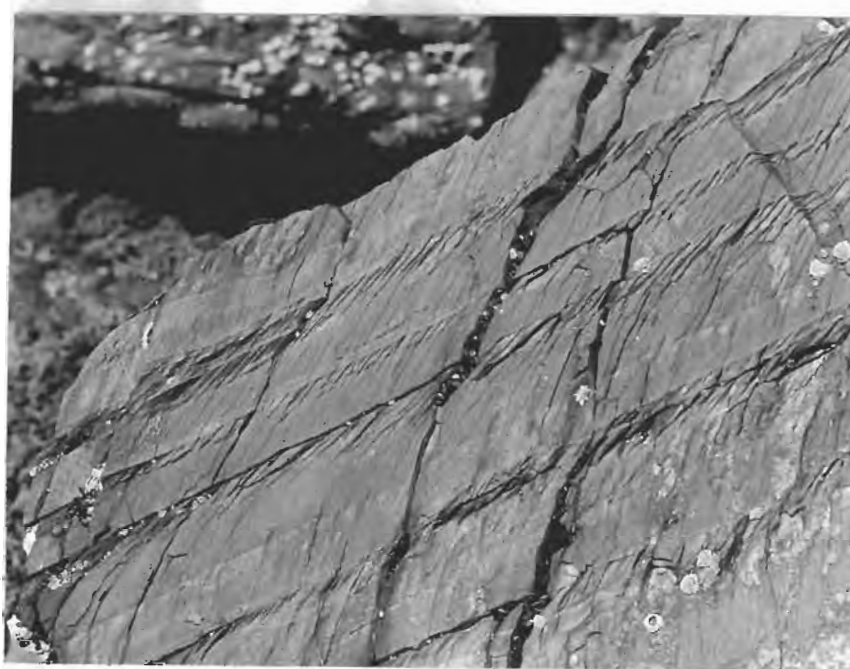


Fig. 3 - 26 (b). Refraction of cleavage in an interbedded sandstone-slate sequence on the limb of a fold from Area E, Sulphur Creek. The width of the photograph is approximately 30 cms.

(2) By continuous generation of a new cleavage in pelitic layers rotating in a constantly oriented stress field.

(3) By interlayer shear.

(4) By differential compaction.

In order to consider which, if any, of these mechanisms has operated at Sulphur Creek a brief statement of the nature of the refracted cleavage is necessary. Firstly, the refracted cleavage is the same cleavage as has been described earlier in this chapter - a penetrative cleavage in the pelites and a non-penetrative cleavage in the sandstones. Secondly, the amount of refraction is geometrically related to the position of the cleavage in the fold. There is no refraction in the hinge region, and refraction increases as the limbs approach parallelism with the axial surface. Thirdly, refraction is most common in the western parts of the Sulphur Creek area, and because the cleavage can be traced eastwards to where there is no refraction in comparable fold situations, it is reasonable to assume that the refracted cleavage was initially planar.

This last criterion eliminates the possibility of refraction being caused by different angles of internal friction in sandstones and slates since if the refraction is caused by an inherent property of the different rock types, it should have equal development in all comparable fold situations. Furthermore, for the different angles of internal friction to have any influence on the orientation of the cleavage, the cleavage must be formed as a shear plane, and this possibility has been rejected for the P1 cleavage at Sulphur Creek.

Voll (1960) proposed a mechanism of cleavage formation in which there is a continuous generation of a new cleavage in a rotating body. If there were continuous generation of cleavage in the pelitic bands, each new generation obliterating the old cleavage while there was only one generation of cleavage in the psammite, it is possible that refraction could be produced. However, no examples of a relict early cleavage have been found in the Sulphur Creek area, so that if such a mechanism operated, the successive generations of cleavage formed at very small angles to the old cleavage and completely reoriented the platy minerals. Yet the rotation of the planar fold elements in Areas C and D (Figs. 3-6 and 3-8) indicates that the cleavage formed while a relatively small amount of deformation was accomplished. On the basis of these considerations the continuous-generation mechanism can be dismissed.

In competent-incompetent folding interlayer shear accompanied by rotation of the competent layers towards the axial surface, is one of the dominant mechanisms of deformation. The strain is concentrated in the slaty bands. Thus, if at a certain stage a planar cleavage is formed throughout the fold, continuing deformation will cause,

(i) the cleavage in the sandstone to rotate out of parallelism with the axial plane, forming a fan divergent outwards from the core, and

(ii) the cleavage in the slate to rotate in an opposite sense to the sandstone cleavage under the influence of shear parallel to the bounding layer.

This is essentially the mechanism outlined by Hills (1963, p.297-8), and could account for all the observed phenomena.

It has been shown that a planar feature developed in a folded sandstone-mudstone sequence which is only partially compacted, will become curved by the subsequent dewatering (Fig. 1-7). The dewatering may occur in any geographical direction (usually parallel to the local plane of flattening) but because the surface area of the competent beds remains approximately constant, loss of water results in a uniform loss of thickness of the layer perpendicular to the bedding, irrespective of the orientation in the stress field. A planar feature which transects the bedding will therefore change its orientation depending on the amount of compaction (Fig. 1-8).

In the case of a folded sandstone-mudstone sequence with occasional graded beds such as at Sulphur Creek, some of the refraction in the limbs can be accounted for by differential compaction. It was noted before that refraction does not occur at the hinge and is most marked in the limbs. This is because at the hinge the cleavage is perpendicular to the bedding and therefore there is no change in its orientation caused by loss of water. On the limbs the cleavage forms an acute angle with the bedding so that refraction caused by differential compaction is to be expected. However, if differential compaction alone caused refraction at Sulphur Creek, it is implied that when the cleavage developed there was more water in the western part of the section than in the eastern part. This is unlikely as the

western part of the section was the most deeply buried part, and therefore might be expected to have had a lower water content than the eastern section.

(c) CONCLUSIONS

From the gross geometry of refracted cleavage it is not possible to distinguish between interlayer shear and differential compaction as possible causes of refraction. The style of folding indicates that there may have been considerable water in the sequence at the time of deformation. Nevertheless, the style of folding also warrants that interlayer shear was one of the dominant modes of strain, and that such strain was concentrated in the pelitic bands. Thus it is concluded that both interlayer shear and differential compaction may have contributed to the formation of the refracted cleavage.

6. THE NATURE OF THE P1 DEFORMATION AT SULPHUR CREEK

Up to this point the main structural features of the Sulphur Creek region have been individually described and interpreted. It is intended here to set out a general synthesis of my interpretation of the events which caused these features from the time of sedimentation to the end of the P1 deformation. In this respect four phases can be distinguished.

(a) THE EARLY DIAGENETIC PHASE

This phase embraces the time from sedimentation until the first deformation as a result of the P1 movement. The sedimentary environment has been fully documented by Gee (unpub. Ph.D. thesis, 1967), and it is sufficient to note that during this period of normal accumulation of geosynclinal sediments, load casts, flame structures and other features were formed. Intraformational open-cast slumps such as in Fig. 3-15(b) were also generated.

(b) THE EARLY P1 PHASE

The exact stage in the diagenetic history when the first P1 movement occurred is not certain. The Sulphur Creek sediments are the highest exposures in the Burnie Slate and Quartzite which is separated from the Ordovician by an almost right-angle unconformity. It is not possible to calculate a depth of burial. However, it is clear that the deformation occurred some time after the open-cast slumping, probably when the sediments were under some load, and the style of deformation indicates that there may have been a considerable amount of water present.

The whole P1 deformation at Sulphur Creek is caused by a persistent dextral couple. During the early deformation the folding was homogeneous in orientation and distribution throughout the sediments. The major synclines and anticlines with their congruous parasitic folds, were formed in the sandstone lenses, and in parts (e.g. Area A) the

sandstones were broken up and surrounded by pelite. The style of folding in the sandstones was concentric but the pelites were extremely ductile, and the overall shape of the profiles is similar. There is no cleavage associated with this early movement.

(c) THE CLEAVAGE FORMATION

The cleavage phase is thought to have been initiated when the water pressures in the pelite greatly exceeded the hydrostatic head and approached the lithostatic pressure. This was caused by sealing-off the sediments in such a manner that the water could not move out quickly enough to relieve the pore pressure developed during the deformation. When this pressure reached the lithostatic pressure there was rapid dewatering, which caused the platy particles in the pelites to orient parallel to the flow channels forming a penetrative slaty cleavage. The water pressures in the sandstones were lower than those in the pelites, and the pelite-bearing water intruded the sandstones forming a non-penetrative cleavage along the channels of intrusion. This cleavage formed perpendicular to the applied maximum compressive stress, and cut across the rocks independently of the existing structures. The volume of the pelites was reduced more than that of the sandstones, and the whole mass probably became stronger and more viscous than before.

(d) THE LATE P1 PHASE

After cleavage formation the dextral couple continued to act on the rock mass. However, the slate was much more viscous than before and the deformation became confined to narrow zones separating larger blocks which did not deform. This heterogeneity can be observed in the southwestern parts of Areas C and D. Folded folds, rotated cleavage, and displacements along the cleavage were formed. The slate being considerably more viscous than before cleavage formation, deformed by fracture and the larger slate areas were completely dissected into small lenses elongate in the cleavage plane. The style of folding was more open and heterogeneous with an increased variation in hinge orientations caused by drag between adjacent blocks. The sandstone beds were "fixed" in the slate after cleavage formation, and thus as the slate continued to compact the common limbs between adjacent hinges were stretched. The straight-bedded outer limbs away from the fold hinges were fractured and at their detached ends were stretched into boudins as they rotated closer towards the axial surface.

CHAPTER 4

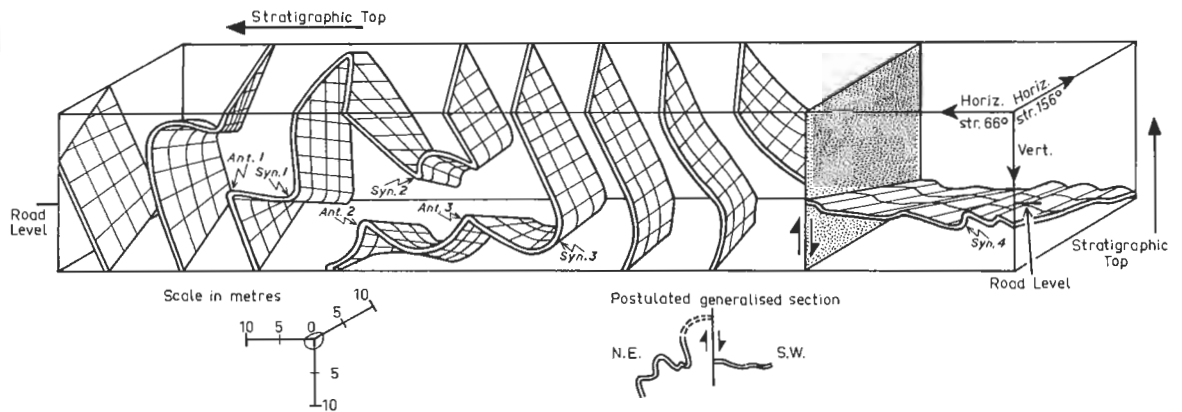
FOLDING IN INTERBEDDED SANDSTONES AND SLATES AT
TULLOCHGORUM, NORTHEASTERN TASMANIA.

1. INTRODUCTION

The Tullochgorum section is on the concave side of a broad corner on the Esk Highway at the 16-miles post from St. Marys to Conara. The section was photographed in a continuous strip, and the photographs were enlarged and used as a base map for all measurements.

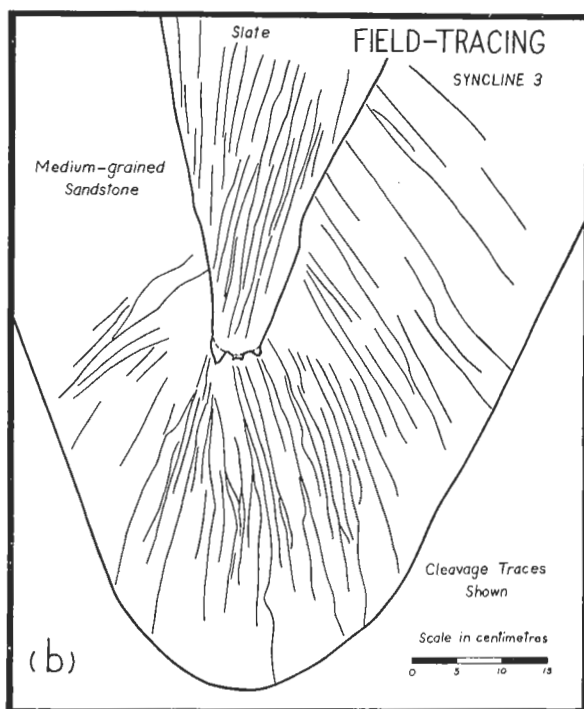
The strip can be divided into two parts. The northeastern part is composed of 60 metres of interbedded sandstones and argillites, overturned and dipping steeply to the southwest, which are separated by a vertical fault of unknown displacement from more gently dipping, right way-up strata at the southwestern end of the section. In the northeastern part there is a folded zone, stratigraphically 10 to 15 metres thick, with a series of three anticlines and three synclines, and it is this zone which has been examined in most detail. These folds are coupled in the sense of an overall drag of the northeastern

BLOCK-DIAGRAM OF TULLOCHGORUM ROAD SECTION ISOMETRIC PROJECTION

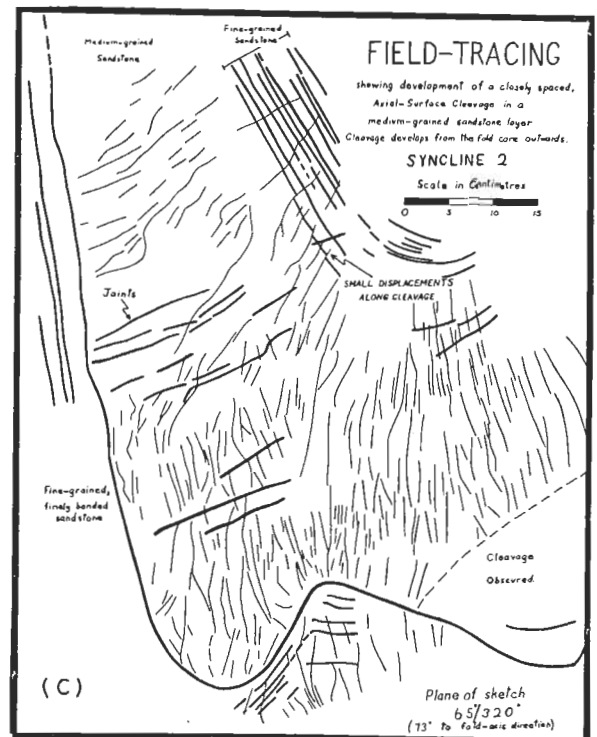


(a)

Layers shown are stratigraphically 10 metres apart



(b)



(c)

side upwards, and Fig. 4 - 1 (a) is a block-diagram showing layers stratigraphically 10 metres apart. In the southwestern part of the section there are some open flexures, one syncline being sufficiently well exposed to be examined in detail.

The composite fold data for the whole section is shown in Fig. 4 - 2 (a). The fold-axes were calculated from bedding-pole distributions, and the bedding / cleavage intersections were calculated stereographically for each point of measurement. Axial planes were estimated both in the field and from stereographic reconstructions for each fold. There is some spread of the fold-axes, although no more than is normal for one phase of folding. Bedding / cleavage intersections give consistent axes except in one case, Syncline 3. The fold-axes on different sides of the fault zone diverge, and this is probably caused by a small amount of rotation of the fault blocks.

Fig. 4 - 3 (a) is a cross-section reconstructed from both photographs and field-measurements. The rocks are composed of two lithic groups, medium-grained sandstones and argillites, and the sandstones which wedge out laterally form 75% of the exposed section. The environment of deposition appears to have been deltaic lagoons where the argillites were formed in bodies of protected water into which the sandstones were sporadically sedimented. Visual estimations of grain-size show that the folding occurred in the zone with the highest proportion of argillite,

FOLD ELEMENTS AND JOINTS

EQUAL-AREA PROJECTIONS

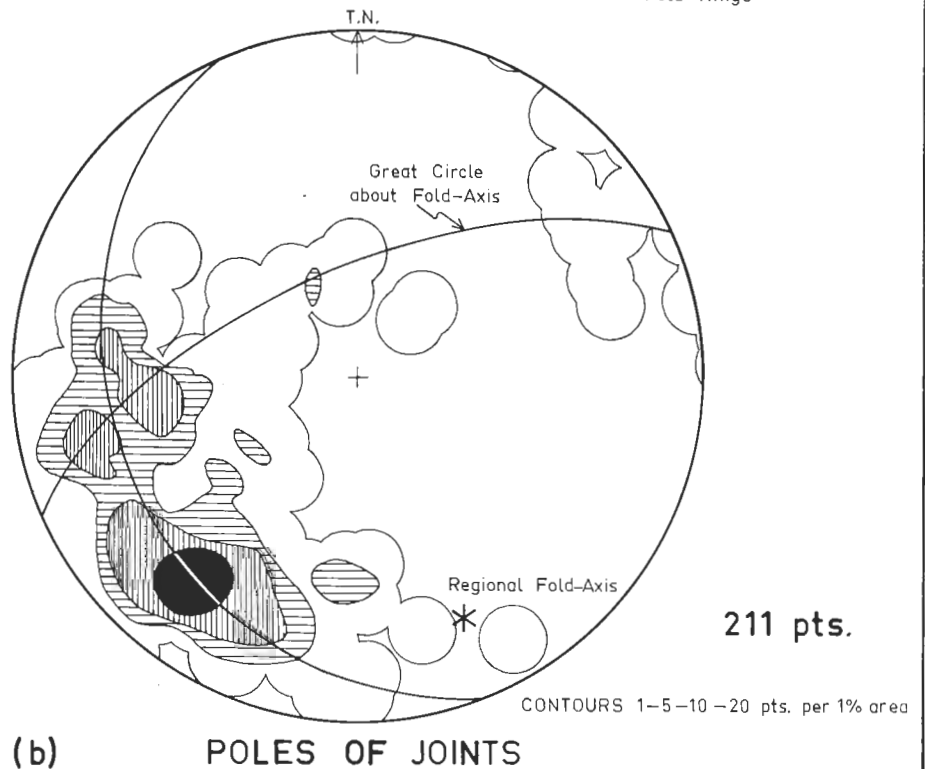
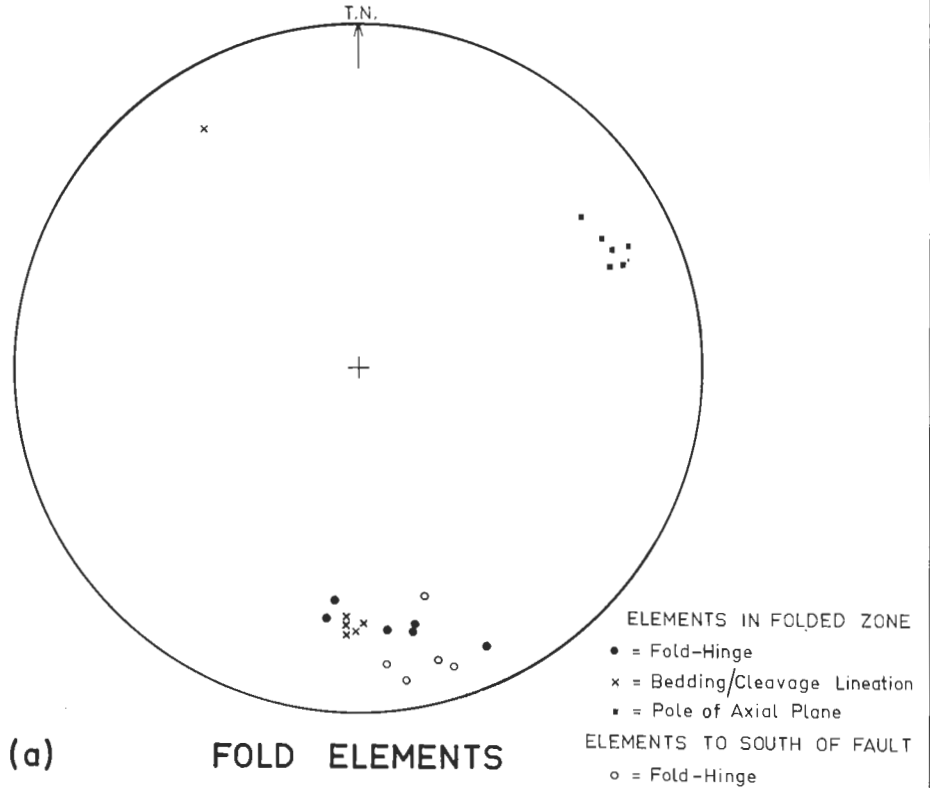
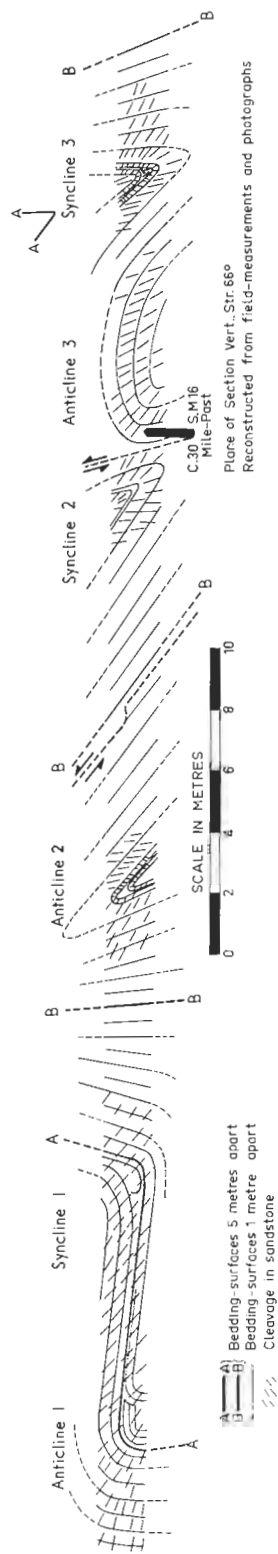


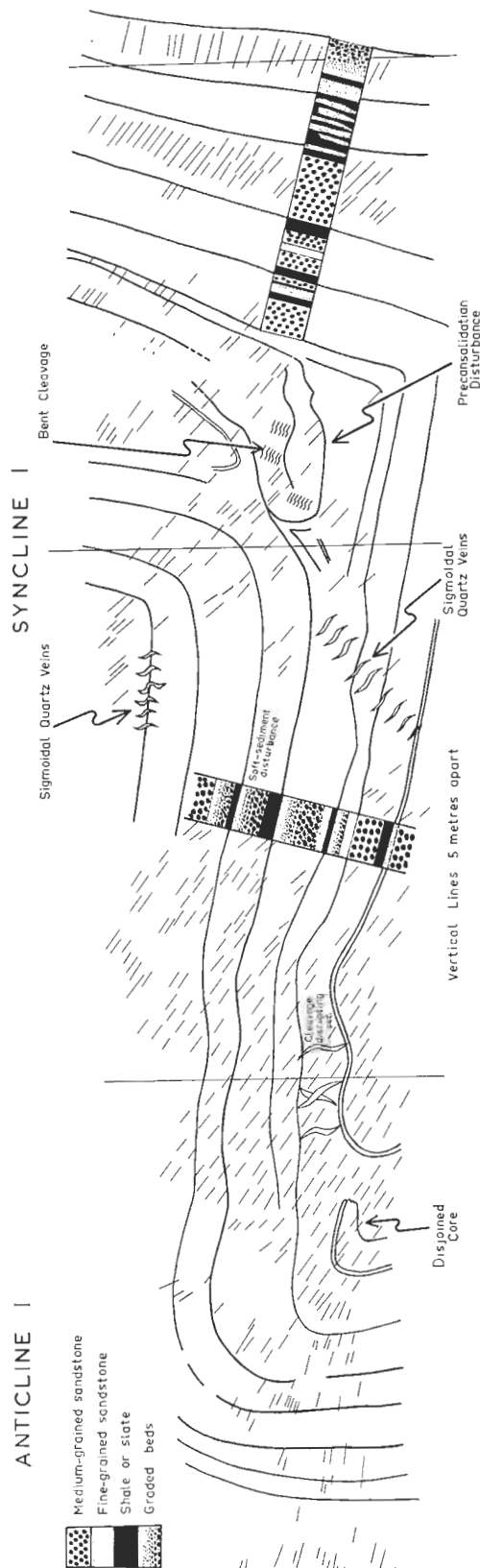
FIG: 4-2

CROSS-SECTION THROUGH FOLDED ZONE, TULLOCHGORUM

(a)



(b)



but within this zone there is considerable variation in the proportion of sandstone.

The style of folding is related to the particular location in primarily concentric folds which occur in the thickest sandstone bands (e.g. Anticlines 1 and 3, and Syncline 1). On the concave side of these concentrically folded bands the thinner sandstone layers have been flattened perpendicular to their axial surfaces and form concertina-style folds such as Anticline 2 and Syncline 3. Both these fold styles are genetically related.

2. STRUCTURAL DESCRIPTIONS

(a) ANTICLINE 1 AND SYNCLINE 1

Anticline 1 and Syncline 1 [Fig. 4 - 3 (b)] are a pair of coupled folds, and Figs. 4 - 4 and 4 - 5 show the structural elements. Both the fold-axes calculated stereographically from bedding-plane measurements, and the axial surfaces are essentially parallel. The style of folding is concentric although primary variations in the thickness of layers are too large to permit useful field-measurement of orthogonal thicknesses. One bed in particular shows large lateral variation in thickness from the anticline to the syncline, and on the steep limb of Syncline 1 it has been thickened to several times its original thickness by a preconsolidation disturbance. Bedding surfaces within this layer are very hard to

STRUCTURAL ELEMENTS, ANTICLINE I EQUAL-AREA PROJECTIONS

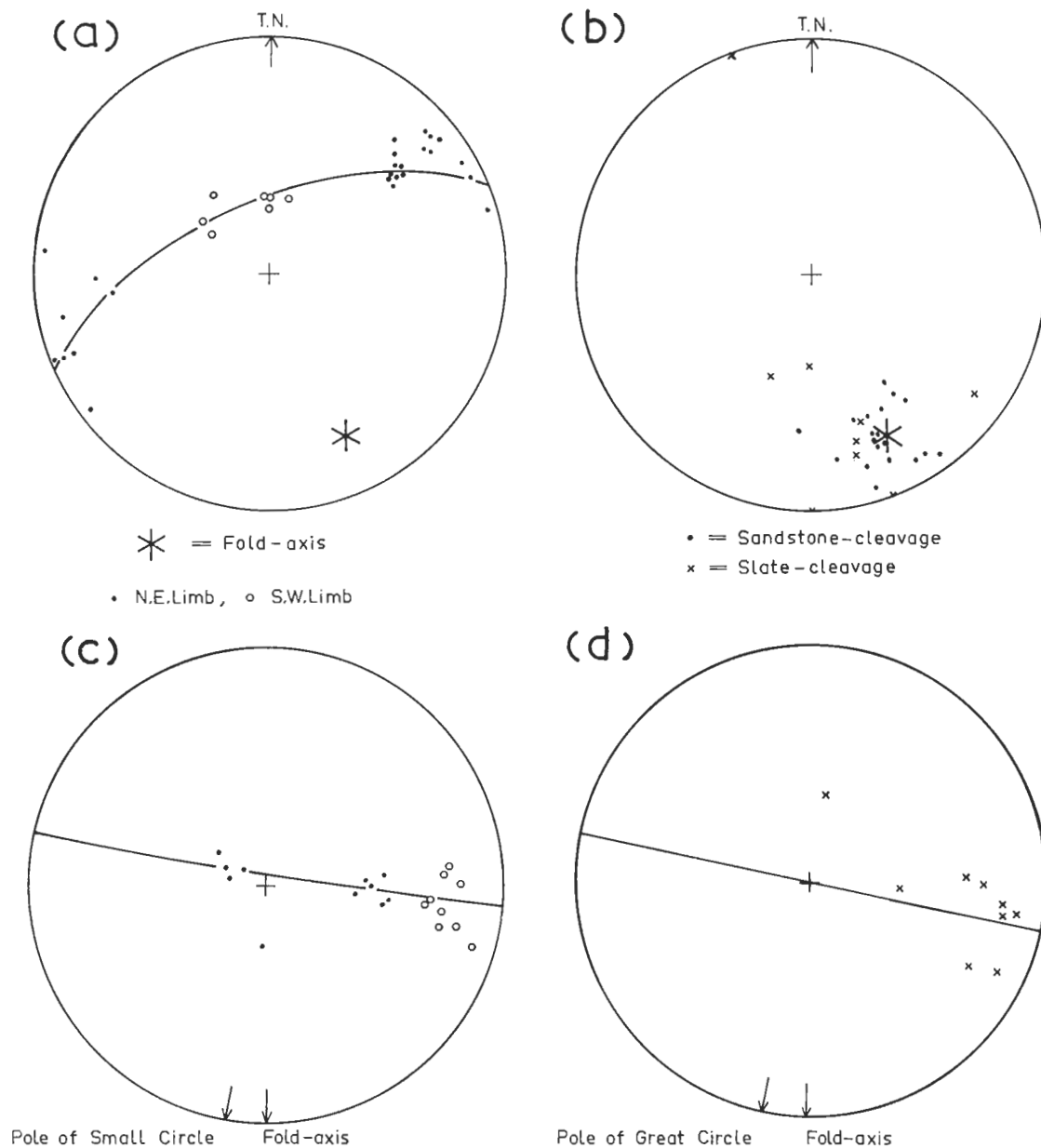


FIG:4-4. (a) Poles of bedding, 32 pts. Fold-axis plunges 27°/158°.
 (b) Calculated bedding/cleavage intersections, 27 pts.
 (c) Poles of sandstone-cleavage rotated as the fold-axis is rotated to the horizontal, 19 pts. 84° small circle is 10° clockwise of fold-axis.
 (d) Poles of slate-cleavage rotated as the fold-axis is rotated to the horizontal, 8 pts. Great circle is rotated 10° clockwise from fold-axis.

trace but are highly contorted and form the structure shown in Fig. 4 - 3 (b).

The core Anticline 1 is disjoined, and the bed that has broken is a fine-grained sandstone layer which is finely laminated in its upper part. There is no evidence of slickensliding, granulation and polishing, or any other indication of brittle-rock fracture, and the broken layer seems completely welded into its surroundings. The cleavage in and around the disjoined core is not refracted or otherwise disturbed, and it appears that this structure formed when the rock was only partly consolidated and capable of welding such a fracture.

The distribution of cleavage in the folds is shown in Figs. 4 - 4 (c) and (d) and Figs. 4 - 5 (c) and (d), after the fold-axes have been rotated to the horizontal. The cleavage in the sandstone in Syncline 1 appears to be reasonably symmetrical about a small circle coaxial with the fold-axis, but in Anticline 1 the small circle is rotated 10° clockwise. The cleavage in the slate does not show any unusual relation with the fold-axis and is approximately parallel to the axial surface. Bedding / cleavage intersections in the sandstone layers give axes showing good agreement with the bedding-pole fold-axes, but the bedding / cleavage intersections in the slate show a variable distribution, probably because of the very small angle between the bedding and the cleavage. Large sigmoidal quartz veins occur throughout these two folds and their significance is considered

STRUCTURAL ELEMENTS, SYNCLINE I

EQUAL-AREA PROJECTIONS

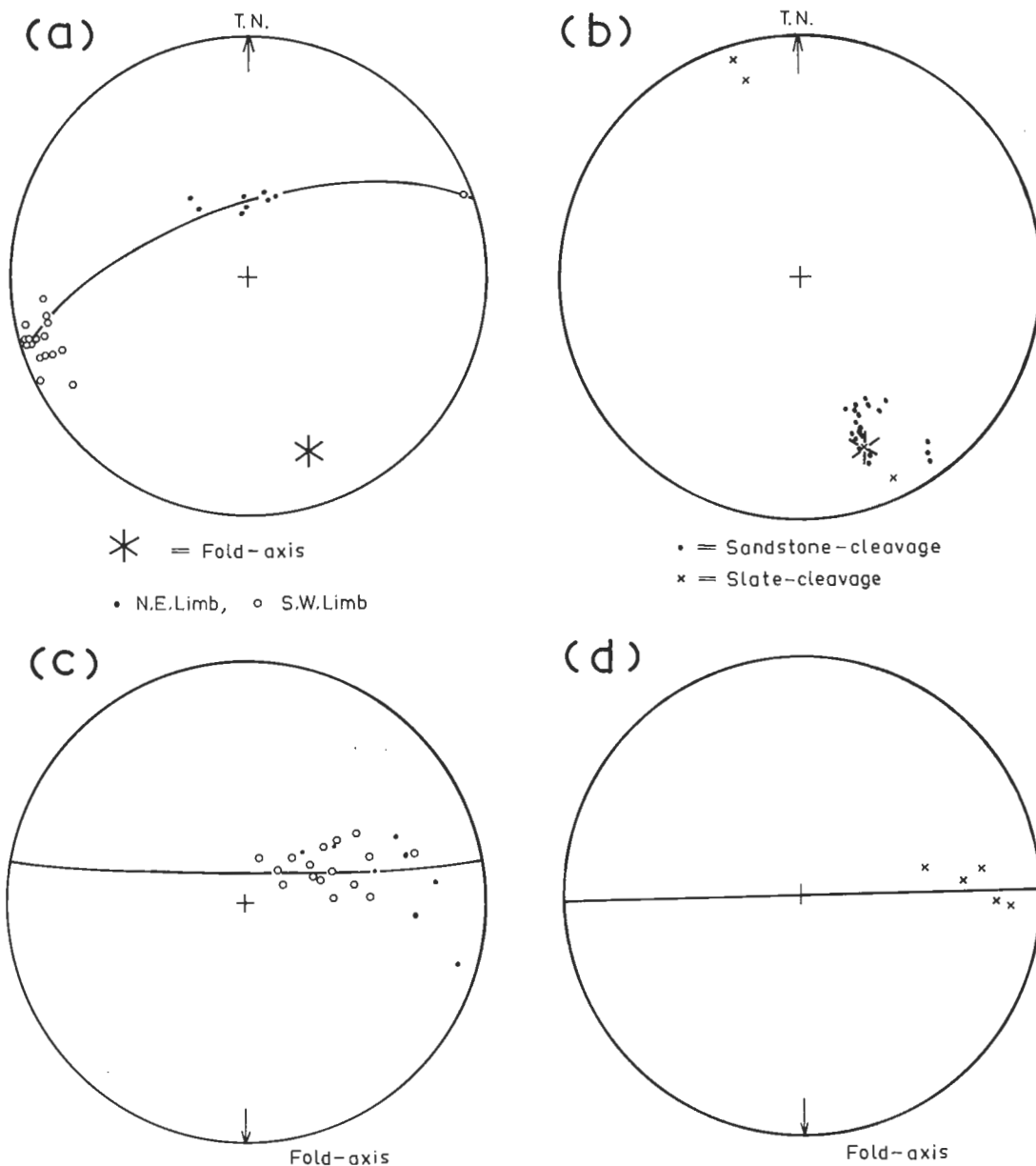


FIG: 4-5 (a) Poles of bedding, 25 pts. Fold-axis plunges $25^{\circ}/160^{\circ}$
 (b) Calculated bedding/cleavage intersections, 24 pts.
 (c) Poles of sandstone-cleavage rotated as the fold-axis is rotated to the horizontal, 24 pts. 80° small circle coaxial with fold-axis.
 (d) Poles of slate-cleavage rotated as the fold-axis is rotated to the horizontal, 5 pts. Great circle is coaxial with the fold-axis.

in the section on jointing.

(b) ANTICLINE 2.

The tracing from photographs of anticline 2 is shown in Fig. 4 - 6 (a). It is the same anticline as figured by Williams (1965, p. 231, Fig. 2), and is composed of interbedded slate and sandstone layers, the latter being 20 to 30 cms. thick. The fold has a small apical angle, and is overturned and facing towards the northeast. It is symmetrical about its axial surface, and the exposed core region is flanked by massive sandstones on the outer arc. The individual sandstone layers have folded to the limit of concentric folding permitted by their proximity to the adjacent competent layers, and flattening in the sandstone layers perpendicular to the axial surface of any particular layer reaches 30% in the hinge region. It is noteworthy that the axial surface is not planar, and changes orientation as it passes from sandstone to slate. The plane which divides the orthogonal-thickness ratios symmetrically in the sandstones is the axial plane of the particular layer, and thus the apparent flattening is not perpendicular to the mean axial plane for the fold.

The geometry of the structural elements is shown in Fig. 4 - 7. The fold-axis defined by the poles of bedding [Fig. 4 - 7 (a)] plunges $23^{\circ}/154^{\circ}$, which is in good agreement with the calculated bedding / cleavage intersections in Fig. 4 - 7 (b). The small apical angle

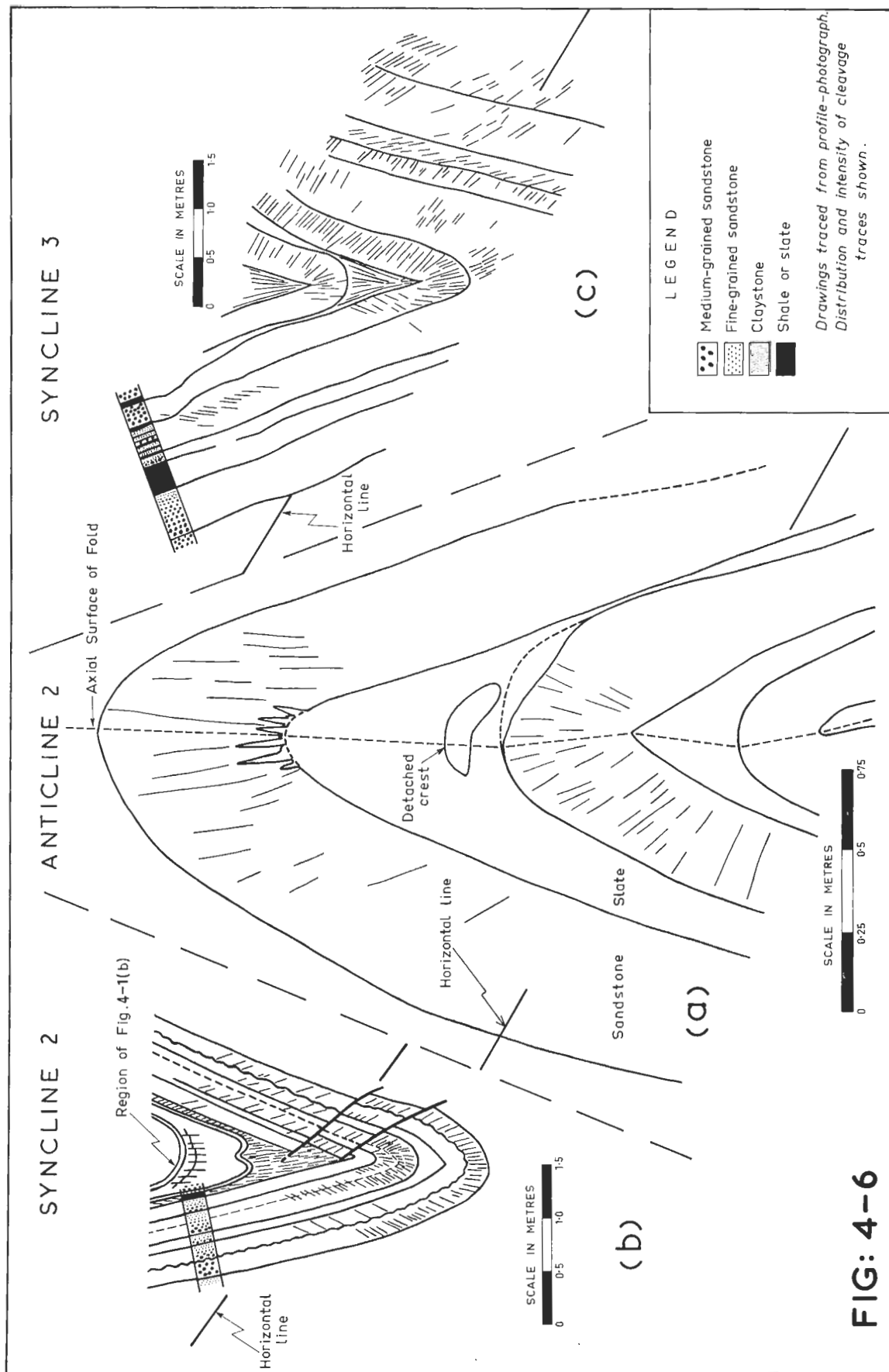


FIG: 4-6

is reflected in the restricted spread of the bedding poles. The cleavage in the sandstone [Fig. 4 - 7 (c)] is distributed reasonably symmetrically about a great circle coaxial with the fold-axis, but the mean cleavage in the slate appears to be inclined to the average axial plane, $57^{\circ}/229^{\circ}$, at 12° in a clockwise sense of rotation [Fig. 4 - 7 (d)].

An interesting phenomenon is the small segment of sandstone which has been detached from the crest of the folded bed. This piece of sandstone appears firmly welded into the slate filling, and must have been detached when such a fracture was capable of being welded. Detachments of this type have not been noted in any other part of the section so that it is probably related to the folding process.

(c) SYNCLINE 2

Syncline 2 [Fig. 4 - 6 (b)] is a tightly compressed, overturned, northeastward - facing fold with the sandstone layers of the outer arc folded in an essentially concentric fashion. The sandstone layers in the core of the fold on the concave side of the concentrically folded layers have been flattened perpendicular to the axial plane, and Fig. 4 - 1 (c) is a tracing of the core made in the field. The pelitic layers have deformed to fill the interspaces between the competent beds, and in the limbs faults caused by extension parallel to the axial surface are terminated in the pelite where strains that are relieved by fracture in the sandstone are accommodated by plastic

STRUCTURAL ELEMENTS , ANTICLINE 2

EQUAL-AREA PROJECTIONS

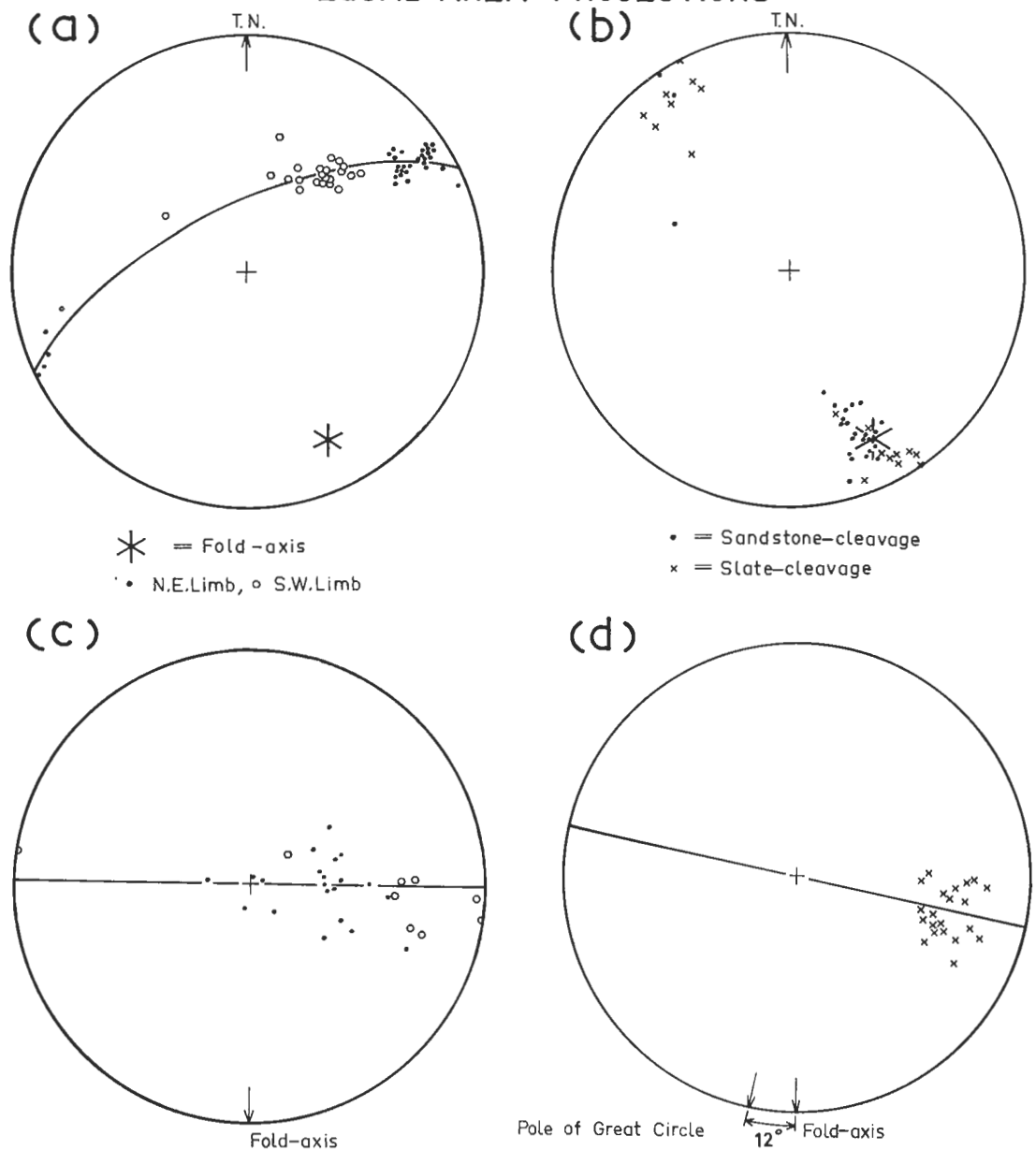


FIG:4-7 (a) Poles of bedding, 55 pts. Fold-axis plunges $23^{\circ}/154^{\circ}$.
 (b) Calculated bedding/cleavage intersections, 42 pts.
 (c) Poles of sandstone-cleavage rotated as the fold-axis is rotated to the horizontal, 29 pts. Great circle is coaxial with the fold-axis.
 (d) Poles of slate-cleavage rotated as the fold-axis is rotated to the horizontal, 21 pts. Fold-axis is inclined 78° to the great circle.

flow. The small faults on the southwestern limb are caused by squeezing against the adjacent Anticline 3 which is composed of stronger, massive sandstones [Fig. 4 - 3 (a)].

The geometry of the structural elements is shown in Fig. 4 - 8. The fold-axis defined by the bedding poles which are clustered in two groups reflecting the long straight limbs and narrow hinge region, plunges $33^{\circ}/171^{\circ}$, and is in good agreement with the bedding / cleavage intersections in Fig. 4 - 8 (b). The poles of the cleavage in the sandstones are distributed symmetrically about a great circle coaxial with the fold-axis, and the poles of the cleavage in the slate are remarkably planar and parallel to the pole of the axial plane, $56^{\circ}/235^{\circ}$. The cleavage in the slate in this syncline is the best approximation to a cleavage parallel to the axial plane of a fold in all the folds examined.

(d) ANTICLINE 3

Anticline 3, in contrast to Anticline 2 and Synclines 2 and 3, is a more open, concentric fold asymmetrical about its axial surface. It is composed of thick, massive, medium-grained sandstone beds with little or no interlayered pelite. Stratigraphically, it lies above the pelitic beds in Anticline 2 [Fig. 4 - 3 (a)], but below the pelitic layers in Synclines 2 and 3. The sandstone beds appear to have bent without fracture, and the overturned northeastern limb has been thinned in a zone of extension.

STRUCTURAL ELEMENTS, SYNCLINE 2

EQUAL-AREA PROJECTIONS

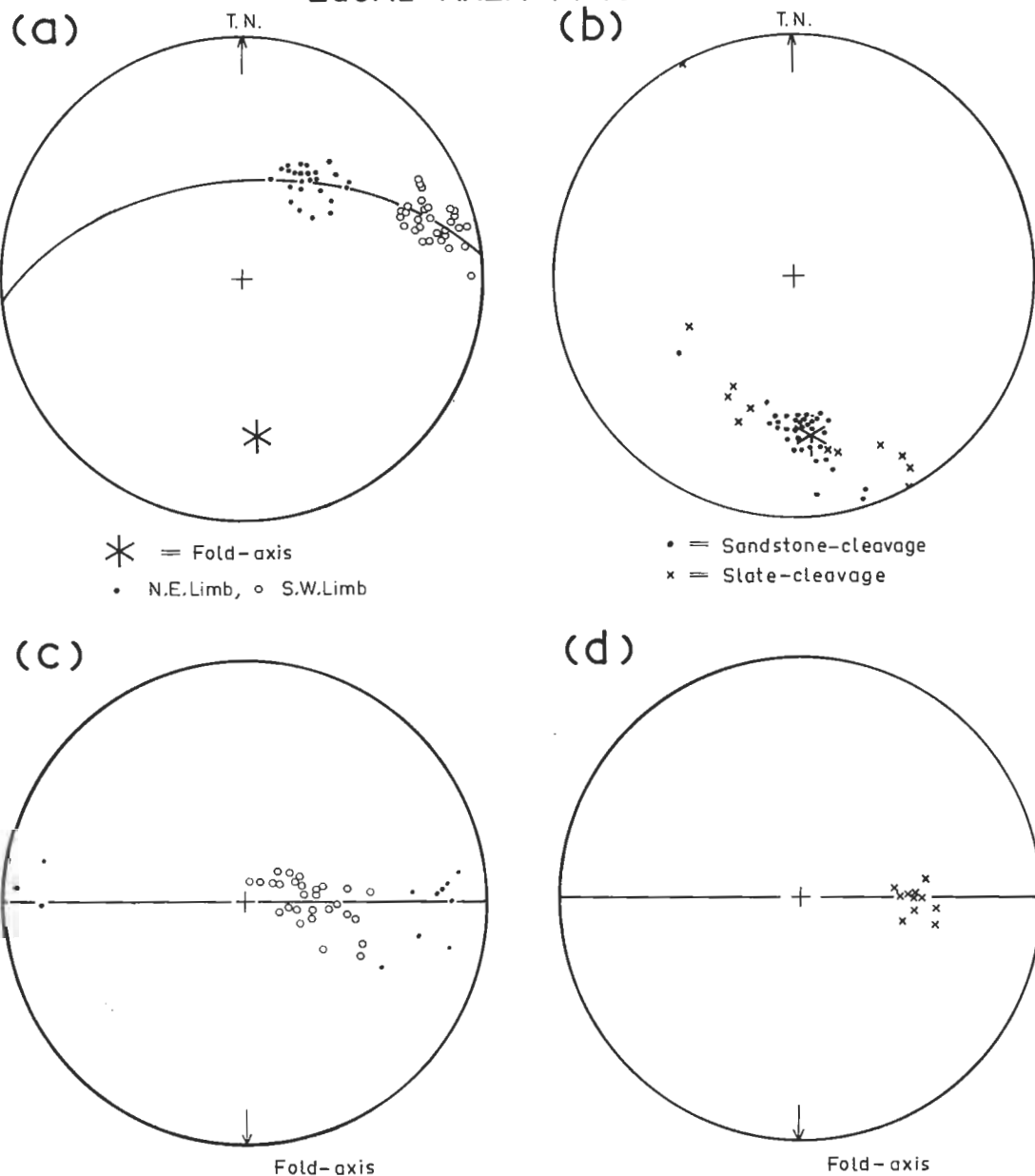


FIG:4-8 (a) Poles of bedding, 55 pts. Fold-axis plunges $33^{\circ}/171^{\circ}$.
 (b) Calculated bedding/cleavage intersections, 45 pts.
 (c) Poles of sandstone-cleavage rotated as the fold-axis is rotated to the horizontal, 40 pts. Great circle is coaxial with the fold-axis.
 (d) Poles of slate-cleavage rotated as the fold-axis is rotated to the horizontal, 11 pts. Great circle is coaxial with the fold-axis.

The geometry of the structural elements is shown in Fig. 4 - 9. The poles of the bedding in Fig. 4 - 9 (a) show a more even great-circle distribution than in any of the other folds, and give an axis plunging $28^{\circ}/173^{\circ}$. The calculated bedding / cleavage intersections in Fig. 4 - 9 (b) show a close agreement with this fold-axis, the tail towards the southeast being caused by the effect of Syncline 3 on the western limb. The poles of the cleavage in the sandstone in Fig. 4 - 9 (c) have a symmetrical distribution between a small circle of 84° and a great circle, both coaxial with the fold-axis. There are too few cleavages measured in the slate to be important, although it may be significant that they show considerable scatter. The axial plane is estimated as $60^{\circ}/235^{\circ}$.

(e) SYNCLINE 3

Syncline 3 is shown in Fig. 4 - 6 (c) and Fig. 4 - 1 (b), and is the same syncline as figured by Williams (1965, p. 234, Fig. 5). In field-outcrop the fold is overturned, but it is symmetrical about its axial surface and has a tightly compressed core of interbedded sandstone and slate, with the outer arc composed of massive sandstones. These massive sandstones on the outer arc in either limb have acted as strong blocks causing most of the deformation in the fold to be localized in the pelitic core. Flattening perpendicular to the axial plane in the core has reached 30%.

STRUCTURAL ELEMENTS , ANTICLINE 3

EQUAL-AREA PROJECTIONS

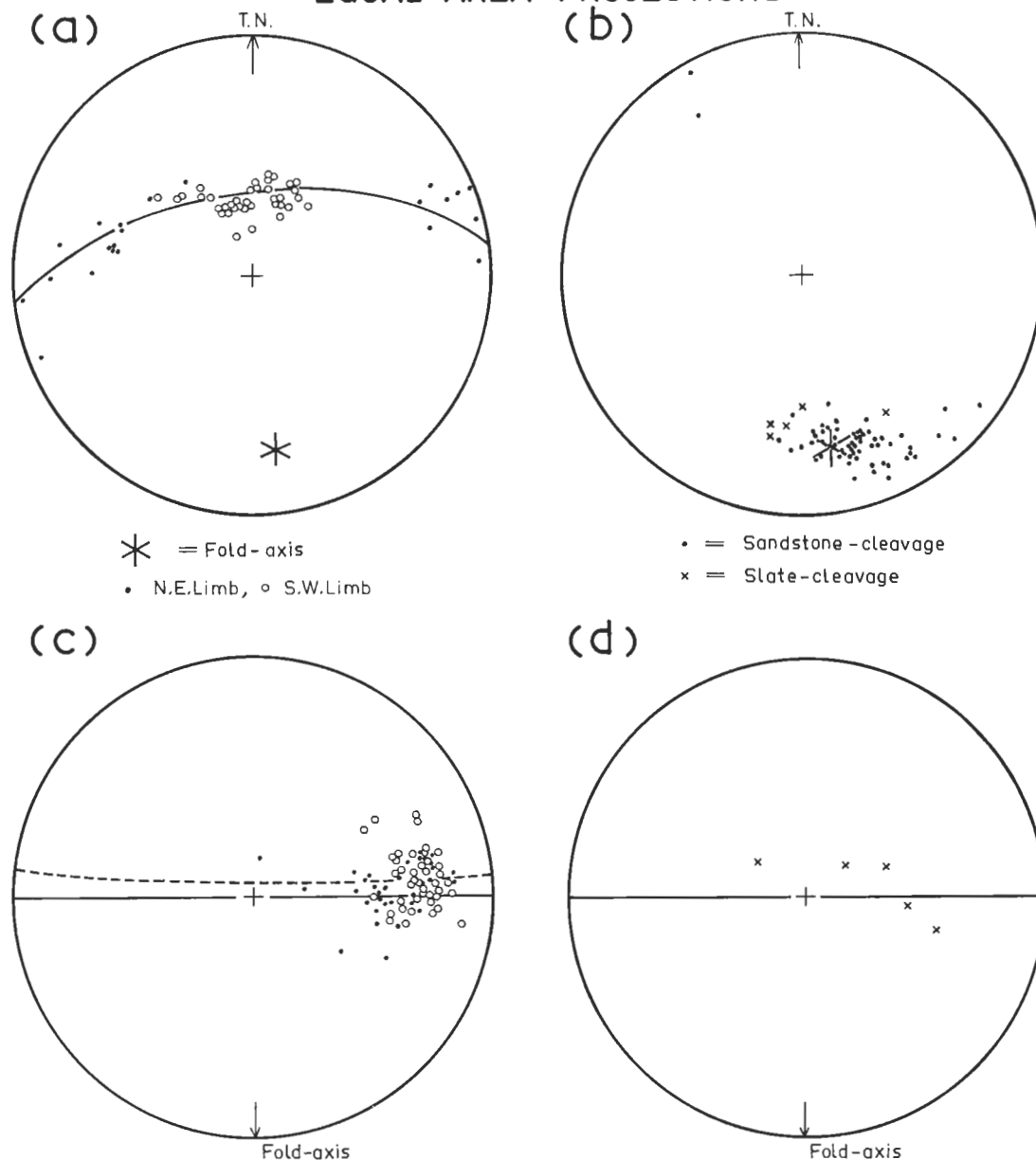


FIG: 4-9 (a) Poles of bedding, 59 pts. Fold-axis plunges $28^{\circ}/173^{\circ}$.
 (b) Calculated bedding/cleavage intersections, 67 pts.
 (c) Poles of sandstone-cleavage rotated as the fold-axis is rotated to the horizontal, 75 pts. Great circle and small circle of 84° are both coaxial with the fold-axis.
 (d) Poles of slate-cleavage rotated as the fold-axis is rotated to the horizontal, 5 pts. Great circle is coaxial with the fold-axis.

The geometry of the structural elements is shown in Fig. 4 - 10, and in many ways this fold is anomalous compared with the other five folds considered. The fold-axis defined by the poles of bedding plunges $12^{\circ}/141^{\circ}$, and this direction lies 20° away from the direction defined by the grouping of the other five fold-axes. The bedding / cleavage intersections in the sandstones, which in each of the other five folds show good agreement with the fold-axis calculated stereographically from bedding poles, are even further divergent from the mean fold-axis than is the bedding-pole fold-axis.

The scatter of the bedding / cleavage intersections is not random but has a distinctly planar trend [Fig. 4 - 10 (b)]. This is caused by rotation between the limbs of the fold about an axis normal to the axial plane. Figs. 4 - 11 (a) and (b) illustrate the disorientation of a β -lineation by rotation of one of the limbs. If one limb is held fixed and the fold-axis rotates through an angle, α , then the lineation on the other limb will rotate through the angle, 2α . The lineation in this case becomes a folded lineation and may be treated as outlined by Ramsay (1960).

In Syncline 3 the amount of rotation is not large and is schematically indicated in Fig. 4 - 11 (c) where the northeastern block has been rotated anticlockwise with respect to the southwestern block. Which block has remained fixed, or whether both blocks have rotated is not known and could be determined only by regional considerations. The parallelism of the bedding / cleavage intersections

STRUCTURAL ELEMENTS, SYNCLINE 3

EQUAL-AREA PROJECTIONS

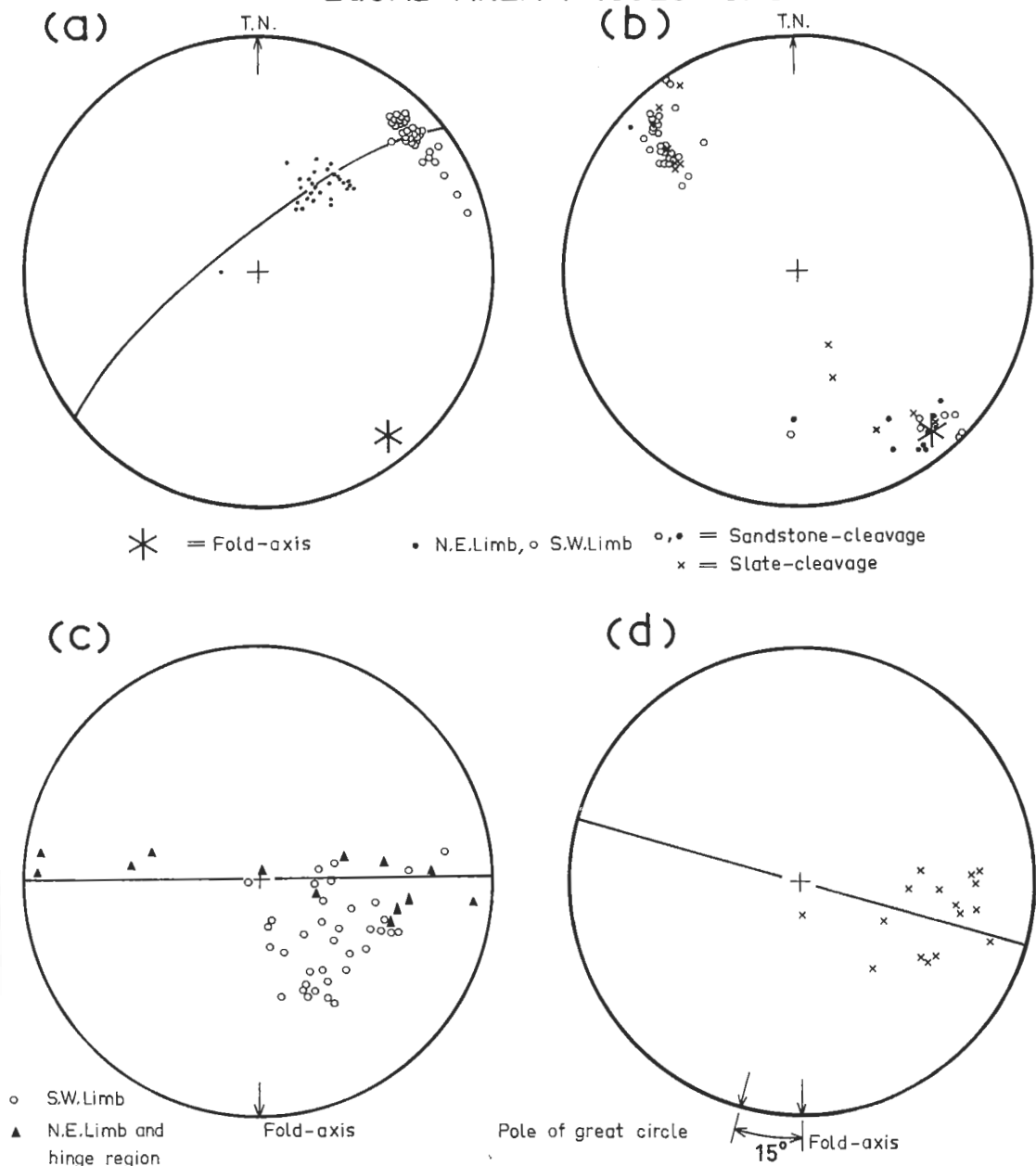


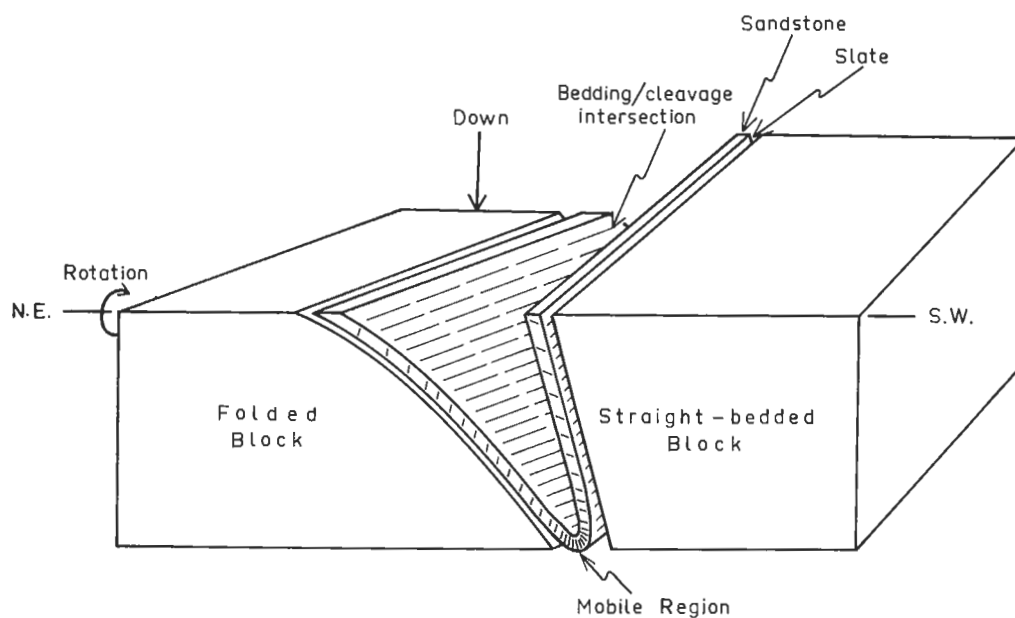
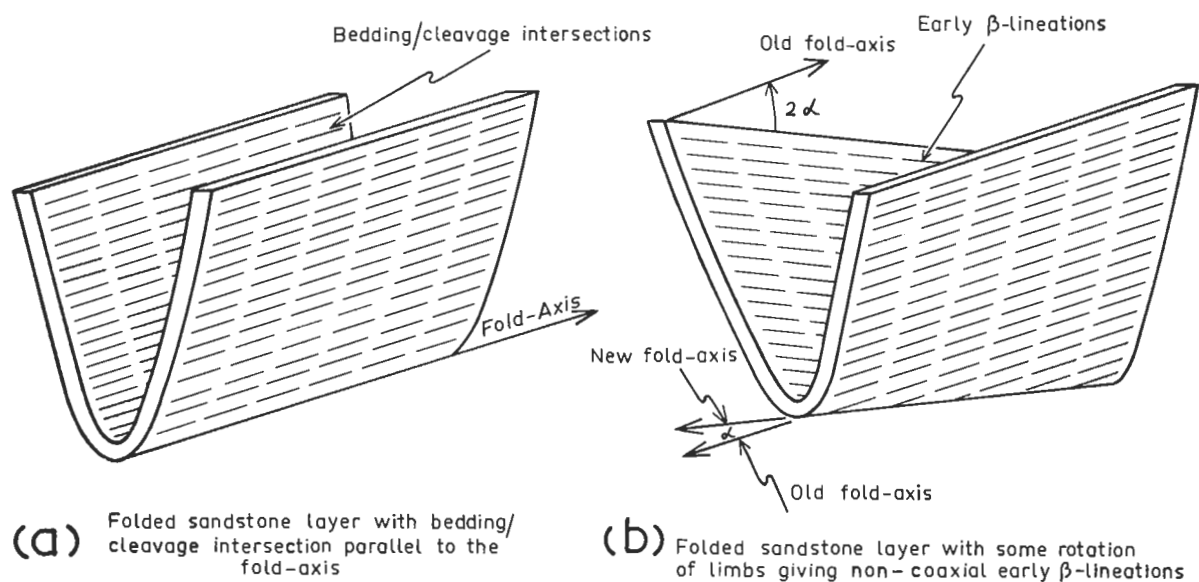
FIG: 4-10(a) Poles of bedding, 66 pts. Fold-axis plunges $12^{\circ}/141^{\circ}$.

(b) Calculated bedding/cleavage intersections, 57 pts.

(c) Poles of sandstone-cleavage rotated as the fold-axis is rotated to the horizontal, 49 pts. Fold-axis is perpendicular to the great circle.

(d) Poles of slate-cleavage rotated as the fold-axis is rotated to the horizontal, 16 pts. Fold-axis is inclined at 75° to the great circle.

EFFECTS OF ROTATION ON β -LINEATION DURING FOLDING



(C) Block-diagram showing sense and type of rotation involved in Syncline 3

with the fold-axes in the other folds indicates that almost all of the rotation in the section was accomplished in this syncline. This scissor-like rotation also accounts for the somewhat anomalous distribution of the poles of cleavage in the sandstone [Fig. 4 - 10 (c)] where the cleavage in the northeastern limb is markedly inclined to the axial plane, $55^{\circ}/231^{\circ}$. The cleavage in the slate is also inclined to the axial plane at 15° in a clockwise sense of rotation.

(f) SYNCLINE 4

Syncline 4 is an open, asymmetrical fold in the southwestern part of the Tullochgorum section where the folding is not as intense as in the northeastern part and the beds are generally gently dipping and right way-up (Fig. 4 - 1). Syncline 4 is the best developed fold of a series of open flexures in this part of the section and the axes of these folds are plotted as open circles in Fig. 4 - 2 (a). The fold is composed of interbedded sandstones and slates with essentially the same fold style as in the northeastern part of the section where more massive sandstone layers form the outer arcs of the concentric folds. However, in Syncline 4 there has been little or no flattening perpendicular to the axial surface which dips gently to the southwest.

The geometry of the structural elements is shown in Fig. 4 - 12. The bedding / cleavage intersections in the sandstone [Fig. 4 - 12 (b)] are in reasonable agreement with the fold-axis, $16^{\circ}/149^{\circ}$, determined from the poles of bedding. However, the bedding / cleavage intersections

STRUCTURAL ELEMENTS SYNCLINE 4

EQUAL-AREA PROJECTIONS

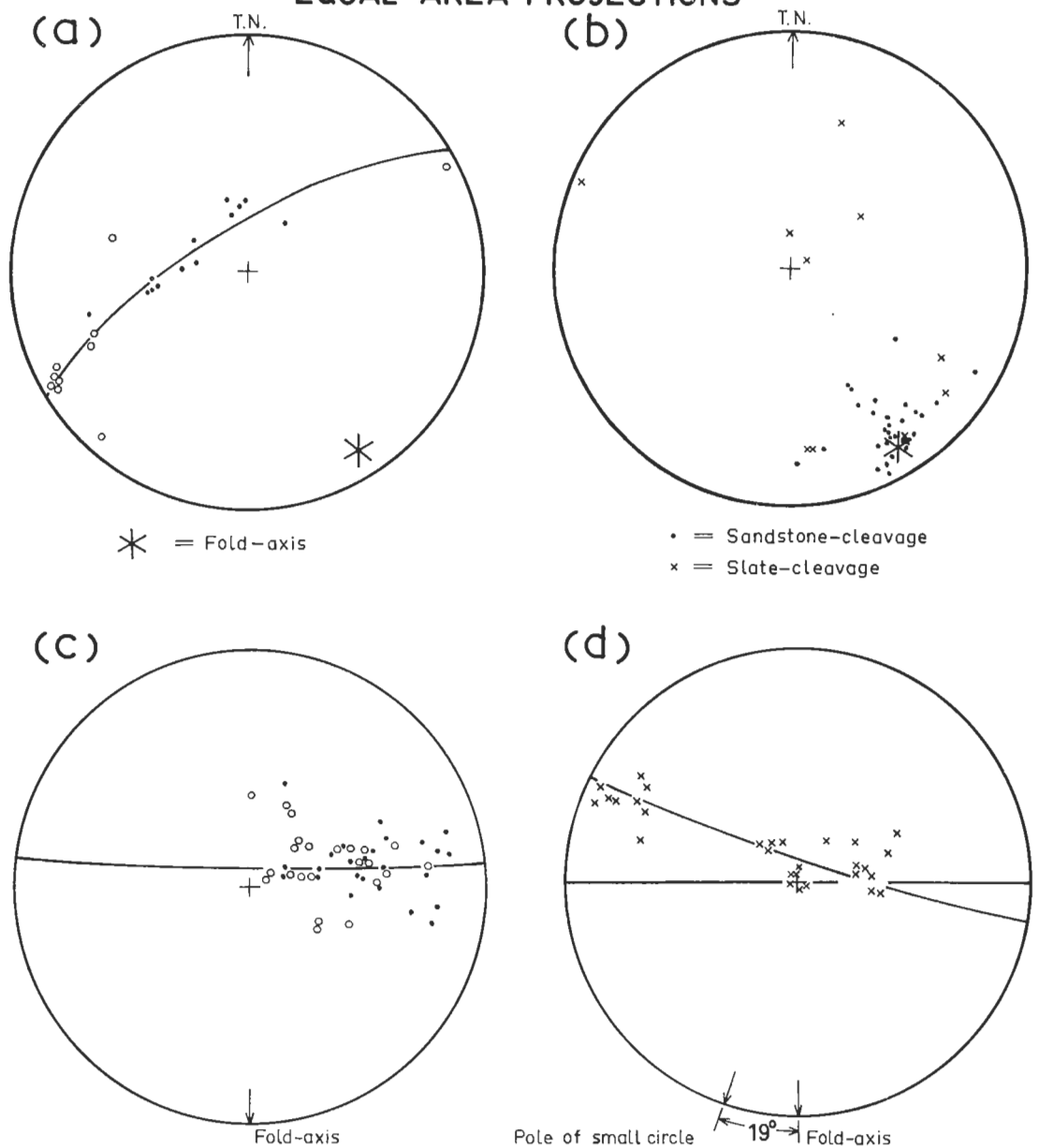


FIG:4-12 (a) Poles of bedding, 23 pts. Fold-axis plunges $16^{\circ}/149^{\circ}$.
 (b) Calculated bedding/cleavage intersections, 40 pts.
 (c) Poles of sandstone-cleavage rotated as the fold-axis is rotated to the horizontal, 48 pts. 84° small circle is coaxial with the fold-axis.
 (d) Poles of slate-cleavage rotated as the fold-axis is rotated to the horizontal, 29 pts. Axis of 82° small circle diverges 19° from the fold-axis.

in the slate show no symmetrical relationship with the fold-axis, and are much more randomly distributed than intersections in the slate in the folds from the northeastern part of the section.

The orientation of the cleavage in the sandstone after the fold-axis has been rotated to the horizontal is shown in Fig. 4 - 12 (c). A small circle of 84° coaxial with the fold-axis is marked, and the cleavage is symmetrically distributed about this surface. However, the cleavage in the slate layers [Fig. 4 - 12 (d)] is not only non-coaxial with the fold-axis but also distributed about a small circle of 82° , the axis of which is 19° oblique to the fold-axis in a clockwise sense of rotation. Although in other folds examined the cleavage in the slate is non-coaxial with the fold-axis, in all cases it is an essentially planar feature. The distribution about a small circle indicates that the cleavage in Syncline 4 has been folded with the bedding. The cleavage maintains a variable, though always acute angle with the bedding throughout the fold, and in the core region it is almost perpendicular to the axial surface. In order to understand this orientation it is necessary to consider the deformation of a pre-existing slate-cleavage in a concentrically folded, interbedded sequence of psammities and pelites.

(g) FOLDED SLATE-CLEAVAGE

When a pre-existing cleavage in a slate in an interbedded sandstone-slate sequence is deformed during cylindroidal concentric

folding of the sandstone layers, the resulting distribution of poles of cleavage may be non-coaxial with the poles of bedding. Hannan (1961) and Stauffer (1964) have considered the geometry of conical folds, Stauffer considering two cases;

(1) pure rotation of the surface with no strain component in the folded plane, and

(2) flattening of a circular conical fold.

In the case under consideration there is a strain component in the folded plane, and no flattening perpendicular to the axial surface.

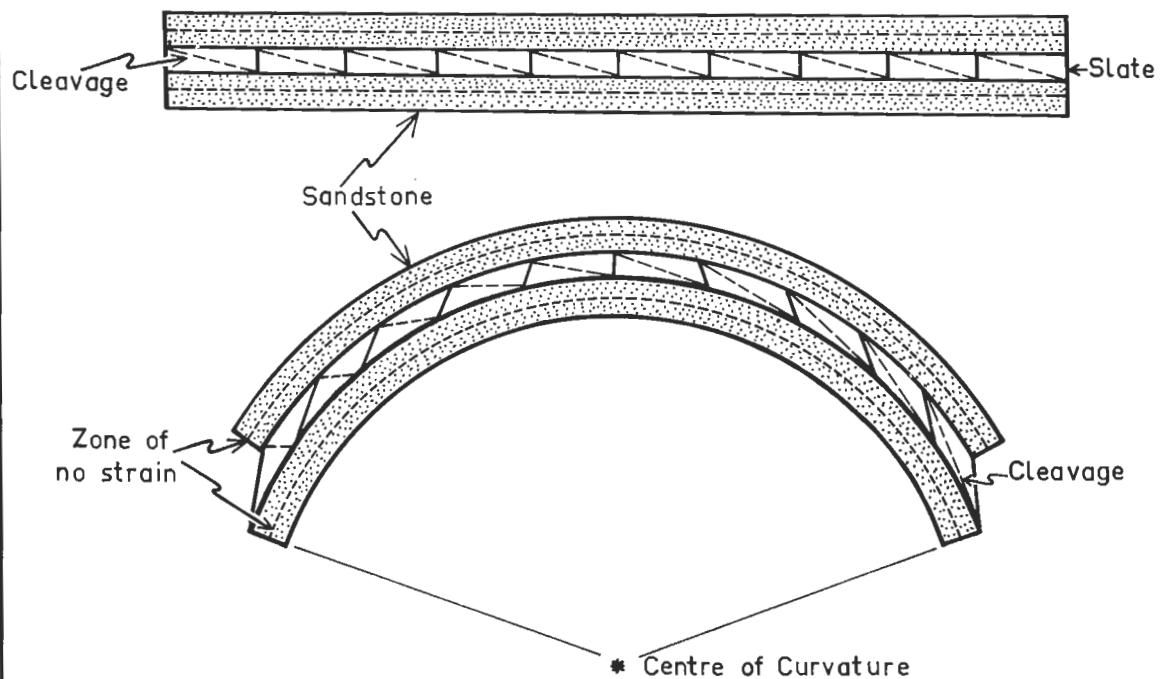
The orientation of the cleavage in Syncline 4 suggests that it is an early developed cleavage, and I have assumed by analogy with the straight-bedded limbs in the northeastern part of the section, that the cleavage had a constant orientation with respect to the bedding before the later folding. The interlayer slip necessary for the concentric style of folding in Syncline 4 was accomplished by layer-parallel shear in the slate bands. Hence deformation of the pre-existing cleavage in the slate during the later folding can be divided into two components.

(1). Strain within the layers parallel to the layer boundaries, and

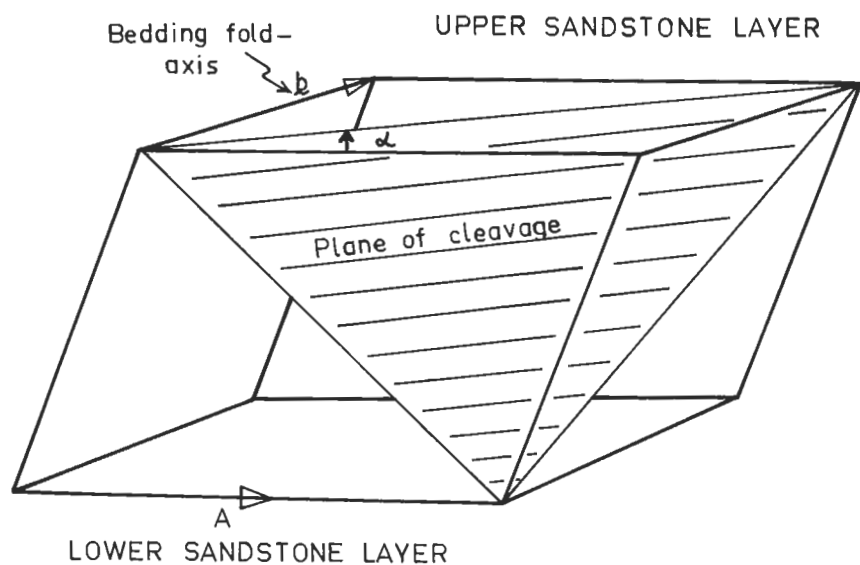
(2). Rotation about the late fold-axis.

Fig. 4 - 13 (a) shows an idealized concentric folding of inter-layered sandstone and slate with the trace of a pre-existing planar structure marked in the slate. The sandstone layers may be considered

CONCERTINA-STYLE FOLDING OF INTERLAYERED SANDSTONES AND SLATES



(a) DEFORMATION OF A CLEAVAGE IN A SLATE BAND BETWEEN ELASTICALLY BUCKLED SANDSTONE BEDS



(b) RELATIONSHIP OF PRE-EXISTING SLATE CLEAVAGE TO A , b , and α

elastic for the purpose of the argument, so that all lines perpendicular to the original layer boundaries in the sandstones will remain perpendicular during the folding. The slate is considered ductile, and deforms by homogeneous simple shear parallel to the layer boundaries. The resulting simple-shear couple in the slate is anticlockwise on the right-hand limb, and clockwise on the left-hand limb and there is a point of no strain at the fold-hinge. During the folding the orientation of the trace of the early cleavage in the slate is altered significantly, as the angle between the bedding and cleavage is increased in the left-hand limb and decreased in the right-hand limb.

In three dimensions [Fig. 4 - 13 (b)] the problem of intralayer strain of the slate may be reduced to simple shear in a direction, A, inclined to the plane of cleavage. The direction of movement is perpendicular to the fold-axis of the layer and parallel to the layer boundaries. The angle, α , which the strike of the plane of cleavage makes with A, remain constant, and all deformation occurs in the vertical plane. The resultant distribution of the poles of cleavage for different amounts of deformation is along a great circle containing the original poles of bedding and cleavage before deformation [Fig. 4 - 14 (a)]. In general the angle, α , between the directrix, A, and the great circle is not 90° . Since the pole of the bedding is fixed, the cleavage in the limb where the bedding / cleavage angle decreases has poles which lie in the smaller segment

NON-COAXIAL FOLDED CLEAVAGE Equal-Area Projections

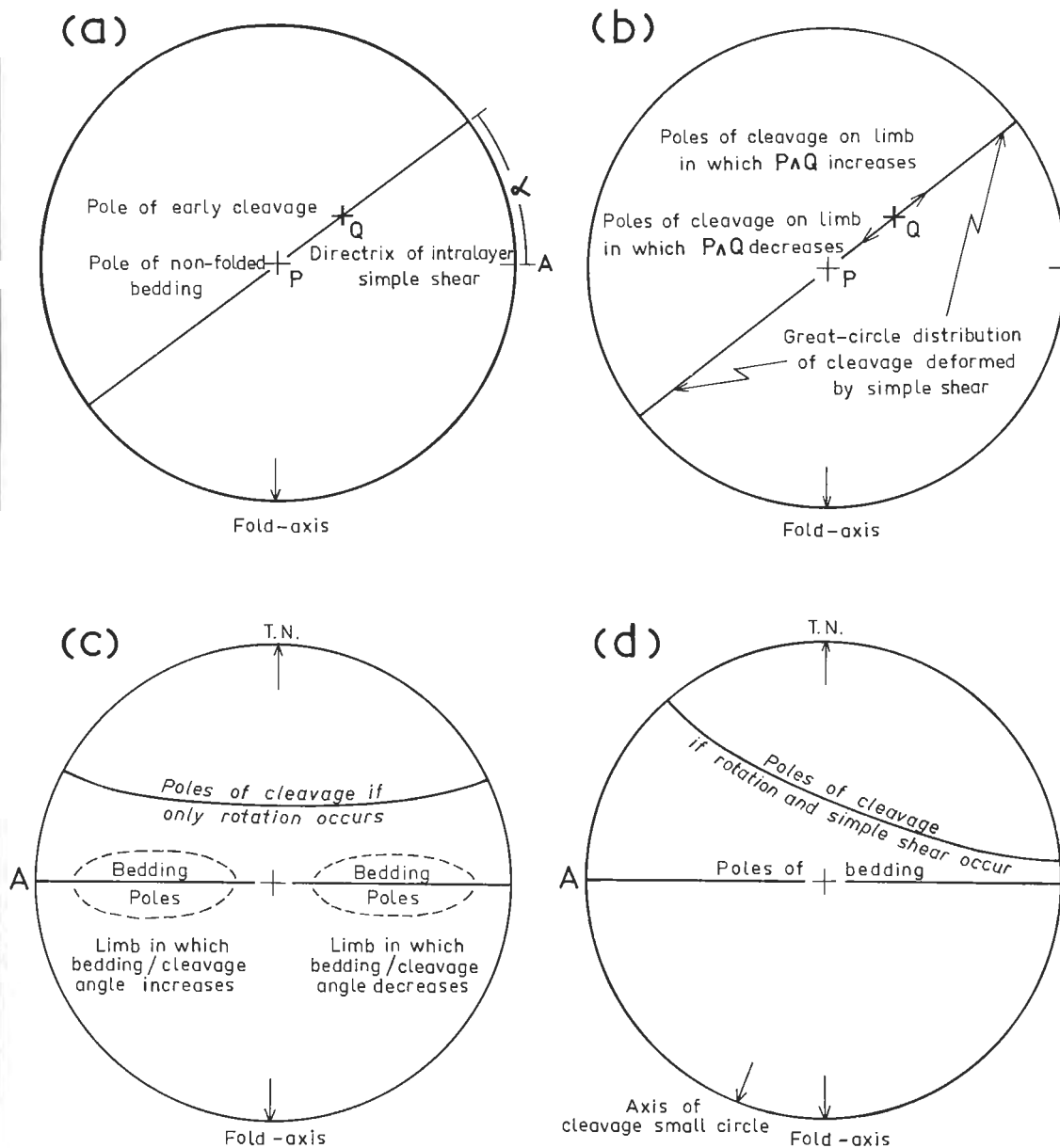


FIG: 4-14 (a) Relationship between the poles of early slate-cleavage, new fold-axis, directrix of intralayer simple shear, A , and the angle, α .
 (b) Great-circle distribution of the slate-cleavage after simple shear along the directrix, A , parallel to the bedding.
 (c) Orientation of the slate-cleavage if it is only rotated about the bedding-pole fold-axis.
 (d) Non-coaxial small-circle distribution of the slate-cleavage after the combined effects of simple shear parallel to the bedding, and rotation about the fold-axis during folding.

of the great circle containing P and Q, and the cleavage in the other limb where the bedding / cleavage angle increases has poles in the larger segment of the great circle [Fig. 4 - 14 (b)].

Stauffer (1964) has shown that the distribution of poles of a surface rotated about an axis oblique to it is a small circle coaxial with the axis of rotation. Thus, if the cleavage were merely rotated with the bedding, the poles of the cleavage would be distributed about a small circle coaxial with the bedding fold-axis [Fig. 4 - 14 (c)]. Furthermore, since the angle between the bedding and cleavage has been shown to increase on one limb and decrease on the other during the folding, the small-circle distribution of cleavage poles will be distorted by rotating one segment of the small circle away from the poles of the bedding, while rotating the poles on the other segment towards the poles of the bedding. If the effects of both strain in the layer and rotation about the bedding fold-axis are combined, the resultant distribution of poles of the cleavage will be of the general shape of Fig. 4 - 14 (d). Thus, where there is both strain and rotation during folding of a slate band which contains a pre-existing cleavage, the poles of the early cleavage will be distributed about an axis non-coaxial with the bedding fold-axis.

In Syncline 4 [Fig. 4 - 12 (d)] the poles of the cleavage lie on a small circle of 82° which is coaxial with an axis that diverges by 19° from the fold-axis. The original angle between the bedding

and the cleavage was small (less than 20°) and has decreased in the gently dipping northeastern limb and increased in the steep southwestern limb. This angle is too small to enable accurate calculation of bedding / cleavage intersections, and thus the calculated bedding / cleavage intersections in the slate in Fig. 4 - 12 (b) have little significance.

(h) JOINTING

The Tullochgorum section contains a large number of joints and quartz veins. Fig. 4 - 2 (b) shows a composite plot of the attitude of all joints and veins measured, and the symmetry is triclinic with no simple relationship to the regional fold-axis. There are, nevertheless, two distinct trends:-

- (1) A girdle of poles perpendicular to the fold-axis, and
- (2) A broad spread of poles which shows no obvious relationship to the fold geometry.

The girdle of poles perpendicular to the fold-axis is largely representative of sigmoidal quartz veins, while the broad spread of poles represents persistent, generally planar quartz veins which tend to cut across the bedding irrespective of its orientation. The girdle of poles perpendicular to the fold-axis is not as prominent as the other distribution because of the smaller number of sigmoidal veins measured. Furthermore, because of the orientation of the section very few joints perpendicular to the fold-axis have been measured. Thus it appears that although 211 joints have been measured, this number

is probably not a good sample of all joints present, and any interpretation of the distribution must be of a broad nature.

The sigmoidal quartz veins are interpreted as having formed as shear fractures which were rotated during folding by continuing deformation towards the tension direction in which they dilated. The relationship of the oblique joints to the folding is not clear. In places the sigmoidal veins appear to cut across them, but in other places the oblique joints transect the sigmoidal veins. On this basis it would appear that the oblique joints are probably contemporaneous with the sigmoidal veins, yet they do not have the geometry of a known fracture system. Their origin has not been determined from existing data.

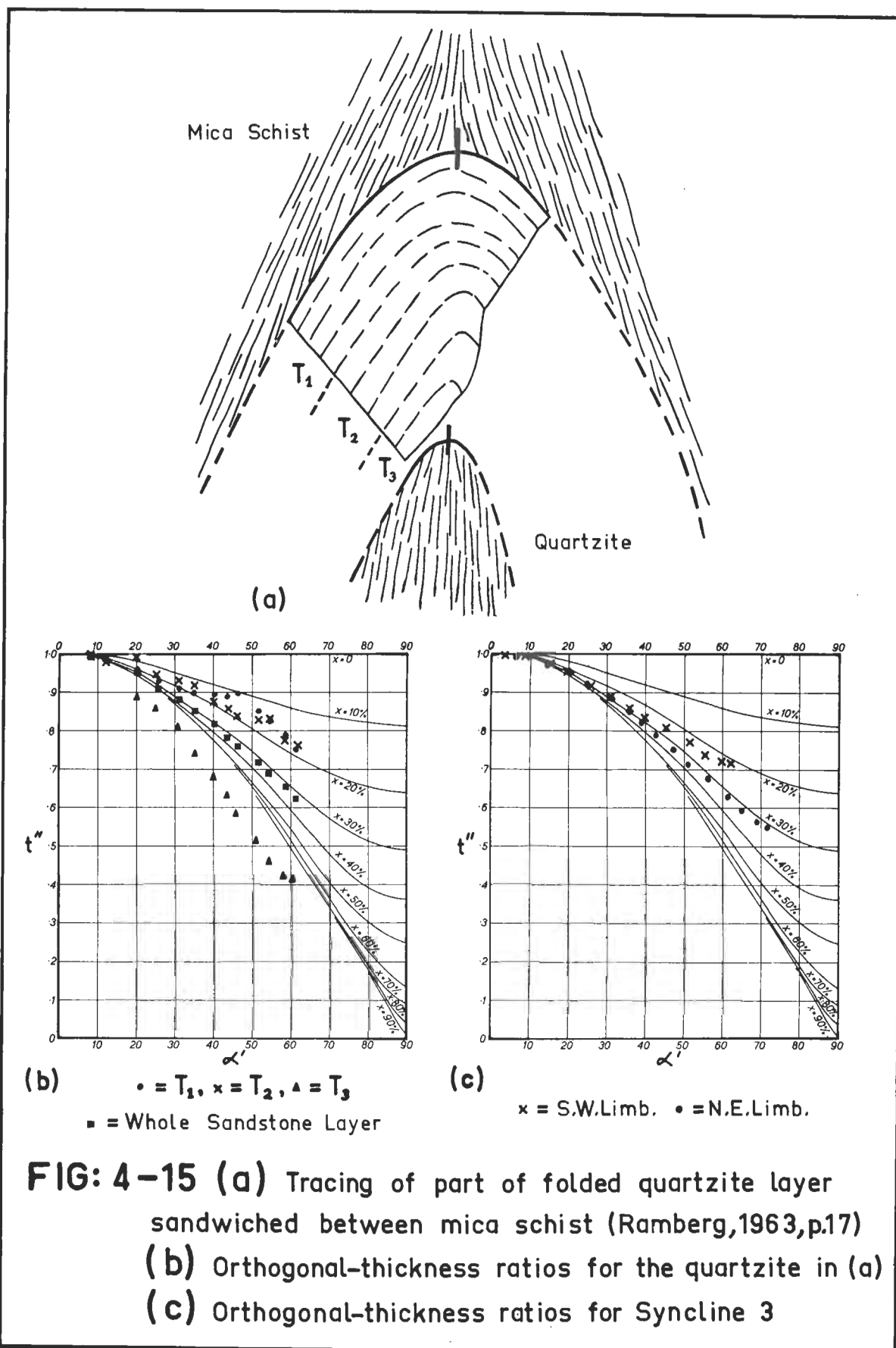
3. FLATTENING

William's method of calculating flattening in originally concentric folds (1965) was developed from a study of the Tullochgorum folds, and is specifically suited for concertina-style folds in which the non-flattened profile in the hinge fits circular arcs. Although for some situations the method has certain advantages over the orthogonal-thickness-ratio method, it is subjected to the same problems of obtaining a good profile section and of being able to orient the inscribed flattened semicircle accurately perpendicular to the fold-axis. Furthermore, the position of the centre of curvature

must be known. Errors involved in the practical application can be serious, and the accuracy of $\pm 2\frac{1}{2}\%$ quoted by Williams (*ibid*, p. 232) may be optimistic.

Ramsay's method of calculating flattening from orthogonal-thickness ratios is not entirely suitable where the layers are thick compared with their radius of curvature and there is some uncertainty about the position of the concave side of the buckled layer. There may also be substantial primary variations in the thickness of layers. Syncline 1 appears to have been localized by a preconsolidation disturbance, and the sandstone layers in both Anticline 2 and Syncline 3 show irregular primary variations of thickness. It was found that by using both Ramsay's and William's methods of calculating flattening, as well as by plotting thickness against distance from the fold-hinge (Ramsay, 1962, p. 311), the following generalized distribution of flattening can be inferred.

(1) The largest percentage of flattening in the sandstone layers occurs in the hinge region. Williams estimated 20% uniform flattening perpendicular to the axial plane in the hinges of Anticline 2 and Syncline 3, and these measurements were verified as approximately true. Orthogonal-thickness ratios from Anticline 2 indicate a uniform flattening of approximately 30% perpendicular to the axial plane on the southwestern limb and approximately 20% on the northeastern limb. In Syncline 3 [Fig. 4 -



15 (c)] orthogonal-thickness ratios correspond to a little more than 30% uniform flattening on the northeastern limb and 20% uniform flattening on the southwestern limb. In both folds these amounts of flattening apply only to the immediate hinge region.

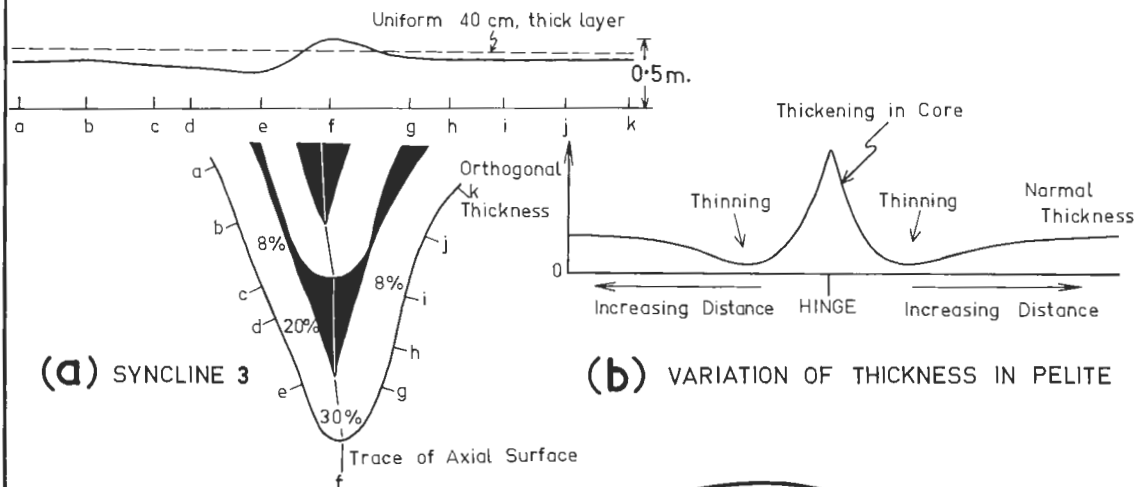
(2) The flattening decreases away from the axial surface. There is differential flattening in any layer with the greatest amount in the hinge zone. Fig. 4 - 16 (a) shows the variation of orthogonal thickness in the lower sandstone layer of Syncline 3. There is approximately 30% uniform flattening in the hinge zone and this decreases to less than 8% a short distance away from the hinge. Detailed measurements on the thickness of groups of sandstone layers away from the hinge zones show that despite sedimentary lensing of individual beds, there is no recognizable variation of thickness irrespective of the orientation of the layers. Furthermore, sedimentary structures such as cross-bedding, flute marks, pseudo-nodules, etc., do not appear distorted away from the core regions, as would be expected if there had been overall flattening of the folded zone.

(3) The percentage of uniform flattening varies in different folds.

There is no measurable flattening perpendicular to the axial surface in the hinge regions of either Anticlines 1 and 3 or Syncline 1, and the maximum flattening is observed in the hinge regions of Anticline 2 and Syncline 2. The flattening is also observed in the hinge regions of Anticline 3 and Syncline 3.

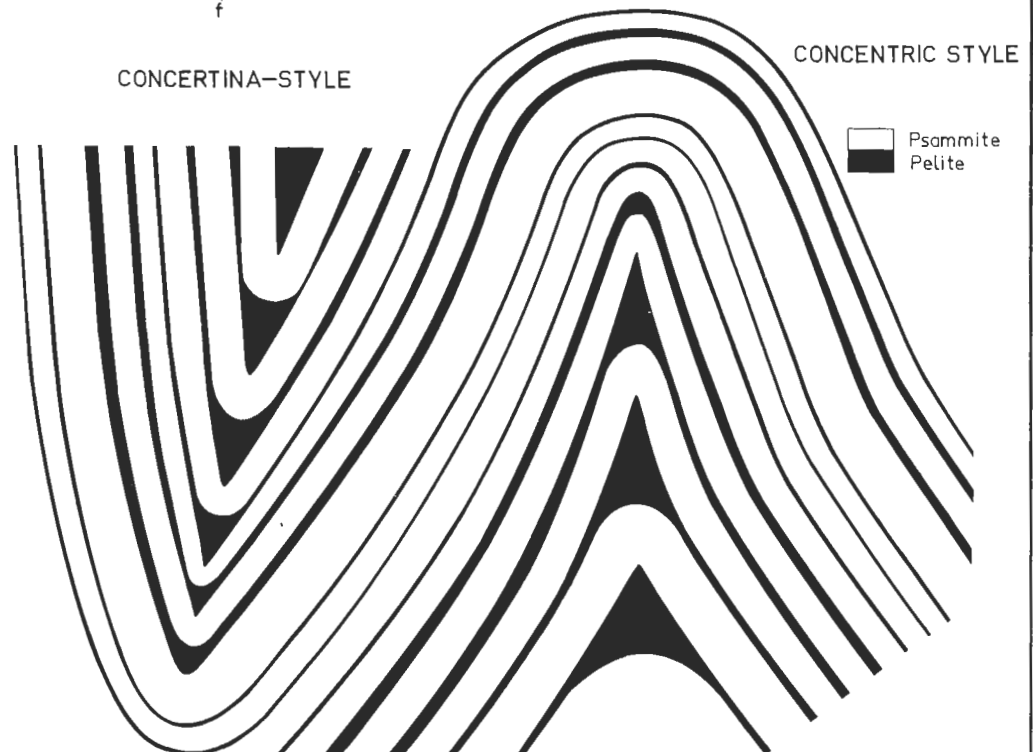
GENERALISED FOLD-STYLE AT TULLOCHG'M

MEASURED ORTHOGONAL THICKNESS, SYNCLINE 3



(a) SYNCLINE 3

(b) VARIATION OF THICKNESS IN PELITE



(c) PROFILE-SKETCH SHOWING GENERALISED STYLE OF FOLDING AT TULLOCHGORUM

The Concertina-style, similar folds in the interbedded sandstones and mudstones, and the Concentric folds in the more massive sandstone beds are both components of one general fold-style

flattening perpendicular to the axial surface occurs in the concertina-style folds which are located on the concave side of the concentric folds. Fig. 4 - 16 (c) is a composite style diagram in which the dependant relationship of the concentric and concertina folds is shown. The compression on the concave side of the concentric folds by the thick sandstone layers has caused the flattening in the concertina folds. When the flattening is considered on this scale it is non-uniform.

(4) Some of the flattening is not parallel to the axial plane. The axial surfaces in both Anticline 2 and Syncline 3 are kinked where they pass from sandstone into slate. The cleavage fan in the slate, convergent towards the convex surface of the fold, is symmetrical about the local orientation of the axial surface, just as is the divergent fan in the sandstones. The most likely plane of flattening which could form the kinked axial surface without destroying the symmetry of the cleavage, is one parallel to the bedding in the straight-bedded bounding zones. A larger amount of flattening in the slate than in the sandstone would cause the originally planar axial surface to rotate further towards the plane of flattening in the slate than in the sandstone, thereby producing the kinked axial surface.

How much of the flattening is of this type has not been determined. It is possible, as Williams suggested (*ibid*, p. 236), that the flattening in the sandstones occurs parallel to the axial

plane only where the cleavage is parallel to it, and that the local plane of flattening in the sandstones is everywhere reoriented parallel to the cleavage. This type of flattening would not reorient the plane of symmetry of the cleavage fan or change the symmetry of the orthogonal-thickness ratios about the axial plane in the sandstone layers. However, this mechanism alone does not account for the kinked axial surface.

4.

CLEAVAGE

(a) GENERAL DESCRIPTION

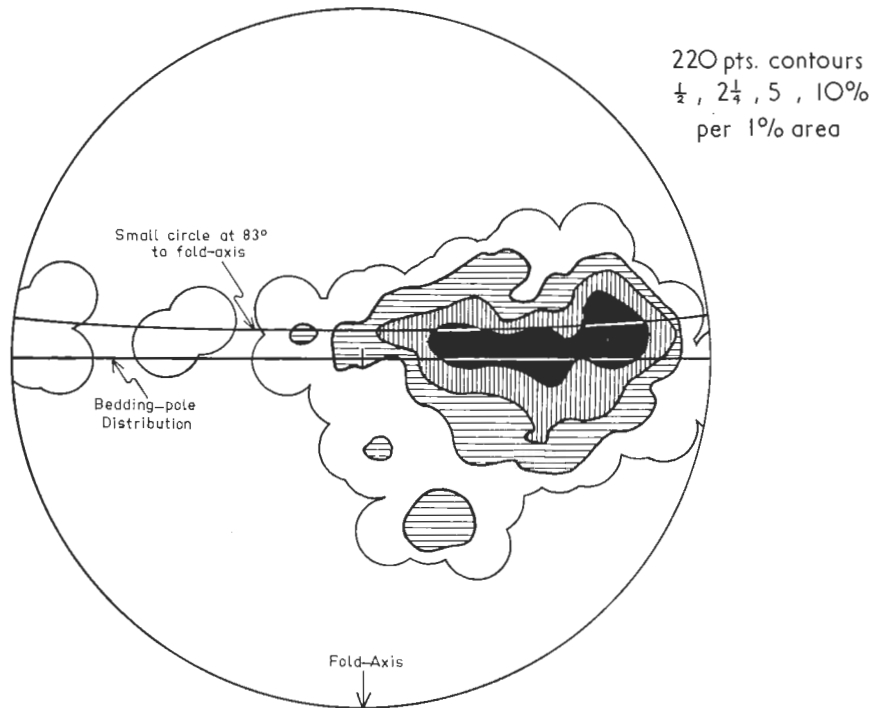
Two types of cleavage can be distinguished in the Tullochgorum folds, and these have been designated sandstone-cleavage and slate- or mudstone-cleavage, depending on the rock in which the cleavage occurs. In hand-specimen the sandstone-cleavage appears to be a non-penetrative fracture type of cleavage. It characteristically makes a large angle with the bedding in the fold limbs, thereby producing a fan which is divergent towards the convex surface of the fold. The sandstone-cleavage is most intensely developed in the vicinity of the fold hinges, but is not restricted to such localities and is found in straight-bedded massive-sandstone units well away from any fold-hinge. The cleavage surfaces anastomose producing lenticular slices elongate in the general plane of cleavage, and there is often

an argillaceous or micaceous coating along these surfaces. Structures such as flames, load casts and pseudo-nodules, which are usually regarded as formed in relatively unconsolidated rocks, tend to be elongated parallel to the cleavage irrespective of its orientation with respect to the bedding. Since there is no apparent flattening of these beds the present orientation of these structures must be related to the development of the cleavage.

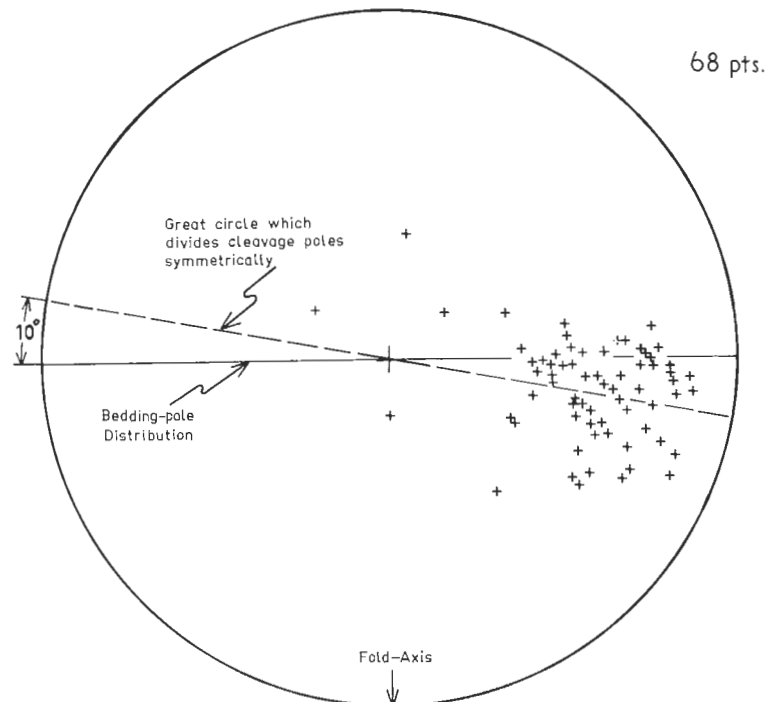
The slate-cleavage is a penetrative, typically slaty type of cleavage which is approximately parallel to the axial surface although it forms a small-angle fan convergent towards the convex surface of the fold. Where thin fine-grained sandstone bands are interbedded with cleaved argillites the sandstone bands are commonly completely disrupted, with fragments oriented parallel to the cleavage. A few plant stems in the pelite are also oriented parallel to the cleavage rather than the bedding. On fold limbs where slates are interbedded with the cleaved medium-grained sandstones the angle of cleavage changes abruptly passing from one rock type to another. However, in the hinge regions on the concave sides of the sandstone layers such as in the fold core of Anticline 2, thin slivers of slate are interdigitated with the sandstone producing a jagged profile.

The distribution of the two types of cleavage collected from all the folds in the section and rotated to a common horizontal axis, is shown in Fig. 4 - 17. The sandstone-cleavage is distributed symmetrically about a zone which lies between an 82° small circle and a great circle ,

COMPOSITE PLOTS OF CLEAVAGE (Equal-Area Projections)



(a) Poles of all sandstone-cleavages rotated
to constant Fold-Axis



(b) Poles of all slate-cleavages rotated
to constant Fold-Axis

both coaxial with the fold-axis. The somewhat asymmetrical distribution is caused by the secondary scissor-like rotation in Syncline 3, but despite this there is readily recognizable a distribution corresponding to a fan coaxial with the fold-axis.

The slate-cleavage shows a markedly different distribution which corresponds to an axial symmetry. However, the mean orientation of the cleavage is not parallel to the axial plane but inclined at an angle of 10° in a clockwise sense of rotation. It is symmetrical about a great circle which is non-coaxial with the fold-axis and diverges by 10° . Reference to the structural elements of individual folds shows that this effect is not caused by the cleavage in all the folds, but only in Anticlines 1 and 2 and Syncline 3. This rotation is interpreted as being caused by the scissor-like rotation in the general axial plane, and as has been shown was accomplished mainly in Syncline 3 but also in Anticlines 1 and 2.

(b) THIN-SECTION DESCRIPTION

In thin-section the sandstone-cleavage consists of lenticles of recrystallized greywacke separated by ribbons of iron-stained argillaceous or micaceous material. The ribbons are of several sizes; the widest being up to 0.3 mms. across and enclosing lenticular slices of greywacke up to 1 cm. wide. These lenticles are elongate in the general plane of the cleavage, and thinner ribbons of pelitic

material branch off the larger ribbons, anastomose throughout the matrix sub-parallel to the cleavage, and enclose sublenticles 3 or 4 detrital quartz grains wide. On a granular scale some ribbons form lenticular outlines around individual quartz grains, but there are parts of the sandstone where the ribbons do not exist on the scale of individual clastic particles.

The cleavage ribbons are severely iron-stained but appear to be composed predominantly of micaceous material. If carbonaceous material were originally present (cf. Sulphur Creek) it has been removed by recent weathering. There are some detrital mica flakes up to 0.5 mms. across which are always bent parallel to the cleavage ribbons where the mica flakes pass into them. In other places the mica flakes are kinked or bent around quartz-grains. Very fine-grained recrystallized sericite which occurs throughout both the ribbons and the lenticles, is parallel to the general cleavage plane, and where the ribbons locally diverge out of this direction the sericite remains parallel to the cleavage plane. The mesoscopic cleavage is formed by the rock splitting along the ribbons rather than along the mineralogical cleavage parallel to the basal plates of the sericite.

There is extensive evidence of shearing in the detrital quartz grains which have undulose extinction, polygonization and areas of fine-grained recrystallization. Some of the larger quartz grains have been elongated into lensoid shapes with an indication of pressure

shadows at the ends. A few sigmoidal porphyroclasts are evidence that there has been some movement along the cleavage surfaces, but the overall sense and distribution of this rotation has not been examined.

These microscopic features agree in essence with Williams' description (1966). It is, however, important to consider the intensity of cleavage development with respect to location in the fold. In general the shearing of clastic particles is greatest in the hinge region, and more intense on the concave side of the bed than on the convex side. The micaceous material in the ribbons has recrystallized quite coarsely along the axial surface with flakes up to 0.2 mms. across and the texture in the coarsest-crystallized part is as drawn by Williams (*ibid.*, p. 117 Fig. 2C). On the limbs the shearing is subordinate and the micaceous ribbons enclose lenticles which have a relatively unaltered greywacke texture. Away from the fold core where the mesoscopic cleavage becomes weak or indeterminate, the thicker micaceous ribbons are absent and a network of thin interconnecting ribbons, elongate in the general direction in which the cleavage is to be expected, anastomose through a normal greywacke texture. Only a few large, detrital grains show evidence of strain.

In the argillite the grain size is generally too fine to enable individual particles to be distinguished microscopically, although very thin sections show there is a strong parallelism of

nearly all the platy particles. The argillites consist predominantly of platy particles, and the ribbon structure which produces cleavage in the sandstones is not developed.

(c) ORIGIN OF CLEAVAGE

(i) Review of Williams' Hypothesis In a series of papers, Williams (1961, 1965 and 1966) has formulated an hypothesis of cleavage formation in the Tullochgorum folds. Briefly, he considers that the cleavage in the sandstones is caused by the development of zones of open texture in granular layers during folding, these zones being infilled with argillaceous matrix and fine quartz particles produced by autogenous grinding. Williams considers that the cleavage in the slate has developed in planes of laminar flow as the slate moved towards the spaces created in the fold crests between the competent layers. While Williams' mechanism of cleavage formation accounts for many of the observed features in the core regions of the folds there are a number of difficulties which arise when the hypothesis is extrapolated throughout the whole section.

Firstly, in consideration of the sandstone-cleavage, Williams (1965, p. 233) states

"...that the cleavages are approximately at right angles to the boundary at the outer arc of the layers".

This is true in the narrow hinge region although even in the

reconstructed, unflattened profile (*ibid.*, p. 231, Fig. 2B), the cleavage makes an angle of 80° with the outer arc on the left-hand limb, 90° at the hinge and 87° on the right-hand limb. This fold is Anticline 2 and further along the limbs away from the hinge the bedding/cleavage angle decreases to less than 50° . In general the bedding/cleavage angle in the limbs of the folds averages 50° to 60° . Williams (*ibid.*, p. 235) explains this as:-

"...a result of a general breakdown in texture adjacent to the hinge area" with

"...movement of material in planes parallel to those of cleavage in the hinge area while cleavage planes are still being formed by granular rearrangements in the flanks of the fold".

Yet movement parallel to the cleavage will not change the orientation of the zones of loose pack in the continuous granular framework in the limbs of the fold since the zones of loose pack are the cleavage zones.

Secondly, although it is accepted that the cleavage in the hinge region is approximately at right angles to the surface on the convex side of a layer, and also that there may be considerable reorientation of the cleavage direction in the limbs, the distribution of cleavage in Anticline 1 and Syncline 1 [Fig. 4 - 3 (b)] does not appear to be related to individual beds. The cleavages in both the sandstone and the slate are essentially parallel and planar throughout the pair of folds,

and a rotation of 30° for the limbs of Anticline 1 and 15° for the limbs of Syncline 1 is sufficient to produce a perfectly planar cleavage throughout the fold couple. Furthermore, in the common limb between the folds the bedding/cleavage angle is as low as 30° , which is difficult to explain on a model of granular rearrangements. A simple explanation of the orientation of the cleavage is that a planar cleavage was impressed on these folds towards the end of their formation, and that a small amount of deformation associated with the tightening of the folds subsequently produced the existing configuration.

Thirdly, the model of equigranular spheres from which the orientation of the cleavage is predicted, does not appear to be justified. The sandstones are generally poorly sorted greywackes and no particular grain-size forms a closed framework. Admittedly it is true that dilatancy is independent of grain-size, and it is quite possible that dilatancy occurred in these beds during deformation, but for the zones of loose pack to become propagated laterally along the beds away from the fold-hinge it is necessary that there is a continuous framework of some particular grain-size. Such a framework does not exist, and in fact the best developed cleavage occurs in layers which have up to 40% argillaceous matrix. Thus, while there may be granular rearrangements with dilatancy during deformation, it is not possible to predict the orientation of cleavage by the geometry of individual granular arrangements.

Fourthly, the cleavage in the slate can not have developed strictly parallel to planes of laminar flow in the argillite. The cleavage distinctly cuts across the slate bands in the limbs, and is either terminated at each end against the bounding sandstones, or passes into the sandstone. If the cleavage in the slate were developed parallel to the planes of laminar flow, then such an orientation implies flow across the sandstone layers, whereas any flow of the slate towards the fold core must necessarily be parallel to the bounding sandstones near the sandstone-slate interface.

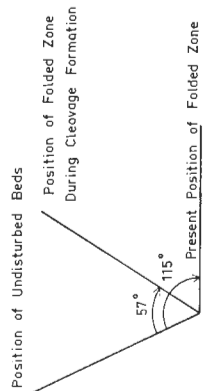
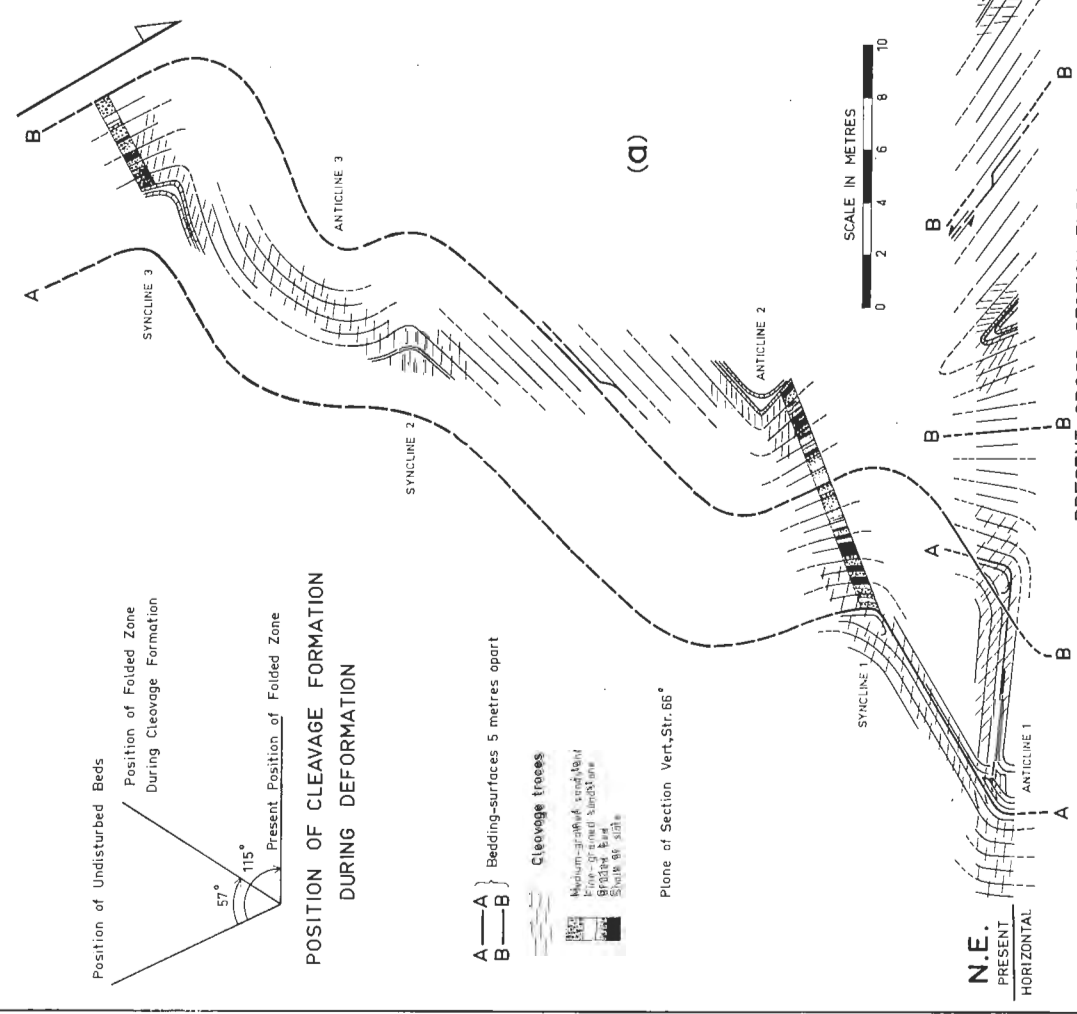
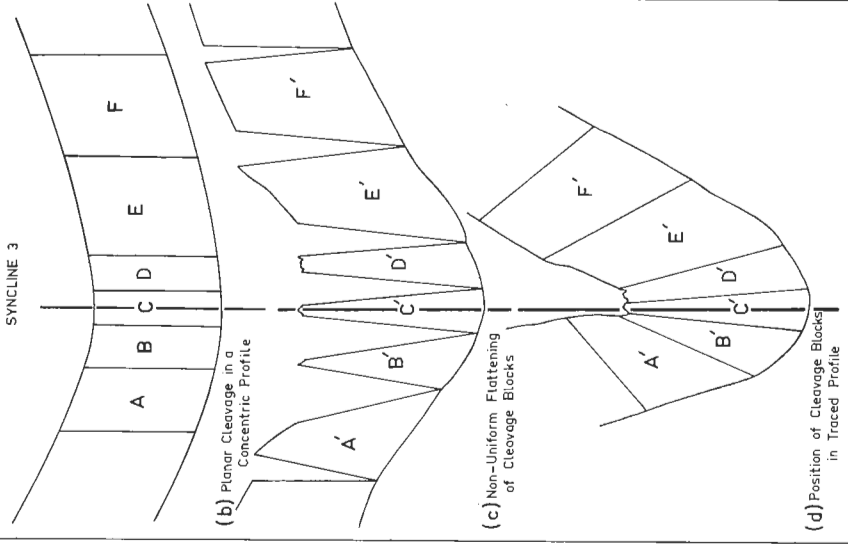
All the observed features, as well as these difficulties with Williams' hypothesis, can be accounted for if the cleavage is considered to have developed as an essentially planar structure at some stage during the folding movement.

(ii) Geometry of a planar cleavage developed during folding.

The folded section reconstructed on the assumption that a planar cleavage was developed at some stage during the folding, is shown in Fig. 4 - 18. The section was reconstructed by taking as the datum direction the present orientation of bedding and cleavage in the straight-bedded region to the northeast of the folded zone and rotating back to parallelism the cleavage in the limbs not immediately adjacent to the fold-hinges. The amount of rotation necessary for each fold varies, the largest rotation of approximately 60° occurring in Anticline 2 and Synclines 2 and 3, and the smallest

RECONSTRUCTION OF FOLDED ZONE, TULLOCHGORUM

FORMATION OF CLEAVAGE FAN



POSITION OF CLEAVAGE FORMATION DURING DEFORMATION



N.E.
PRESENT
HORIZONTAL

S.W.
PRESENT
HORIZONTAL

PRESENT CROSS-SECTION THROUGH THE FOLDED ZONE

FIG:4-18

rotation of 15° in Syncline 1. It is significant that the largest rotations are on the concave sides of the thickest sandstone beds where larger angular rotations are consequent upon any given angular rotation in the more open, enveloping layers.

The rotation of the cleavage to a planar orientation produces fairly uniform apical angles of between 70° and 90° for all the folds, the only exception being Anticline 1 which has an apical angle of approximately 60° . This is in keeping with the idea that, in the early stages of formation, folds in comparable structural locations are fairly regular in style, and that variations in style develop later when the limit of concentric folding is reached and further deformation is accomplished by plastic flow.

Nevertheless, this reconstruction still produces a fan in some of the fold-hinges. Non-uniform flattening can account for this fan, but there is no direct proof that such a process has operated in the Tullochgorum section. To prove that such a mechanism has occurred it is necessary to take one mechanical unit which has been flattened non-uniformly and to examine flattening in different parts of the layer by means of internal markers such as originally layer-parallel surfaces. Such markers are difficult to obtain because slight variations of composition in a layer are likely to localize strain along their boundaries and the layer behaves as a group of thin sub-layers rather than a mechanical unit. Nevertheless, there are a number of folds known in which there are

originally layer-parallel markers that have not acted as separate mechanical units.

Figs. 3 - 10 (b) and 3 - 13 (a) (Sulphur Creek), and Fig. 9 - 1 (Arm River) are examples of folds in which there has been non-uniform flattening between the convex and concave sides of a folded layer. In addition, Ramberg (1963, p. 16, Fig. 14) figures a fold in which there are different amounts of flattening on the convex and concave sides of a quartzite layer. Fig. 4 - 15(a) is traced from Ramberg's diagram and shows the division of the quartzite layer into convex (T_1), middle (T_2) and concave (T_3) subunits by tracing round the basal plates of the micas. The orthogonal-thickness ratios are shown in Fig. 4 - 15, and the layer as a whole has a variation in thickness corresponding to a uniform flattening between 30% and 35%. T_1 and T_2 correspond to approximately 15% uniform flattening, whereas the shape of the orthogonal-thickness-ratio curve for T_3 corresponds almost to a similar fold with an additional amount of flattening at the hinge. There is little doubt that in the early stage of folding this quartzite layer has acted as one mechanical unit, as it is vastly different in composition from the surrounding slate, but there has certainly been a large amount of flattening in the concave side of the quartzite layer in the hinge region. Therefore a reason must be found why the concave side of this fold, as well as of other folds, has undergone an increased amount of deformation whereas the convex side has remained

relatively undeformed.

It may be inferred from the pattern of non-uniform strain that the layer was visco-elastic during folding, and a model of deformation can be constructed as follows:- Initially the sandstone layers are buckled elastically until the yield limit of the granular fabric is reached and shear occurs between individual grain contacts. Once a grain contact has been broken it is not readily re-established so that the yield limit is progressively lowered as more contacts are broken. In this way the granular fabric in the concave side of the layer collapses and plastic deformation occurs. There is no strain hardening and this permits a large amount of plastic flow on the concave side of the layer with little or no flow on the convex side.

There are two possible models of cleavage formation associated with such visco-elastic folding. In one model the cleavage can be regarded as geometrically related to the stress distribution in the fabric of the buckled layer. The spatial orientation of stress will change around the buckled layer (Ramberg, 1963, Biot, 1961 and others), and consequently the cleavage will be fanned. However, the angular relations between the cleavage and the layer will not be constant for folds in different environments. The actual stress in any part of the buckled layer is dependant on both the confining pressure and the buckling stress, and if the confining pressure on the grain contacts is sufficiently large, the contribution of the buckling stress

may be negligible and a planar cleavage will result. All variations between a cleavage which maintains a constant angular relationship with the bedding, and a planar cleavage, are possible. Nevertheless, in one outcrop the effect of the confining pressure should be relatively uniform so that, if an essentially planar cleavage is formed, such as in Anticline 1 and Syncline 1, there is no reason to expect a cleavage fan to be formed in adjacent folds.

The other model is one in which the cleavage forms perpendicular to the greatest pressure applied to the intergranular fluid. This direction will be determined by the orientation of the external forces causing the folding, and will be essentially planar and parallel to the general axial plane. However, the relationship of the cleavage to individual folds is incidental, and the cleavage may well be oblique to the axial surfaces of some folds. Such a situation is indicated in Anticlines 1 and 2, and Syncline 3. If, after such a planar cleavage forms, there is non-uniform flattening of the type indicated in the hinge region of Syncline 3 (Fig. 3 - 18), a cleavage fan will be formed in the hinge as well as between the limbs.

There is one problem with this model as applied to the Tullochgorum section, and this is that the sandstone bands in Anticline 2 and Syncline 3 have to be rotated further than the thicker outer limbs in these folds to produce a perfectly planar cleavage. There are a number of possible explanations, but it

may be simply due to the fact that the cleavage is not formed immediately throughout the whole folded zone. A certain amount of rotation may be accomplished while the cleavage is being propagated parallel to the axial plane. If this is so, the cleavage will begin to form in the fold cores and move outwards into the layers of smaller curvature. However, such an interpretation is only speculation since available evidence can neither prove nor disprove that there was a perfectly planar cleavage. The divergences which exist are relatively unimportant and do not conflict with the idea of an essentially planar cleavage that formed throughout the whole sequence at some stage of the deformation.

The mechanism proposed requires that the cleavage in the slate also was planar and initially parallel to the cleavage in the sandstone. However, the cleavage in the slate may have been considerably modified in orientation by later movements. After the planar cleavage had formed, continuing folding developed an increasingly large space in the hinge region between the competent beds, and this space was filled by slate from the limbs. This movement could have been accomplished either by rotation and slip of the cleavage in a manner similar to the slip of cards in a pack between two boards, or by flow oblique to the cleavage. The thinning in the slate immediately adjacent to the hinge is shown in Fig. 4 - 16 (b), and it indicates that at least some bodily flow from the limbs has occurred. Probably slip and flow along the

early cleavage, as well as flow oblique to it, have operated.

It is significant that the slate-cleavage in the core is symmetrical about the line joining the apex of one layer to the cusp of the next, rather than about the overall axial plane. In parts the plane of symmetry of the slate-cleavage diverges up to 20° from the plane of flattening in the interbedded sandstone layers. Hence it can not be said that the cleavage in the slate has simply formed perpendicular to the direction of maximum stress. Its initial orientation may have been perpendicular to the direction of maximum stress, but the present orientation of the cleavage in the slate has to be accounted for by later movements.

(iii) Nature of the cleavage. The cleavage in the sandstones is produced by anastomosing micaceous or argillaceous ribbons. In the core regions of the folds these ribbons have recrystallized as muscovite flakes of the same diameter as the detrital quartz grains. However, in the limbs recrystallization is much less pronounced and it appears that when the micaceous ribbons were first formed they consisted of very fine argillaceous or micaceous material of the same composition as the argillite or the matrix of the greywacke beds.

The spacing of these main ribbons on a scale larger than the detrital grains indicates that their formation was not controlled by individual granular rearrangements. Thinner branches from the main ribbons anastomose around detrital grains forming lenticles,

and the spacing and distribution of these smaller ribbons has been influenced by the individual detrital particles. However, in parts of limbs of the folds even the smaller cleavage ribbons are spaced on a scale larger than the size of individual grains, and small lenticles of undisturbed greywacke fabric are surrounded by narrow cleavage ribbons.

If the cleavage were essentially planar when formed, it is implied that the cleavage was formed while there was only a small amount of deformation. The stage of rotation which the folded zone (considered as a whole) would have reached at the time of cleavage formation, is shown in Fig. 4 - 18 (a). In its present configuration the folded zone has been rotated approximately 115° from the orientation of the straight-bedded bounding zones, and the planar cleavage would have been formed after 57° of rotation. The intensity of cleavage developed can not be related to the amount of rotation during deformation, although the cleavage is most intensely developed on the concave side of the competent layers in the hinge area where there has been increased shearing and plastic deformation.

The orientation of structures such as flames, load-casts, pseudo-nodules and other features usually referred to as "sedimentary" is always elongate in the plane of the cleavage. This orientation could have been produced from original sedimentary structures if there were considerable flattening or simple shear along the cleavage surfaces. However, ripple marks and current cross-bedding do not

appear to be grossly distorted, indicating that extreme smearing-out has not occurred.

All these features which are not easily explicable by conventional hypotheses of cleavage formation (see Chapter 3), become meaningful if the cleavage was formed by the movement of water out of the rocks during folding. The water-movement hypothesis is outlined in the section on Sulphur Creek, and I postulate that it could also have operated in the Tullochgorum folds.

Initially the sandstone layers were buckled elastically and most of the strains were relieved by interlayer slip accompanying concentric folding. The pore pressure of the intergranular water did not equal the confining pressure so that most of the lithostatic load was borne on the grain-to-grain contacts. However, during the deformation an increasing proportion of the applied pressure was taken by the intergranular water. When the water pressure approached the lithostatic pressure there was a collapse of the card-house pack of platy particles in the pelites, and the mud-bearing water moved out of the section through both sandstones and argillites parallel to the general axial plane thereby initiating a cleavage.

The movement of water, the formation of the argillaceous (now micaceous) ribbons and the reduction in load pressure on the granular fabric, facilitated shearing of the grain-to-grain contacts on the concave side of the elastically buckled sandstone layers. Once the shearing of grain contacts was initiated the rate of collapse

increased since cohesive grain contacts were hard to re-establish.

The collapse of the granular framework proceeded from the concave side towards the convex side of the layer, and there was plastic flow parallel to the cleavage planes.

When the excess water was lost from the section the pore-pressure decreased and the confining pressure on the granular fabric increased. On the limbs where the grain-to-grain contacts in the original granular fabric had not been disturbed by bending, the sandstone beds were rigid with respect to the time of deformation, and there was no flattening. In the fold-hinges where collapse of the fabric had been aided by elastic buckling forces, the sandstones became incompetent and continued to deform by intergranular plastic flow. The field-tracing in Fig. 4 - 1 (c) represents a sandstone layer in which the original granular fabric has been destroyed, and a closely spaced, axial-surface cleavage has been arrested as it was developing outwards from the fold core.

The intergranular shearing along the cleavage ribbons caused fracture and polygonization of the detrital quartz, and there is also crystallization of fine sericite throughout the matrix. Shearing and recrystallization is greatest on the concave side of the sandstone layers where the quartz grains display pressure shadows, and the mica has crystallized into recognizable muscovite flakes. Snowball-sericite rolls are evidence that there has been movement along some of the cleavage ribbons.

In the limbs the crystallization of sericite is weak or non-existent, and some of the quartz porphyroclasts were strained and fractured as the style of deformation became increasingly more brittle. Continued deformation of the folded zone from the position of cleavage formation to its present position, was accomplished by the rotations permitted by plastic flow in the hinge regions, and the cleavage in the slate was reoriented as the pelite moved to fill the spaces formed between the competent layers.

Nevertheless, there are some differences in environment between the folding at Tullochgorum and that at Sulphur Creek. The style of folding at Tullochgorum indicates that the rocks were more consolidated when they were deformed than were the rocks of Sulphur Creek. Furthermore, there is a higher proportion of sandstone in the Tullochgorum rocks which has influenced the style of folding, and the cleavage appears to have formed half-way through the deformation at Tullochgorum rather than towards the end as at Sulphur Creek. The Tullochgorum environment probably corresponds to the environment which existed near Howth at the time of the P1 deformation, and the water content of the sediments would have been lower than that at Sulphur Creek during the P1 folding.

5. HISTORY OF STRUCTURAL EVOLUTION

The structural evolution of the Tullochgorum folds can be conveniently divided into four phases or stages.

(a) SEDIMENTARY AND EARLY DIAGENETIC STAGE

The interbedded sandstones and mudstones are characteristic of a deltaic environment where the normal deposition was fine argillite with sporadic influxes of medium-grained sandstone. Load casts, ripple marks (mostly current ripples), cross-bedding, graded bedding, disrupted shale beds and small-scale slumps and other structures characteristic of this environment were formed. The early stages of consolidation appear to have been quite normal.

(b) EARLY FOLDING STAGE

At some stage during the progressive burial and compaction of the sediments the folding was initiated. There appears to have been less water in the sediment at the time of folding than at Sulphur Creek, although the rocks were certainly not fully compacted. In the early stages of deformation there were marked differences between the sandstones and the mudstones, and the sandstones were folded in a strictly concentric manner. These folds may have been initiated by elastic instability. In this early stage the pore pressure of the interstitial water was

less than the lithostatic pressure though probably considerably greater than the hydrostatic head to be expected for the particular depth of burial. As deformation proceeded the pore pressure increased, and progressively more load was taken from the grain-to-grain contacts onto the water.

(c) CLEAVAGE FORMATION

When the deformation was about half completed the pore pressure approached or even equalled the lithostatic pressure. At this stage there was very little difference in strength between the sandstones and the pelites, and the excess water was being forced out of the sediments perpendicular to the maximum applied pressure (i.e. parallel to the average axial plane of the folds). However, the rate of loss of water was not large enough to prevent an overall rise in pore pressure, and when the water pressure exceeded a certain limit there was a rapid orientation of platy particles in the pelites parallel to the direction of water movement. This orientation greatly increased the permeability of the rock, and the flow of water through both the sandstones and the mudstones out of the section formed ribbons of argillaceous material which comprise the cleavage in the sandstones.

At this stage many of the flame structures, convolute folds, pseudo-nodules, etc., were either formed or reoriented parallel to the cleavage by the movement of water through the almost completely

disaggregated sandstones. Elastic stresses in the hinge regions of the buckled sandstone layers were also relieved by the collapse of the granular framework, and considerable flattening may have occurred.

(d) LATE FOLDING STAGE

When the cleavage ribbons were formed the excess water was rapidly lost from the section. The loss of water increased the friction between the sandstone layers and there was a general rise of temperature which caused a weak crystallization of sericite in the cleavage ribbons. The strongest crystallization occurred in the fold-hinges where the granular framework of the sandstones had been broken down, and deformation was proceeding by intergranular shearing. Continuing deformation caused the fold limbs to be rotated closer together until the present configuration of the section was attained. During the latter part of the deformation there was an anticlockwise, scissor-like rotation of the whole zone, and this was accommodated mainly in Syncline 3. The open folds to the southwest of the normal fault were formed after the cleavage, thereby accounting for the folded cleavage in the slate. However, the relationship of this normal fault to the folding can not be clearly established except that it postdates the formation of the cleavage.

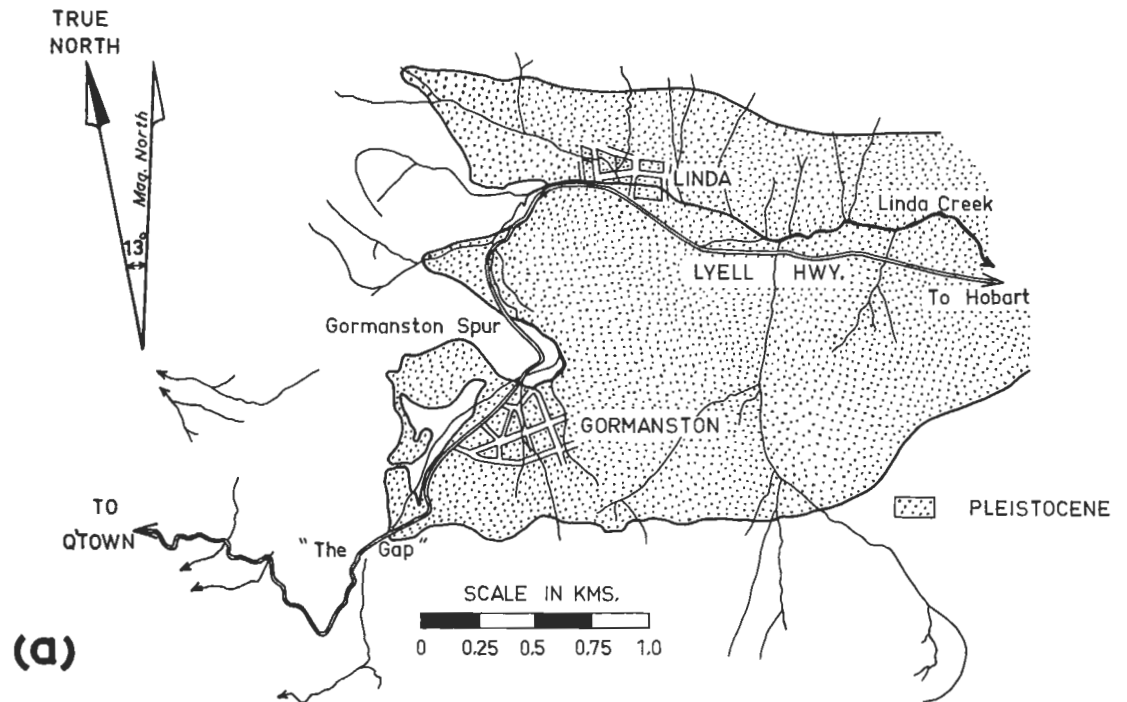
CHAPTER 5

INTRAFORMATIONAL STRUCTURES IN THE PLEISTOCENE GLACIAL
MORaine AT GORMANSTON, WEST COAST OF TASMANIA.

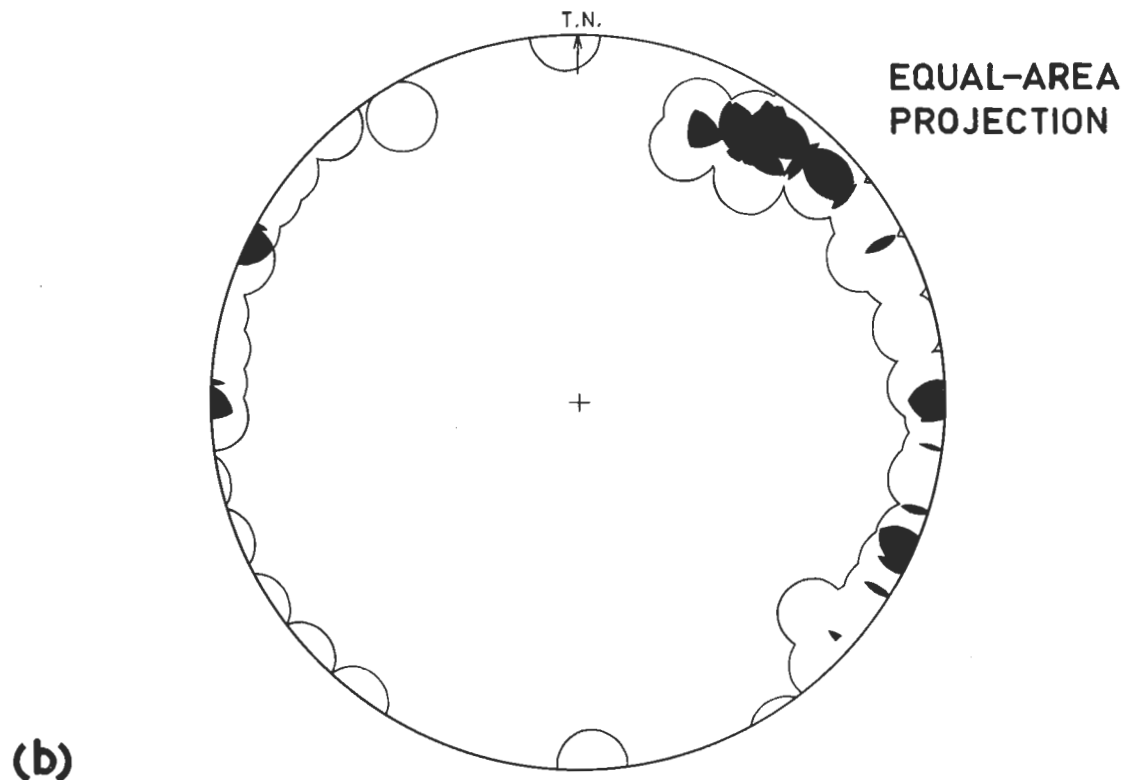
1. INTRODUCTION

The glacial deposits at Gormanston, West Coast of Tasmania are part of a terrestrial moraine at the head of the Linda Valley [Fig. 5 - 1 (a)], and the rhythmites in the moraine were the first of their kind recorded in Australia (Lewis, 1936, p. 30). Bradley (1954, p. 196) suggested that the Gormanston deposits were formed in a small lake between the nose of a distributary glacier which was moving up Linda Valley, and "The Gap" (just west of Gormanston township) which was an overflow channel. Subsequent workers (Carey, 1955, p. 176, Ahmad *et al.*, 1959, p. 15, and Davies, 1962) have supported this view. Radiocarbon dating (Gill, 1956, p. 80) on fossil wood collected from towards the base of the moraine gives an age of $26,480 \pm 800$ years B.P.

GLACIAL MORAINE AT GORMANSTON



30 FOLD-HINGES



CONTOURS 1 and 2 points per 1% area

FIG: 5-1

My interest in these deposits was to study some of the many, small-scale, intraformational-fold structures. The study is by no means exhaustive although the structures presented are representative of most classes of intraformational disturbance in the moraine. The method of analysis involved cutting (with a shovel) profiles of folds perpendicular to the local fold-axis, and washing and abrading the face with water; these profiles were then photographed and sketched in the field.

Most of the structures I have considered in this chapter were observed in the road cutting at the head of the moraine, and some others were studied on the southern flank of Gormanston Spur. Till occurs up to 1360 feet and has been reported to a height of 1400 feet just south of The Gap (Ahmad *et al.*, *ibid.*, p. 15). A small gully, a tributary of Linda Creek, has eroded along the contact between the moraine and the underlying quartzites and schists, and at the present time the stream has not cut into the bedrock.

The moraine consists of interbedded till, outwash sands and rhythmites. Ahmad *et al.* (*ibid.*, p. 15) have outlined a section exposed in a gully near the Lyell Highway, but the sequence is not simple. The lateral extent of any group of beds can not be traced, and it appears that in detail the moraine consists of small basins separated by outwash gravel deposits, rather than a uniform succession of horizontal beds that extend laterally.

Nevertheless, three main types of sediment can be distinguished, viz. (1) White Clay, (2) Brown Clay, and (3) Outwash Sands and Gravels.

The white clay (34944-5) occurs either as very thin laminations (down to one millimetre thick) in the medium-grained, yellow sand, or as bands of finely laminated clay several metres thick. The finest white clay is very soft and plastic to handle, but there are variable amounts of very fine silt admixed. The brown clay (34946) is not as plastic to handle as the white clay, and occurs in thick bands of very finely laminated material. It is not associated with the outwash sands, although it does occur adjacent to thick bands of white clay.

The outwash sands and gravels are very coarsely stratified and contain bands of pebbles and boulders, some of which are more than two metres in diameter. Cross-bedding is very common, and although there are a few thin layers composed wholly of plastic white clay, there is no silt or clay fraction in the matrix of the sands. A massive black or dark brown clay (34943) at the base of the moraine represents a peaty deposit formed on the basement of Gordon Limestone.

The various coloured clays were washed to remove the silt fraction and it was found that the darker the clay the finer the particle size. The white clay settled through 50 cms of water in less than ten minutes, whereas the black clay took

two days to settle through the same distance. Differential thermal analyses carried out by third-year students show that all the clays apart from the black peaty clay which is a chloritic type, are composed predominantly of kaolinite.

2. STRUCTURAL DESCRIPTIONS

(a) GENERAL DESCRIPTION

The orientations of the fold-hinges of 30 structures were measured, and the plot in Fig. 5 - 1 (b) shows that they tend to be distributed randomly in the plane of the bedding which dips 10° to 15° towards the northeast. The axial surfaces of the folds are generally highly contorted and also appear to be randomly oriented. The slight dip of the sediments is probably caused by differential compaction, as the moraine thickens sharply away from the head of the valley. The many different structures have been classified into a number of categories.

- (1) Compaction structures.
- (2) Diapiric folds.
- (3) Convolute folds.
- (4) Miscellaneous folds.

Compaction structures are formed by differential compaction around boulders and pebbles which have been rafted into the clay. They are usually quite simple in style, although irregularly shaped

boulders produce complicated fold shapes. Diapiric folds are very common in the interbedded clays and sands, and the sand is usually diapiric upwards into the clay. The folds are characterized by broad, open synclines and narrow, tight anticlines. Convolute folds are formed in the brown-clay bands and are usually very complicated in detail. These three categories account for most of the observed structures, and other types of structures, individually not common, are classed as miscellaneous.

(b) COMPACTION STRUCTURES

Fig. 5 - 2 (a) (i) is a tracing of a photograph of a simple compaction fold over a quartzite boulder. The matrix is finely laminated, brown clay with a small amount of fine sand admixed, but there are no discrete sandy layers. The quartzite boulder has distorted the clay laminae from the horizontal in three ways.

- (1) Under the boulder there is a broad, shallow depression three or four times as wide as the boulder. The depression is symmetrical, and the layers immediately below the surface on which the rock was deposited have been stretched and thinned without fracture.
- (2) The layers between the two surfaces which just wrap around the top and the bottom of the boulder are turned upwards where they abut against the rock. The dotted line shows the original level of the depositional

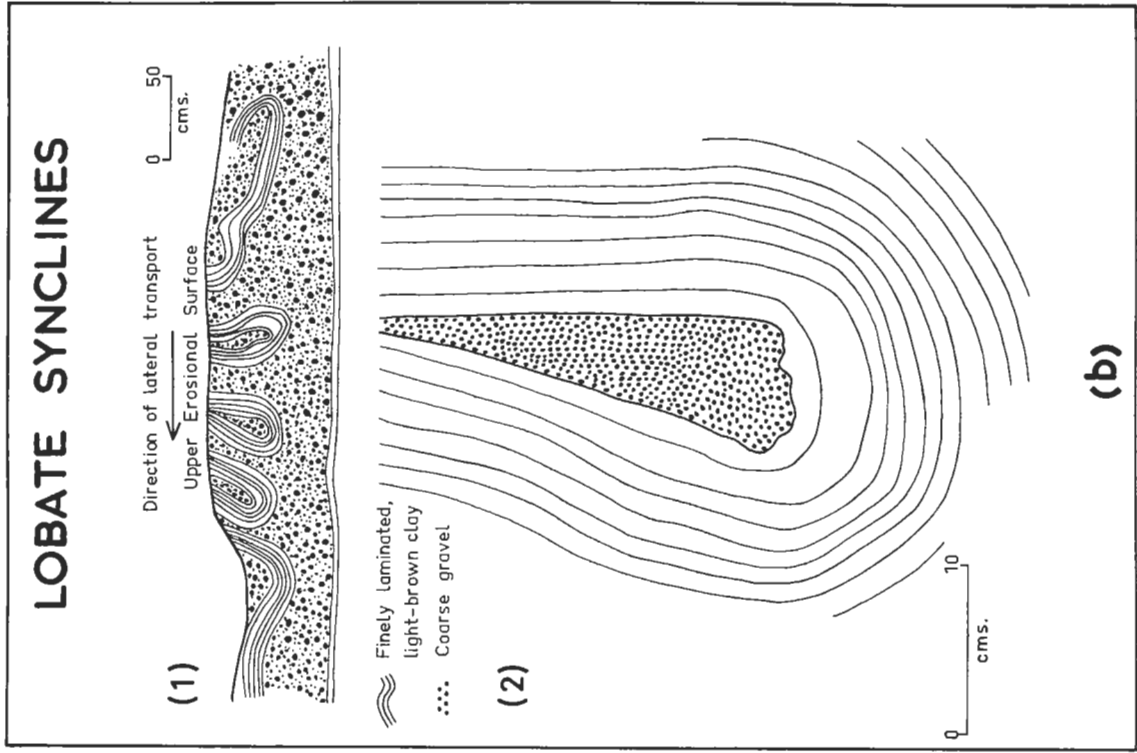
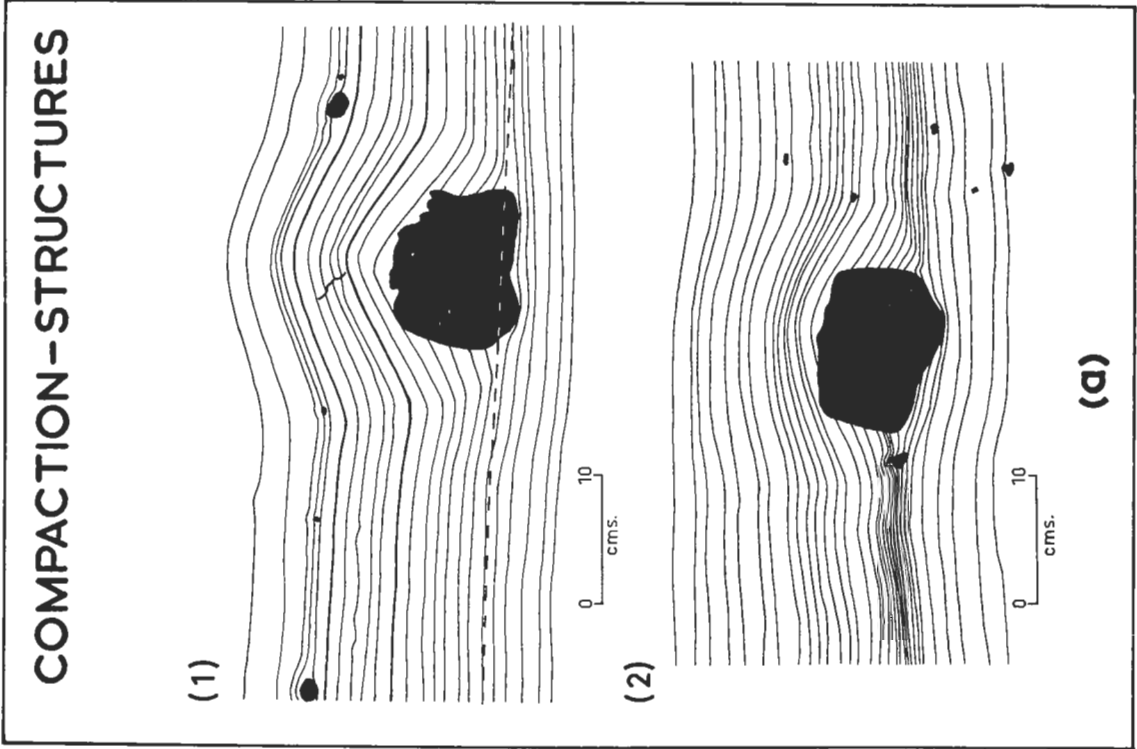


FIG: 5-2

surface extrapolated from the horizontal strata away from the boulder, and assuming that the layer which just covers the top of the rock was originally horizontal, the clay has compacted to 55% of its original thickness.

- (3) The layers above the boulder have been thinned by stretching during differential compaction. Measurements show that the profile-area of the fold between any two surfaces is the same as the cross-sectional area the layers would have occupied if there had been no boulder present. The amount of thinning of any layer in the fold crest is directly proportional to the amount of stretching of the layer during the formation of the fold.

Fig. 5 - 2 (a) (ii) is a tracing of another compaction fold around a quartzite boulder from the same outcrop as Fig. 5 - 2 (a) (i). The general form of the compaction structure is similar to Fig. 5 - 2 (a) (i) except that the base of the rock is more angular than the base of the boulder in Fig. 5 - 2 (a) (i), and the downward projection has pierced the laminae closest to the depositional surface. The discontinuous laminae abutting against the boulder have the same upturned edges caused by adhesion of the clay layers to the boulder soon after deposition and subsequent stretching during compaction. Measurements show that the clay in this fold also has compacted to 55% of its original thickness.

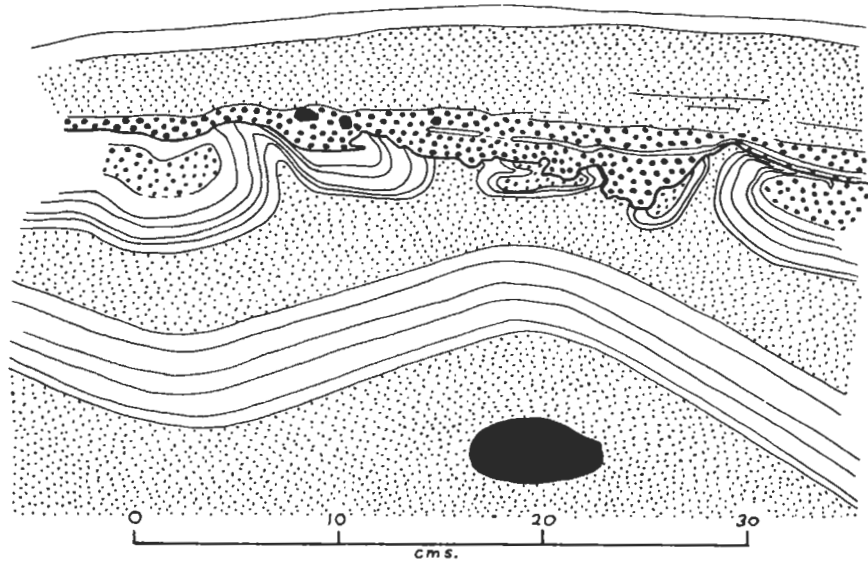
(c) DIAPYRIC FOLDS

Fig. 5 - 3 shows tracings from photographs of three examples of intraformational, diapiric folds. In Fig. 5 - 3 (a) there is a broad anticline over a pebble and the sediment is an alternation of thick bands of structureless, medium-grained sand and thinner layers of fine-grained sand and clay. The upper band of clay layers has been disrupted, forming a series of small folds facing away from the crest of the anticline. The upper surface of these folds has been eroded, and the overlying sediment is a sandy grit above which a medium-grained sand lies conformably. The style of folding tends towards concentric in the broad tumour and also in the fairly open synclines. However, in the anticlines the folds approach a similar style, with diapiric intrusions of medium-grained sand piercing right through the clay band to form isolated synclinal pods that resemble pseudo-nodules.

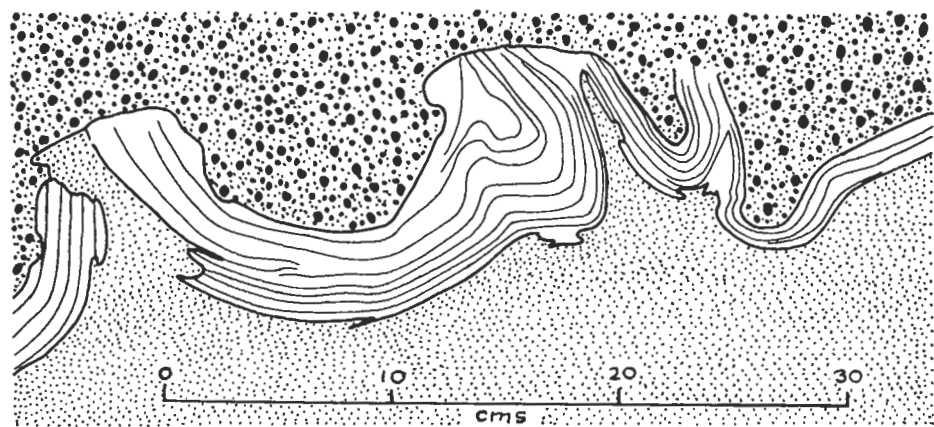
Two conclusions can be drawn about the origin of these folds. Firstly, the folds have formed at, or near the sediment-water interface as indicated by the truncation of the anticlines - and secondly, that the supratenuous, compaction fold over the pebble must have been present at the time of erosion, although in a diminished form. The latter conclusion is justified by the symmetrical sense of slip of the clay laminae down either limb of the anticline.

DIAPIRIC FOLDS

(a)



(b)



(c)

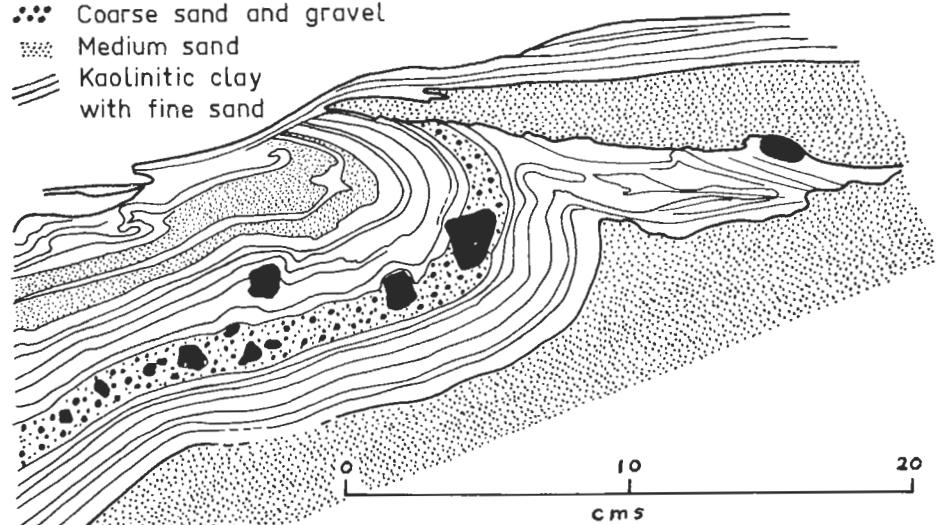


FIG: 5-3

The dissection of the clay band on the crest of the anticline has caused the clay layers to slide down the fold limbs, but this dissection is not likely to have been caused by erosion from bottom currents. Firstly, the anticline could have had only a very small closure when the clay band was deposited, and secondly, it requires very strong currents to erode clay once it has been deposited. When clay layers are eroded it is usually by plucking of whole layers to produce intraformational breccias, and none of these has been observed.

The most likely explanation is that the folding was caused by excess water pressure in the sand. Brief experiments in the field show that the clay layers are remarkably impermeable but that the sand acts as a good aquifer. The distributary glacier flowing up the Linda Valley was almost certainly a wet-base glacier (Carey and Ahmad, 1961), and as such the water pressures in the ground moraine would have been significantly greater than the hydrostatic pressure expected at that level. This high-water pressure would cause an unstable situation whereby there would be a tendency for the water to move upwards through the sediments to the free-water interface. In the tracing the sand appears to have been diapiric upwards into the clay band. When the high-pressure water breached the crest of the anticline it would have enabled the clay bands to slide off, producing a sense of overturning of the folds down the limbs. A subsequent

current eroded the tops of the folds and laid down the sandy grit after which normal deposition proceeded.

Fig. 5 - 3 (b) is a tracing of diapiric folds from a photograph shown in Fig. 5 - 4 (a). The medium-grained sand ($\phi=2$) appears to have been mobile and diapiric through a band of light-yellow clay into a pebbly gravel. Many of the pebbles in the photograph are not part of this overlying gravel, but residual pebbles from the present erosional surface. The style of folding is comparable with the style in Fig. 5 - 3 (a) where broad, open, essentially concentric synclines are separated by tight, similar anticlines along which the medium-grained sand has penetrated, and in places has broken right through the clay band.

The diapiric folds in Fig. 5 - 3(b) are considered to have formed in essentially the same manner as those in Fig. 5 - 3 (a) although the crests of the anticlines in Fig. 5 - 3 (b) have not been eroded. When the relationship between the clay band and the overlying gravel is examined in detail, the contact is found to be conformable except at the crest of each anticline where the underlying sand has broken through. The diapiric intrusion of the sand probably occurred after the gravel had been deposited, and the anticlines have been extended upwards by the flow of water out of the underlying sand. The crests of the anticlines did not reach the sediment-water interface,



Fig. 5 - 4 (a). Broad, concentric synclines and tight, similar anticlines in a clay band. The folds were caused by diapiric intrusion of the medium-grained sand. Six-inch rule shown.

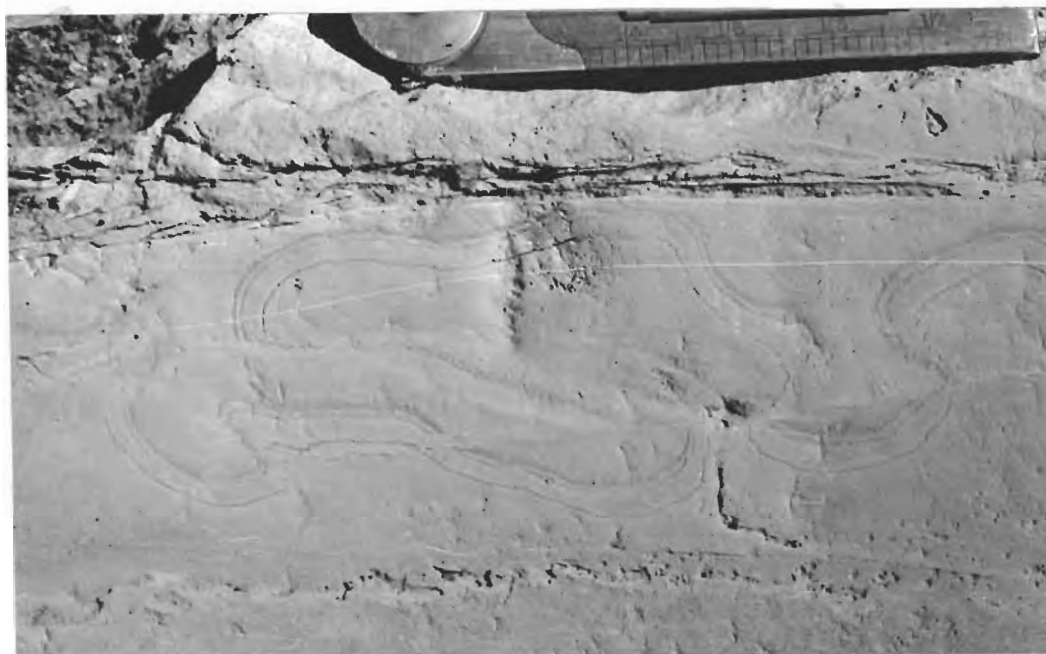


Fig. 5 - 4 (b). Unusual, mushroom-shaped folds in a silty-clay band. The three surfaces outlining the folds are very thin, kaolinite layers. Part of the six-inch rule shown.

although they may not have been far beneath it.

Fig. 5 - 3 (c) is a tracing from a photograph of another diapiric anticline from an outcrop adjacent to those in Fig. 5 - 3 (a) and (b). The clay band is composed of several thin clay laminations with a layer of coarse grit in the middle. The medium-grained sand intruded along the right-hand limb to what was the depositional surface, and the upper part of the right-hand limb was eroded. This diapiric fold formed at, or near the sediment-water interface, and the sediment deposited after the fold had formed is the uppermost clay band shown.

Fig. 5 - 2 (b) (i) is a sketch from a photograph of a layer of lobate synclines which are composed of finely laminated, light-brown clay which wraps around cores of coarse gravel. The isoclinal synclines which are separated by narrow, diapiric anticlines are in the form of pods, elongate and narrowing upwards, and are set in a layer of coarse gravel that penetrates between each pod. Fig. 5 - 2 (b) (ii) is a tracing from a photograph of one of the pods in which the gravel core is elongated upwards. However, the clay layers maintain almost perfectly concentric geometry indicating that the limbs have not been stretched.

The origin of comparably shaped lobes in deltaic and geosynclinal environments is commonly attributed to the sinking of coarse sand into an underlying silty layer. The sand is

supposed to have higher bulk density than the silt at the time of deposition, and this density contrast provides the potential energy (Emery, 1950, and Kaye and Power, 1954).

However, in this case the matrix in which the clay layers are located is a coarse gravel which certainly had a higher bulk density than the clay at all times. Furthermore, measurement of the length of the clay layers in the exposed section shows that there has been overall lateral shortening.

The present configuration of the lobate synclines is thought to have been caused partly by lateral movement of the clay band from right to left, and partly by water pressures in the gravel exceeding the normal hydrostatic pressure. The clay was broken up into segments by the underlying gravel piercing the anticlines, and the movement of the gravel up the anticlines may have been caused by the upward flow of the high-pressure water. There has been considerable flow in the gravel to allow the lobes to be piled together in their present position.

(d) CONVOLUTE FOLDS

Convolute folding in which there appears to be a genuinely random distribution of fold-hinge directions and axial surfaces, occurs quite commonly in the thick bands of finely laminated brown clay. The layers which have been disturbed usually contain lenses of fine-grained sand. Larger-scale folds in the clay

bands which bound individual convolute layers may involve one or more disturbed zones, but even these more regular folds are always bounded top and bottom by undisturbed horizontal beds.

Figs. 5 - 5 and 5 - 6 are photographs of convolute folds in the brown clay. In Fig. 5 - 5 (a) the bounding layers have been folded in a concentric manner into a series of broad, open synclines and narrow, diapiric anticlines. The convolute folds in the intervening incompetent layers are bulbous contortions which have a core of very fine-grained sand surrounded by a thin skin of brown clay. There is some extension in the vertical direction in the sharp anticlines caused by diapiric piercement from below.

Fig. 5 - 5 (b) shows several bands of convolute folds bounded top and bottom by essentially horizontal beds. In the lower part of the photograph there is a box fold above which is a zone of convolute bedding that passes laterally into essentially undisturbed layers. In the upper, right-hand part of the photograph the convolute bands have broken through the intervening undisturbed layers and have formed a diapiric structure. There is also a small diapiric anticline in the upper left-hand part of the photograph.

Fig. 5 - 6 (a) is an example of convolute folding where more than one layer has been disturbed although the zone as a whole is bounded top and bottom by straight-bedded, horizontal

layers. In detail the folded zone consists of bands of finely laminated, brown clay which is folded concentrically and separated from the next band by a highly contorted, lighter-coloured band containing some very fine-grained sand.

In Fig. 5 - 6 (b) the deformation is not as intense as in Fig. 5 - 5 (a), and the interbedded sequence of brown clay and fine-grained sand has been folded disharmonically by movement from left to right. The clay bands are folded concentrically and separated from the adjacent bands by fine-grained sandy layers in which there are many convolutions. These incompetent layers have served as zones of décollement.

All the structures in Figs. 5 - 5 and 5 - 6 were caused by liquefaction of the fine-grained sand. The cause of the liquefaction is not apparent, although in Fig. 5 - 5 (a) and 5 - 6 (b) there has been local lateral movement. Nevertheless, very fine-grained sand is the grain-size most liable to be liquified (Terzaghi, 1957). Clay particles are held together by electrostatic forces, and hence bands composed predominantly of clay cohere, and fold in a concentric fashion.

The open synclines and tight anticlines in the upper layers are produced by the diapiric action of the quicksand. When a layer is liquefied the whole load is placed on the intergranular water which is forced from the layer through the high points. However, the clay bands are almost impermeable, and thus a large

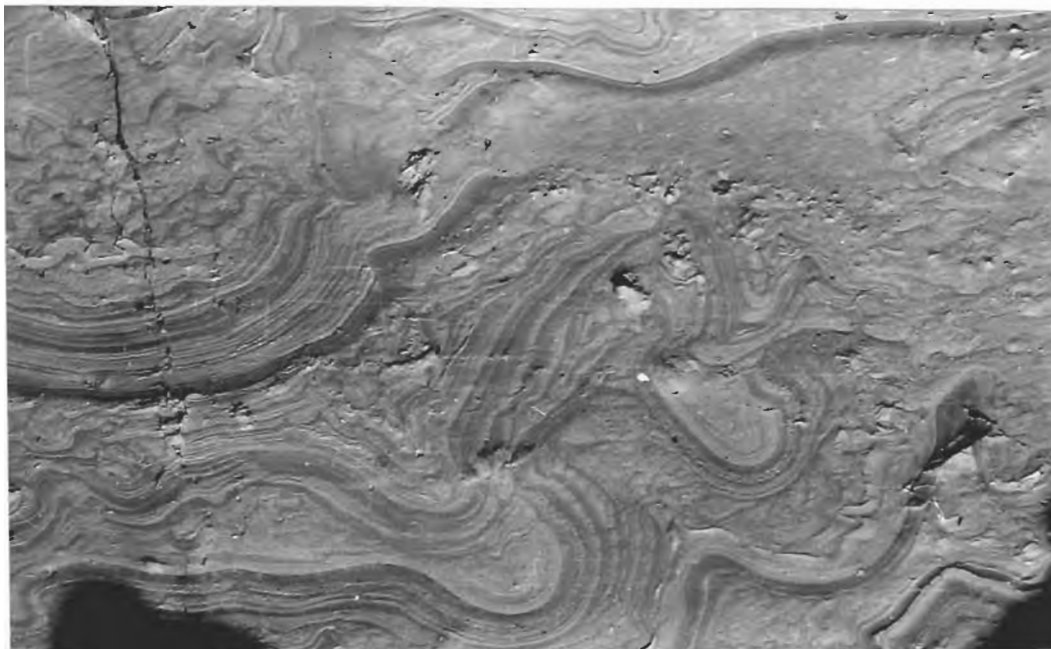


Fig. 5 - 6 (a). Close-up photograph of convolute folds in a silty band in the brown clays. Width covered by the photograph is approximately 15 cms.

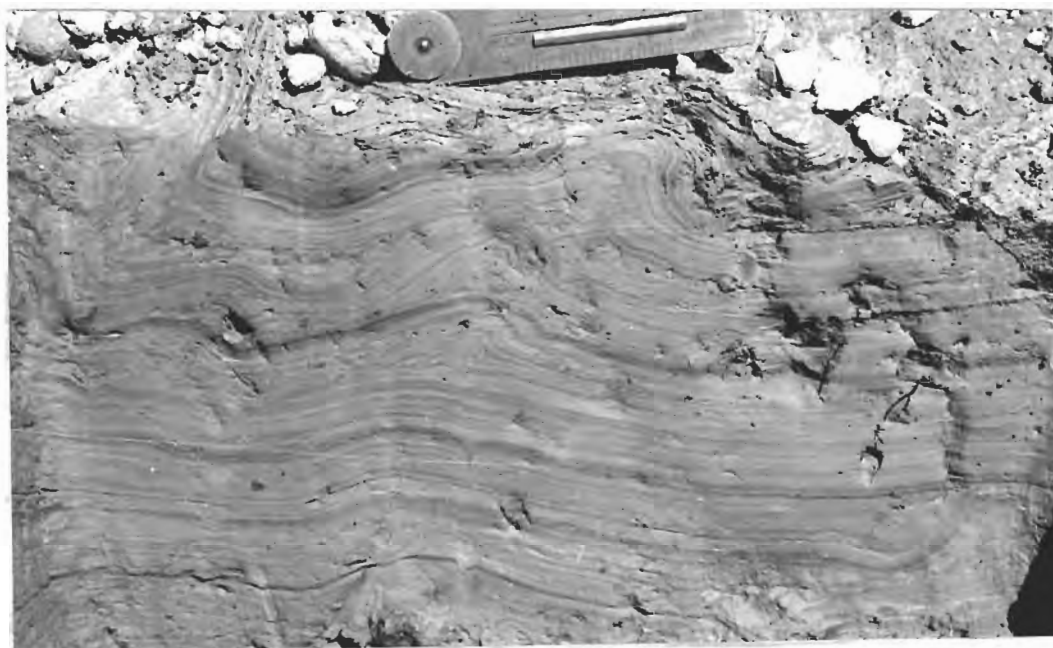


Fig. 5 - 6 (b). Less intense folding in the brown clays where there has been layer-parallel slip between bands of clay layers folded in an essentially concentric fashion. The silty bands serve as zones of décollement. Six-inch rule shown.

amount of deformation in the quick band is possible before the excess water escapes. Considerable lateral transport can be accomplished on such lubricated layers, although in many cases little or no lateral movement has actually occurred.

(e) MISCELLANEOUS STRUCTURES

Fig. 5 - 7 (a) is a tracing from photographs of a series of intraformational folds. The folded zone is composed of white clay which handles like putty, and some very thin, fine-grained, sandy layers that mark the original bedding. Above the white clay is a band of fine-grained structureless sand that has acted incompetently, and the folded zone is bounded top and bottom by undisturbed, horizontal layers.

The individual folds form a regular series of anticlines and synclines, overturned and facing to the left. The overturned common limb between the anticlines and the synclines is sheared-out or thinned by flowage. The upper surface of the clay band has been squeezed against the fine-grained sand producing box-folds - a style very similar to the intraformational folds in the Lisan Formation in Israel (Chapter 6). The style of folding varies from left to right, the folds on the left being open with an essentially concentric layer in the middle of the clay band. Towards the right the folds become tighter with more closely spaced axial surfaces, and the concentric character is subordinate.

MISCELLANEOUS FOLD STRUCTURES GLACIAL DEPOSITS, GORMANSTON

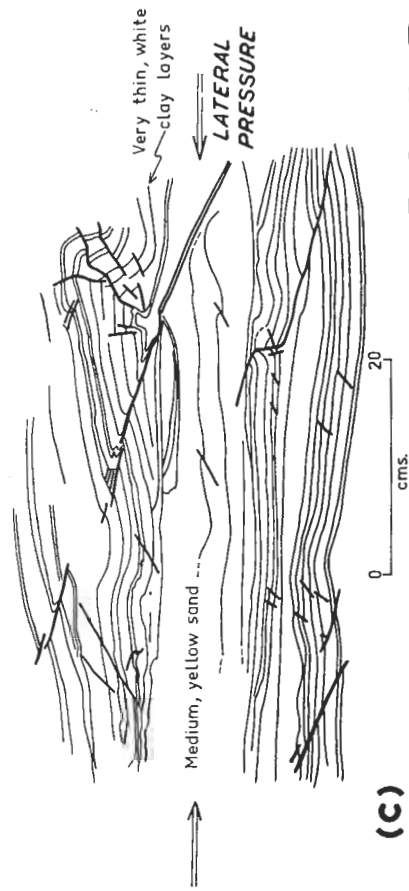
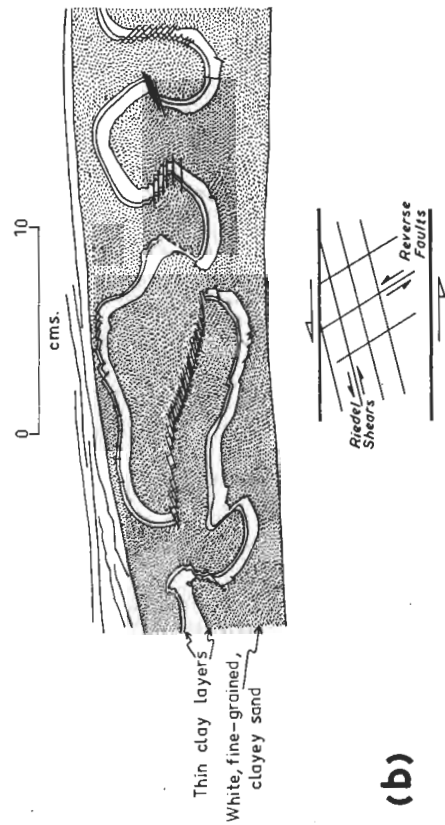
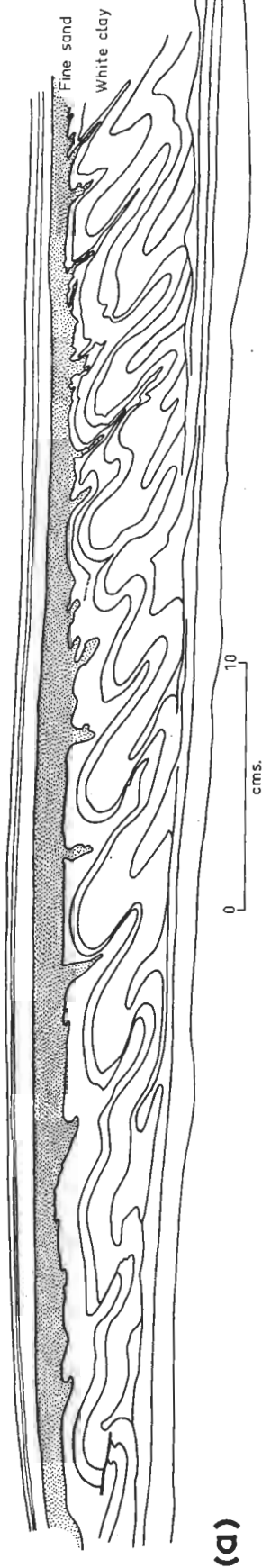


FIG: 5-7

The folded clay band increases in thickness from left to right as the axial surfaces come closer together, but measurements show that the axial-profile area of each fold remains approximately constant.

In the field, as one progresses further to the right the folds become even more closely spaced and highly contorted, until the layering is barely discernible. About 1.5 metres to the right of the traced section the folded layer thins over a very short distance, then thickens and passes into another series of folds facing away from the thinned region with fold-hinges almost at right angles to the hinges of the traced folds.

These folds are interpreted as caused by liquefaction of the clay band in the region of the thinned zone. The lithostatic load on the clay band is supported by

- (a) the hydrostatic head of the water, and
- (b) the pressure remaining on the particle-to-particle contacts of the clay fabric.

When the clay was liquefied all the load was taken on to the water, and thus the local water pressure was greater than the water pressure further along the layer where part of the overburden was still supported by the clay fabric. This caused lateral movement of the water, together with suspended clay, and there was local shortening and thickening in the layer adjacent to the liquefied region.

The initial flexures formed in the clay band adjacent to the liquified zone were concentric, but as the water pressure in the layer increased the clay fabric was weakened allowing flow folding to prevail. However, since the wavelength of the initial flexures was probably determined by the thickness of the mechanical units, and these thicknesses were the same throughout the folded zone, the axial-profile areas remained constant. The flat crests of the anticlines were caused by squeezing of the clay against the fine sand as the high-pressure water moved out of the quick-clay band. Thus, the highly contorted clay band adjacent to the liquefied region passes into more open, concentric folds which in turn pass into undeformed bedding.

Fig. 5 - 7 (b) is a tracing from a photograph of an unusual style of intraformational folding, and Fig. 5 - 4 (b) is a photograph of one of the folds. The disturbed band is composed of a white-coloured, fine-grained mixture of sand and clay which handles like putty, and the surfaces marked represent very thin layers composed wholly of clay. The material between these layers is the same clay-sand mixture as in the surrounding disturbed band.

The style of folding indicated by the unshaded layer, is essentially concentric with rather bulbous, balloon-shaped folds. There has been considerable lateral shortening, and the length of the unshaded layer is twice the horizontal width of the section.

The limbs are characterized by many small, parallel faults with a sense of displacement enabling the folds to assume a mushroom shape. These faults fall into two groups: those making a small angle with the bounding layers are Riedel shears, and those making a high angle are reverse faults. The faults can be recognized only by displacements of the three, thin clay layers, as the silty-clay matrix itself is structureless.

The balloon-shaped folds are interpreted as having formed by a combination of flow and fracture in a dilatant granular body under shear. The couple that has operated is shown in the idealized diagram below the tracing. A small strain on a dilatant granular body tends to increase the volume of the fabric (Brown and Hawksley, 1947, and Andrade and Fox, 1949), and the deformation can proceed either by allowing water to fill the increased void space or, if the void space can not be increased, by fracturing and granulating the grain-to-grain contacts in the granular fabric to allow the particles to move into a closer pack. In the folded layer in Fig. 5 - 4 (b) the water apparently has not been able to seep through the impermeable clay layers to relieve the pressures caused by dilatancy. The granular fabric has been fractured mainly on two shear systems - Riedel shears and reverse faults - although there are also some small extension fractures in the crest of the largest anticline.

The fracturing of the granular fabric has not affected the disturbed band as a whole since the shears, which are marked only by displacements on the clay layers, do not pass from one limb of the folds to another. The big displacement indicated in the overturned, left-hand limb of the largest anticline, has been accommodated in the core of the fold and does not affect the other limb. The matrix has undergone considerable plastic flow but the layer bounded by the thin clay laminations, which layer has the same composition as the matrix, has been folded in a concentric style, and fractured on a regular pattern.

The lateral shortening indicated by the concentric layer implies that the disturbed zone has locally increased up to twice its original thickness. Since the deformation is closed-cast this thickening implies that the superimcumbent sediment has been uplifted with respect to the lower layers. This uplift could have been accomplished by lateral sliding of the overlying sediment from a higher location so that, although the folded layer has been thickened, the overall centre of gravity has been lowered.

It is also likely that since the clay layers are so thin and yet have prevented water moving into the concentric band to relieve the pressures caused by dilatancy, the deformation has been relatively rapid, and the silty clay probably behaved as a fluid. It is quite possible that the silty clay in the

disturbed band was liquefied so that the whole load was borne by the ground water.

Fig. 5 - 7 (c) is a tracing from a photograph of a conjugate, box-type fold in the unconsolidated sands. The surfaces shown represent very thin bands of white clay in medium- to fine-grained, yellow sand. The sand itself is structureless, and the small faults can be recognized only by the displacement of the clay bands, or by thin strips of clay which occur along some of the sinistral shears.

The box fold has been produced by movements along conjugate shears which make an angle of 20° to 30° with the bedding. The sinistral shears that make an angle of 20° with the average bedding orientation, are developed as a few, prominent fractures which extend through many layers. The dextral shears are less prominent but more numerous, and individuals do not extend through many layers. The angle they make with the bedding is 30° , a little steeper than the sinistral shears.

This type of folding is interpreted as caused by lateral pressure exerted along the bedding with the easiest relief in a vertical direction. The fracturing in unconsolidated, essentially cohesionless sand is caused by dilatancy. When the lateral squeezing was initiated, the sand, having a granular fabric, tended to expand slightly, and the thin clay layers prevented water moving in to fill the increased pore space.

Before the water could seep in to relieve the stress, the granular fabric was fractured on a normal shear pattern for lateral compression of a solid body. Subsequent to the deformation, there was sufficient time for water to move in, relieve the intergranular stresses, and heal the fractures. The thin bands of clay aligned along some of the sinistral shears may have been brought in by the initial influx of water into the dilated fabric. However, apart from where there are clay layers along them, the fractures have ceased to become surfaces of weakness, and the sand can be regarded as structurally homogeneous in its present state.

3. INTERPRETATION

(a) ORIGIN OF THE CONTORTIONS

Despite the great variety of intraformational disturbances present in the Gormanston moraine it is possible to generalize the style of folding. In most cases the clay layers have behaved as completely competent, coherent units, while the bands of sand have been incompetent and cohesionless. The clay layers tend to maintain their orthogonal thickness, while the sand shows irregular variations in thickness. Nevertheless, in the narrow, diapiric anticlines and a few bands of quick clay, the clay layers have a geometry more allied to similar

or flow folds, indicating that in places the clay has behaved in a fluid manner.

I have interpreted most of the folds examined as having been caused by excessive water pressures developed in the sandy bands. Dilatancy in the granular bands together with local lateral pressure, make a subordinate contribution to the style of deformation. The ultimate origin of these forces is a matter for debate, and probably can not be solved unequivocally without detailed experiments. Fairbridge (1947) has given an excellent summary of the possible causes of intraformational disturbances in glacial varves, and of the seven hypotheses proposed he favours gravitational slumping as the cause for most of the Australian Carboniferous examples that he examined. Since 1947 the recognition of slumped sediments has become more widespread, and Fairbridge's opinions on these examples appear well founded. However, the type of glacial deposit Fairbridge examined is probably different from the Gormanston moraine since terrestrial glacial deposits are not likely to be preserved for more than a few million years (Carey and Ahmad, 1961).

Gravitational slumping does not appear to be the main cause of deformation at Gormanston. Despite the assertions of some writers to the contrary, slumping associated with lateral movement produces dimensional orientation of fold elements (e. g. the syntaphral slumping at Paga Point). The random

distribution of fold-hinges [see Fig. 5 - 1 (b)] indicates that there has been little, if any, consistent lateral movement in the Gormanston moraine.

All the intrastratal disturbances that have been observed at Gormanston can be explained when it is realized that the moraine was probably formed from a wet-base glacier. The water percolating through the ground moraine of a wet-base glacier supports much of the ice load (Carey and Ahmad, 1961), and since the height of the ice is usually considerably greater than the level of the terminal melt water, there is an excessive water pressure in the moraine. This high pressure causes upwelling of the ground water and accounts for the diapiric action of the sand.

Lateral pressure was a subsidiary, although operational force in the moraine. The box folds, and some of the convolute folds, have been formed mainly by lateral pressure or local lateral movement. Sutton (1963), Bradshaw and Inglesmith (1963) and many earlier workers have described structures caused by alternate freezing and melting of ground water. Charlesworth (1957, 1, p. 559) noted that the lower limit of frozen ground is probably uneven owing to variations in the pattern of water circulation. The water-ice transformation which involves an increase in volume of approximately 9%, is sufficient to cause the amount of lateral deformation observed.

(b) CONCLUSIONS

Three main conclusions can be drawn from this work.

- (1) The intraformational folds in the Gormanston moraine are both open- and closed-cast.
- (2) There is a large range of fold styles but the clay bands generally have been coherent and maintain orthogonal thickness, whereas the sand has been cohesionless and varies irregularly in thickness.
- (3) Most of the structures have been produced by excessive water pressures developed in the sand. Dilatancy, and lateral pressure caused by alternate freezing and thawing of the ground, are subordinate causes of deformation.

CHAPTER 6

EARLY-DIAGENETIC, INTRAFORMATIONAL FOLDING IN THE
PLEISTOCENE LISAN FORMATION, ISRAEL

1. INTRODUCTION

The Lisan Formation in Israel (Langozky, 1963) is composed of 25 to 40 metres of Upper Pleistocene sediments which are thought to have formed in a lacustrine environment. The Lisan deposits are the only sediments which are well correlated throughout the Rift Valley, and they overlies unconformably the Hamarmar Formation which measures 70 metres in its thickest outcrop, although the base is not exposed. The sediments of the Lisan are composed mainly of gypseous marls and sandstones, and are virtually unconsolidated. Within the formation there are several bands of contorted layers separating almost horizontal, non-contorted marls. Professor S. W. Carey took a series of profile photographs of these contortions at co-ordinates 1835/0545 (Palestine Grid) in a canyon, Nahal Parazim, which

is a tributary of the Pitulim. Mr. Y. Langozky of the Geological Survey of Israel kindly collected samples from the actual layers in the photographs, and these samples, together with the photographs, form the basis of this study.

2. PETROLOGY

The Lisan Formation is light-coloured with alternate light and dark laminations. The sediments collected by Mr. Langozky were first disaggregated in 0.01 N solution of sodium oxylate, and then washed in fresh water. Samples were mounted in both glycerine and water, and were examined microscopically.

The clastic particles in the dark bands (34520, 34523, and 34525-6) are predominantly quartz, feldspar, green amphibole and chlorite, with minor quantities of zircon, rutile and an opaque iron mineral. The larger grains reach 0.05 mms. diameter, and are moderately well rounded, but there is a considerable proportion of fine, angular silt. In addition, 10% to 20% of the sediment is composed of perfectly formed calcite rhombs.

The light-coloured bands (34521-2 and 34524) are composed almost entirely of aragonite needles up to 0.01 mms. long and 0.002 mms. across. These crystals aggregate in a number of ways forming crosses and spherules up to 0.02 mms. across. Contacts between crystals are at the ends of the needles rather

than along their sides. Brownian motion of the small crystals suspended in water can be observed under the microscope, and it is possible that such motion at the time of formation of the aragonite crystals caused aggregation into crosses, spherules and groups of spherules.

Langozky (1961, p. 155) notes that the ratio between detrital and chemical sediments in the Lisan Formation is 1:3. The aragonite in the light-coloured bands is believed to have been chemically precipitated, as is also the calcite in the darker bands. Bentor, and Vroman (1960, p. 68) conclude that

"The lighter, more chalky and gypseous, varves represent the summer deposits, while the darker varves, which are richer in clay material, were formed during the winter."

Thus the light-coloured bands were formed predominantly by chemical precipitation during the hot, dry summers; the dark bands by influxes of silt in the wetter winters.

Picard (1943, p. 151), Bentor and Vroman (*op. cit.*) and Langozky (*op. cit.*) have all concluded that the sediments of the Lisan Formation (*sensu. stricto*) were deposited under lacustrine conditions. Langozky has deduced that the waters were to 2 to 3 times more dilute than those of the lake in which the underlying Hamarmar Formation was deposited, and the Hamarmar lake resembled the present Dead Sea in volume and composition. The greatest thickness of sediment covering the contorted layers

was probably about 20 metres, and certainly less than 50 metres. However, it is not known what thickness of sediment overlaid the contorted zones at the time of deformation, although the structures are closed-cast.

3. STRUCTURAL DESCRIPTIONS

The folded zone in Fig. 6 - 1 (a) lies between undisturbed beds. It consists of two bands of light-coloured, relatively competent layers which are separated, both from themselves, and from the bounding strata, by dark incompetent material. The four most competent layers, which are also the lightest coloured layers, have been stippled. Layers 1, 2 and 4 (34524) are rhythmically banded, aragonite-rich layers, while layer 3 (34525) is more coarsely stratified and, in addition, has a silt fraction of 20% to 30%. The aragonitic layers have been competent during deformation, and the incompetent layers are composed predominantly of fine-grained sand.

Considered in its entirety, the folded zone faces towards the left, which is towards the Dead Sea. Individual folds vary from upright to asymmetric, overturned, and facing to the left. The right-hand limbs of the anticlines are always longer than the left-hand limbs, and the axial surfaces of some of the folds are involuted.

LATERAL SLIP ON FOLD ZONE

PLEISTOCENE LISAN FORMATION, ISRAEL

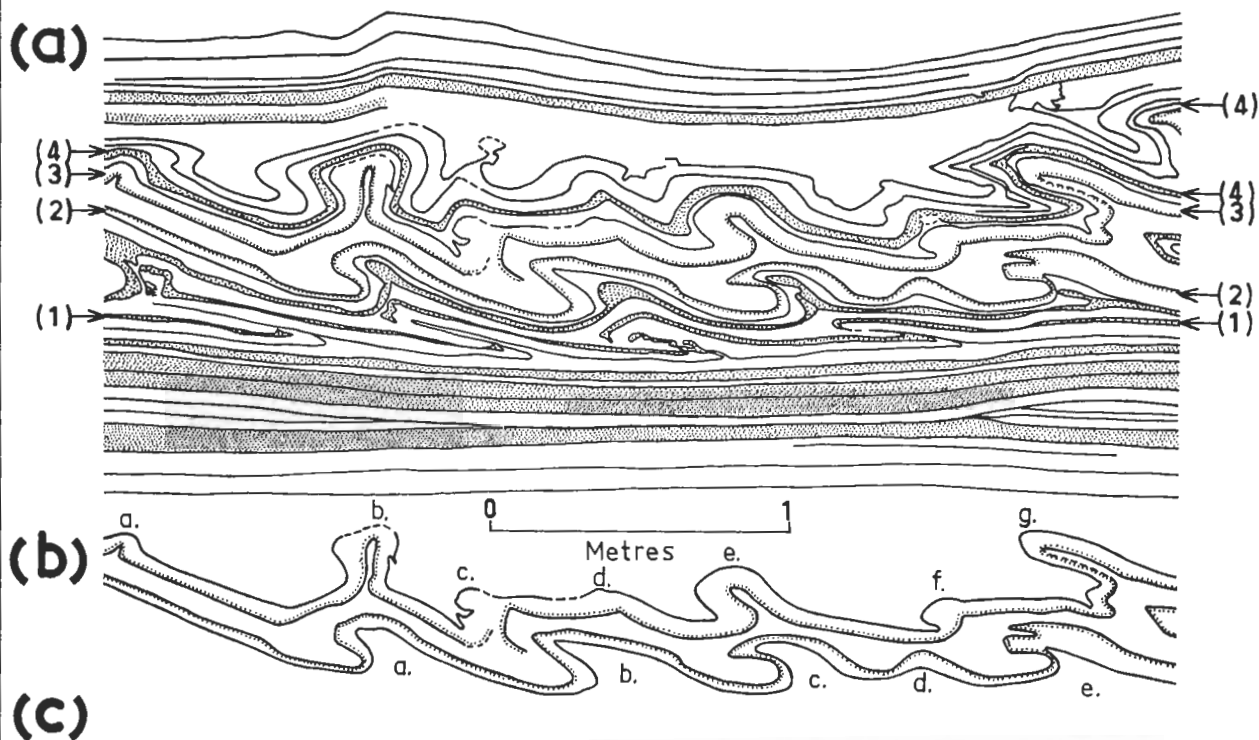


FIG: 6-1

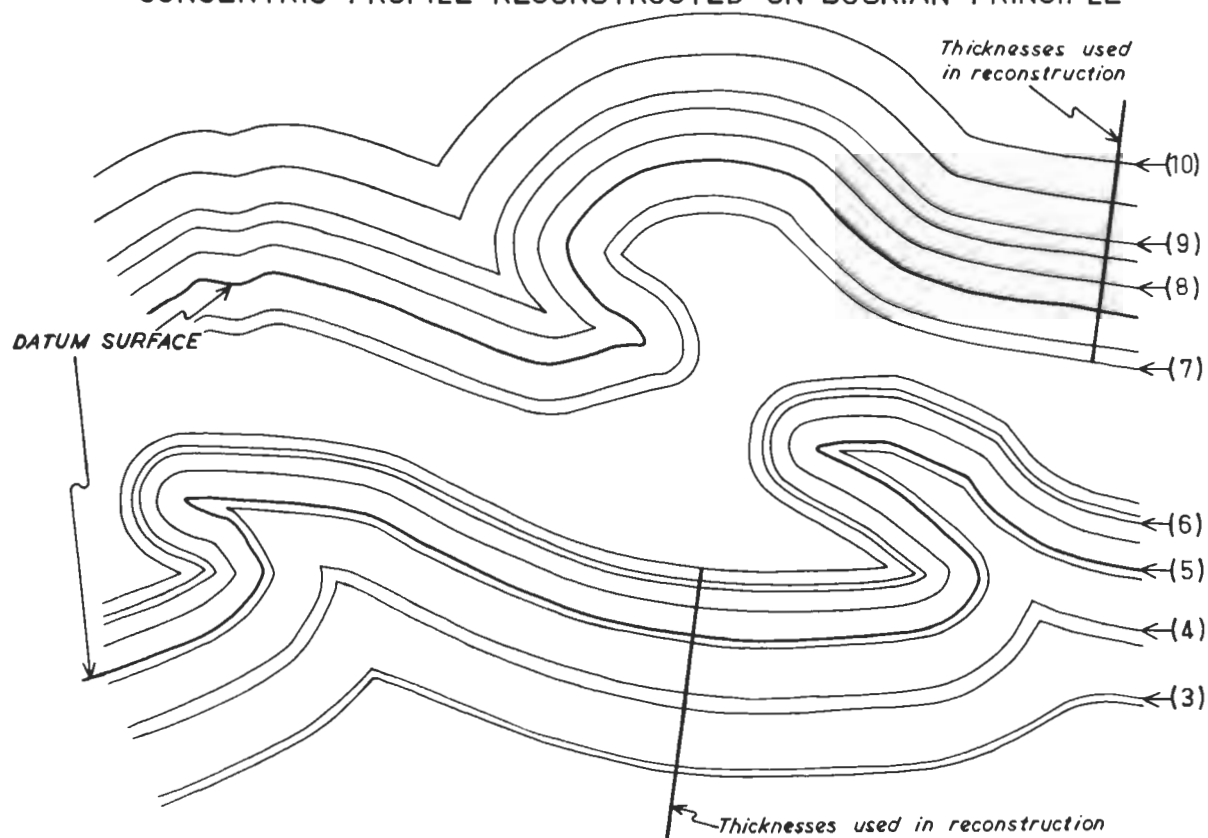
The lengths of the competent layers 1 to 4 were measured with dividers in order to determine the amount of shortening in the section. The ratios of the unfolded length to the horizontal length for Layers 1 to 4 are as follows:- Layer 1 - 1.4₉; Layer 2 - 1.4₈; Layer 3 - 1.4₇; Layer 4 - 1.5₀. It is remarkable that these ratios compare so well in spite of the thickening and thinning of parts of the layers depending on their position in the folded band. These ratios correspond to a shortening of 33% in the horizontal direction.

In addition to lateral shortening, there has been considerable movement between the upper and lower bounding layers. The folds in both the upper and lower folded bands show sufficient similarity in wavelength and shape to suggest that initially each fold involved both bands, and that later during deformation the upper and lower groups of layers acted independently. Fig. 6 - 1 (b) shows the probable correlation between the folds in the upper and lower bands, and indicates a lateral movement of about 1 metre in the middle incompetent band.

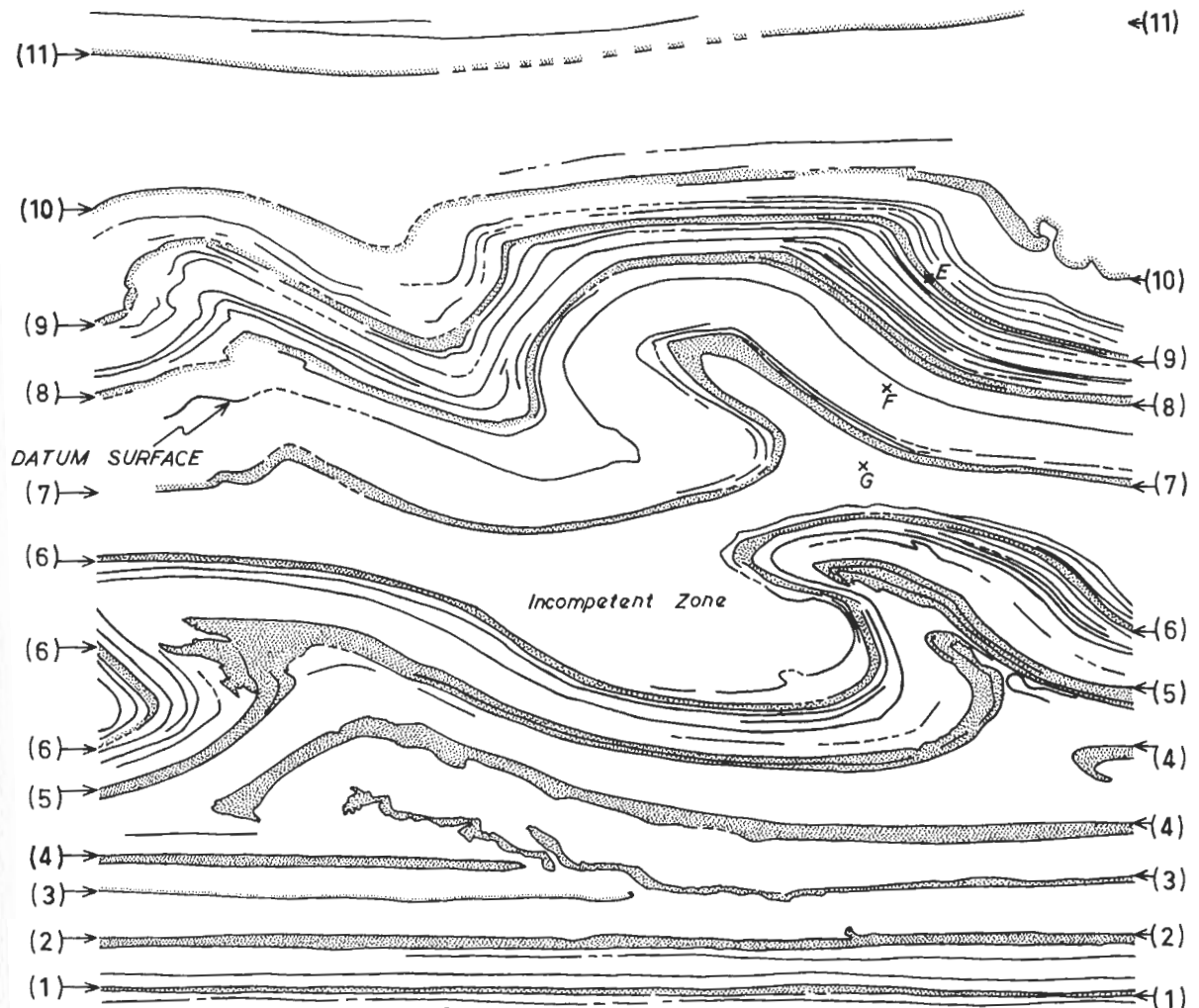
Fig. 6 - 2 (a) is a tracing of the fold in Fig. 6 - 1 (c). Ten individual laminae of gypseous marl have been stippled, and individual surfaces are numbered as shown. Two surfaces which are associated with the thickest competent bands were selected and have been marked in as thick lines in the overlay

191

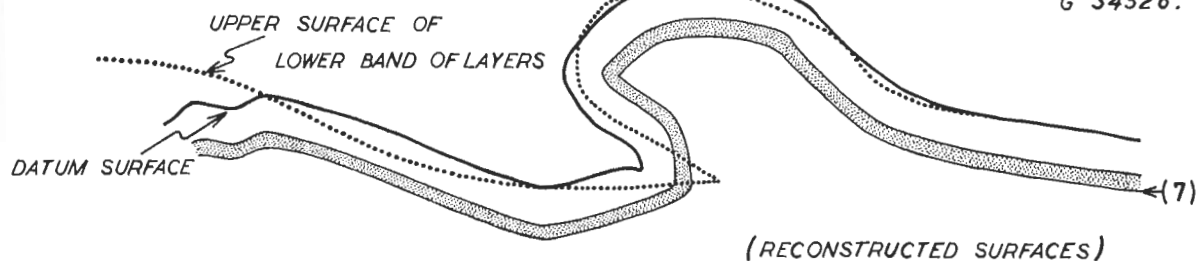
CONCENTRIC PROFILE RECONSTRUCTED ON BUSKIAN PRINCIPLE



DISTORTED CONCENTRIC FOLD PLEISTOCENE LISAN FORMATION, ISRAEL



CATALOGUE NOS E 34524,
F 34525,
G 34526.



(b) FOLD-SHAPE COMPARISON BETWEEN THE UPPER AND
LOWER BANDS OF LAYERS

FIG: 6-2

to Fig. 6 - 2 (a). From these two surfaces, one the upper surface of the aragonite-rich silt layer [Surface 3, Fig. 6 - 1 (a)], and the other the upper surface of an aragonite layer in the fine silt between Surfaces 1 and 2 [Fig. 6 - 1 (a)], a concentric profile has been constructed using an averaged thickness for each layer. When a comparison is made between the reconstructed concentric profile and the actual profile, a number of conclusions can be drawn.

- (1) The reconstructed upper surface of the lower band of layers fits quite well with the datum-surface used in the reconstruction of the upper band of layers [Fig. 6 - 2 (b)].
- (2) The crest of the anticline has been thinned in a vertical direction, but extended horizontally. The geometry is what would be expected if the anticline had been squeezed against a rigid upper boundary while still able to extend laterally.
- (3) The cross-sectional area of the inner cores of the folds in both the upper and lower bands has been reduced in comparison with the reconstructed profile. The geometry corresponds to the geometry that would occur if the incompetent material were squeezed out of the fold core or decreased in volume with respect to the competent layers.

- (4) Despite the modifications noted, the geometry of the folding is essentially concentric.

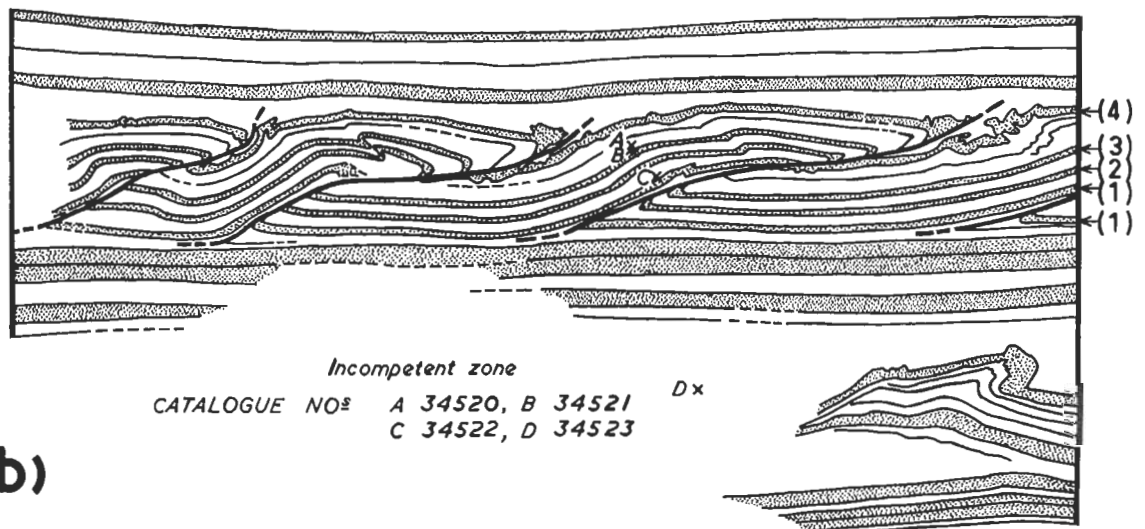
It should be noted that the reconstructed upper surface of the lower fold [Fold (c) in Fig. 6 - 1 (b)] did not originally fit into the upper fold [Fold (e) in Fig. 6 - 1 (b)]. Nevertheless, the shape of Fold (e) in the lower folded band is almost identical with the shape of Fold (c), and the comparison is justified.

Fig. 6 - 3 (b) is a photograph of a series of small-scale, nappe-like folds which are remarkable both for the regular reproduction of style from one individual to the next, and for the constant sense of displacement. These nappe-like folds are confined to one band of sediments which invariably has a fine-grained, structureless sand or silt at the top. The beds above and below the folded zone appear to be undeformed, and as no truncations of the upper layers has been seen in any of the folded zones, the deformation was closed-cast. In Fig. 6 - 3 (a) [a tracing of Fig. 6 - 3 (b)] four thin layers (1 to 4) have been stippled, and their lengths through the horizontal width of the section were measured. All four layers are between 1.50 and 1.53 times as long as the present horizontal width of the section, which corresponds to a shortening of approximately 33%.

The thrust faults along which the nappes have glided are geniculate surfaces. Where each thrust cuts through the originally horizontal layers it is inclined at 25° to 30° . At

SMALL-SCALE, NAPPE-LIKE FOLDS PLEISTOCENE LISAN FORMATION, ISRAEL

(a) Unfolded length : length of section \div 1.5



(b)



(c)

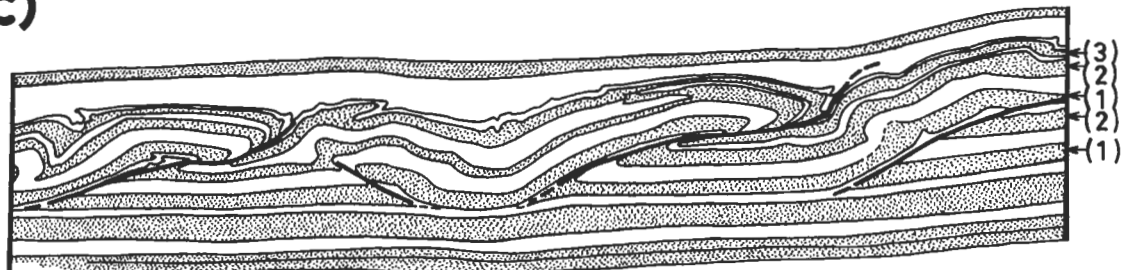


FIG: 6-3

the original top of the folded layers the thrust surfaces extend horizontally up to the point where the overriding sheet reaches the adjacent nappe. From this point the slip surface steepens and the nose of the overriding nappe is crumpled and shortened. Thus the sedimentary slices are arranged in a series of open S-shapes separated by open Z-shaped slip surfaces. In any folded band there is one particular layer along which the nappes have glided and in the examples studied the mobile layers are light-coloured - probably aragonitic silt.

Fig. 6 - 3 (c) is a tracing from a photograph of a folded zone from a different branch of the wadi where the same nappe structures as in Figs. 6 - 3 (a) and (b) are developed. The lengths of the three layers, 1, 2 and 3, as measured with dividers are respectively, 1.58, 1.50 and 1.32 times the width of the present horizontal section, although the value for layer 3 may be too low because of many minor plications that could not be adequately taken into account.

One of the geniculate thrust surfaces is facing contrary to the general direction, and as it is traced upwards it terminates in a small fold the axial surface of which has been involuted so that the nose of the fold in the upper layer faces in the same direction as the noses of the other nappe folds. The origin of this thrust is not clear, but it appears that since its formation its upper part has been rotated by the

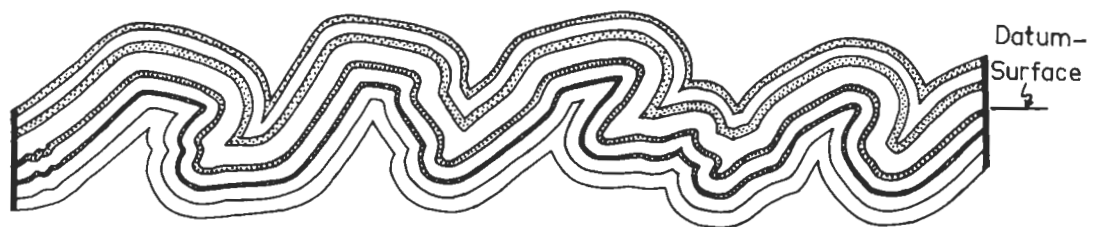
general movement from left to right.

Fig. 6 - 4 (a) is a photograph showing a zone of box-type folds above which there is a series of nappes with large horizontal displacement. Both the box folds and the nappes face towards the right, but whereas box folds are closed-cast and confined to one band of sediment, the nappes cut across several sedimentary layers. Both the nappes and the box folds reflect a large amount of lateral shortening.

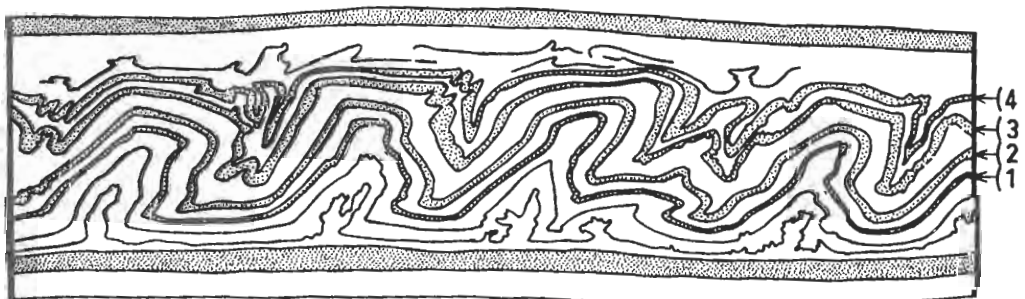
Fig. 6 - 4 (b) is traced off the layer of box folds, which is the same set of folds as in De Sitter (1964, p. 327, Fig. 250). Four of the light-coloured layers have been stippled and are numbered 1 to 4. The length of each of these layers is between 1.65 and 1.70 times the present horizontal width of the section, which corresponds to a shortening of 40%. The transparent overlay, constructed on the Buskian principle using the upper surface of layer 2 as the initial form, correlates closely with the actual profile showing that the folding is essentially concentric. The main deviations from ideal concentric geometry are

- (1) Thinning of the troughs and crests of the box-shaped folds, and
- (2) Intricate contortion of the layers on the concave side of the cusp in any fold. Layers on the top and bottom of the folded band are contorted more than those in the middle of the band.

Concentric Profile reconstructed on Buskian Principle from layer (2)



INTRAFORMATIONAL BOX-FOLDS PLEISTOCENE LISAN FORMATION IN ISRAEL



Unfolded length: section-length (1) 1.67 , (3) 1.68 ,
for numbered layers (2) 1.65 , (4) 1.70 .

0 2
Metres

FIG: 6-4

The folded band is composed predominantly of alternations of light- and dark-coloured layers, and the light-coloured layers have been most competent. The well-laminated, folded zone is capped by an apparently structureless band of grey silt or sand in which there are some pebbles, and this layer has been incompetent during the folding. The layer in which slip has been accomplished at the base of the folded zone is also a grey silt. The layers above and below the folded zone are well bedded and apparently undisturbed by the deformation.

4. ORIGIN OF THE INTRASTRATAL CONTORTIONS

Picard (1943, p. 155) commented that there were still two unsolved problems in connexion with the Lisan sediments, one of these being the origin of the intrastratal contortions, and he suggested that perhaps they could be explained by the hydration of anhydrite. Such an origin can be dismissed on three counts. Firstly, there is very little gypsum in the contorted layers. Secondly, there are non-contorted layers both above and below the folded zone with a higher gypsum content than the contorted layers, and thirdly, the lateral shortening indicated by the folding is approximately 33% which is the maximum that could occur if the layers were 100% gypsum.

The lateral shortening indicated by the concentric folding could have taken place in either of two ways. In one model there may have been a considerable horizontal movement between the upper and lower blocks causing the overall length of the contorted bands to shorten, and in the other model there may have been alternate zones of stretching and shortening along any one contorted band. Which of these two mechanisms has operated can not be deduced from existing data, but could be checked in the field as in the latter model the contorted band should pinch and swell when traced laterally over a distance.

Langozky (1966, *pers. comm.*) considers that the contortions have developed by slump towards the Dead Sea graben-trough. He notes that the Lisan Formation dips easterly towards the western margin of the Dead Sea at inclinations from 0.5° to 4° , and that dip measurements in the Lisan sediments in the Pitulim Valley do not always coincide with the regional dip of the Lisan Formation. The occurrence of lacustrine sediments [Hamarmar Formation (?)] 85 metres above the highest known level of the "Lisan Lake" (Langozky, 1963), and also on top of the neighbouring Mt Sdom, are independent testimony of Late Pleistocene or Recent movements in the graben.

The development of individual folds is instructive. I have demonstrated that most of the folds approximate closely to a concentric style, but the distortions are significant. In Fig. 6 - 2 (a) the crest of the anticline has been thinned in a vertical direction, and extended horizontally. This could not have been caused by simple gravitational compaction of a concentric profile, since the original thickness in the vertical direction which would be the same in both the crests and adjacent troughs, should have compacted to the same thickness in both locations. It appears that the crest of the anticline has been squeezed against the over-lying undeformed layer, and extended plastically in a horizontal direction. A similar mechanism has operated for other folds in Fig. 6 - 1 (a) and Fig. 6 - 4 (a).

All the structures must have been formed closed-cast with respect to the uppermost deformed surface, for nowhere is there a truncation of the folded layers. If the small-scale, nappe-like structures had formed in an open-cast situation it is unlikely that they would not have been eroded. The structureless, grey silt or sand which caps most of the deformed layers appears to have been highly disturbed, and probably acted as an upper décollement zone.

The chemically precipitated, aragonitic layers have been competent, and the detrital silt layers incompetent. The forces which bound the aragonite needles into crosses and spherules may have been sufficient to maintain cohesion during deformation. There were no corresponding intergranular forces in the detrital layers which consequently were cohesionless and incompetent.

In my opinion, the geometry of these contorted layers and their mechanism of deformation can be explained best in terms of the development of relatively high water pressures in certain zones during creep towards the Dead Sea graben which was actively subsiding. During the creep a stage was reached in certain zones where grain-to-grain contacts were disrupted, and the overburden load - significant, although small, since the maximum depth of burial of the folded zones is 25 to 40 metres - was taken on the pore water of the silty layers. The intergranular forces between the detrital particles in these silt layers were negligibly small, but the stronger intergranular forces in the finer grained, chemically precipitated layers were sufficient to maintain cohesion.

The loss of cohesion in certain zones reduced the effective viscosity of the folded zone markedly, and thus the intervening strata behaved as rigid sediments. As well as the lateral shortening indicated by the concentric folding, other horizontal

displacements were accomplished, as indicated in Fig. 6 - 1 (b). The escape of the high-pressure water out of the folded zones caused the crests of the anticlines to be squeezed against the undeformed bounding zones. Deformation continued until the excessive water pressure was relieved, after which the contorted zone gradually recovered a viscosity comparable with that of the intervening undeformed layers. Movement did not necessarily occur on all the deformed zones at the same time.

5. CONCLUSIONS

Five main conclusions can be drawn from this study.

- (1) The style of folding in the contorted layers is essentially concentric.
- (2) The aragonitic layers are competent; the detrital silty layers incompetent.
- (3) Lateral shortening of the order of 33% is indicated in the folded bands, and slightly more shortening is associated with the nappes.
- (4) The deformation is closed-cast, and probably caused by slumping towards the Dead Sea graben.
- (5) Both the modifications to the basic concentric style and the mechanism of movement can be explained simply by the development of high water pressures in the incompetent layers.

CHAPTER 7

FOLDING IN THE CONTACT AUREOLE OF A QUARTZ-DIORITE
DYKE, NORTHEASTERN TASMANIA

1. INTRODUCTION

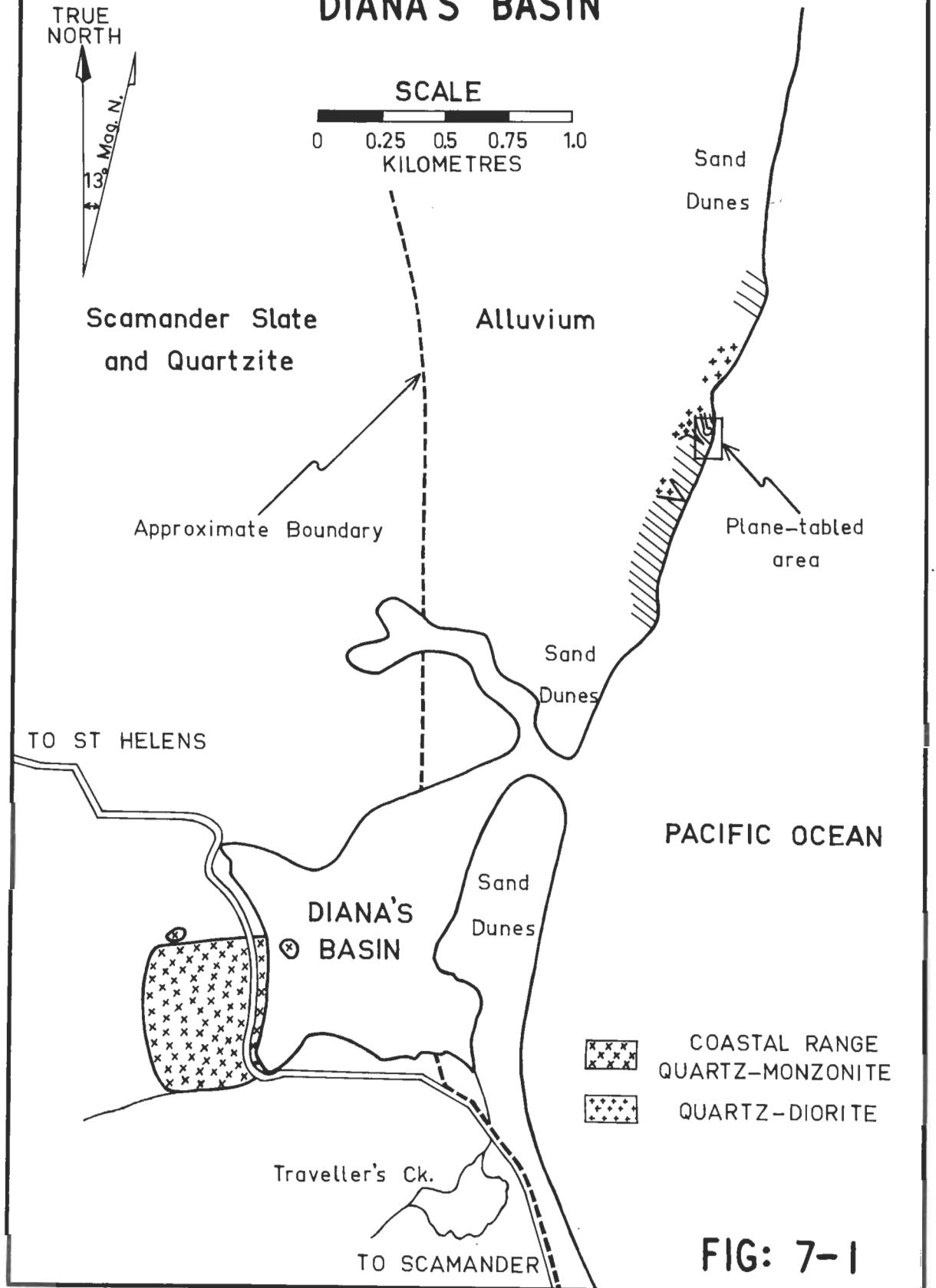
On the coast of northeastern Tasmania, about one mile north of Diana's Basin, near St Helens, there is a well-exposed contact between quartz diorite and siliceous mudstones which may be part of the Scamander Slate and Quartzite (see Fig. 7 - 1). Walker (1957) has shown that the Late Devonian (McDougall and Leggo, 1965) quartz monzonite intrudes the Scamander Slate and Quartzite with sharp transgressive contacts. Walker (*ibid*, p. 32) noted that,

"Diorite porphyry apophyses, sills and dykes occur within the granitic mass and penetrate the country rocks up to 75 feet from the contact zone. ...They cut the aplite dykes, and therefore are slightly younger than the quartz monzonite massif and aplite dykes."

and (p. 33),

"Plagioclase is more basic than that in the quartz

GEOLOGICAL SKETCH-MAP DIANA'S BASIN



monzonite and usually approaches labradorite in composition."

The quartz-diorite dyke about one mile north of Diana's Basin is one of these dykes.

McNeil (1960) plane-tabled part of the area and incorporated a preliminary report as an appendix to his Honours thesis. The most notable features of the exposure are the plastic style of folding immediately adjacent to the quartz diorite and the occurrence of basic-plagioclase feldspars in the contact zone. In order to study these problems a more extensive area was plane-tabled by D. McP. Duncan and myself, and the map agrees in all essential details with that of McNeil.

2. STRUCTURE














(a) GENERAL

Fig. 7 - 2 is an outcrop map showing the distribution of measured foliations and fold elements. Three rock types have been distinguished, viz. hornfels, quartz diorite and quartz dolerite. The hornfels is dense and fine-grained with slight textural and colour banding parallel to the original bedding. The sediments are relatively unmetamorphosed away from the quartz diorite, and to the south extend uninterrupted for half a mile, dipping steeply on a constant strike of 138° . Small-scale cross-bedding is common in some of the

IGNEOUS CONTACT ZONE DIANA'S BASIN

Plane-tabled by C.McA. Powell and D.McP. Duncan 1965

LEGEND

-  Sediments (bedding traces shown)
-  Quartz-diorite
-  Quartz-dolerite
-  Contorted bedding and Quartz-diorite lobes
-  Boundary in region of 100% outcrop
-  Probable boundary in region of limited outcrop
-  Possible boundary in region of no outcrop
-  Limit of 100% outcrop
-  Bedding, with dip shown
-  Overturned bedding
-  Bedding, with measured facing
-  Fold-hinge with plunge in degrees and axial plane with dip
-  Approximate low-water mark

Tidal range averages 1.5 metres

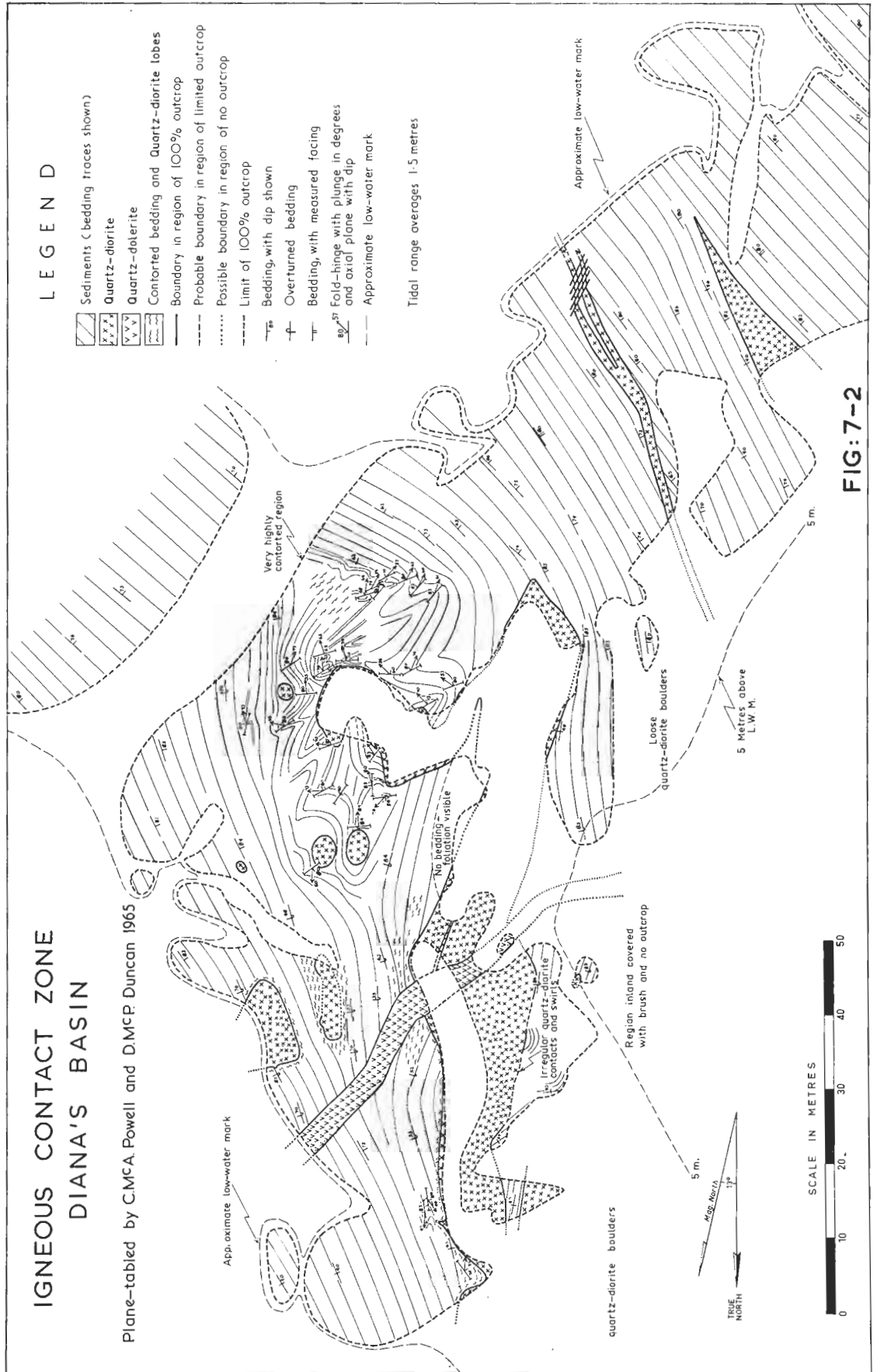


FIG: 7-2

layers, and indicates that stratigraphic top of the whole area is towards the south. There are at least three zones (two to three metres thick) south of the mapped area in which there have been intraformational folding in the sedimentary or early diagenetic stage.

The quartz diorite extends north and west for at least half a mile so that the area may be regarded as the southeastern contact of a stock-like body. There is only one outcrop of quartz diorite south of this area and this also extends westward. In the mapped area the quartz-diorite outcrops are all related to one main dyke with which the folding is associated, and to the south there are two smaller dykes adjacent to which there has been no folding.

Most of the folding is limited to a band of sediments on the northeastern side of the main dyke. This zone does not extend laterally out to sea, and all the folds are adjacent to the main dyke or small quartz-diorite pods connected to it. The northeastward-striking, quartz-dolerite dyke is a later dilational feature.

(b) FOLDING

(i) Brief Description. Two classes of folds can be distinguished in the field.

(1) Irregular, highly contorted folds, many in the form

of envelopes around pods of quartz diorite which are always immediately adjacent to a larger mass of quartz diorite.

Fig. 7 - 3 (a) shows some quartz-diorite lobes from the northern end of the outcrop where the sediments have been thinned and expanded around each lobe. It is not possible to measure accurately the orientation of these lobes because they are small-scale and the tough hornfels does not allow excavation of layers. Nevertheless, they do not appear to have a strongly preferred orientation.

(2) More regular, larger-scale folds in which there have been both competent and incompetent layers. These are the folds bedding traces of which are shown in Fig. 7 - 2. The style of folding varies from bed to bed and from one part of the area to another. The sandstone layers furthest from the quartz-diorite dyke tend to maintain their orthogonal thickness, whereas those layers immediately adjacent to the dyke have considerable variations in thickness. The essentially concentric style of some of the layers is shown in Fig. 7 - 3 (b).

Figs. 7 - 4 (c) and (d) are tracings from photographs of intraformational folds caused by the intrusion of a granodioritic vein remote from the quartz-diorite dyke. The sandstone layers have been competent with respect to the granodiorite. If the folds are to be regarded as pre-intrusive structures in which certain beds have been selectively replaced by granodiorite, it

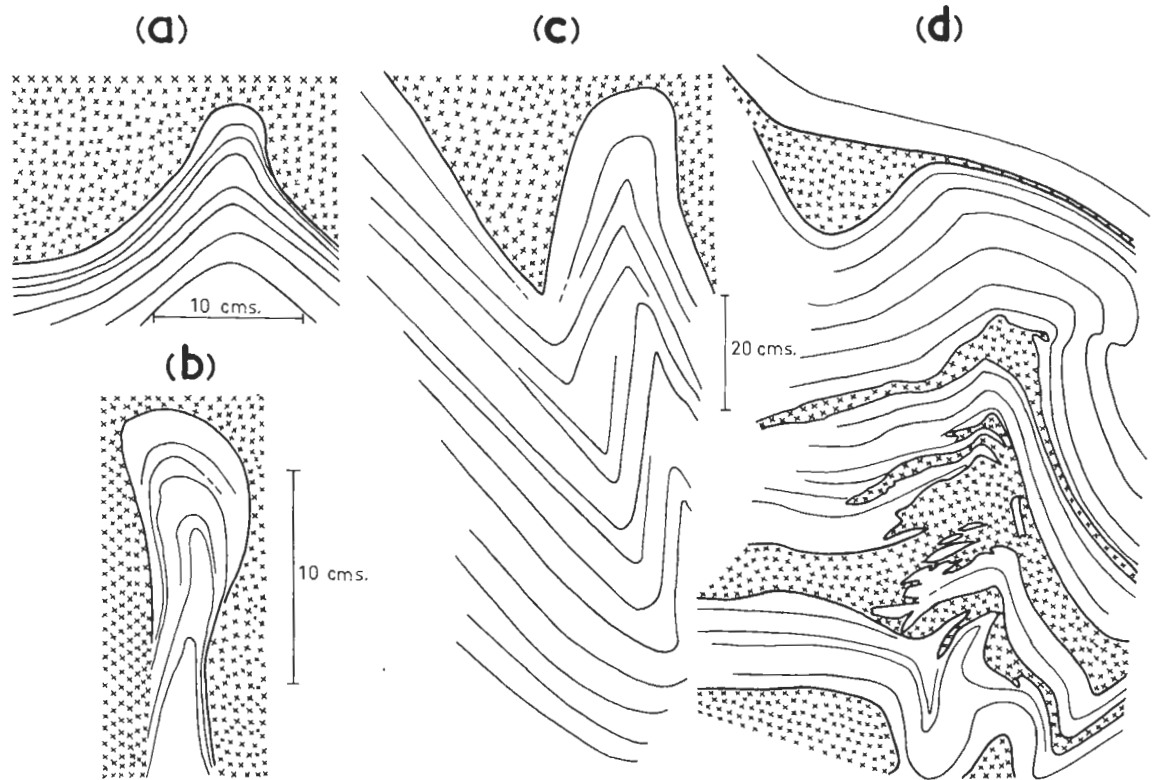


Fig. 7 - 3 (a). Quartz-diorite lobes from the northern end of the outcrop. The sedimentary layers enclosing each lobe have expanded in surface area and decreased in thickness. Main quartz-diorite dyke is to the right-hand side. The hammer is approximately 30 cms. long.



Fig. 7 - 3 (b). Essentially concentric style of folding in some mudstone-layers away from the quartz-diorite contact. Six-inch rule shown.

FOLDS CAUSED BY QUARTZDIORITE MAGMA



FORMATION OF QUARTZDIORITE LOBES

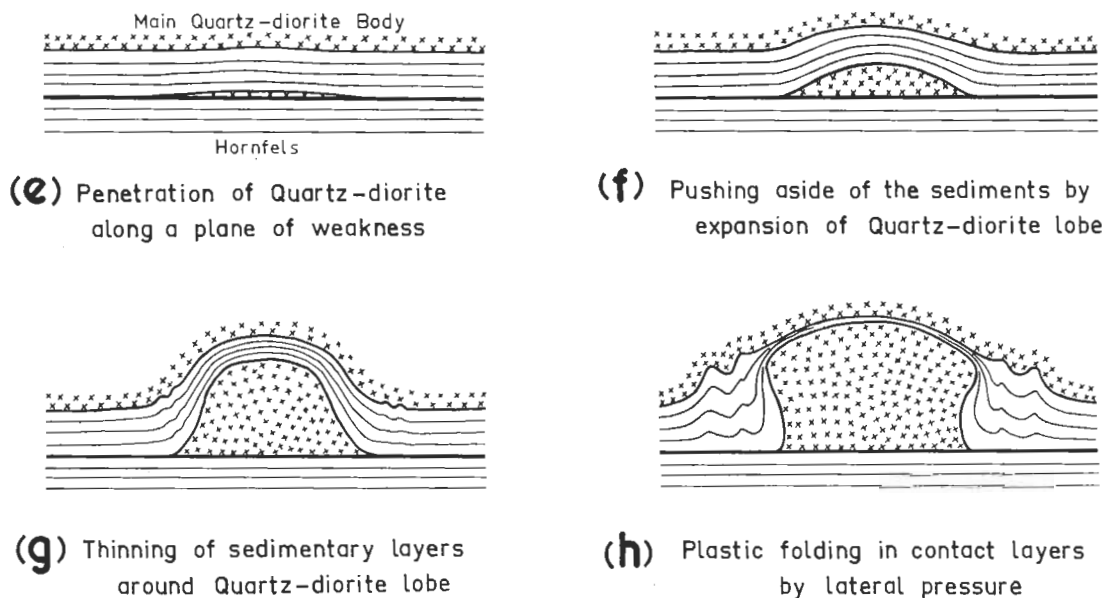


FIG: 7-4

is anomalous that the granodiorite has replaced the incompetent siltstones rather than the more permeable sandstones. A more likely interpretation is that the quartz-diorite veins lubricated the bedding surfaces and accommodated the strain developed by concentric folding of the sandstone layers.

(ii) **Rotation of the Bedding.** The bedding orientations can be conveniently divided into two groups on a scale of metres.

- (1) Those which are related to individual fold-hinges, and
- (2) Those which are not specifically related to individual fold-hinges.

Fig. 7 - 5 (a) is an equal-area projection of 87 bedding orientations which are related to individual fold-hinges. They form a complete girdle about an axis $65^{\circ}/180^{\circ}$. Fig. 7 - 5 (b) is an equal-area projection of 32 fold-axes, most of which were calculated from the bedding readings by the π method. The maximum concentration is at $79^{\circ}/171^{\circ}$ which is in reasonable agreement with the axis in Fig. 7 - 5 (a). A mean fold-axis of $71^{\circ}/175^{\circ}$ is taken.

Fig. 7 - 5 (c) is an equal-area projection of 72 bedding orientations which were not specifically related to individual fold-hinges on the scale of metres. They form a partial girdle about the mean fold-axis. The cross marks the orientation of the bedding from the straight-bedded zone which extends southward at a constant attitude for more than a kilometre.

STRUCTURAL ELEMENTS, DIANA'S BASIN

EQUAL-AREA PROJECTIONS

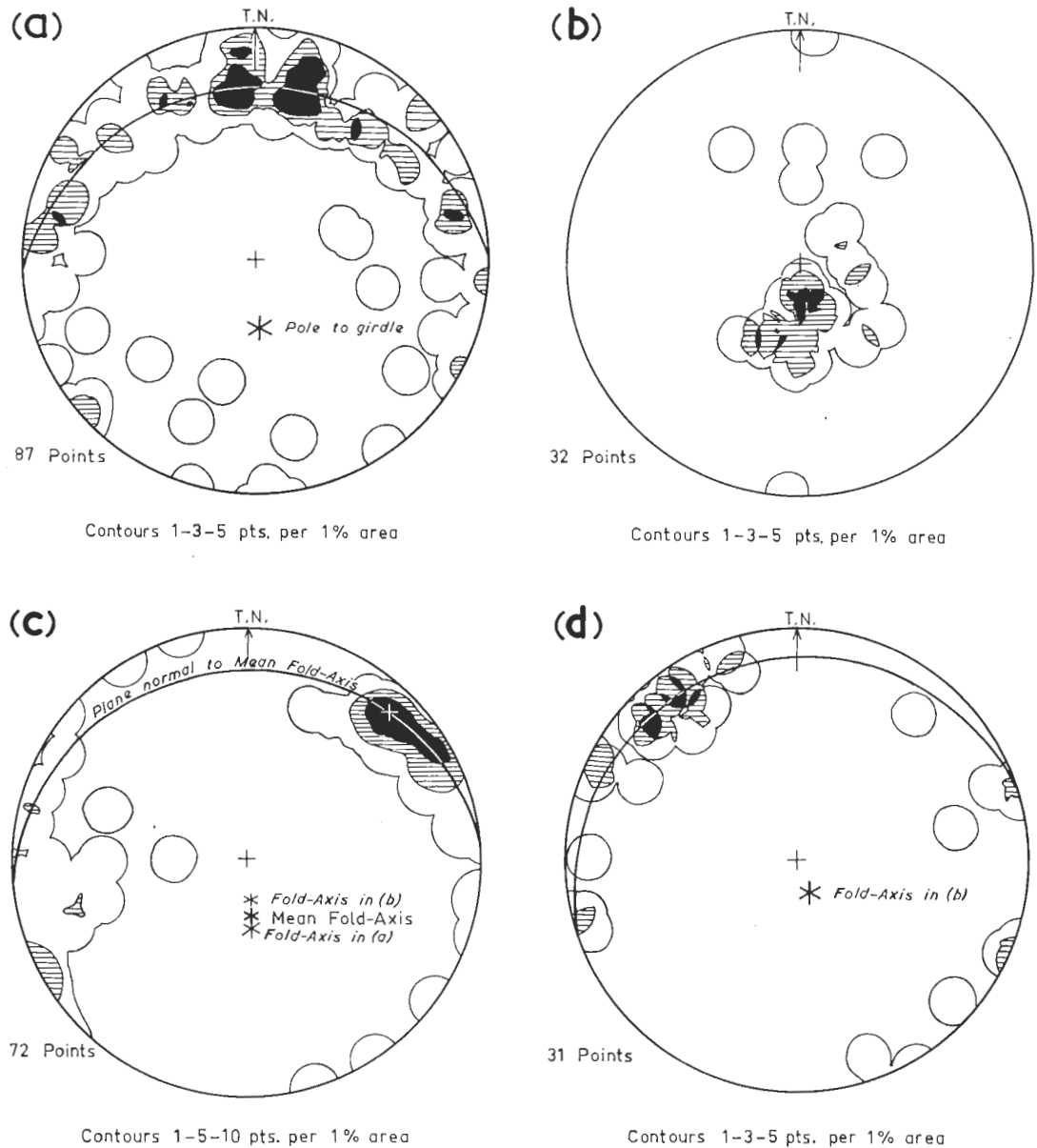


FIG: 7-5. (a) Poles of bedding specifically related to individual fold-hinges. Pole to girdle $65/180^\circ$
 (b) Fold-Hinges. Maximum concentration $79/171^\circ$
 (c) Poles of bedding not specifically related to individual fold-hinges. Mean fold-axis $71/175^\circ$. Cross marks bedding to the South.
 (d) Poles of Axial Planes.

The bedding in the folded zone may be regarded as having a polarity with respect to the constant orientation to the south, and this polarity corresponds to a clockwise rotation about the mean fold-axis. Fig. 7 - 5 (d) is an equal-area projection of the poles of 31 axial planes. These, too, form a partial girdle about the average fold-axis in Fig. 7 - 5 (b).

3. PETROGRAPHY

(a) QUARTZ DIORITE

The main body of quartz diorite (34955) a few hundred metres north of the mapped contact is a coarse-grained, even-textured rock with some dark enclaves. Many of the enclaves appear to be xenoliths of hornfels, but there are several "basic clots" composed mainly of mats of hornblende and plagioclase. The quartz diorite contains 70% plagioclase and 25% quartz, the remaining 5% consisting of biotite (with some alteration to penninite) and accessory zircon and magnetite. No potassium feldspar has been found in the slides examined. The plagioclase occurs both as strongly zoned crystals and as albitic patches. The zoned crystals show normal, reversed and oscillatory zoning with an overall normal trend from basic-labradorite cores to oligoclase rims. They form 30% to 40% of the rock, and together with the quartz and biotite are included in poikilitic patches of albite. The basic-plagioclase cores are commonly

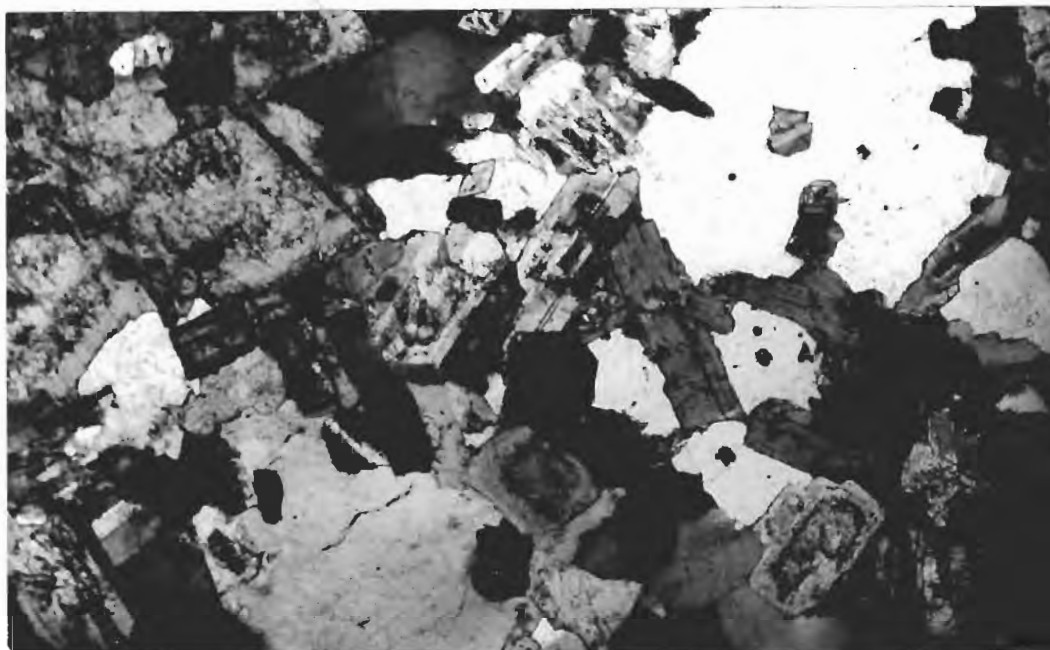


Fig. 7 - 6 (a). (34951B) Quartz diorite from the main dyke. Small, zoned labradorite crystals and biotite flakes are set in more coarsely crystallized quartz and sodic plagioclase. The width of the field of the photograph is approximately 4 mms.

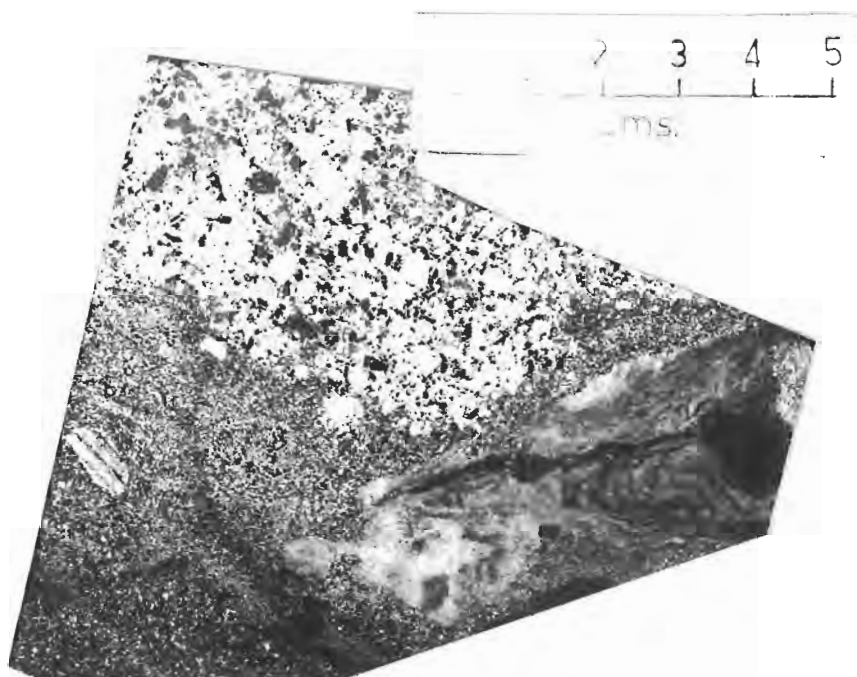


Fig. 7 - 6 (b). (34961) Plastic folding in the hornfels immediately adjacent to the quartz-diorite contact. The banding is original compositional banding in the hornfels. Scale is shown.

altered to sericite, and more rarely to epidote and chlorite. Patchy zoning also occurs in the zoned plagioclase.

The quartz diorite (34951) in the main dyke is considerably darker and finer grained (average grain size 2 to 3 mms.) than the main body. It is composed of 55% plagioclase, 25% quartz, 15% biotite (with some alteration to penninite) and accessory magnetite, zircon, and tourmaline. There are some dark, fine-grained patches which are composed almost entirely of mats of hornblende and plagioclase, with minor biotite and quartz. The plagioclase in the dyke rock occurs both as well-formed, zoned crystals and as irregular albitic patches. All types of zoning are found, and there is an overall normal trend from basic-labradorite cores to oligoclase rims. Albitic patches form poikilitic textures in places surrounding hornblende, quartz, biotite and zoned plagioclase crystals. The hornblende is a common green variety, and the biotite is strongly pleochroic from reddish brown to almost colourless.

(b) HORNFELS

The hornfels (34948, 34954 and 34958) not closer than 10 metres to the quartz diorite is a very fine-grained, quartz-sericite rock with some biotite and small quantities of chlorite, magnetite, tourmaline and zircon. Equidimensional, unstrained quartz grains, 0.05 to 0.1 mms. in diameter, form 60% of the

rock and are set in a very fine sericitic matrix which surrounds each grain and imparts a typical cement-like texture. In places the sericite has recrystallized to recognizable muscovite flakes *detrital* with a maximum size of 0.1 mms. diameter. Biotite is much coarser grained, up to 0.3 mms. diameter, and appears identical in colour with the biotite in the quartz diorite. The biotite commonly contains needle-like inclusions of rutile, and also small magnetite crystals which show hexagonal or octagonal sections. Small grains of tourmaline and zircon appear to be rounded detrital particles which have been included in the recrystallized quartz.

As the hornfels is traced towards the quartz-diorite dyke three important changes can be observed.

(1) The average grain-size of the quartz is progressively coarser towards the quartz diorite, and the cement-like texture is almost destroyed.

(2) Well-formed plagioclase crystals up to 5 mms. across occur within 5 metres of the quartz-diorite contact, and the crystals are complexly zoned with an overall normal trend from basic-labradorite cores to albite rims.

(3) Irregular patches of albite up to 5 mms. across and containing inclusions of quartz and sericite from the matrix, are found in parts of the hornfels.

The boundary of the plagioclase-bearing hornfels is not marked by any substantial lithic break, and the contact is irregular and transgressive to the sedimentary layers. The original bedding has been almost completely obliterated in the plagioclase-bearing rock which has an intrusive relationship to the finer-grained host in the outer part of the aureole. In polished hand-specimens (34949) the contact is generally sharp, although in thin-section (34956 and 34957) both rocks are typically hornfelsic.

The maximum size of the plagioclase crystals in the hornfels decreases away from the quartz diorite, but terminates abruptly at a size of 2 mm. at a distance of not more than five metres from the contact. As well as the individual, zoned plagioclase crystals in the hornfels there are also patches of albite or oligoclase up to 5 mm. across which have a poikilitic texture with respect to smaller inclusions of quartz and basic plagioclase. In most parts the grain-size of the sericite in the plagioclase-bearing hornfels is only slightly coarser than that of the sericite in the fine-grained hornfels, although in places individual muscovite flakes up to 0.5 mms. diameter can be recognized. The presumed originally equidimensional quartz grains set in a cement-like matrix [Fig. 7 - 7 (a)] have been transformed into an interlocking mosaic of quartz with scattered patches of sericite [Fig. 7 - 7 (b)].

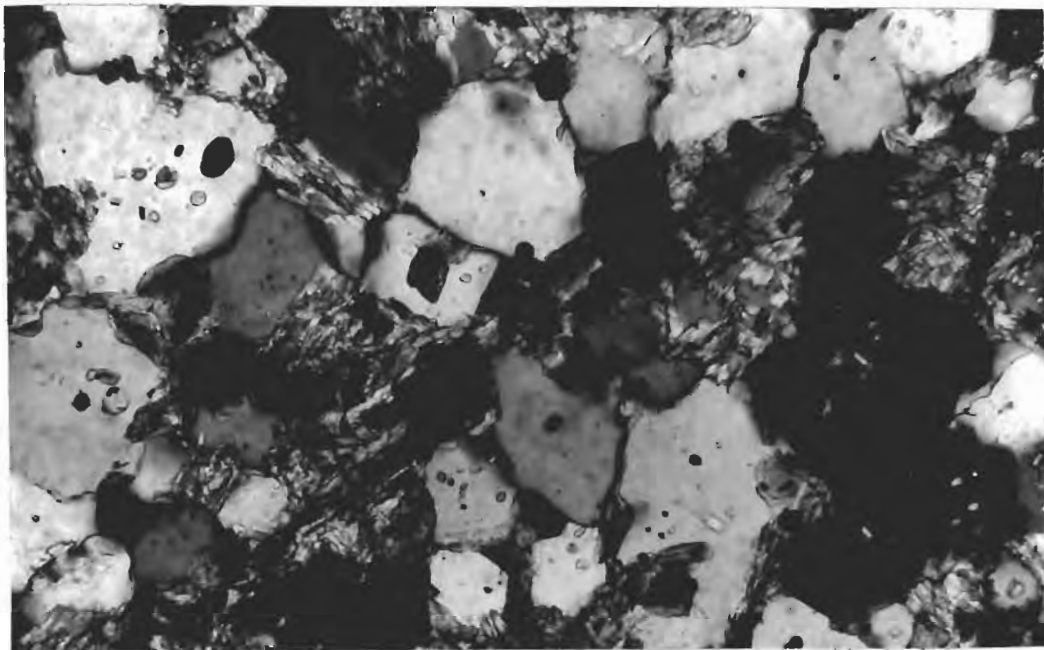


Fig. 7 - 7 (a). (34948) Cement-like texture in the hornfels away from the quartz-diorite contact. The width of the field of the photograph is 0.8 mms.

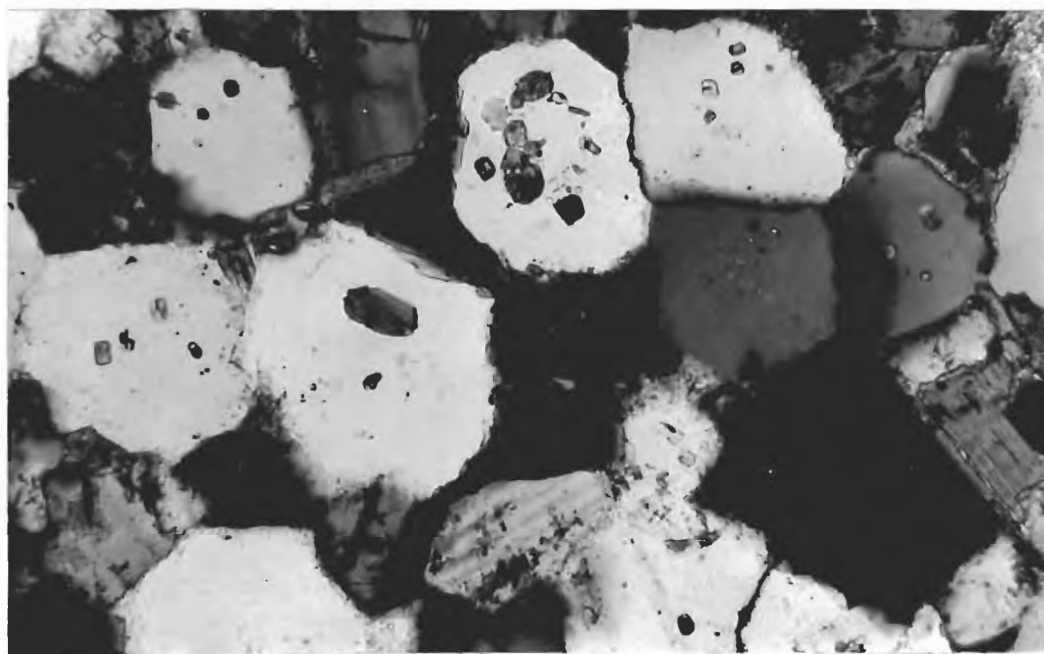


Fig. 7 - 7 (b). (34950) Hornfels texture immediately adjacent to the quartz-diorite contact. Quartz grains appear to have recrystallized 2 to 3 times coarser than in Fig. 7 - 7 (a). The width of the field of the photograph is 0.8 mms.

(c) GRANODIORITIC VEINS

Medium-to coarse-grained, thin granodioritic veins with less than 2% mafic minerals cut through all parts of the hornfels. They are composed predominantly of quartz and plagioclase with minor muscovite and some biotite, and have chilled margins and disoriented xenoliths. The plagioclase which is close to albite in composition has a completely different form from the well-zoned crystals found in both the main dyke and the hornfels, and occurs as ill-defined, irregular crystals up to 5 mms. across. These unzoned crystals are strongly altered to sericite in places, and have inclusions of both quartz and muscovite.

(d) HORNFELS CONTACT ZONE

The hornfels contact zone is a narrow zone less than 50 cms. wide, in which quartz-diorite lobes occur. In detail the contact zone is highly contorted, but the boundary between the quartz diorite and hornfels is a sharp interface. Zoned plagioclase crystals occur on both sides of the contact, but whereas the average grain-size of the quartz diorite is 2 to 3 mms., in the hornfels the grain-size is only 0.2 to 0.3 mms. In thin-section the quartz diorite has an igneous, poikilitic texture and the hornfels a recrystallized cement-like texture. There are many, small irregular folds which indicate that this

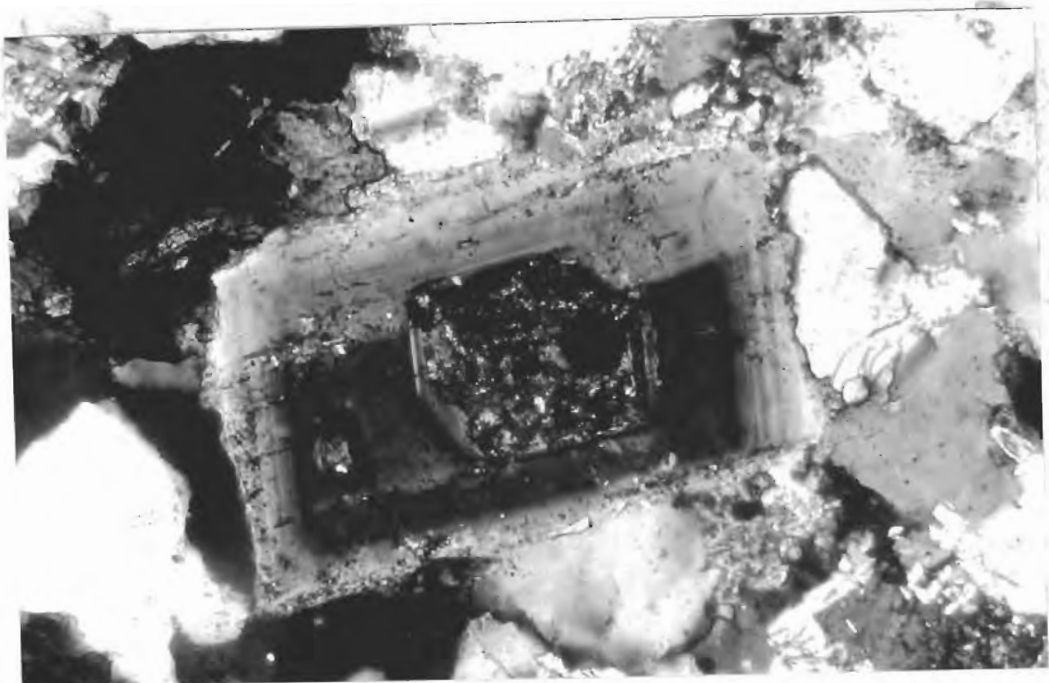


Fig. 7 - 8 (a). Rock No. (34956) Zoned plagioclase crystal in the hornfels contact zone. Variation of extinction angles is shown by the dotted line in Fig. 7 - 9 (c). The altered core is the same size as the quartz grains in the hornfels, and is believed to have been intruded as a solid crystal. The outer zones have crystallographic outlines and have grown *in situ*. The width of the field of the photograph is 0.8 mms.

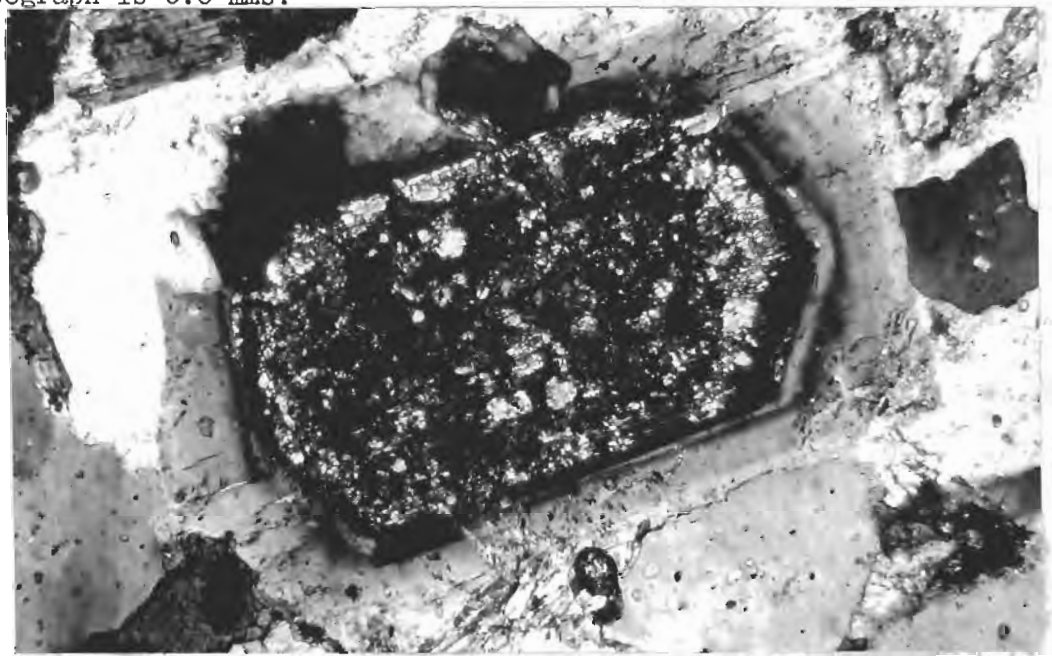


Fig. 7 - 8 (b). Rock No. (34950) Zoned plagioclase crystal in the hornfels contact zone. Variation of extinction angles is shown by the dotted line in Fig. 7 - 9 (a). Diameter of the altered core is 0.4 mms. The outer zones have inclusions of the hornfels matrix. The width of the field of the photograph is 0.8 mms.

zone has been plastically deformed [Fig. 7 - 6 (b)].

(e) ZONED PLAGIOCLASE CRYSTALS

Complexely zoned plagioclase crystals are found in the quartz diorite and in the hornfels within five metres of the contact. Extinction angles were measured on a normal microscope stage from those sections which were cut approximately perpendicular to (010), and some zone curves are presented in Fig. 7 - 9. Each crystal was measured from its edge into the core, and crystals were selected from three different structural localities. Figs. 7 - 9 (a) and (b) represent feldspars in a hornfels about three metres away from the contact; Figs. 7 - 9 (c) and (d) are from feldspars in the hornfels immediately adjacent to the contact, and Figs. 7 - 9 (e) and (f) represent feldspars from the main quartz diorite.

The feldspars on which zoning was measured in the hornfels are all less than 1 mm. in diameter although the largest plagioclase crystals in these rocks reach 5 mm. across. This is because the cores of the large feldspars tend to be severely altered to sericite with some chlorite and epidote, whereas the smaller crystals which have relatively small inner cores for their size compared with the large feldspars, are less altered. However, all the strongly zoned plagioclase crystals have altered cores, and where the core is not completely altered, it is basic labradorite.

ZONING IN PLAGIOCLASE

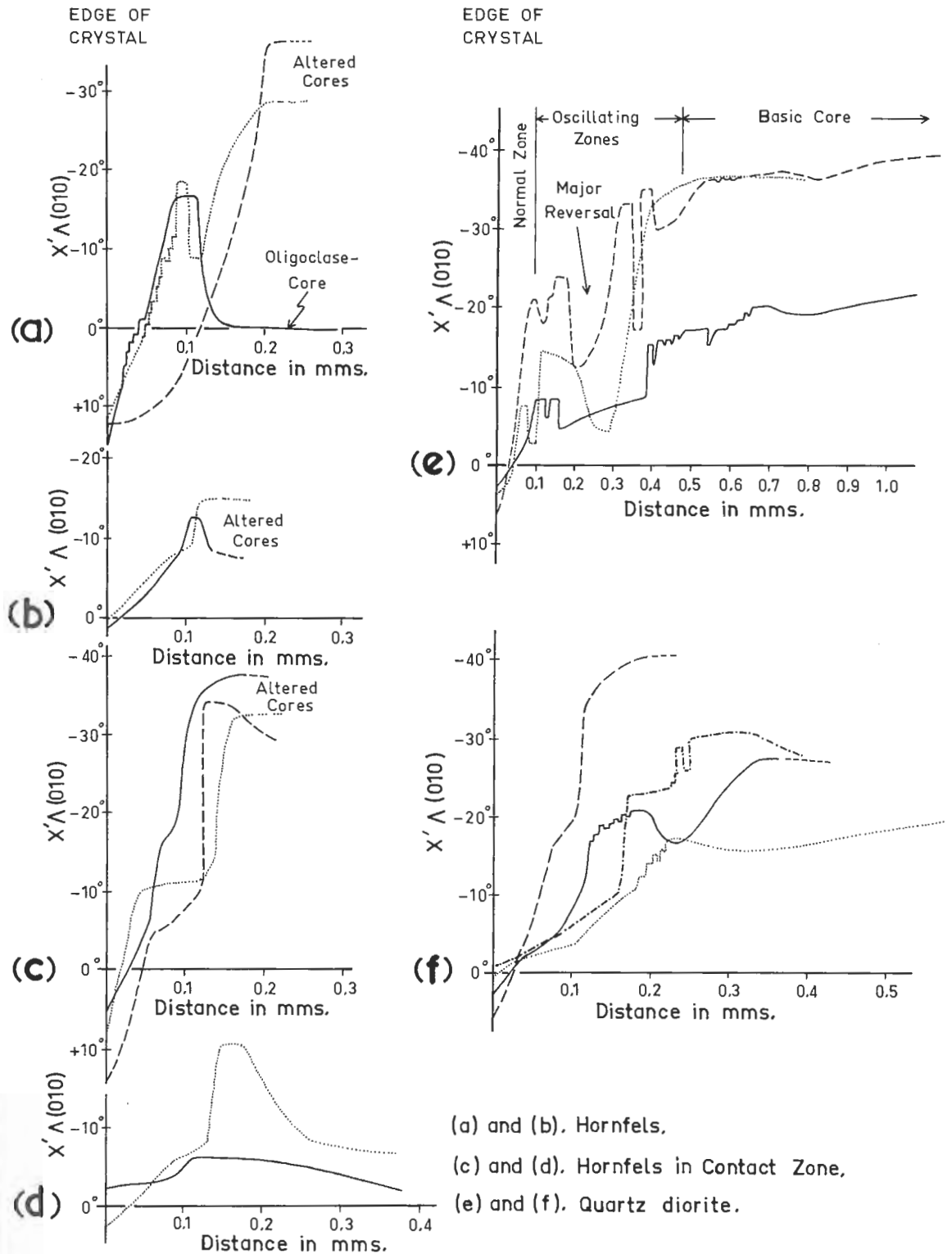


FIG: 7-9

Some zoned feldspars have extinction angles indicating cores of composition An₆₀ to An₇₀.

Zoning from the basic cores outwards follows a normal pattern, but the zoning is not smooth as there are many small oscillations, and generally one marked reversal, between the altered core and the outside rim. This outside rim is generally thin with strong zoning of the normal type approaching albite on the outer edge. Some cores show patchy zoning and have been replaced by oligoclase; in a few cases this replacement is complete.

The plagioclase crystals in the quartz diorite show a large variation in size and in distribution of zones, and some of the smaller crystals are as strongly zoned as the larger ones. Fig. 7 - 9 (e) shows zoning in three medium-sized crystals which can be divided into three parts. There is a basic-labradorite core of variable diameter, an annulus of oscillatory zones with one major reversal and a growth discontinuity along which small inclusions are aligned, and an outer, thin normal zone. The smaller crystals [Fig. 7 - 9 (f)] show the same range of composition although the labradorite cores may be quite small.

The plagioclase in the quartz diorite shows a good correlation of form in broad outline (Greenwood and McTaggart, 1957), although in detail the correlation is poor. The width of individual zones varies from one crystal to another and

from one side of a crystal to another, and there is poor correlation of value. The plagioclase in the hornfels also shows a fair correlation of form in broad outline, but very poor correlation in detail. The correlation of value is reasonably good.

4. STRUCTURAL INTERPRETATION

(a) INTRUSIVE NATURE OF THE QUARTZ DIORITE

There are no serious doubts that the quartz diorite is essentially intrusive or has replaced an intrusive. The disoriented xenoliths [Fig. 7 - 10 (a)], the terminated beds [Fig. 7 - 10 (b)], the dilatant shape of the dyke in the southern part of the mapped area (Fig. 7 - 2), the expansion of layers around the quartz-diorite lobes in the contact zone [Fig. 7 - 3 (a)], and the discordant shape of the quartz-diorite outcrop in many places (Fig. 7 - 2) are sufficient evidence. Nevertheless, there are several points of controversy, two of which I have attempted to deal with.

- (1) The relationship of the quartz diorite to the folding, and
- (2) The origin of the basic-plagioclase feldspars in the hornfels.

(b) ORIGIN OF THE QUARTZ-DIORITE LOBES

The quartz-diorite lobes are confined to the plastically folded contact zone immediately adjacent to the main bodies of



Fig. 7 - 10 (a). Disoriented xenoliths in a quartz-diorite dyke south of the main dyke. There is a narrow chilled margin. Six-inch rule shown.



Fig. 7 - 10 (b). Terminated beds in the middle of a quartz-diorite dyke to the south of the main dyke. The fault which terminates the main group of beds does not extend into the dyke walls. The hammer is 30 cms. long.

quartz diorite. Some of the larger lobes at the northern end of the main dyke are shown in Fig. 7 - 3 (a). Adjoining layers bifurcate and can be traced around individual quartz-diorite lobes, proving that the lobes are intrusive bodies. Such shapes are found nowhere else in the half-mile section south of the quartz-diorite contact, so that there is no evidence to suggest that they are not magmatic emplacements.

Empirically, it appears that the quartz diorite has penetrated initially along a bedding surface or some other weakness in the wall rock. The embryonic lobe then expanded, plastically deforming the side adjacent to the main body of quartz diorite and also squeezing the layers laterally. The side adjacent to the main mass of country rock, however, is relatively undeformed. This progression of events is outlined diagrammatically in Figs. 7 - 4 (e) to (h).

Fig. 7 - 11 (a) shows a quartz-diorite lobe in the early stages of formation with a thinned band of layers encompassing it. Fig. 7 - 11 (b) shows a lobe which has pushed back into the main body of magma and has folded the layers on either side by lateral pressure. Fig. 7 - 12 (a) is a somewhat oblique section, but shows the detail of a fold which has had pressure exerted on it from the left, while Figs. 7 - 4 (a) and (b) are tracings from photographs of other folds which occur at the quartz-diorite contact. In both the latter folds there



Fig. 7 - 11 (a). A quartz-diorite lobe in the early stages of formation with a thinned band of sediment encompassing it. Six-inch rule shown.



Fig. 7 - 11 (b). A quartz-diorite lobe which has pushed back into the main intrusive body and also pushed laterally causing plastic folding. Six-inch rule shown.

has been lateral pressure exerted, and this has caused the folds to become globular shaped and almost detached.

An explanation of the formation of the quartz-diorite lobes was sought in terms of increasing water pressure in a cooling silicate melt. This phenomenon is caused by the increasing concentration of water in the residual fluid as the various silicate phases crystallize out. However, the mechanism poses problems when applied in detail, and does not provide a satisfactory solution. Thus, the origin of the quartz-diorite lobes has not yet been determined.

(c) ORIGIN OF THE FOLDING

The main problem concerning the folded zone is whether the folding was caused by the intrusion, or whether the quartz diorite merely intruded a folded zone. It has been shown in Fig. 7 - 5 that the fold-axis defined by both the folded bedding and the individual hinges is the same as the axis of rotation of the straight-bedded zones. This implies that the axis of rotation of the bedding during intrusion was the same as the axis of folding, which could be coincidental. However, there is no record of folding on such a steep axis in adjacent rocks where plunges rarely exceed 30° . Furthermore, most of the folding occurs on the northeastern side of the dyke, and it is clearly limited to a zone between two undeformed zones

(Fig. 7 - 2). It seems unusual that the folding does not extend either laterally along this zone, as would intraformational, nontectonic folding, or into the adjacent bounding zones as would metamorphic, tectonic folding. The simplest explanation consistent with all the facts is that the folding has been caused by the intrusion of the quartz diorite.

(d) NATURE OF THE QUARTZ DIORITE DURING INTRUSION

There are three main lines of evidence which indicate the physical state of the quartz diorite and the country rock during intrusion.

- (i) The plastic folding in the contact zone.
- (ii) The basic plagioclase in both the quartz diorite and the hornfels.
- (iii) The nature of the contact.

(i) The plastic folding in the contact zone. The contact zone in which the plastic style of folding occurs is a narrow band surrounding the quartz diorite, and it is always less than one metre wide. This type of folding in igneous contact zones is usually attributed to one of three conditions.

- (1) Intragranular plasticity of minerals at high temperatures (Pitcher and Read, 1960 and 1963).
- (2) Partial melting of the rock (Spry and Solomon, 1964).
- (3) The presence of an introduced interstitial melt (Thomas and Smith, 1932, p. 289).

Intragranular plasticity of minerals at high temperatures is the property commonly used to explain the complex solid-state deformations in metamorphic terrains, and the rocks develop a characteristic foliation and preferred orientation of minerals as in schists and gneisses (Pitcher and Read, *op. cit.*). At Diana's Basin there is no foliation developed in the plastically folded contact zone, and the quartz grains are equidimensional as in a typical hornfels. They have recrystallized to several times their original size, but the relict cement-like texture is still recognizable. Thus it appears that there was very little intragranular deformation.

Partial melting of the hornfels can be dismissed because there is no evidence of glass or, indeed, any mineral assemblage which indicates a temperature in excess of 600°C. Sericite, which persists right up to the contact, decomposes in the presence of quartz at approximately 600° to 650° C. to form potassium feldspar and sillimanite (Deer, Howie and Zussman, 1962, 3, p. 24), neither of which minerals has been found. Nor is the presence of an introduced interstitial melt likely. Apart from the absence of potassium feldspar it is anomalous that the sericite should have recrystallized so finely adjacent to the contact if a melt had been present. The muscovite in the adjacent quartz diorite is ten times as large.

The texture of the hornfels in the plastically folded contact zone indicates that deformation was accomplished by intergranular movements. The style of deformation also indicates that there was an almost complete lack of cohesion between the grains. This cohesionless, intergranular style of deformation is typical of folding in unconsolidated sediments in which there has been a pore pressure equal to the confining pressure. Since the plastic folding is strictly confined to the contact zone which in parts transgresses the sedimentary layering, it is clear that the disaggregation of the hornfels was related to the intrusion of the quartz diorite.

A simple explanation of the plastic style of folding is provided if there were developed in the contact zone a pore pressure approximately equal to the lithostatic load. The abundance of sericite implies that this pressure would have been essentially a high water pressure, and the deformation would thus be caused by small stress differences in the disaggregated hornfels. The pore pressure would decrease outwards from the quartz diorite so that progressively more load would be borne by grain-to-grain contacts and the plastic behaviour would be restricted to the zone in which the pore pressure approximately equaled the confining pressure. As the load taken by grain-to-grain contacts increased, the sedimentary layering would provide a heterogeneous resistance to differential stress, and bedding-

plane slip would become the dominant style of deformation. Thus the folds become more concentric outwards from the quartz-diorite contact.

- (ii) The basic plagioclase in both the quartz diorite and the hornfels.

Strongly zoned crystals of plagioclase with basic-labradorite cores occur in both the quartz diorite and the hornfels. The overall correlation between the crystals in the quartz diorite and those in the hornfels is not good since many of the crystals in the quartz diorite have large basic cores, whereas the size of the cores in the hornfels is generally much smaller in proportion to the size of the crystal. However, there is reasonably good form and value correlation between the outer zones in both the quartz diorite and the hornfels. The general form is a set of oscillatory zones with an overall normal trend and one major reversal, rimmed by an outer, thin though strong, normal zone.

This agreement in both form and value indicates that the plagioclases have been subjected to similar variations of environmental conditions in the latter stage of their history. Inclusions of equidimensional quartz grains in some of the outer zones of the plagioclases in the hornfels indicate that these zones have grown *in situ*. However, no detrital inclusions have been found in the labradorite cores which invariably show good crystallographic outlines although they are considerably altered.

The outer zones which reflect these crystallographic outlines (Fig. 7 - 8) are quite fresh. None of these features is like the features described from plagioclases considered to have been formed by metasomatism.

Mish (1949, p. 387), an ardent metasomatist, invoking a metasomatic origin for granites of batholith size, writes,

"Early phases of the growth of plagioclase porphyroblasts are present in every thin section. These early crystalloblastic patches are small, often still turbid, and have ill-defined borders. The porphyroblast has become large but still lacks crystal form. Finally crystal faces begin to develop, but relict inclusions of groundmass grains may still be preserved."

At Diana's Basin the basic-plagioclase cores are well crystallized, and although there have been more sodic rims grown there are no turbid, early porphyroblasts. From these considerations I conclude that the basic-plagioclase cores are not formed by metasomatism of the hornfels, but were mechanically emplaced, and that the outer rims grew afterwards.

(iii) Nature of the contact.

The contact between the quartz diorite and the hornfels is quite regular in broad outline (Fig. 7 - 2), and indicates that the quartz diorite is a dilatant dyke. However, in detail there are many perturbations, and pods of quartz diorite appear throughout the narrow zone of plastic folding. In hand-specimen there is no difficulty in distinguishing quartz diorite from

feldspar-bearing hornfels; there is a sharp change in colour, grain-size and texture. Nevertheless, there is no obviously chilled margin immediately adjacent to the plastic hornfels, although the middle of the quartz-diorite dyke is somewhat coarser than its margins.

In thin-section, the gradual increase in grain-size of the hornfels accompanied by progressive destruction of the cement-like texture, can be traced in towards the quartz diorite, but there is a sharp break in grain-size at the contact. The coarsest hornfels at the contact has an average grain-size of 0.4 mms. whereas the grain-size of the adjacent quartz diorite averages 2 to 3 mms. The plagioclase crystals reach 5 mms. in diameter on both sides of the contact but the labradorite cores in the hornfels are generally less than 0.5 mms. across.

A possible explanation of the origin of the labradorite cores is afforded by the high water-pressure hypothesis. If the water pressure in the quartz diorite approached the lithostatic load, and this pressure decreased outwards from the quartz diorite into the country rock, then outward-moving hydrous fluids might carry some small plagioclase crystals a limited distance through the disaggregated country rock. As Martin (1952, p. 333) noted,

"The walls can not be regarded as firm or in any way stationary."

The passage of plagioclase crystals would be inhibited where the pore pressure was not large enough to overcome grain-to-grain contact loads and thereby allow the granular fabric of the hornfels to dilate. Thus the plagioclase crystals are restricted to within 5 metres of the quartz-diorite contact, and the feldspar-bearing hornfels has an intrusive or vein relationship with respect to the outer, fine-grained hornfels.

(e) INTERPRETATION OF THE HISTORY OF INTRUSION

In my opinion, the quartz diorite at the time of intrusion was a silicate melt containing labradorite crystals. Since the most common rock in northeastern Tasmania is high-level intrusive granite (*sensu lato*), and the regional grade of metamorphism is low, the level of intrusion at Diana's Basin was probably within a few kilometres of the surface. Nevertheless, the somewhat basic composition of the quartz diorite when compared with the granites indicates that the quartz diorite intruded from a lower level, and a fairly rapid ascent could have caused local high water pressures. The sandstones and mudstones, essentially vertical at the time of intrusion, were rotated and folded about an axis plunging steeply to the south. The larger-scale concentric folding was accomplished in the early phase of intrusion.

As the melt cooled and crystallized the water pressure increased until it was approximately equal to the lithostatic

pressure on the country rock. The penetration of this high-pressure fluid into the mudstone caused loss of cohesion between the grains, and the contact hornfels became a disaggregated, granular mass susceptible to plastic deformation. Nevertheless, the pressure was not totally hydrostatic as there was a gradient from the approximately lithostatic pressure in the quartz diorite to a pressure closer to the hydrostatic head in the pores of the more distant country rock.

This pressure gradient caused aqueous solutions, together with some small, solid particles, to filter through the plastic, disaggregated country rock immediately adjacent to the contact. The basic-plagioclase cores were thus solidly emplaced in the hornfels within five metres of the contact, and the quartz-diorite lobes, with accompanying plastic folds, were formed. There was no partial melting of the hornfels, and complete mixing with the quartz diorite was prevented by the outwardly directed pressure gradient.

As the melt continued to cool and crystallize the water pressure was gradually reduced, and more of the load was borne by grain-to-grain contacts in both the hornfels and the quartz diorite. In the latter stages of crystallization the quartz diorite, being a granular body, was susceptible to dilatancy upon any small deformation [Fig. 7 - 12 (b)], and the hornfels was reset firmly in its sericitic matrix. In the very late stage,



Fig. 7 - 12 (a). An oblique section showing some of the detail of the plastic folding along the margins of the quartz-diorite dyke. Pressure has been exerted from the left. The width of the photo is approximately 15 cms.



Fig. 7 - 12 (b). Intrusion of sediment back into the quartz diorite, probably caused by dilatancy in the quartz diorite in the late stages of crystallization. Six-inch rule shown.

as the quartz diorite continued to settle, quartzo-feldspathic fluids passed into the country rock in veins, and also throughout the matrix, forming diffuse albite crystals.

CHAPTER 6

FOLDING IN A HORNFELS ADJACENT TO A DOLERITE CONTACT,
REMARKABLE CAVE, S. E. TASMANIA

1

INTRODUCTION

Remarkable Cave is a blow-hole about three miles south of Port Arthur on Tasman Peninsular, formed by weathering along a set of strong, vertical joints which trend southeasterly. At high tide the water reaches the northern entrance to the cave, but at low-water it is possible to walk right through. Geologically, Remarkable Cave is located in Lower Triassic sandstones immediately above a sill-like intrusion of Middle Jurassic dolerite, and the horizontal contact is well exposed 200 metres east of the cave. Apart from a few, open domes and basins within 2 metres of the dolerite, the sandstones east of Remarkable Cave are essentially horizontal and undisturbed.



Fig. 8 - 1 (a). Northeastern side of Remarkable Cave where horizontal sandstones (right-hand side) have been downstoped (left-hand side) into mobilized sediment which overlies dolerite.



Fig. 8 - 1 (b). Southwestward-facing wall at the southern opening of Remarkable Cave. Irregular folding of originally horizontal layers is outlined by chaotic banding in the mobilized sediment. The hammer is approximately 30 cms. long.

In contrast the rocks at Remarkable Cave itself are highly contorted, a feature which is atypical of contacts between dolerite and sandstone in Tasmania (McDougal, 1962, p. 284). The contact hornfels can be divided into two types of rock, one lying above the other. The upper rock type, which is conformable with the overlying, undisturbed sandstones has retained its original layering and is folded in a concentric fashion. It is underlain by a coarser-grained, almost structureless, grey rock which contains many irregular, "flow" folds. The contact between the dolerite and hornfels can not be seen at Remarkable Cave, but by extrapolation from the exposed contact to the east it lies just below sea-level.

2

PETROGRAPHY

The upper part of the hornfels appears to have been a medium- to fine-grained sandstone composed predominantly of quartz with some sodic plagioclase and minor quantities of zircon and opaque iron minerals. There are no argillite bands, and the fine-grained, dark layers were originally quartzose silts. Although the quartz appears to have recrystallized, and new minerals such as zeolite and margarite have formed, some relicts of the sedimentary texture are still recognizable, and the overall grain-size has not been changed markedly.

The unmetamorphosed sandstones above the hornfels are medium- to coarse-grained and have well-developed cross-bedding.

The underlying, highly contorted hornfels appears to have undergone more radical changes. It is medium- to coarse-grained with quartz crystals up to 0.5 mms. diameter, and patches of zeolite several times as large. The original sedimentary texture can not be recognized and in places there is graphic intergrowth of quartz and potassic feldspar. Nevertheless, the overall texture is not igneous and the rocks are remarkable for the unusual, low-grade metamorphic minerals.

Zeolites occur in all the thin-sections examined. Three separate varieties can be distinguished of which stilbite and heulandite have been positively identified, and other zeolites may also be present.

Stilbite. Optically negative with a medium 2V; dispersion $r < v$; optic plane parallel to the one good cleavage; parallel extinction.

Heulandite. Occurs more rarely than stilbite in crystal aggregates up to 5 mms. across. Optically negative with a large 2V; very low refractive index and birefringence; optic plane perpendicular to cleavage; parallel extinction. X-ray diffraction (R. J. Ford, 1967, *pers. comm.*) on a crystal showing herring-bone intergrowth (34967) showed the three main peaks of heulandite.

Zeolite [possibly *ferrierite* (?) (34964)]. Optically positive with a medium 2V; dispersion $r < v$; optic plane parallel to the one good cleavage with a weak parting perpendicular to it; extinction almost parallel.

Other zeolites may also be present.

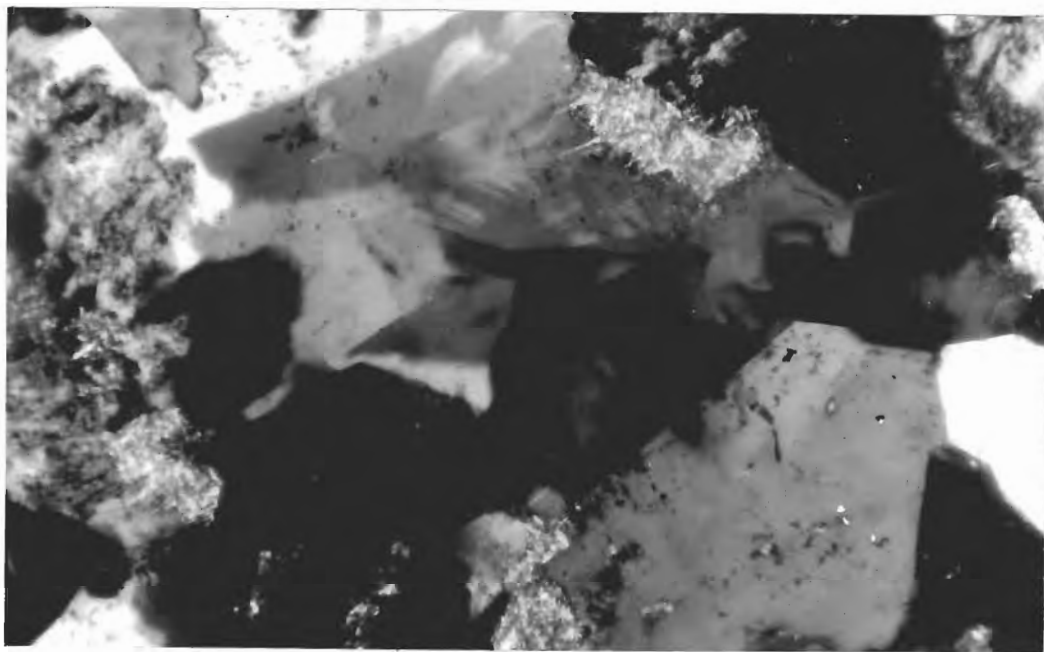


Fig. 8 - 2 (a). (34972). A zeolite patch showing the intricate twin structure in the zeolite and the rational crystal faces on the quartz facing into the zeolite in the lower part of the photograph. X 150. Crossed polaroids.

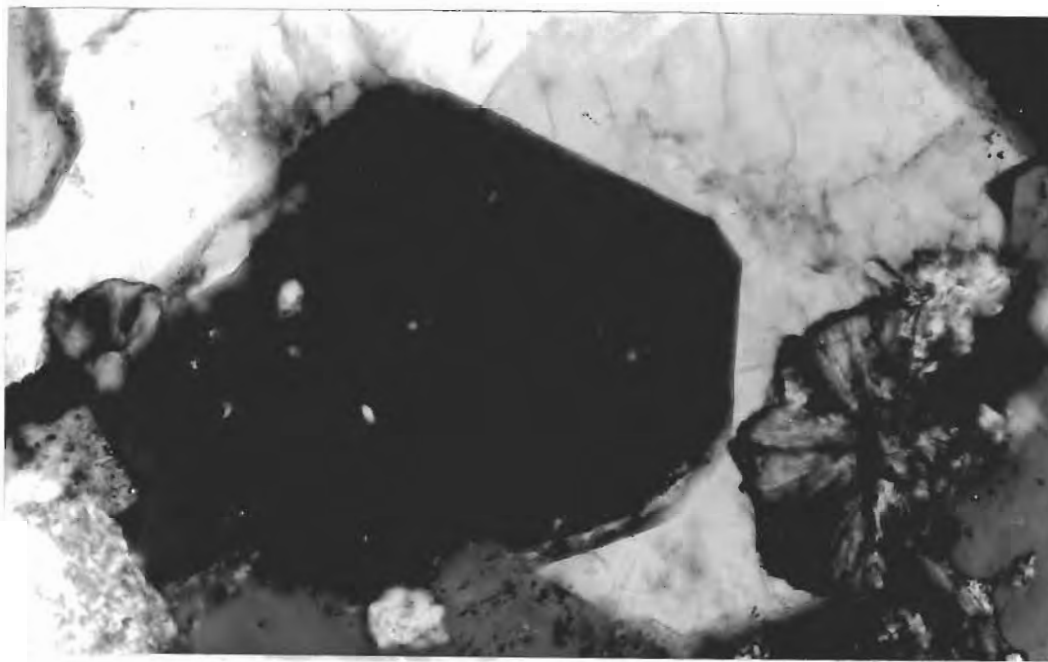


Fig. 8 - 2 (b). (34964) Euhedral quartz crystal and a chlorite spherulite surrounded by zeolite. X 250. Crossed polaroids.

The brittle mica, *margarite*, is particularly common and widespread. It occurs as pale-yellow crystals and has an extinction angle of 13° with the good basal cleavage. *Cancrinite* is also present and is distinguished from *quartz* by the lower refractive index, slightly higher birefringence and uniaxial negative, interference figure. In parts the cancrinite has a yellow alteration product along the weak cleavage.

Chlorite is very common throughout the hornfels. It is mostly a common green variety but some penninite and serpentine have been identified. There are a number of distinctive forms in which the chlorite (or serpentine) occurs.

(1) As radiating crystals in small spherulites. The chlorite is generally colourless and the spherulites are everywhere surrounded by zeolite although in some places they are arranged along the margins of brown biotite flakes.

(2) In large clumps as a green or brown alteration product of a ferromagnesian mineral. The fibrous mineral has a radiating structure and is probably serpentine.

(3) As scattered, green or yellowish-green crystals which in places have a pseudo-hexagonal form.

(4) As colourless, pale-yellow or green encrustations on biotite flakes. The chlorite appears to have nucleated on the (001) surface of the biotite and grown away from it at a constant angle. Such overgrowths are generally associated with zeolite patches.

There are two varieties of *biotite* present. One is pleochroic from deep reddish-brown to pale pinkish yellow or colourless, while the other is pleochroic from olive green to pale yellow. The reddish-brown biotite is scattered throughout the hornfels and is four or five times as large as the quartz grains in the relatively unmetamorphosed sediments. In places it has grown partly around the quartz grains, which indicates that it has been formed during metamorphism. The olive-green biotite is rarer and does not appear to be spatially related to the reddish-brown variety although both occur in 34965. However, whereas the brown biotite is scattered throughout the rock the olive-green variety is restricted to small patches where the grain size of the quartz is three or four times larger than the surrounding host rock.

The colour of the reddish-brown biotite is not always constant. The shade in the direction of the basal plates varies from a dark brown with no red tinge to a much lighter, almost reddish, chocolate-brown hue. Furthermore, the reddish-brown biotite exhibits a variable amount of alteration to chlorite, and there may or may not be overgrowths. The olive-green biotite does not show any alteration, overgrowth or variation in colour.

The quartz is remarkable for its unusual form. In the finer-grained, upper hornfels the quartz exists predominantly as

equidimensional grains, commonly rounded, though sometimes angular. However in the lower hornfels the grain-size is 2 to 3 times larger, and the quartz grains are very heavily embayed [Fig. 8 - 3 (a)]. Close examination reveals that the protuberances between the embayments are commonly bounded by straight, rational, crystallographic faces [Fig. 8 - 3 (b)].

I have interpreted these embayment shapes as growth forms, not resorption textures, for two reasons. Firstly, resorption of grains would not be expected to produce re-entrant angles between adjacent rational faces, and secondly, the embayments are best developed where the grain-size of the quartz is largest. Even in a single thin-section where there is some variation in grain-size, the embayments are best developed in the coarsest parts.

3

FOLDING

(a) GENERAL STATEMENT

The style of folding is quite variable, although most structures have some element of concentric folding. In general, the large folds tend to be more concentric than the smaller ones, and in several places a broad, open, concentric fold may have small, similar-style parasitic folds associated with it. Nevertheless, all the folds are disharmonic, and the

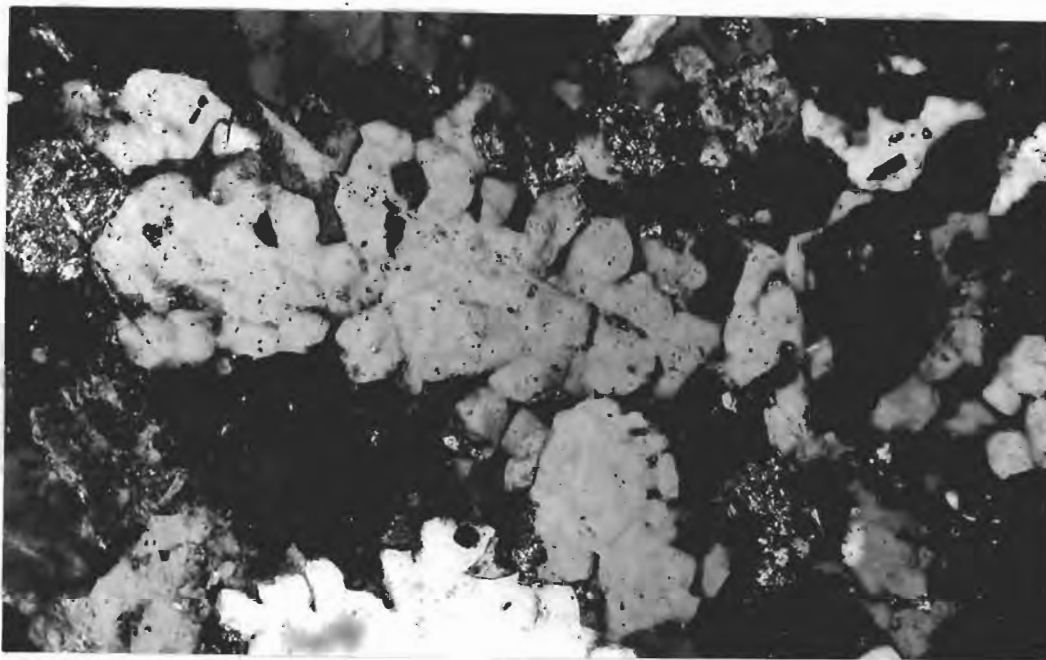


Fig. 8 - 3 (a). (34964) Typical growth form in heavily embayed quartz
X 100. Crossed polaroids.

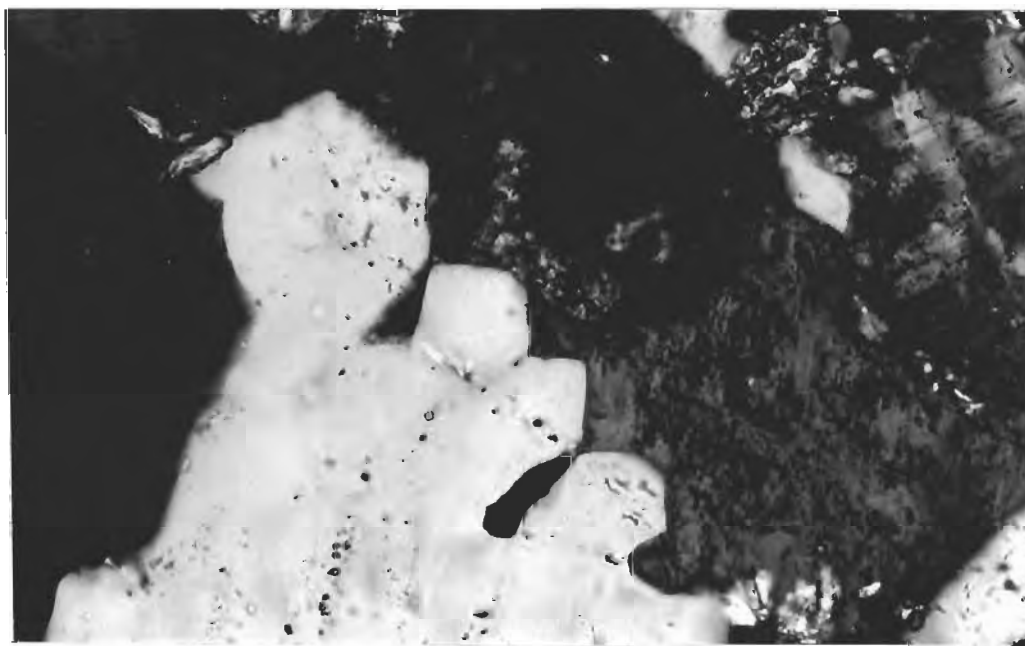


Fig. 8 - 3 (b). (34964). Re-entrant, rational, crystallographic
faces in quartz. X 300. Crossed polaroids.

incompetent zones are composed of highly contorted sediment which is slightly coarser grained than the competent sandstones and mudstones.

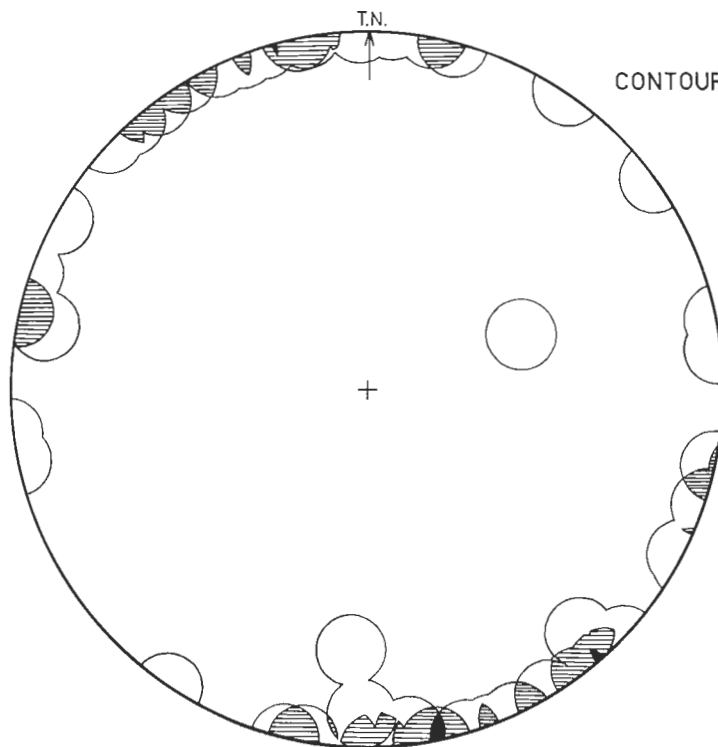
In the upper part of the hornfels the folds are characterized by competent beds which maintain their orthogonal thickness, separated disharmonically from one another by tongues of mobilized sediment. In places thin layers are detached from the main sheaf of foliae, and folded in a very irregular, disjunctive fashion resembling folds normally formed in sedimentary or diagenetic environments. The folds nearest the dolerite contact are the most chaotic and irregular. The proportion of highly contorted, "mobilized" sediment increases towards the dolerite contact so that in the lower part of the cave individual bands of sandstone, approximately maintaining orthogonal thickness, are surrounded by coarser grained material in which original layering can not be recognized. At the bottom of the cave wall the original layering has been so completely obliterated that the mobilized sediment has the appearance of a homogeneous crystalline rock.

The 33 fold-hinges measured [Fig. 8 - 4 (a)] are distributed in a subhorizontal girdle which is the attitude of the overlying undeformed sandstones. Although the distribution within this girdle is not completely random, there is a broad spread and the preferred orientation may be a function of sampling rather

FOLD ELEMENTS, REMARKABLE CAVE

33 FOLD-HINGES

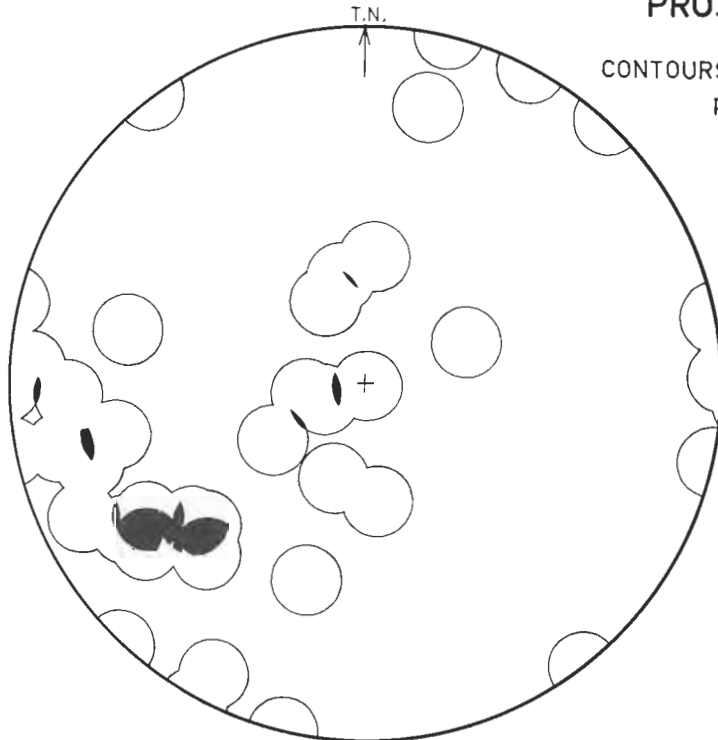
(a)



CONTOURS 1,3 and 5 points
per 1% area

33 POLES OF AXIAL PLANES

(b)



EQUAL-AREA
PROJECTIONS

CONTOURS 1 and 3 points
per 1% area

FIG: 8-4

than reality. In the lower part of the hornfels, the few fold-hinges measured appear to be almost completely randomly oriented. The axial planes do not show any significant grouping although the distribution shown is not random. In the upper part of the hornfels the axial surfaces tend to be vertical, or almost vertical, while lower in the outcrop they are much more random, and many are involuted.

(b) DETAILED DESCRIPTIONS

Fig. 8 - 5 shows several profile sketches traced from photographs. All the sketches are oriented with the vertical up the page. Fig. 8 - 5 (a) is a hinge-fold between the undisturbed horizontal (upper) sandstones and a group of strata, two or three metres thick, which has been rotated downwards into the mobilized sediment and (?) dolerite by partial stoping. The two outer bands of sandstone in the sketch are folded concentrically, but they are separated from each other, somewhat disharmonically, by a zone of mobilized sediment in which there are numerous irregular, small-amplitude contortions.

Fig. 8 - 5 (b) is located on the eastern wall of the northern entrance to Remarkable Cave. It indicates how layers, individually folded concentrically, are separated by mobilized sediment which has penetrated along bedding surfaces. Within these bands of irregular thickness marked

RHEOMORPHIC-FOLD PROFILES

REMARKABLE CAVE, S.E. TASMANIA

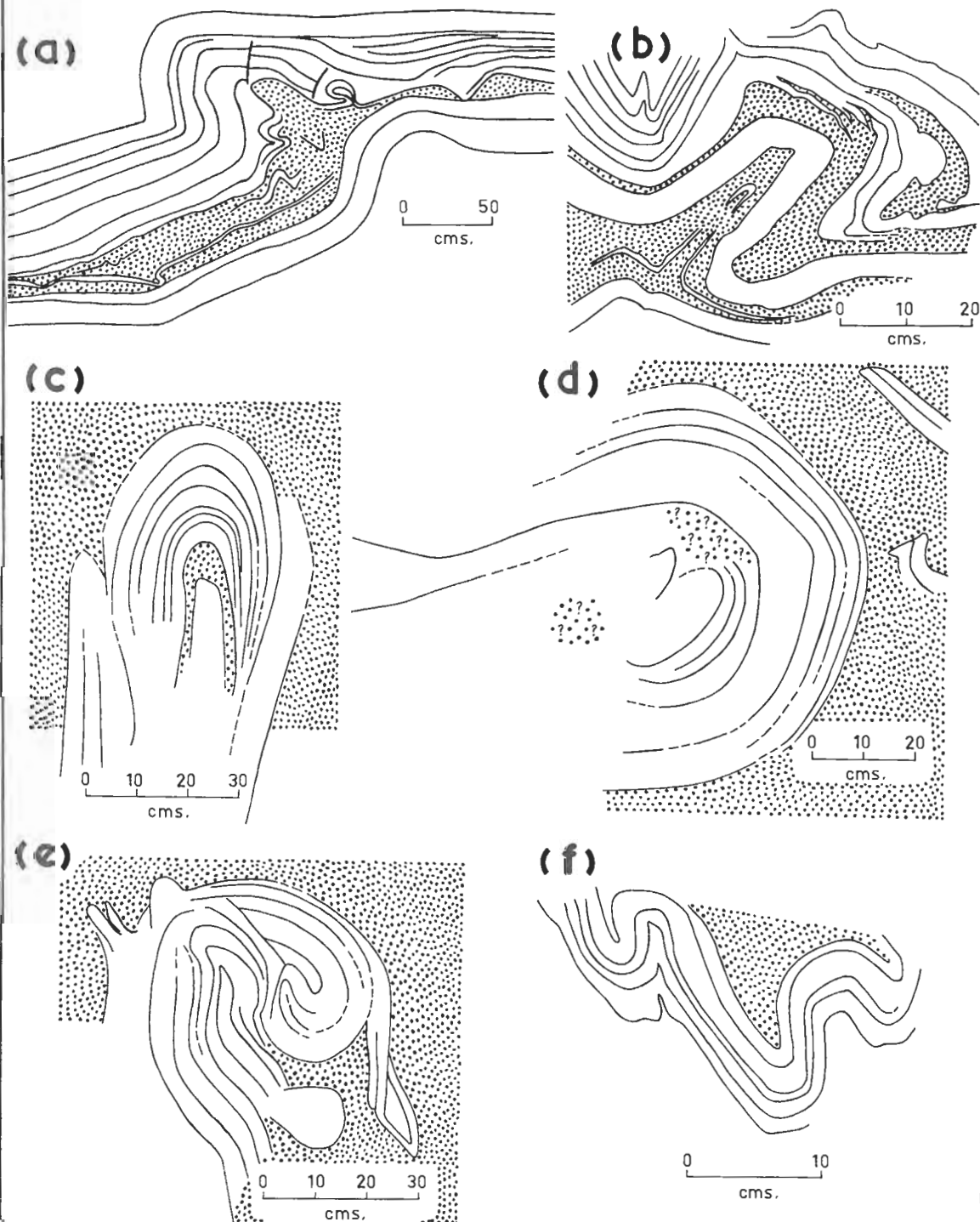


FIG:8-5

as mobilized sediment, there are several very thin sandstone layers which have been peeled-off the thicker layers and folded disjunctively on a very small scale.

Figs. 8 - 5 (c) to (f) are sketches of folds located closer to the dolerite contact than those in Figs. 8 - 5 (a) and (b). The style of folding is more irregular, and there has been considerable thickening and thinning of the sandstone layers. Fig. 8 - 5 (c) is an inverted, lobe-shaped structure with its lower limbs pinched right out. It appears to have been formed by stretching the limbs in the vertical direction. Fig. 8 - 5 (d) is part of a sandstone layer which is almost involuted. It is located close to the base of the cave wall at the southern entrance shown in Fig. 8 - 1 (b). The sandstone layer has maintained its orthogonal thickness but is completely detached from other sandstone layers. The axis of folding is horizontal, but an adjacent hinge is almost vertical. Fig. 8 - 5 (e) is located a metre or two south of Fig. 8 - 5 (d), and is completely involuted. The axis of folding is sinuous and the structure is suitably described as a balled-up, "comma" fold. Fig. 8 - 5 (f) is located in the same part of the cave wall but is folded on a more regular style and has a relict concentric geometry.

Figs. 8 - 6 (a) and (b) are profile sketches traced from photographs of small-scale, intraformational folds located

further away from the contact than the folds in Fig. 8 - 5.

The disturbed layers occur between thicker bands of undeformed horizontal sandstones. In Fig. 8 - 6 (a) 2 one of the main groups of layers, AA' - BB' has been divided into thin slices parallel to the axial plane. The thicknesses parallel to the trace of the axial plane are shown in Fig. 8 - 6 (a) 3 with the lower surface, AA', straightened out. The geometry is not similar, and orthogonal-thickness ratios correspond to a uniform flattening perpendicular to the axial surface of less than 10%. Thus the style of folding is essentially concentric.

In Fig. 8 - 6 (b) 1 the fold form is more angular. Axial thicknesses were measured on the band, CC' - DD', and are shown in Fig. 8 - 6 (b) 3 where the lower surface, CC' is straightened out. The variation in axial thickness is considerable, and as with the fold in Fig. 8 - 6 (a) corresponds closer to concentric rather than similar folding. Orthogonal-thickness ratios correspond to uniform flattening perpendicular to the axial plane in the hinge region of between 20% and 30%. However, since the axial thickness at the hinge is approximately equal to the average thickness of the layer away from the core region, there has actually been no flattening, and the equivalent effect is caused by simple shear of a concentric profile parallel to the axial surface.

INTRAFORMATIONAL PROFILES

REMARKABLE CAVE

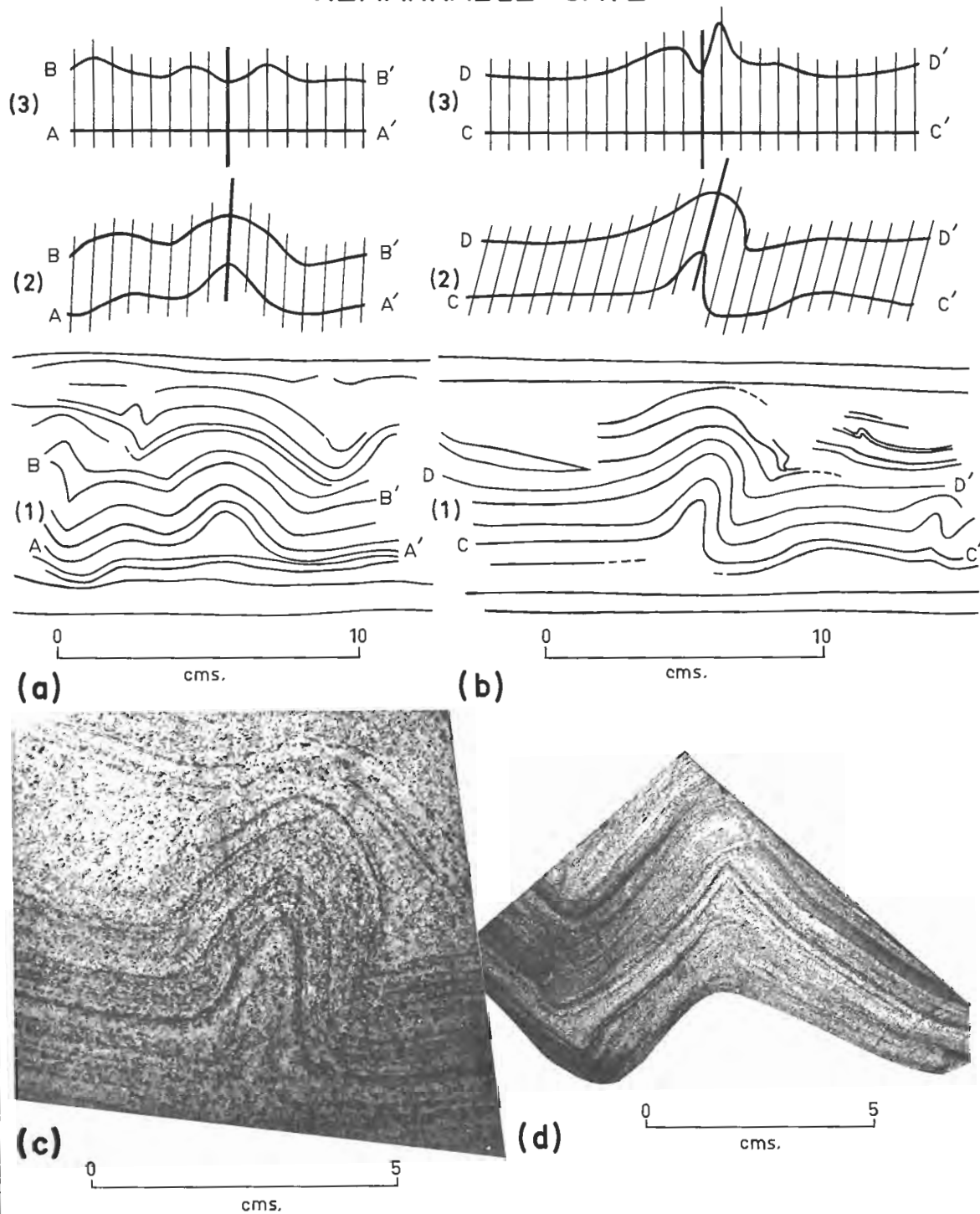


FIG: 8-6

In total aspect there has been no shortening in the folded zone. In any part, shortening in one layer is accommodated by stretching in the layers above or below, and when any layer is traced laterally it passes into alternate regions of shortening and stretching. The hinge regions appear to be loci of weakness and incipient mobilization, and there appears to have been some similar (flow) folding as well as the basically concentric mode. The geometry is almost what would be expected if there had been a series of small convection cells developed in the folded zone, and this style has many similarities with the expansion fold figured by Hills (1963, p. 69, Fig. III - 21).

Fig. 8 - 6 (c) is a photograph of a polished hand-specimen from which a large thin-section (34974) was made, and the style of folding is comparable with that of Figs. 8 - 6 (a) and (b). The orthogonal-thickness ratios in the hinge region correspond to a uniform flattening of 20% to 30%, yet the axial thickness at the hinge is not significantly different from the average thickness of the layer away from the hinge. Thus the present fold shape is produced by simple shear parallel to the axial surface in the hinge area together with a concentric profile.

In thin-section the rock is remarkably homogeneous in both texture and grain-size; the grains show no strain related to the folding, and zeolites pervade the whole rock. The grain-size of the quartz has increased by growth in scattered patches,

and the grain boundaries are very angular, re-entrant shapes.

There is little doubt that in its present textural state this rock would deform homogeneously under directed stress. There would be neither layer-parallel slip which must have occurred to produce the concentric profile, nor the irregular thickening and thinning on the limbs of the fold adjacent to the crest. The heterogeneity of deformation implied by the style of folding must have existed before the present texture, and perhaps mineralogy, developed. Nevertheless, when all factors are taken into account, there is no evidence to suggest that the middle layer in the photograph was ever markedly different texturally or mineralogically from either the upper or lower layer. It seems likely, then, that folding occurred when the rock was in a condition such that small, even minute, stress differences were capable of causing relatively large deformations.

Fig. 8 - 6 (d) is a photograph of a polished surface of a somewhat angular, disjunctive fold in which the more competent layers have broken at, or near the fold-hinges. In thin-section, these competent layers do not appear different in either texture or composition from the incompetent layers, and it is concluded that in this example also the folding must have occurred before the present texture was developed.

Fig. 8 - 7 is a photograph of a very large thin-section (34975). The photograph is smaller than natural size, the



Fig. 8 - 7. Photograph of a very large thin-section (34975). The disjunctive style of folding was caused by the intrusion of coarse-grained, zeolite-bearing hornfels from the left-hand side. The width of the thin-section is approximately 20 cms.

width of the thin-section being approximately 20 cms. The disjunctive style is characteristic of the folding caused by local intrusion of coarse-grained, zeolite-bearing rock which is the light-coloured material in the photograph, into the upper hornfels. The dark bands are finer grained than the light-coloured bands, and have been broken-up in a manner resembling "quickstone" folding. The shape of the mobilized sandstone in Fig. 8 - 7 indicates that the folding was caused by bodily intrusion from left to right.

Zeolite occurs throughout the rock, and the only differences between adjacent layers are variations in grain-size and proportions of dark minerals. Detrital plagioclase grains can be recognized in the intrusive rock by their sharp angular boundaries which commonly transect compositional zones and polysynthetic twins.

4

INTERPRETATION

The rheomorphism of the country rock at Remarkable Cave is unusual for the Jurassic dolerite contacts in Tasmania.

McDougall (1962, p. 284) notes that,

"...mobilized country rock has been found with the Red Hill dyke..."

and that,

"...near Port Arthur on Tasman's Peninsular... numerous rheomorphic veins intrude the roof of a well-exposed dolerite sheet. These are the first recorded cases of rheomorphism associated with the Tasmanian dolerite intrusions".

The rheomorphism can not be attributed to either partial melting of the rock, or the presence of an introduced interstitial melt. The same arguments as applied at Diana's Basin can be used to exclude temperatures in excess of 600°C. Likewise, as at Diana's Basin the absence of a metamorphic foliation excludes the possibility of intragranular plasticity to account for the mobilization of the rock.

The peculiar, zeolite-rich mineralogy associated with chlorite, serpentine and olive-green biotite, indicates temperatures probably below 300°C (Coombs *et al.*, 1959). Stilbite, margarite, cancrinite and chlorite are all indicators of a hydrous, calcium-rich environment. The temperature when some of these minerals formed may have been well below 300°C.

The style of folding in the lower part of the hornfels testifies to the extreme plasticity of the rock, whereas the characteristic concentric, disharmonic and disjunctive folds in the upper part indicate increasing competence away from the dolerite. Disjunctive folds as in Fig. 8 - 7 are formed by the intrusion of the mobilized lower part of the hornfels into the upper parts. In my opinion, this rheomorphism is satisfactorily accounted for by the development of intergranular water pressures equal to the load pressure.

The water was probably not connate water of the sediments for several reasons.

(1) The sandstones above the hornfels are quite permeable and would have been unlikely to retain pore water during a gradual increase of temperature accompanying a dolerite intrusion.

(2) The dolerite has many other contacts with the sandstones and all these contacts are knife-sharp (McDougall, *op. cit.*). Thus, whatever caused the high water pressures at Remarkable Cave can not have been a general property of the sediments.

(3) The presence of both reddish-brown biotite and an olive-green biotite, together with the alteration of the reddish-brown biotite to chlorite and serpentine, indicates that there has been a change in environment since the initial metamorphism. The reddish-brown biotite is a normal product of thermal metamorphism, whereas the olive-green biotite indicates hydrothermal, low-grade conditions (Schwartz, 1958, p. 167).

From these considerations I have concluded that initially the sandstones were baked into a normal, contact hornfels with the development of reddish-brown biotite, and that later a quantity of calcium-rich, hydrous residuum was locally disgorged from the cooling dolerite sheet causing the folding and peculiar mineralogy.

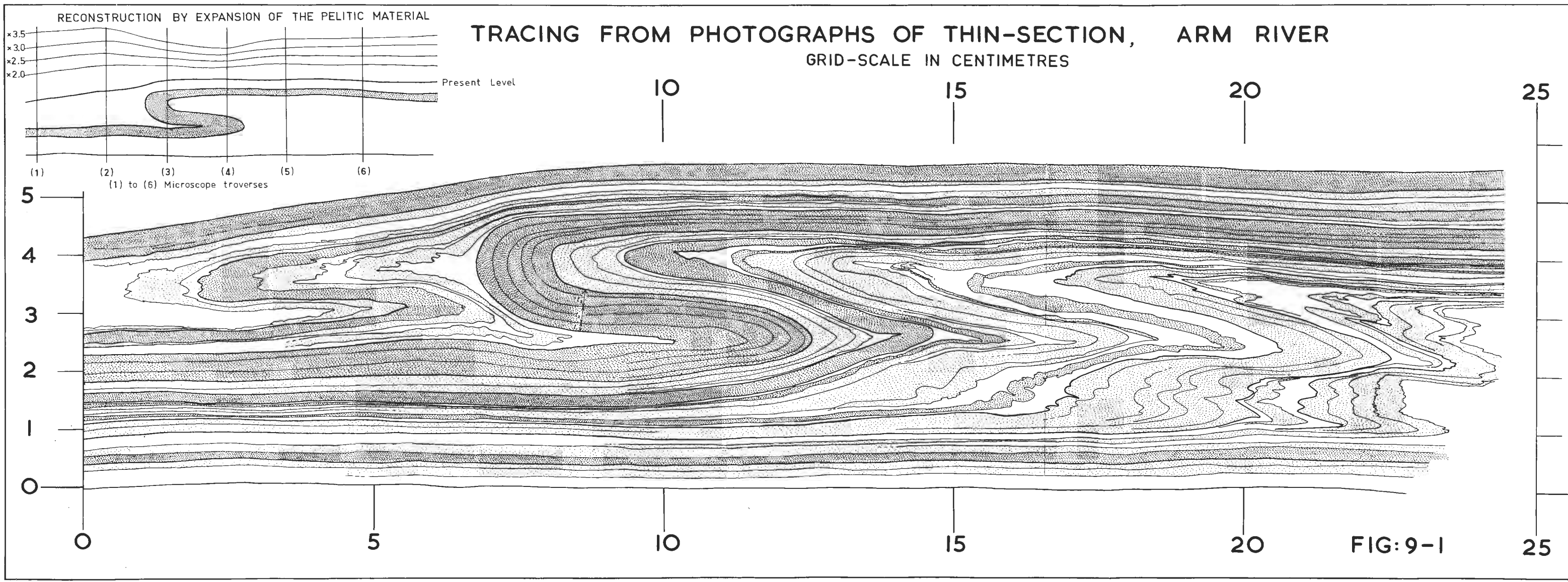
CHAPTER 9

MISCELLANEOUS FOLDS

1 A SMALL-SCALE INTRAFORMATIONAL FOLD FROM
 ARM RIVER, NORTHERN TASMANIA

(a) INTRODUCTION.

Fig. 9 - 1 is a tracing from photographs (Fig. 9 - 2) of a large thin-section of an intraformational fold from the Howell Group quartzite in a road cutting on the main road to Rowallan at approximately $41^{\circ}40' 2''$ S, $146^{\circ}13' 2''$ E, which is a little more than a mile north of the junction of the Arm and Mersey Rivers, northern Tasmania. The specimen was collected by Dr. A. H. Spry (1966, *pers. comm.*) who attributed the fold to the F2 phase in the Precambrian, although he noted that no earlier F1 folds have been found at this location. Spry (1962b, p. 142) noted that the road cutting



"...exposes a number of isoclinal folds. The folds are all of the same style and their axial planes are parallel but axes only a few feet apart plunge west at angles ranging from 5° to 45°."

The folds are intraformational, and each folded zone is separated from adjacent folded zones by apparently undisturbed, straight-bedded strata. There is a strong lineation, which is 10° divergent from the fold-axis in the specimen examined.

Unfortunately the relationships between the Howell Group and the Precambrian in other parts of Tasmania are not clear. It is entirely possible that the Howell Group was deposited after the F1 phase of folding had affected the Older Precambrian, and thus it is not yet possible to correlate between the deformational surfaces developed in this fold and the metamorphic surfaces S1 and S2. Nevertheless, I shall attempt to show that the characteristics of this particular fold are what would be expected from the deformation of a partially lithified sediment in which the pelitic layers contained up to 60% water. This fold may thus be representative of a group of early diagenetic folds in the Precambrian of Tasmania.

(b) STRUCTURAL DESCRIPTIONS

(i) Flattening. In the tracing of the fold (Fig. 9 - 1) the layers have been classified as psammitic, semi-pelitic and pelitic, the psammitic layers having been closely stippled,





the semi-pelitic layers more openly, and the pelitic layers are not stippled at all. The psammitic layers contain greater than 90% of quartz, the pelitic layers less than 20%, and the semi-pelitic layers contain varying intermediate proportions of quartz and platy minerals. From both the tracing and the photograph it can be seen that although the fold profile is propagated along the trace of the axial surface in the manner of a similar fold, the psammitic layers tend to maintain their orthogonal thickness and the pelites fill the interspaces. The style of folding is thus strongly disharmonic from layer to layer, with deformation concentrated in the pelitic layers.

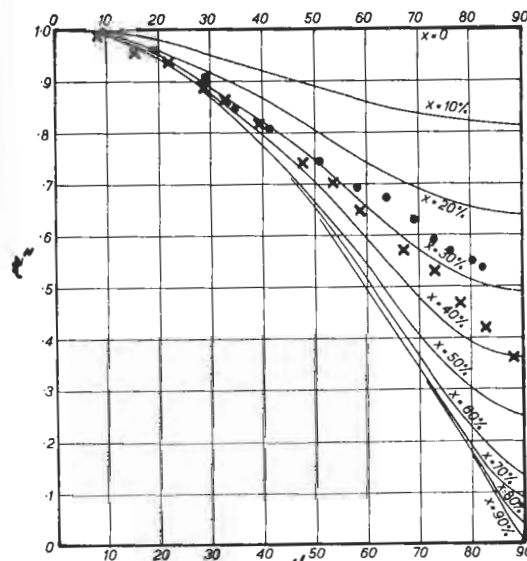
Orthogonal-thickness ratios were measured on the main psammitic layer which is composed of 95% of quartz, and which appears to have acted as a single mechanical unit. Thin strings of platy minerals mark originally very thin, layer-parallel, pelitic laminae and enable the psammitic layer to be divided into subunits. These have been designated T_1 , T_2 and T_3 , as shown in Fig. 9 - 1, with T_1 the uppermost layer, T_3 the lowest. Although the sedimentary facing of the fold has not been determined, I have assumed for the purpose of this analysis that the tracing has been oriented right way-up. Thus the upper fold is referred to as the antiform and the lower fold as the synform.

It can be seen by inspection that the upper and lower limbs of the antiform and synform, respectively, are thinner than the common limb between them. The orthogonal λ -thickness ratios for the whole layer around both the antiform and the synform, and also the ratios for the subunits of the synform, are shown in Fig.

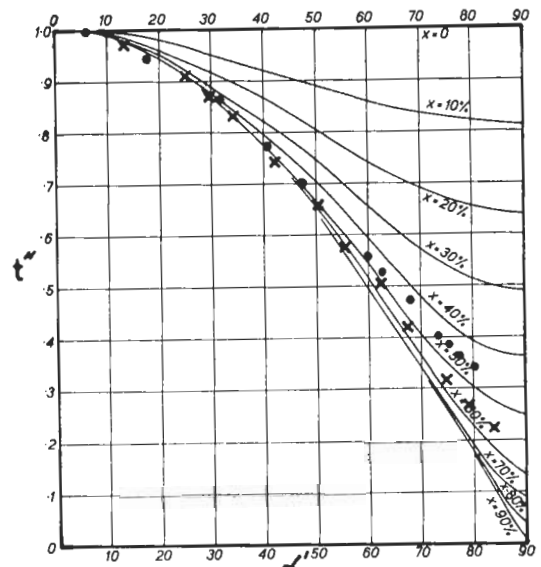
9 - 3. The equivalent flattening perpendicular to the axial surface is approximately 30% in the antiform and is slightly less in the common limb, slightly greater in the upper limb. In the synform the amount of equivalent flattening is larger, being between 40% and 50% on the common limb and approaching 60% on the lower limb.

The percentages of equivalent flattening in the sublayers of the synform are shown in Figs. 9 - 3 (c) and (d). T_1 is on the concave part of the layer; T_3 the convex side. The geometry of T_1 is very close to perfect similar geometry, whereas T_3 has an equivalent flattening of a little less than 40%. This increase in equivalent flattening on the concave side of the psammitic layer is readily seen in the fold tracing, and around the antiform T_1 is flattened less than T_3 , although the effect is not as prominent as in the synform. This pattern of equivalent flattening may indicate that elastic strains induced by buckling are relieved by increased plastic flow on the concave side of the layer (See Fig. 4 - 15).

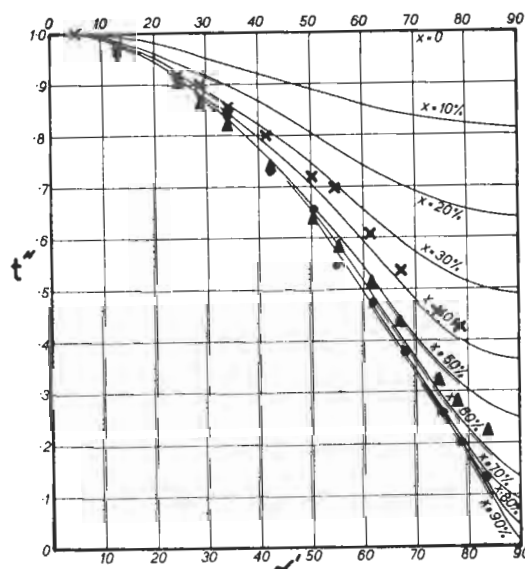
ORTHOGONAL-THICKNESS RATIOS THICK PSAMMITIC BAND, ARM RIVER



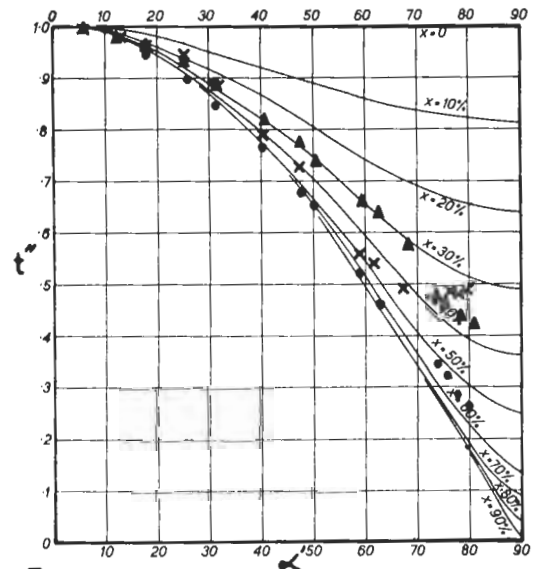
(a) ANTIFORM
Whole Layer



• = Common Limb
x = Outer Limb
(b) SYNFORM
Whole Layer



(c) LOWER LIMB



• = T_1
▲ = T_2
x = T_3
(d) COMMON LIMB

(c) and (d) from SYNFORM

(ii) Microscopic Structure. [Large thin-section (34979) and three orthogonal sections (34980A), (34980B) and (34980C)].

Up to 95% of the psammitic layers is composed of an interlocking mosaic of quartz 0.02 mms. to 0.05 mms. in diameter. There are some small grains of albite up to 0.1 mms. across which may be detrital, and rounded, detrital grains of zircon, tourmaline and an opaque iron mineral also reach 0.1 mms. diameter. Small flakes of muscovite the same size as the quartz grains are scattered throughout the quartz mosaic. The pelitic bands are composed of unidentified, very fine-grained, brown material which is probably iron-stained clay or sericite. The amount of quartz in the pelitic bands is variable, and the irregular, angular outlines indicate that the quartz may be original detrital grains.

The cleavage is produced by parallel ribbons, up to 0.1 mms. wide, composed of pelitic material which has intruded through all except the thickest psammitic bands. In places the pelitic material is crystallized into sheaves of light-brown mica up to 1 mm. long, and this mica is distinctly different from the small, colourless muscovite flakes scattered throughout the psammite.

Fig. 9 - 4 (a) [Location (15.5, 2.5) in Fig. 9 - 1] is a photograph of a thin psammitic layer in a thicker band of semi-pelite. The psammitic layer is composed of almost

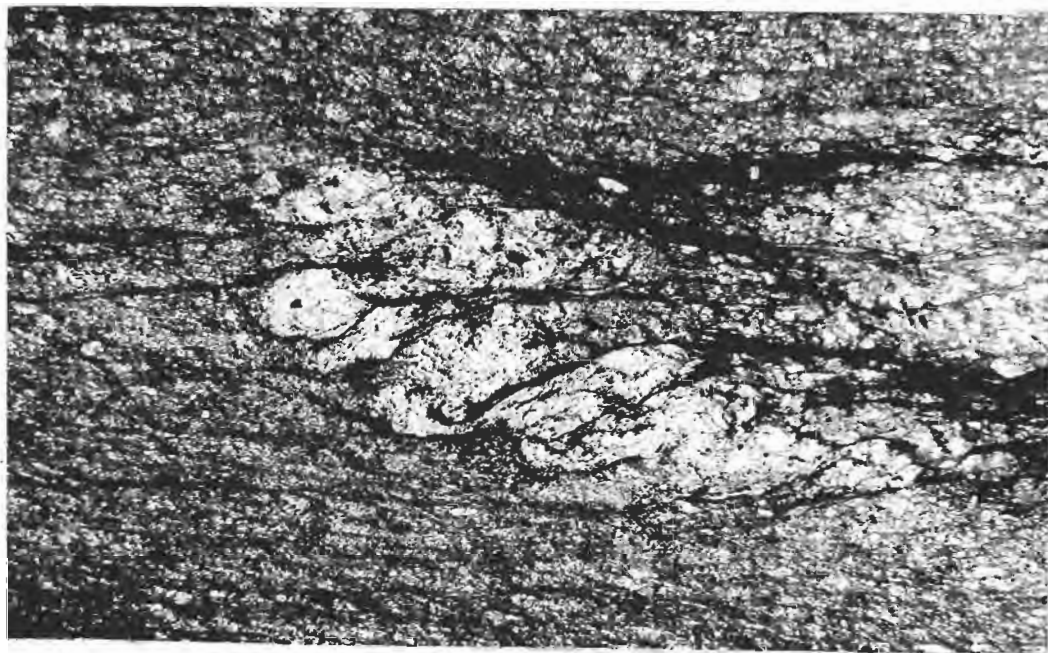


Fig. 9 - 4 (a). (34979) Location (15.5, 2.5) in Fig. 9 - 1.
Cleavage ribbons which transect a fold core in a thin psammitic
layer. X 22. Plane-polarized light.

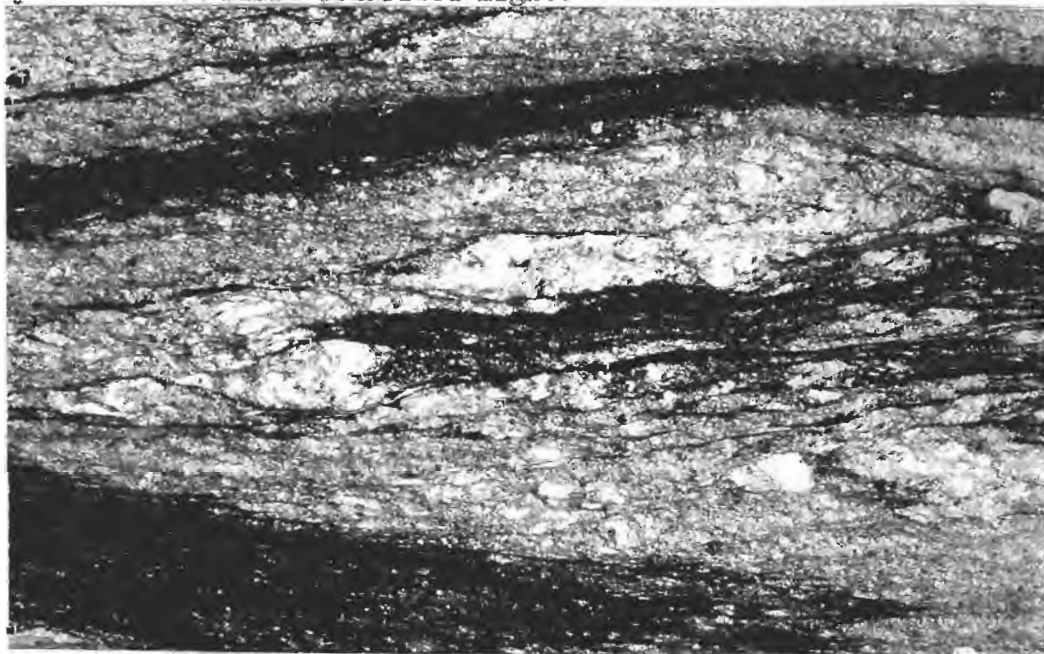


Fig. 9 - 4 (b). (34979) Location (19.5, 3.7) in Fig. 9 - 1.
Intense development of cleavage ribbons in a fold core. X 22.
Plane-polarized light.

100% quartz which, in its present state, is a continuous interlocking mosaic. In the semipelite the quartz is more angular, and each grain is usually surrounded by dark, pelitic material. The parallel cleavage ribbons are 0.02 to 0.05 mms. thick, and are spaced at distances an order larger. The ribbons pass right through the quartz-rich fold core and continue into the semi-pelite. In places the pelitic material in the cleavage has crystallized as a mica slightly pleochroic in pale browns.

Two important conclusions can be drawn from the configurations in Fig. 9 - 4 (a).

(1) The cleavage in both psammite and pelite is the same phenomenon, and probably formed synchronously in both materials.

(2) Any hypothesis of cleavage formation invoking a layer-delimited cause is excluded.

Fig. 9 - 4 (b) [Location (19.5, 3.7) in Fig. 9 - 1] depicts another fold core in which there has been an intense development of cleavage ribbons. The psammitic layer has been almost completely dissected, and there has been considerable displacement in the profile section along some of the cleavage ribbons. The psammitic band which has an element of concentric geometry when considered as an entity, must have behaved incompetently well before the deformation was finished. In many of these micro-folds it appears that initially the folding proceeded by

layer slip which decreased in importance during deformation as simple (and pure) shear parallel to the axial surface predominated. In the case of the cleavage in Fig. 9 - 4 (b), there can have been no deformation transverse to the pelitic ribbons since their formation, as they are essentially planar. The concentric geometry must therefore have been produced by layer-parallel slip before cleavage formation after which all deformation was either simple or pure shear parallel to the cleavage surfaces.

Fig. 9 - 5 (a) [Location (14.5, 3.8) in Fig. 9 - 1] shows a very thin, ptygmatically folded, psammitic layer in a pelitic band. Despite the intense crenulation in the psammite, the bounding surfaces of the enclosing pelite appear relatively straight. The sense of coupling of these parasitic folds is congruent with drag of the upper layers towards the adjacent hinge, but the crenulations are just as intensely developed in the fold core, so that they were not caused solely by drag.

Most examples of ptygmatic folding are recorded in localities where quartzo-feldspathic veins appear to have intruded rheomorphic country rock. The viscosities of the intruding and intruded materials are thought to be very similar. If the folding in Fig. 9 - 5 (a) is of a comparable mechanical nature, it may indicate that at some stage during the



Fig. 9 - 5 (a). (34979) Location (14.5, 3.8) in Fig. 9 - 1.
 Ptygmatic folding of a thin psammitic layer in a thicker pelite
 band. X 22. Plane-polarized light.

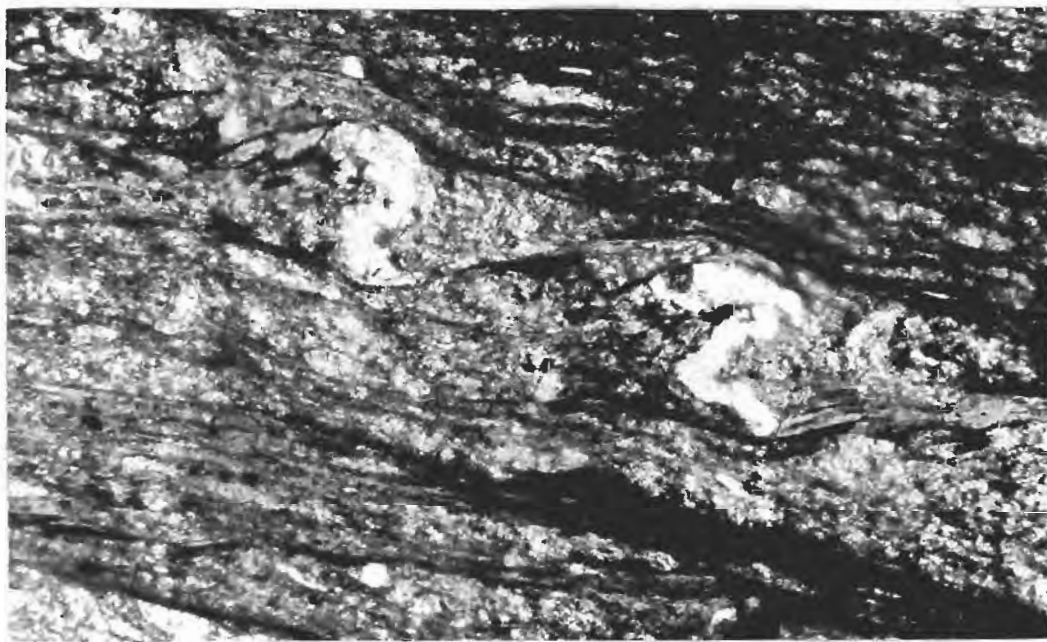


Fig. 9 - 5 (b). (34979) Location (20.0, 3.4) in Fig. 9 - 1.
 Sigmoids developed in a thin psammitic layer. X 55. Plane-
 polarized light.

formation of the fold there were very similar viscosities in all rock types. High water pressures approaching the lithostatic load could cause this condition.

Fig. 9 - 5 (b) [Location 20.0, 3.4 in Fig. 9 - 1] shows the remnants of a thin psammitic layer which has been broken up into sigmoidal folds. At first sight it might appear that shearing along the cleavage surfaces produced the sigmoids, but this is not the case. Any reconstruction must begin with the psammitic layer parallel to the overall layering which runs from the upper left to the lower right in the photograph. Because of this the couple which has produced the sigmoidal shapes must have been a dextral rotation; yet the displacement along the cleavage is sinistral.

This apparent anomaly can be explained by considering the deformation in its successive stages. Initially deformation was predominantly layer slip which produced a series of dextrally coupled buckles or drag folds in the psammitic layer. Later the cleavage ribbons parallel to the axial surface of the parental fold were propagated throughout the rock disrupting the buckled psammitic layer. After cleavage formation the style of deformation changed and all simple-shear movement was parallel to the newly created cleavage surfaces. This later movement reversed the sense of displacement between adjacent sigmoids as the shear fold continued to develop. There may

also have been some flattening perpendicular to the cleavage.

(c) INTERPRETATION

Spry (1962b, p. 148) suggested

"...that mineral assemblages of chlorite to garnet grades were produced...during F1 and that these were folded into large recumbent folds during F2 at garnet grade."

F1 is the designation applied to a phase of movement which occurred along a foliation while garnets were growing. No folds have been positively identified as belonging to F1, although there appear to be some folds which predate F2. Nevertheless, even if there are folds which predate F2, and which may have axial surfaces parallel to the surface S1, it can not be proved that F1 and the formation of S1 were synchronous. All that can be shown is that there was movement along S1 while garnet-grade minerals were growing. It is entirely possible that S1 had been formed at an earlier stage of deformation and at a different grade of metamorphism, and that at a later stage there was movement along the surface while the garnet grade of metamorphism was reached.

There is no evidence that this particular fold was formed at the chlorite or garnet grade of metamorphism. Firstly, there are no minerals that indicate a grade of metamorphism above the lowest greenschist facies. The unidentified clay

or sericitic material has crystallized in part only to recognizable micas, and the albite grains are probably detrital. Secondly, the cleavage appears identical in geometry and gross composition to the cleavage at Sulphur Creek and Tullochgorum which developed in very low-grade conditions. Where the ribbons have recrystallized to relatively coarse sheaves of mica, the crystallization clearly postdates the initial formation of the ribbons. Thirdly, the fabric of the quartz mosaic which is reasonably well developed and can be recognized by rotating the thin-sections between crossed polarizers, appears to be homogeneous throughout the fold. There is no obvious variation in preferred orientation related to the position of the very tight fold-hinges. A rock folded so tightly and intricately in the chlorite or biotite grade of metamorphism would be expected to have a preferred dimensional or optical orientation related to the local fold geometry. Hence I have concluded that the fabric of the quartz mosaic is clearly superposed.

Apart from these considerations there are several features which suggest that deformation may have occurred when the pelite contained a considerable amount of water.

(1) The fold limbs in regions where there is a high proportion of pelite are convex towards the axial surface. This somewhat unusual configuration is to be expected if there was dehydration of the pelite after folding (See Chapter 1).

(2) The disharmonic style of folding between layers of different composition indicates marked differences in viscosity, as well as ease of layer-boundary slip. Such conditions are characteristic of early diagenetic folding (See Sulphur Creek).

(3) The apparent identity of the cleavage ribbons with those at Sulphur Creek and Tullochgorum indicates that a comparable, very low-grade environment may have existed at the time of cleavage formation.

(4) The folded zone thins where the amount of pelite is largest, and this is to be expected if the pelite had compacted after deformation.

The tracing of the thin-section in the upper left-hand part of Fig. 9 - 1 shows the outline of two layers as well as the outline of the main psammitic layer. Six traverses, numbered as indicated, were made across the profile and the thicknesses of pelite and psammite were counted microscopically with a graduated ocular.

If the conclusion that there was considerable water present in the pelite at the time of deformation is valid, it should be possible to expand the pelite and reconstruct a geometrically more simple profile than the existing one. It is a characteristic of such intraformational, early diagenetic folds that the upper and lower bounding surfaces of the folded zone are parallel after deformation. To make this reconstruction the

present thickness of pelite has been expanded by various factors, and the restored upper surfaces drawn. An expansion of the pelite to 2.5 times its present thickness produces an approximately level upper surface, and this implies that 60% of the volume of the pelite has been lost by dehydration since deformation. Nevertheless, there are a few complicating factors. Firstly, such a calculation assumes that the psammitic material has not been compacted, as the expansion of the pelite is relative to an unchanging psammite thickness. The psammite may well have compacted up to 10% so that the reconstructed thicknesses are minimal. Secondly, there may have been some thinning over the psammitic parts during compaction. Thinning accomplished by stretching occurs over boulders during compaction at Gormanston. Thirdly, there is a possible error in the estimation of the relative proportions of compactable and incompactable material. The pelitic layers are generally too fine for individual grains to be distinguished, and there may be variation in the proportions of platy and granular minerals. In view of these complications I consider that the approximation of the reconstructed upper surface to a planar bounding surface is remarkably good.

(d) CONCLUSION

The main conclusion of this analysis is that this intraformational fold has the geometry of a fold which may have developed when there was up to 60% of water in the pelite. There are no immediate repercussions on the structural evolution of the Precambrian of Tasmania as deduced by Spry, although several conclusions could be drawn if, and when, these folds are correlated with the deformational episodes resolved elsewhere.

2. FOLDS IN THE MARTINSBURG SLATE, PENNSYLVANIA

The rocks from which Maxwell (1962) developed his hypothesis for the formation of slaty cleavage by water movements during folding, are the Martinsburg Slate of the Delaware Water Gap area of Pennsylvania and New Jersey. Behre (1933) compiled a comprehensive report, entitled "Slate in Pennsylvania", in which he included several drawings of fold profiles exposed in quarry faces. I have used some of these drawings to determine the equivalent amount of flattening, and to compare them with some Tasmanian folds.

In general, Behre describes the folding as of "similar" type with noteworthy thickening of troughs and thinning in the limbs. The folds have variable apical angles, and there is a marked tendency toward northward overturning which varies

from a few degrees off the vertical to a nearly horizontal position. Behre (*ibid.*, p. 157) considers there are strong reasons to believe that most of the folds were firstly formed with essentially vertical axial surfaces, and were rotated to various attitudes later during the diastrophic history. He claims that the thickening in the hinge regions is the same irrespective of the orientation of the axial surface of the fold, and has concluded (*ibid.*, p. 29) that the cleavage surface (a flow or slaty cleavage) formed perpendicular to the direction of maximum compression. In my calculations I have used the axial plane as the datum-plane for estimating apparent flattening, and in all cases except one (*ibid.*, p. 320, Fig. 79), the cleavage is parallel to the axial surface.

Fig. 9 - 6 (a) (Behre, 1933, p. 22, Plate 5B). Orthogonal thicknesses were measured on the band between the marked lines which is just below the knee of the man in the photograph. The upper limb shows thickness ratios approaching an almost perfectly similar geometry which, if caused by uniform flattening perpendicular to the axial surface, represents an amount of at least 70%. The lower limb corresponds to uniform flattening of between 35% and 40%. Since there is no reason to suppose that the mechanical characteristics of the band are markedly different on the upper limb from the lower limb, the difference in apparent flattening is probably caused by simple

FOLD PROFILES IN THE MARTINSBURG SLATE

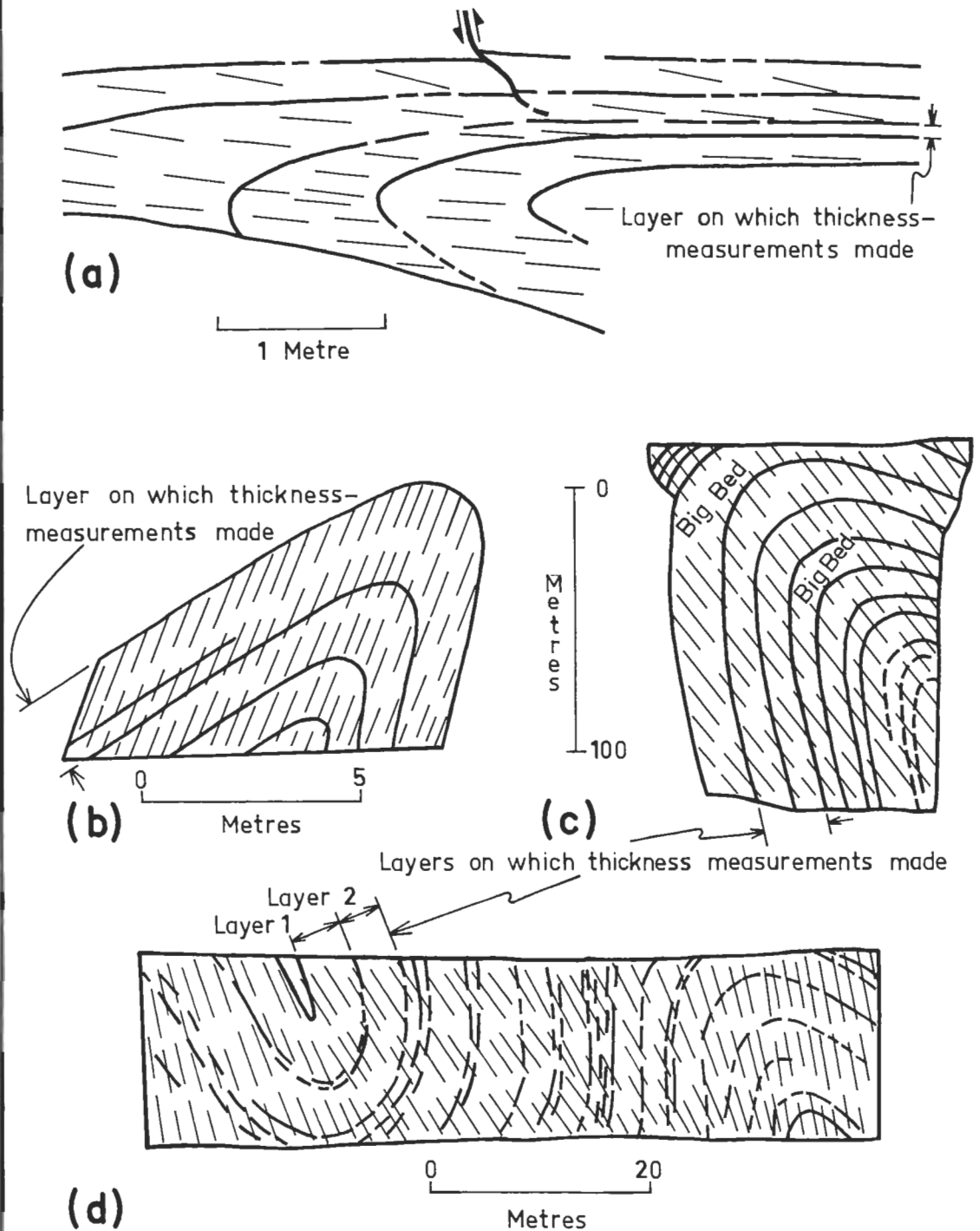


FIG: 9-6 PROFILES TRACED FROM BEHRE, 1933.

Cleavage traces shown as thin lines. (a) Edelman quarry, Lehigh-Northampton district (Behre, Plate 5B, p.22). (b) Lehigh Gap quarry (Behre, Fig. 79, p.320). (c) Manhattan quarry, Slatedale (Behre, Fig. 49, p.155). (d) Eureka quarry, Slatington (Behre, Fig. 48, p.155).

shear of the upper limb parallel to the axial surface.

Fig. 9 - 6 (b) (*ibid.*, p. 321, Fig. 79). Measurements on the sharp overturned anticline in the southwestern wall of the Leligh Gap quarry were made on the layer of ribboned slate fifteen feet thick. The cleavage diverges 10° from the axial plane, but the apparent flattening is symmetrical about the axial plane and not the cleavage. Both limbs have orthogonal-thickness ratios corresponding to 30% uniform flattening, but the amount of flattening in the hinge region appears to be less - 20%. This increase in apparent flattening in the limbs is probably caused by stretching or simple shear of the limbs parallel to the axial surface.

Fig. 9 - 6 (d) (*ibid.*, Fig. 48). Measurements were made on two layers in the syncline at the northern end of the eastern wall of the Eureka quarry, near Slatington. This apparently is the same fold as in Plate 5A (Behre, p. 22). The orthogonal-thickness ratios of the layer immediately adjacent to the core in the photo, correspond to fairly uniform flattening of 20% perpendicular to the axial plane, although the overturned southern limb may be flattened slightly more than the right way-up northern limb. The layer adjacent to the convex side of this bed shows a smaller percentage of flattening; 5% to 10% on the northern limb and 15% and on the southern limb. This indicates that there may be a small amount of differential and nonuniform

flattening in the hinge region and is comparable with some of the distributions at Sulphur Creek and Tullochgorum. The adjacent anticline to the south was not measured because there seems to be some irregularity in the layers, perhaps primary variation.

Fig. 9 - 6 (c) (*ibid.*, p. 155, Fig. 49). Orthogonal thicknesses were measured between the two Big Beds in the northeastern wall of the Manhattan quarry, near Slatedale. The northern limb appears to be flattened uniformly perpendicular to the axial surface by 30%, the southern limb by a slightly larger amount, perhaps 40%.

CONCLUSIONS

(1) The overall style of folding is not similar, but lies approximately half-way between the similar and concentric end-members. This implies at least some layer-parallel slip during deformation.

(2) The amount of apparent flattening is comparable with measurements in the slates at Sulphur Creek.

(3) The orthogonal-thickness ratios are symmetrical about the axial surface even where the slaty cleavage diverges from it, thereby implying that there has been little flattening related to the formation of the cleavage.

(4) Apart from the different scales of folding, there is no significant difference between the geometry of these folds and that of some of the folds in the slates at Sulphur Creek.

(5) It appears that whatever mechanism of cleavage formation operated in the Martinsburg slates could equally well have operated at Sulphur Creek, and *vice versa*.

3. RECUMBENT, ZIG-ZAG FOLDS IN THE FRANCISCAN CHERTS, CALIFORNIA

Fig. 9 - 7 is a tracing from a photograph on the cover of a Special Report published by the California Division of Mines (Goldman, 1959). The folds are in interbedded cherts and argillites which form lenses up to several hundred feet thick in the Franciscan Chert, California. In the tracing, the competent chert layers are light-coloured, and the incompetent argillite is black. Horizontal is parallel to the length of the page and, although no scale was given, Goldman (*ibid.*, p. 9) states,

"The chert layers are half an inch to six inches thick, but average about 2 inches",

which makes the tracing approximately one tenth natural size. The folding is a typical concertina style, and the fold form is propagated along the trace of the axial surface in the profile almost unchanged from one chert layer to the next. In the fold-hinges, the chert layers are rounded on the convex side and have a sharp angular cusp on the concave side. Measurements of thickness parallel to the trace of the axial surface show that there has been considerable flow of the argillite into the hinge regions.

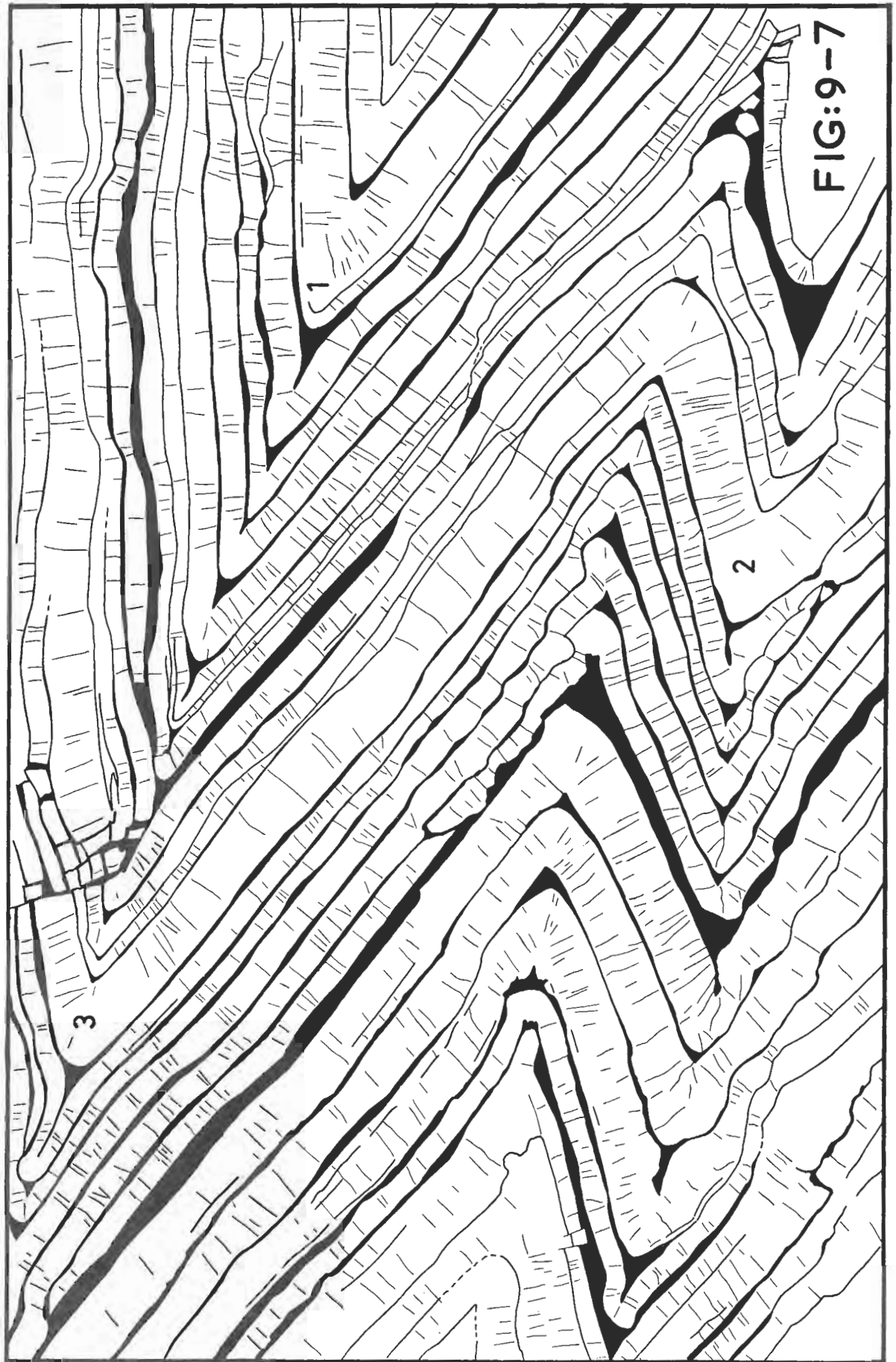


FIG:9-7

Orthogonal-thickness ratios were calculated for three hinges, and these have been numbered 1, 2 and 3 on the tracing. The layers adjacent to Hinge 1 are shown as Fig. 9 - 8 (a), and the orthogonal-thickness ratios in Fig. 9 - 8 (d). It can be seen that the geometry of Hinge 1 approximates closely to a similar fold, or to a concentric fold that has been uniformly flattened at least 50% perpendicular to the axial surface. Hinge 2 also has similar geometry, but in Hinge 3 the orthogonal-thickness ratios correspond to an apparent uniform flattening of between 35% and 40% perpendicular to the axial surface. Inspection of other hinges (e.g. on the convex side of Hinge 3) shows that all variations between concentric and similar folds exist. Nevertheless, most hinges have some degree of similar geometry.

In order to test whether the similar geometry was produced by simple shear or by flattening, a reconstruction of the region of Hinge 1 was attempted [Fig. 9 - 8 (b)]. In the concertina folds, the only part used in the orthogonal-thickness calculations is the narrow hinge region, and since the long limbs are straight it is not possible to say what the original thicknesses of the layers were. Nonetheless, because there is a thickening of the argillite in the hinge region if it is measured parallel to the trace of the axial surface, there was at least some concentric folding. There appear to be two possible modes of deformation which combined with the concentric folding, could produce the existing geometry.

FLATTENED CONCENTRIC PROFILE FRANCISCAN CHERT, CALIFORNIA

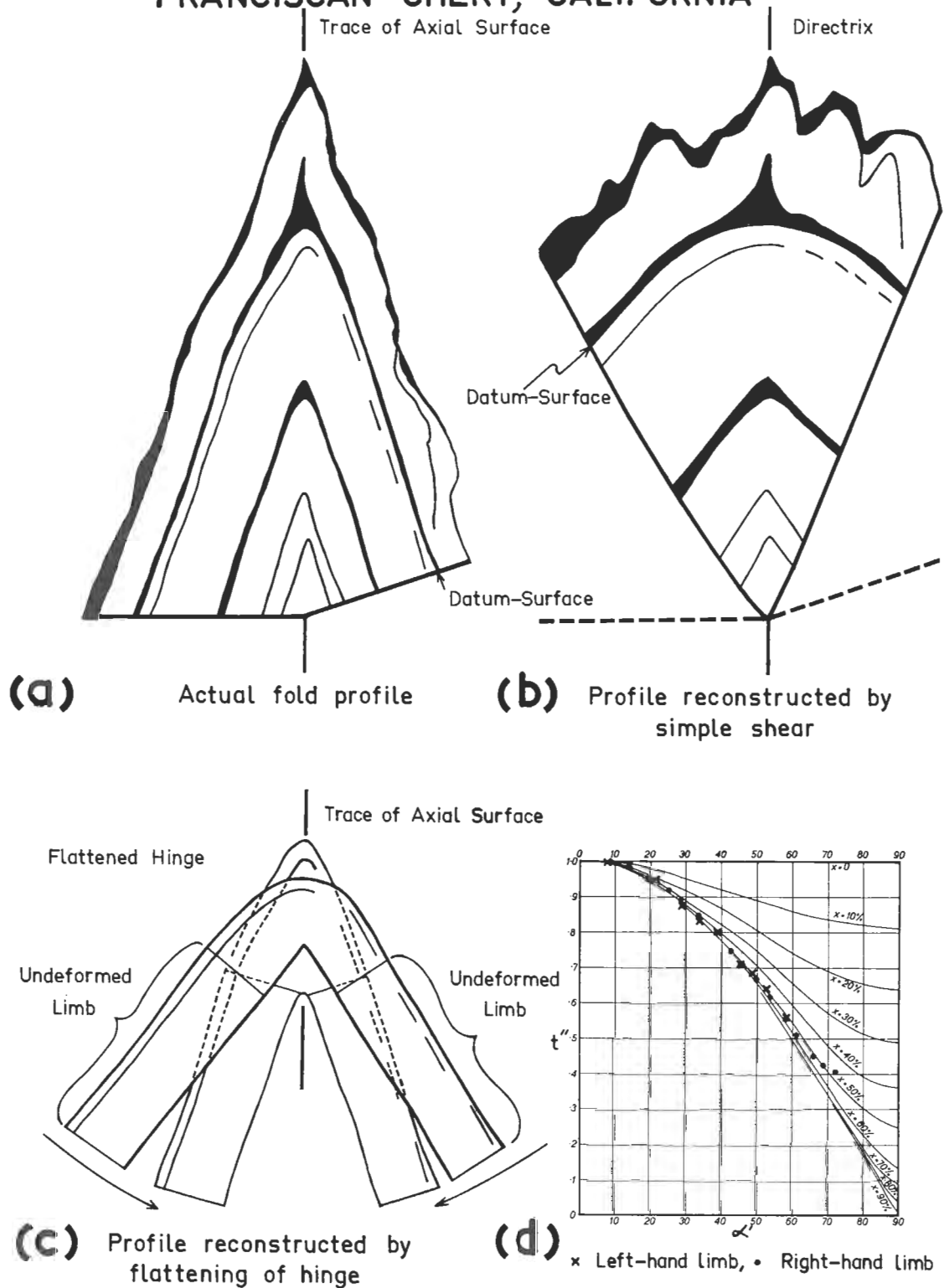


FIG:9-8

In one model, it is possible that after a certain amount of concentric folding, heterogeneities between layers became negligible, and further deformation proceeded by simple shear parallel to the axial surface. In the other model there was collapse of the hinge region of the folded layer after, or during the concentric folding, and flattening in the hinge region perpendicular to the axial surface was accompanied by rotation of the limbs.

Fig. 9 - 8 (b) shows a reconstruction of the region of Hinge 1 by the simple-shear mechanism. The convex surface of the layer in Hinge 1 was taken as the datum-surface, and the layer was reconstructed to a concentric profile by simple shear parallel to the axial surface. The effect on the adjacent layers is striking. The layer on the concave side of the datum-layer still shows a certain amount of similar geometry, and the apical thickness is almost one and a half times the orthogonal thickness in the limbs. On the convex side of the datum-layer there are many irregularities of thickness which were not present before the reconstruction. In addition, the hinge region tends to be thinner than the limbs, which is opposed to the thickness distribution in the layers on the concave side of the datum-layer. Thus, while it is possible to reconstruct a concentric profile from a partly similar profile for one layer by simple shear parallel to the axial surface, the adjacent layers

are deformed into complicated shapes. Simplicity demands that any reconstruction preserves the uniformity of fold style in all parts of the profile, and thus this simple-shear mechanism is precluded as a possible origin of the similar geometry.

The alternative to simple shear is pure shear. It is well to note that hypotheses of either uniform or differential flattening satisfy the geometrical requirements of any one layer. However, as noted before, different layers have different amounts of equivalent flattening along the same axial trace, and one or two layers are folded in an almost concentric fashion. Thus uniform flattening of the whole section parallel to the axial surface can be dismissed.

The best explanation of the fold geometry is in terms of differential flattening involving a collapse of the hinge region with concomitant rotation of the undeformed limbs. Fig. 9 - 8 (c) shows the reconstruction of Hinge 1 from its present form to a concentric fold. The layer has been divided into a hinge region and two limbs which have been simply rotated undeformed while the hinge region was flattened by 50% perpendicular to the axial surface. It is interesting to note that in this reconstruction it is not possible to fit the layer on the concave side without first flattening it. This is in accordance with the idea that the hinges on the concave side of the thicker chert layers are flattened more than those on the convex side, and the

notion is borne out by inspection of the many hinges in Fig. 9 - 7. It is also important to note that this reconstruction can be repeated *ad infinitum* to produce uniform concentric profiles in all the hinges in the profile.

There is a marked similarity between the style of deformation in this example from the Franciscan cherts, and some of the later, recumbent folds at Paga Point, Port Moresby. As in this example, the mode of deformation at Paga Point also appears to have been interlayer slip in the limbs with some flattening in the hinges producing an overall similar, concertina-style fold which is a combination of Ramsay's Class 1C in the chert layers and Class 3 in the argillite.

The Franciscan cherts are thought to have been chemically precipitated (Taliaferro, 1934, and Goldman, *op. cit.*), and Taliaferro (*ibid.*, p. 225) concludes that the chert layers became brittle soon after deposition. Nonetheless, it is quite clear that in the folding in the tracing the chert maintained its cohesion, and was capable of deforming plastically with time. Elastic stresses were concentrated at the hinges during folding and were relieved by flattening. The cracks which are arranged perpendicular to the layer boundaries do not increase in intensity in the hinge regions, and I interpret them as contraction cracks formed by dehydration of the silica gel.

CHAPTER 19

VARIATION IN FOLD STYLE

1. INTRODUCTION

Fold style is a term which refers to both the form of folds and their mode of formation. In most studies of folding the style is considered in terms of the geometry or morphology of the folds, but there have been some attempts (Beloussov, 1960) to consider fold style in terms of the kinematics and mechanics of formation. In this final chapter, I shall attempt to show that although there is a wide variation in the geometry of folds, this variation can be interpreted fairly readily in terms of only a few mechanical principles.

Very early in the history of structural geology, at the turn of the century, two basic styles of folding -- similar and concentric -- were recognized. These two geometrical types have been considered by many geologists as end-members of a continuous series of real folds. This is only partially true, for as Ramsay

(1967, *in press*) noted,

"...the two models ... are but two unique types in a whole field of possible geometrical models..."

Ramsay has extended the continuous series beyond both the concentric and similar end-members, and divided the spectrum into five categories, *viz.* Classes 1A, 1B (concentric), 1C, 2 (similar) and 3.

Although all fold shapes cannot be described in terms of this classification (e.g. disjunctive folds, irregular "flow folds", detached cores, etc.), it is possible to give a general indication of fold style in most cases.

2. GEOMETRICAL ANALYSIS OF FOLDS

(a) THE BEHAVIOUR OF GEOLOGIC MATERIALS IN DIFFERENT ENVIRONMENTS

Inspection of the range of fold styles from a variety of environments reveals that the relative competence of certain materials varies depending on the conditions at the time of folding. In deformations in sedimentary and early-diagenetic environments the order of competence is generally

pelite > limestone > psammite,

while in most late-diagenetic, and low- and medium-grade metamorphic environments the order is

limestone ≈ psammite > pelite,

and in high-grade metamorphic environments the order of competence is

psammite > limestone > pelite.

Apart from the structures in the contact aureoles, the folds I have considered in this thesis have all formed under sedimentary, diagenetic or low-grade metamorphic conditions, and the main transition is the change in relative competence of the pelites and psammites. The folds in the contact zones have also been considered because they have many similarities with folds formed in sedimentary or diagenetic environments.

Although it is generally true to say that argillites are more competent than sandstones in sedimentary or early diagenetic folding, a great range of fold styles is possible even in a single layer. For example, in the intraformational folds in the glacial varves at Gormanston, the clay layers are folded in a concentric style in the broad, open synclines, but in a similar style in the adjacent, tight anticlines. It is true that in both the synclines and the anticlines the interbedded sand has been incompetent, but in rocks more consolidated at the time of deformation, such as those at Sulphur Creek and Tullochgorum, adjacent folds in any particular layer tend to have comparable fold styles. In superficial deposits fold styles range through all five Classes, 1A to 3, whereas in the more consolidated rocks the range of styles is restricted to the concentric - similar series (Classes 1B to 2).

Pelite is not always the most competent material in sedimentary or early diagenetic folds. In the folded cherts and argillites

at Paga Point, and also in the Franciscan chert of California, the most competent material during the folding was the chert (or silica gel, as it must have been soon after precipitation). At Paga Point where there has been progressive syntaphral sliding, it is significant that the sandstones involved in the recumbent folding at the western end of the section were competent with respect to the argillite. This may imply that at least the latter part of the folding occurred when the rocks were reasonably well consolidated.

In the intraformational folding of the Pleistocene Lisan Formation of Israel, the most competent bands are composed of chemically precipitated aragonite bands, and the fine-grained, detrital sands were incompetent. In the diagenetic or low-grade metamorphic conditions exemplified at Sulphur Creek, Tullochgorum, Arm River and Piper's River, as well as in the Delaware Water Gap area, U.S.A., the pelite is everywhere incompetent with respect to the sandstones, although the sandstone dykes along the cleavage surfaces in the Martinsburg Slate (Maxwell, 1962) indicate that the sandstones were not competent at all times during the folding.

(b) VARIATION OF STYLE IN A SINGLE FOLD

One of the most important properties of folds is that the fold style must vary in different parts of a fold, except in the special case of ideal similar folding. Thus a concentric fold

must pass along its axial surface into a décollement or a zone of different fold style. Even in folded psammites and pelites where the upper (or lower) surfaces of successive layers of the same rock type have identical shapes thereby producing an apparently similar profile, there are different fold styles in the different rock types. Thus the concertina-style folding at Tullochgorum, which has an overall similar shape, is formed by folds of Classes 1B or 1C in the psammite alternating with folds of Class 3 in the pelite, and the concertina folds themselves are situated on the concave sides of concentric folds.

Fold style is not necessarily constant for a particular rock type in any one locality, even in late diagenetic or low-grade metamorphic environments. Where there is a range in thickness of the layers of one particular type of material, it is possible to have a range of fold styles depending on the relative positions of the thick and thin layers. Thus, at Sulphur Creek and Tullochgorum the thick sandstone bands are folded in a concentric fashion, and the thin sandstone beds on the concave sides of these folds have been flattened by variable amounts to form folds of Class 1C. Similarly, in the Pleistocene Lisan deposits of Israel the thin, white, aragonite-rich layers are curved broadly around the convex sides of the intraformational folds, but are highly contorted on the concave sides. This variation in fold style is not random, and is dependent on the position of the competent layers in the

larger-scale folds.

The dependence of fold style on relative position within a fold occurs on all scales down to the scale of grains, as is shown by the large thin-section from Arm River. Thus, although it is true that the parasitic folds on the concave side of a thick competent layer are tighter, and perhaps flattened, when compared with parasitic folds on the convex side, this generalization holds only for the scale of the larger fold. Smaller folds which are parasitic with respect to the first-order parasitic folds have the same type of variation in style as the first-order folds, and this relationship may extend through many orders of scale.

(c) VARIATION OF STYLE IN DIFFERENT ENVIRONMENTS

It is quite commonly assumed that the style of folding in superficial deposits indicates flowage; that with increasing compaction and lithification the style tends to be concentric, and that as the grade of metamorphism is increased the style tends toward "flow folds". Rickard (1963, p. S2, Fig. 1) uses this idea to disagree with Bradley's suggestion that

...zig-zag folds in greywackes are due to mass sediment slip towards the geosynclinal trough. (ibid., p. S2).

In the sequence of fold-style development assumed by Rickard, zig-zag folds develop at slightly higher metamorphic grades than concentric folds which belong to the lowest metamorphic grades,

and thus zig-zag folds can not occur before induration of the sediments. The recumbent zig-zag folds at Paga Point and in the Franciscan cherts vitiate this reasoning!

All styles of folding occur in unconsolidated sediments. No particular fold shape is unique to one environment. Thus most styles of folding which occur in metamorphic rocks can be found in the glacial moraine at Gormanston. If a generalization is to be made about fold style, it could be said that the range of fold styles decreases with increasing grade of metamorphism. Hence, while all five classes of folds, 1A to 3, are present in superficial deposits, low-grade metamorphic rocks generally have only folds of Classes 1B, 1C and 2, depending on the rock types present. In rocks of higher metamorphic grade folds of Class 1B are rare, and most folds formed under medium-grade metamorphic conditions belong to Classes 1C and 2. In high-grade conditions irregular folds which do not fit into this classification may occur, but there is little range of style.

3. MECHANICAL ANALYSIS OF FOLDS

(a) GENERAL STATEMENT

One of the more usual approaches to the mechanical interpretation of folds is based on the concept that a certain mechanism will give rise to a certain geometry, so that by recognizing the geometry of

the fold the mechanism of folding can be specified. Thus Carey (1962, p. 95) considers that,

"Similar folding is not just a more intense development from concentric folding; the two types are at the opposite ends of a behaviour spectrum."

This is correct, but although it is true that a certain mechanism produces a certain geometry, a given geometry may have been produced by many different mechanisms.

One of the best known dilemmas in this respect is the impossibility of distinguishing between simple and pure shear merely from the shape of a deformed body. Additional information is needed to discriminate between the two modes of deformation, such as knowledge of the symmetry or orientation of the deformed body with respect to its original position or the deforming movement. For this reason the "flattenings" I have determined from orthogonal-thickness ratios can not, in most cases, be ascribed unequivocally to pure, rather than to simple shear. However, there are sufficient examples in which pure shear can be demonstrated as the mode of deformation, to justify a tentative suggestion that, in this thesis, most of the folds with partial similar geometry have been deformed by pure, rather than simple shear. In this concluding section I shall attempt to consider briefly some of the basic mechanical factors influencing the style of folding.

(b) SCALE IN MECHANICAL INTERPRETATIONS

Mechanical interpretations of deformed rocks are usually formulated for two fundamental scales.

- (1) The scale of layers, and
- (2) The scale of grains.

The layers important in deformation are the layers that act as mechanical units, and they may range in thickness from fractions of a millimetre, as postulated in the formation of crenulation cleavage (Rickard, 1961), up to hundreds of metres (Currie *et al.*, 1962). Commonly, but not necessarily, sedimentary beds are the mechanical layers during deformation.

Granular deformation may be considered as either movement between grains, or movement within grains. In this thesis, I have considered folds in which the layers have been both active and passive mechanically, but most of the deformation has been intergranular. Intragranular deformation is typical of higher-temperature and higher-pressure environments.

(c) THE ROLE OF LAYERING IN DEFORMATION

One of the most intriguing problems of structural geology is why layers act as mechanical entities in some folds, and are merely passive markers in others. Concentric folding requires that the material to be folded consists of discrete layers or lenses separated by surfaces along which considerable movement can occur. The cohesion across the layer boundaries must be

lower than the internal cohesion of the competent layers. By contrast, in ideal similar folding the cohesion throughout the mass is homogeneous, and the rocks behave isotropically.

This difference in the behaviour of layers poses a problem on the granular scale. Why should the cohesion between grains in a sandstone be greater than the cohesion between platy mica flakes in one environment, and yet less in another? Clearly there are factors other than inherent properties of the rocks, which cause the diverse behaviour of layers.

(d) POSSIBLE MECHANICAL CAUSES OF VARIATION IN FOLD STYLE

I have shown empirically that in general the range of fold styles decreases with increasing depth and grade of metamorphism. Carey (1962, p. 117), reasoning from a theoretical standpoint writes,

"The important point is that rising temperatures and fluid pressures carve bigger slices from the viscosities of the more 'competent' rocks than from those whose viscosities were already low, leading thus to a convergence of viscosities... and similar folding."

Convergent viscosities in adjacent layers is probably the fundamental reason why the range of fold styles in any one environment decreases with increasing depth of burial and grade of metamorphism. Nevertheless, convergent viscosities do not explain why the fold style may vary in similarly situated environments. There are four principal factors that control the variation of fold style.

(i) The rate of application of stress difference.

In general, for a given situation, if the rate of application of the stress difference is very slow, similar or "flow" folds are produced; if the rate of application is more rapid, concentric folding occurs, and if the rate is even greater fracture rather than flow prevails. The rate of strain must be considered relative to the rock viscosities, for although a particular strain rate will cause a certain style of deformation in one situation, the same rate of strain may cause an entirely different style in another environment.

(ii) Temperature. The commonly postulated effect of temperature is that increasing temperature lowers both the viscosities, and the range of viscosities of the rocks. Thus, under a given stress difference an increase in temperature will cause a greater rate of deformation, or, conversely, under a given strain rate a style of folding more allied to similar or "flow" folding will occur. On a granular scale an increase in temperature increases the "plasticity" of the constituent minerals, and intragranular movements are a larger proportion of the total deformation.

(iii) Confining pressure. The effect of increasing the confining pressure is to increase the strength of the rock slightly. This effect acts in the opposite way to the effect of temperature, but since an increase in pressure is usually accompanied

by an increase in temperature, the effects of confining pressure alone can rarely be observed. Nevertheless, in general the effect of increasing confining pressure dominates in the shallower levels of the earth's crust, and the effects of temperature are increasingly important with greater depths.

(iv) Pore pressure.

The effect of varying the pore pressure is to vary the load borne on the granular fabric of the rock. Pore pressure equal to the confining pressure enables the whole weight of the superincumbent rocks to be taken on the interstitial fluid instead of the granular fabric of the rock. Thus, heterogeneities in the strength of the fabric, so necessary for concentric folding, are eliminated, and the rock is capable of behaving as an isotropic medium with respect to any applied stress difference.

To decide which of these factors has been operative in any given case is difficult, and commonly impossible. Temperature, confining pressure and strain rate are well-known and accepted controls on the style of deformation, but the role of pore pressure is often neglected. In the interpretation of each deformed area in this thesis, I have attempted to show difficulties in explaining all the observed configurations in terms of temperature, confining pressure and strain rate, and I have outlined the possible role of pore pressure.

In particular, I have attempted to show that high water pressures may be the significant factor in deformation in sedimentary or early diagenetic environments such as in the glacial moraine at Gormanston, and the intraformational slumps in Israel. I have attempted to show that the development of high water pressures may be the only plausible explanation of cleavage formation in the very low-grade rocks at Tullochgorum, Sulphur Creek and divers other places, and I have also attempted to show that the plastic, intergranular style of folding in the contact aureoles at Diana's Basin and Remarkable Cave may, too, have been caused by high water pressures.

It is almost impossible with our present state of knowledge to prove the one-time existence of a departed, high water pressure. Detailed examination of the geometry of individual folds may at least throw doubt on some of the more conventional hypotheses of cleavage formation, and trace-element studies on the pelitic ribbons which line the cleavage surfaces in the sandstones are a possible future line of research. Let it suffice for me to conclude that in these studies in folding I have been able to interpret more features in terms of pore pressure than in terms of any other factor, or combination of factors.

REFERENCES

- AHMAD, N., H.A. BARTLETT and D.H. GREEN. 1959. The glaciation of the King Valley, western Tasmania. *Pap. Proc. R. Soc. Tasm.*, 93, 11-16.
- ANRADE, E. da C., and J.W. FOX. 1949. The mechanism of dilatancy. *Proc. phys. Soc. Lond.*, 62, Sect. B, 483-500.
- BADGLEY, P.C. 1965. *Structural And Tectonic Principles*. New York, Harper and Row.
- BEHRE, C.H. Jr. 1933. Slate in Pennsylvania. *Bull. Pa geol. Surv.*, 15 4th ser., M 16, 400 p.
- BELOUSSOV, V.V. 1960. The conditions of fold formation. 21st *Int. geol. Congr.*, pt. 18, 326-334.
- BENTOR, Y.K., and A. VROMAN. 1960. The Geological Map of Israel, 1: 100,000 Sheet 16: Mount Sdom. 2nd ed., *Geol. Surv. Israel*, Jerusalem.
- BIOT, M.A. 1961. Theory of folding of stratified viscoelastic media and its implications in tectonics and orogenesis. *Bull. geol. Soc. Am.*, 72, 1595-1620.
- BRADLEY, J. 1954. The geology of the West Coast Range of Tasmania. *Pap. Proc. R. Soc. Tasm.*, 88, 193-244.
- BRADSHAW, R., and D. INGLESMTIH. 1963. Permafrost structures on Sully Island, Glamorgan. *Geol. Mag.*, 100, 556-565.
- BROWE, C.B. 1938. On a theory of gravitational sliding applied to the Tertiary of Ancon, Ecuador. *Q. Jl geol. Soc. Lond.*, 94, 359-370.
- BROWN, R.L., and P.G.W. HAWKSLEY. 1947. The internal flow of granular masses. *Fuel, Lond.*, 26, 159-173.

- BRYAN, W.H., and O.A. JONES. 1962. The bedded cherts of the Neranleigh-Fernvale group of south-eastern Queensland. *Proc. R. Soc. Qd.*, 73, 17-36.
- BURNS, K.L. 1964. Devonport. *Explan. Rep. geol. Surv. Tas.*, 1. 1-mile Geol. Map Ser., K 4 55-6-29.
- CAREY, S.W. 1955. A new record of glacial grooving near Queenstown, Tasmania. *Aust. J. Sci.*, 17, 176.
- CAREY, S.W. 1962. Folding. *J. Alberta Soc. Petrol. Geol.*, 10, 95-144.
- CAREY, S.W. and N. AHMAD. 1961. Glacial marine sedimentation. *Proc. 1st Internat. Symposium on Arctic Geology*, 865-94.
- CHARLESWORTH, J.K. 1957. *The quaternary era: with special reference to its glaciation*. London, Arnold.
- CLOOS, E. 1947. Oolite deformation in the South Mountain fold, Maryland. *Bull. geol. Soc. Am.*, 58, 843-918.
- COLLETTE, B.J. 1958. On the origin of schistosity. *Proc. K. ned. Akad. Wet.*, 61, ser. B, 121-139.
- COOMBS, D.S., A.J. ELLIS, W.S. FYFE, and A.M. TAYLOR. 1959. The zeolite facies, with comments on the interpretation of hydrothermal syntheses. *Geochim. cosmochim. Acta*, 17, 53-107.
- CURRIE, J.B., H.W. PATNODE, and R.P. TRUMP. 1962. Development of folds in sedimentary strata. *Bull. geol. Soc. Am.*, 73, 655-674.
- DAVIES, J.L. 1962. Cainozoic - geomorphology and glaciation. *J. geol. Soc. Aust.*, 9, 243-248.
- DEER, W.A., R.A. HOWIE, and J. ZUSSMAN. 1962-3. *Rock-Forming Minerals*. London, Longmans.

- DONATH, F.A. 1961. Experimental study of shear failure in anisotropic rocks. *Bull. geol. Soc. Am.*, 72, 985-89.
- EMERY, K.O. 1950. Contorted pleistocene strata at Newport Beach, California. *J. sedim. Petrol.*, 20, 111-115.
- FAIRBRIDGE, R.W. 1946. Submarine slumping and location of oil bodies. *Bull. Am. Ass. Petrol. Geol.*, 30, 84-92.
- 1947. Possible causes of intraformational disturbances in the Carboniferous varve rocks of Australia. *J. Proc. R. Soc. N.S.W.*, 81, 99-121.
- FOURMARIER, P. 1956. Remarques au sujet de la schistosité en général avec application aux terrains paléozoïques de l'Ardenne et du massif schisteux Rhénan. *Geologie. Mijnb.*, 18, 47-56.
- GEE, R.D. 1967. *The tectonic evolution of the Rocky Cape geanticline in northwest Tasmania*. Unpub. Ph.D. thesis, Univ. of Tasm., 351 p.
- GILL, E.D. 1956. Radiocarbon dating for glacial varves in Tasmania. *Aust. J. Sci.*, 19, 80.
- GLAESSNER, M.R. 1952. Geology of Port Moresby, Papua. *Sir Douglas Mawson Anniversary Volume*, Univ. of Adel., 63-86.
- GOLDMAN, H.B. 1959. Franciscan chert in California concrete aggregates. *Spec. Rep. Calif. St. Min. Bur.*, 55, 28 p.
- GREENWOOD, H.J. and K.C. McTAGGART. 1957. Correlation of zones in plagioclase. *Am. J. Sci.*, 255, 656-666.
- HAMAN, P.J. 1961. Manual of the stereographic projection. *West Canadian Research Publications*, Calgary, Ser. 1, No.1.

- HARRISON, J.V., and N.L. FALCON. 1936. Gravity collapse structures and mountain ranges, as exemplified in south-western Iran. *Q. Jl geol. Soc. Lond.*, 92, 91-102.
- HILLS, E.S. 1963. *Elements Of Structural Geology*. London, Methuen.
- KAYE, C.A., and W.R. POWER. 1954. A flow cast of very recent date from northeastern Washington. *Am. J. Sci.*, 252, 309-310.
- KRUYT, H.R. 1952. *Colloid Science*. London, Elsevier.
- LANGOZKY, Y. 1961. Remarks on the petrography and geochemistry of the Lisan and the Hamarmar formations. *Bull. Res. Counc. Israel*, 11 G, 155.
- 1963. High-level lacustrine sediments in the rift valley at Sdom. *Israel J. Earth-Sciences*, 12, 17-25.
- LEWIS, A.N. 1936. Varved shales from Tasmania. *Aust. Geogr.*, 2, 30.
- MCDUGALL, I. 1962. Differentiation of the Tasmanian dolerites: Red Hill dolerite-granophyre association. *Bull. geol. Soc. Am.*, 73, 279-316.
- , and P.J. LEGGO, 1965. Isotopic age determinations on granitic rocks from Tasmania. *J. geol. Soc. Aust.*, 12, 295-332.
- McKEE, E.D., M.A. REYNOLDS, and C.H. BAKER. 1962. Experiments on intraformational recumbent folds in cross-bedded sand. *Prof. Pap. U.S. geol. Surv.*, 450-D, 155-160.
- McNEIL, R.D. 1960. *The geology of the Mt. Elephant and Piccaninny Point area*. Unpub. Hons. thesis, Univ. of Tasm., 187 p.

- MARTIN, M.R. 1952. The structure of the granite massif of Flamanville, Manche, north-west France. *Q. Jl geol. Soc. Lond.*, 108, 311-341.
- MAXWELL, J.C. 1962. Origin of slaty and fracture cleavage in the Delaware Water Gap area, New Jersey and Pennsylvania. 281-311. In ENGEL, A.E.J., H.L. JAMES, and B.F. LEONARD, *Editors*, Petrologic studies: A volume in honour of A.F. Buddington. *Geol. Soc. Am.*, 660 p.
- MEANS, W.D. 1963. Mesoscopic structures and multiple deformation in the Otago schist. *N.Z. Jl Geol. Geophys.*, 6, 801-816.
- MISCH, P. 1949. Metasomatic granitization of batholithic dimensions. Pt. 2. Static granitization in Sheku area, northwest China. *Am. J. Sci.*, 247, 372-406.
- MONTGOMERY, J.N. 1930. In *The oil exploration work in Papua and New Guinea conducted by the Anglo-Persian Oil Company on behalf of the Commonwealth Government of Australia, 1920-29*. 4, London, H.M.S.O.
- NORTON, R.D. 1930. Ecologic relations of some foraminifera. *Bull. Scripps Instn Oceanogr. tech. Ser.* 2, 331-388.
- O'DRISCOLL, E.S. 1964. Simple and pure shear. *Nature, Lond.*, 201, 672-674.
- van OLPHEN, H. 1963. *An introduction to clay colloid chemistry, for clay technologists, geologists, and soil scientists*. New York, Interscience Publishers.
- PICARD, L. 1943. Structure and evolution of Palestine. *Bull. geol. Dept. Hebrew Univ.*, Jerusalem, 4, No. 2-3-4, 187 p.

- PITCHER, W.S., and H.H. READ. 1960. The aureole of the main Donegal granite. *Q. Jl geol. Lond.*, 116, 1-36.
- 1963. Contact metamorphism in relation to manner of emplacement of the granites of Donegal, Ireland. *J. Geol.*, 71, 261-296.
- RAMBERG, H. 1963a. Strain distribution and geometry of folds. *Bull. geol. Instn Univ. Uppsala*, 92, 1-20.
- 1963 b. Fluid mechanics of viscous buckling applicable to folding of layered rocks. *Bull. Am. Ass. Petrol. Geol.*, 47, 484-505.
- RAMSAY, J.G. 1960. The deformation of early linear structures in areas of repeated folding. *J. Geol.*, 68, 75-93.
- 1962. The geometry and mechanics of formation of "similar" type folds. *J. Geol.*, 70, 309-327.
- 1967. *Folding And Fracturing Of Rocks*. New York, McGraw-Hill.
- REESMAN, A.L., and W.D. KELLER, 1965. Calculation of apparent standard free energies of formation of six rock-forming silicate minerals from solubility data. *Am. Miner.*, 50, 1729-1739.
- RICKARD, M.J. 1961. A note on cleavages in crenulated rocks. *Geol. Mag.*, 98, 324-332.
- 1963. Review discussion of quickstone hypothesis. S1-S2. In *Syntaphral tectonics and diagenesis - a symposium*. Univ. Tasm.
- RIGBY, J.K. 1958. Mass movements in Permian rocks of Trans-Pecos, Texas. *J. sedim., Petrol.*, 29, 298-315.
- RUTTEN, M.G. 1955. Schistosity in the Rhenic massif and the Ardennes. *Geologie Mijnb.*, 17, 104-110.

- 1956. Note on schistosity. *Geologie Mijnb.*, 18, 57-58.
- SCHWARTZ, G.M. 1958. Alteration of biotite under mesothermal conditions. *Econ. Geol.*, 53, 164-177.
- de Sitter, L.U. 1939. The principle of concentric folding and the dependence of tectonic structure on original sedimentary structure. *Proc. K. ned. Akad. Wet.*, 42, 412-430.
- 1957. Cleavage folding in relation to sedimentary structure. *20th Int. geol. Congress*, pt. 5, 1, 53-64.
- 1958. Boudins and parasitic folds in relation to cleavage and folding. *Geologie Mijnb.*, 20, 277-286.
- 1964. *Structural Geology*. 2nd ed. New York, McGraw-Hill.
- SPRY, A.H. 1962a. The Precambrian rocks. 107-126. In "The Geology of Tasmania". *J. geol. Soc. Aust.*, 9, 107-362.
- 1962b. *Some aspects of the stratigraphy, structure and petrology of the Precambrian rocks of Tasmania*. Unpub. Ph.D. thesis, Univ. of Tasm., 317 p.
- , and M. SOLOMON. 1964. Columnar buchites at Apsley, Tasmania. *Q. Jl geol. Soc. Lond.*, 120, 519-545.
- STAUFFER, M.R. 1964. The geometry of conical folds. *N.Z. Jl Geol. Geophys.*, 7, 340-347.

- SUTTON, R.F. 1963. Involutions in surficial deposits, N.W. Ontario. *Bull. geol. Soc. Am.*, 74, 789-794.
- TALIAFERRO, N.L. 1934. Contraction phenomena in cherts. *Bull. geol. Soc. Am.*, 45, 189-232.
- TERZAGHI, K. 1957. Varieties of submarine slope failures. *Saertr. tekn. Ukeblad*, no. 43-44, repr. 1461, 1-16.
- THOMAS, H.H., and W.C. SMITH. 1932. Xenoliths of igneous origin in the Trégastel-Ploumanac'h granite, Côtes du Nord, France. *Q. Jl geol. Soc. Lond.*, 88, 274-296.
- TURNER, F.J., and L.E. WEISS. 1963. *Structural Analysis Of Metamorphic Tectonites*. New York, McGraw-Hill.
- VOLL, G. 1960. New work on petrofabrics. *Lpool Manchr geol. J.*, 2, 503-567.
- WALKER, K.R. 1957. The geology of the St. Helens-Scamander area, Tasmania. *Pap. Proc. R. Soc. Tasm.*, 91, 23-40.
- WATERHOUSE, J.B. and J. BRADLEY. 1957. Redeposition and slumping in the Cretaceo-Tertiary strata of S.E. Wellington. *Trans. R. Soc. N.Z.*, 84, 519-548.
- WELLER, J.M. 1959. Compaction of sediments. *Bull. Am. Ass. Petrol. Geol.*, 43, 273-310.
- WHITTEN, E.H.T. 1966. Sequential multivariate regression methods and scalars in the study of fold-geometry variability. *J. Geol.*, 74, 744-763.

- WILLIAMS, E. 1961. The deformation of confined, incompetent layers in folding. *Geol. Mag.*, 98, 317-323.
- 1965. The deformation of competent granular layers in folding. *Am. J. Sci.*, 263, 229-237.
- 1966. An analysis of the deformation in a fold in north-east Tasmania. *Geol. Mag.*, 103, 115-119.
- YODER, H.S. 1955. Role of water in metamorphism. *Spec. Pap. geol. Soc. Am.*, 62, 505-524.

APPENDIX I

DEFINITION OF TERMS

Throughout this thesis I have used many technical terms related to folding, and in this appendix I have set out the meaning I import to each term. The greater part of this list has been prepared by Professor S.W. Carey in an unpublished synopsis on folding, and I have used this material *verbatim*. However, not all the terms prepared by Professor Carey are contained in this appendix, and a few extra terms that I have adopted are marked with an asterisk. German (G), Dutch (D), French (F) and Russian (R) equivalents of many of the terms are given in brackets.

General Terms

A *fold* is a deformation of a pre-existing surface within a rock to become a continuous curved surface convex in a single sense (G. *Falte*, D. *plooi*; F. *pli*; R. *Складка*). *Folding* is the process whereby folds are produced (G. *Faltung*; D. *plooiing*; F. *plissement*; R. *Складчатость*). The deformed surface is called an *s-surface* (G. *s-Fläche*; S-*поверхность*). The folded rock may or may not be a sediment. The s-surface need not be bedding, nor need it have been a plane surface. Faults, unconformities, foliations, veins, in fact any pre-existing surfaces may be folded. A fold produces a continuous curve; discontinuity implies rupture, which is not folding. The fold is limited by the *inflection line* where the convexity changes to concavity, and the adjacent fold begins.

Differential curvature. The curvature at any point of an s-surface has a maximum radius of curvature R_1 and a minimum radius of curvature R_2 . Three limiting cases occur where (i) $R_1 = R_2$ and the curvature at the point is spherical (ii) R_1 is infinite and the curvature at the point is cylindrical (iii) R_1 and R_2 are both infinite and the curvature at the point is planar.

The *hinge* of a folded s-surface is the locus of minimum R_2 . Where R_2 has a minimum value over an area (i.e. the fold profile is a circular arc in the neighbourhood of the hinge), the hinge is the locus of the mid-point of the circular arc. Note that the hinge may or may not be straight or confined to a plane, and that the minimum radius of curvature is not necessarily constant.

The *profile* of a folded s-surface through a point is the line of intersection of the s-surface and a plane through the point normal to the hinge.

The *apex* of a folded s-surface in any section of it, is the point of intersection of the hinge and the section.

The *axis of a fold* traditionally has been used in the sense of hinge as defined above. It has also been used for the locus of the apex in sections and on plans. More recently it has been used in a statistical sense (from π or β diagrams) to express the mean direction of the hinge throughout the fold. All other uses of the term axis are now covered by adequate properly defined terms and the statistical usage is growing, hence I adopt this usage. To be consistent the terms axial surface and axial trace should be replaced by hinge surface and hinge trace, but the former terms have priority and are quite firmly established and universally used.

The *axis of a fold* is the statistical mode of the directions of the hinges within the fold. (G. Achse; D. aslijn; F. axe; Р.ось складки).

Textbooks of structural geology mostly use the term "*axial plane*" to specify a median surface within the fold. This "*axial plane*" is not necessarily nor even commonly a plane. Hence this usage should be discontinued in favour of "*axial surface*". The idea behind the concept of axial surface is intuitively simple -- it is the surface which divides the fold as symmetrically as possible. But it is not easy to define that surface rigorously, and few have attempted to do so. However the axial surface can be defined uniquely in terms of hinge.

The *axial surface* of a fold is the surface generated by the hinges of the s-surfaces of the fold. (G. Achsenfläche; D. assenvlak; F. surface axiale; Р.Осевая поверхность).

The *axial plane* of a fold at a point on the axial surface is the plane tangential to the axial surface at that point. (G. Achsenebene; D. assenvlak; F. plan axial).

The *axial trace* of a fold with respect another surface (such as the ground surface or some reference plane) is the line of intersection of the axial surface and the given surface.

The *core* of a fold is that part lying nearest the axial surface.

The *envelope* of a fold is the part farthest from the axial surface.

Terms referred to Stratigraphic datum

An *anticline* (Gr. $\alpha\nu\tau\iota$ opposed $\chi\lambda\eta\nu\sigma$ bend) is a fold in which the convexity is towards the younger strata. (G. *Antiklinale*; D. *anticlinaal*; F. *anticlinal*; R. *антиклиналь*).

A *syncline* (Gr. $\sigma\nu\nu$ together $\chi\lambda\eta\nu\sigma$ bend) is a fold in which the convexity is towards the older strata. (G. *synklinale*; D. *synclinaal*; F. *synclinal*; R. *синклиналь*).

The *limb* of a fold is the part bounded between adjacent axial surfaces. (G. *schenkel*; D. *vleugel*; F. *flanc*; R. *крыло*).

Terms referred to horizontal datum

The *plunge* of a fold at a point on its axial surface is the angle between the horizontal and its hinge, measured in the vertical plane including or tangential to the axial line at that point. (G. *Abtauchen*; D. *onderduiking*; F. *plongement*). The *pitch* of a fold at a point in its axial surface is the angle between the horizontal and the hinge, measured in the plane tangential to the axial surface at that point. (G. *Gefälle*, *Einschieben*; D. *duiking*; F. *chute* *Ряжение*). The *rake* of a fold at a point on its axial surface is the angle between the hinge of the fold and the strike of the s-surface, measured in the plane tangential to the s-surface at that point. The term rake is rarely used in relation to folds, but is sometimes useful for some other structures. In summary:

The angle between the axis and a horizontal line is:

plunge, if measured in the vertical plane
pitch, if measured in the axial plane
rake, if measured in the s-surface.

Dimensions of folds

The *amplitude* of a fold in a given s-surface in a given profile is half the distance measured along its axial trace in that profile from the apex to the intersection with that axial trace of the straight line joining the apices of the adjacent folds. (G. *Amplitude*; D. *amplitude*; F. *amplitude*; R. *амплитуда*) (For example, in an anticline, measurement from the apex along the axial trace to the line joining the apices of the adjacent synclines

The *wave-length* of a fold in a given s-surface on a given profile is the sum of the normals from the two adjacent apices to the axial trace of the fold. (G. *Wellenlänge*; F. *longueur d'ondes*; Р. ДЛИНА ВОЛНЫ). (For example, in an anticline, draw the axial trace to the profile, and draw normals to this trace from the apices of the adjacent synclines. The sum of these normals is the wavelength of the anticline).

Hinges of folds

The hinge of a fold may be *rectilinear*, plane-curved, or non-planar. The axial surface of a fold may be plane *uniaxial* (where it has a rectilinear generator) or *polyaxial* where there is no rectilinear generator. A plane axial surface may occur with a rectilinear or plane-curved hinge. A uniaxial surface may occur with a rectilinear or non-planar hinge. Rectilinear hinges are penetrative, curved hinges are not. The contradictory term "plane fold" for a fold with a plane axial surface should be dropped.

A uniaxial fold is usually called a *cylindrical fold*. (G. *zylindrische*; D. *cyindrische*; F. *cylindrique*; Р. ЦИЛИНДРИЧЕСКИЙ).

A *cylindroidal* fold approximates towards a cylindrical fold. (G. *zylindroidale*; Р. ЦИЛИНДРОИДНЫЙ).

A *paraboloidal* has parabolic profile and parabolic hinge or approximates to these shapes. (G. *paraboloidale*; F. *paraboloidal*; Р. ПАРАБОЛОИДНЫЙ).

Most *diapiric* (Gr. δια through, παρο pierce) folds are of this form.

A paraboloidal fold has a medial line which corresponds to the axis of the coaxial parabolas which make up the fold, but doesn't correspond to the axis of a cylindrical fold. It is analogous to the diretrix of a similar fold as defined by Hills, but does not correspond to the diretrix of the parabolas in the geometrical sense.

Sigmoidal folds. The horizontal axial traces of sigmoidal folds are inflected like an elongated sigma or its mirror image. They are normally doubly plunging and commonly occur en echelon (from F. *échelle*, ladder). (Р. СИГМОИДАЛЬНЫЙ).

Attitude of folds

The *attitude* of a fold is the dip of its axial surface. (G. *Anordnung*; D. *stand*; F. *allure*) A fold is said to *face* the steeper (or most rotated) limb. The direction in which a fold faces is called its *facing*.

*Vergence** (Wood, 1963, p. 654) is the sense of rotation implied by the shape of the fold, and may be designated "sinistral" (anticlockwise) or "dextral" (clockwise).

A *polyclinal fold* shows a variety of attitudes in different parts of the fold. This may simply mean that it is non-cylindroidal or it may be due to the superposition of unrelated movements.

Some have urged the use of appropriate letters of the alphabet which resemble the fold profile to describe the shapes of folds and their attitudes, particularly Z, S, M, A, N and V. Z has been widely used for flat-limbed folds with an overturned middle limb, but Fleuty (1964) would still use Z or S when the axial surface is steep like an N or a M. Fleuty considers sense of coupling (sinistral or dextral) the important criterion and would use Z or S for the above irrespective of attitude. Others however consider the distinction of horizontal over-riding and upward differential movement more important than a dextral or sinistral couple which in both these cases is reversed by looking at the profile from the other side. For my part I will mean by Z-fold a steep middle limb in larger flatter limbs.

A fold is *upright* if its axial surface is a vertical plane. (G. *aufrechte Falte*; D. *rechttopstaande ploo*i; F. *pli droit*; R. *прямая с.*).

A fold is *symmetrical* if its axial surface is a vertical plane and its limbs form a mirror image about the axial plane. (G. *symmetrische Falte*; D. *symmetrische ploo*i; F. *pli symétrique*; R. *симметричная с.*). Some authors use symmetrical for all upright folds but Fleuty (1964, p. 482) has observed that an upright fold may be asymmetrical when one limb is thinned.

asymmetrical if its axial surface is inclined and the limbs dip in opposite directions. (G. *asymmetrische Falte*; D. *asymmetrische ploo*i; F. *pli dissymétrique*; R. *асимметричная*).

overturned if the dip of both limbs is towards the same side of the fold, one limb having been rotated through more than a right angle. (G. *überkippte Falte*; D. *overbellendè ploo*i; F. *pli renversé*; R. *опрокинутая складка*). ("Overfold" is a synonym).

recumbent if the axial surface approximates to horizontal. (G. *begende Falte*; F. *pli couché*; R. *лежащая складка*).

inverted if progressively younger strata occur down dip along the anticlinal axial surface. (R. *перевернутая складка*). Note that a fold limb is inverted in an overturned fold, the strata having been turned through more than a right angle. A fold is inverted if its axial surface is turned through more than

a right angle.

involuted if its axial surface is itself folded.

reclined when the line in the axial surface normal to the hinge is approximately horizontal and the hinge has a significant dip. Fleuty (1964, p. 488) suggests 10° as the upper limit for "approximately" and the lower limit for significant.

An *antiformal syncline* is an inverted syncline. The fold is convex towards the older strata, hence it is a syncline but the strata are arched upwards as an antiform.

Similarly a *synformal anticline* is an inverted anticline.

Mutual relations of fold limbs.

The *angle of a segment* of a fold is the dihedral angle between the tangent planes at the ends of the segment.

The *angle of a fold* at a point is the angle, measured in the profile through that point, between the tangent planes to the limbs of the fold at the points of inflection where the fold passes into the adjacent folds. (G. *Faltemwinkel*; D. *plooingshoek*; F. *angle du pli*) This angle reduces from a limiting 180° in the gentlest folds to 90° in moderate folding to zero in *isoclinal* folding and *box folds* and to negative values in *fan folding*.

The terms open and closed are used by many authors to indicate the magnitude of the fold angle, but there is no consistent definition. According to Longwell and Flint (1955, p. 283) a fold is closed when the angle and the axial surface is less than about 45° , but according to Stoces and White (1935, p. 119-121) the fold is not closed until the limbs cease to diverge from the axial surface, i.e. the fold becomes isoclinal. According to Bailey and Robyn Willis (1934, p. 62) the fold is closed when the limbs cannot bend closer without distorting the bedding, and according to Billings (1942, p. 42) a fold is closed when the deformation is sufficiently intense to cause flowage of the more mobile beds, so that the beds thicken and thin. The concept closed (закрптая) is used in the same sense in the Russian literature.

Fleuty*(1964) uses the fold angle to define open 70° , close 30° , and tight 0° , and this is the way in which I have used the terms. An objection may be raised that a closed fold has another quite different meaning in that a fold is said to be *closed* if a horizontal plane cuts one or more s-surfaces of the fold in a closed trace. However, the horizontal datum has little significance in the type of analysis with which I have been involved, so that no confusion arises.

between the tangent plane

A fold is *angular* if the angle of a short segment near the hinge is much smaller than the angle of long segments in the limbs. (G. *scharf, spitz*; D. *spitz*; F. *aigu*; R. *крытая складка угловатая* С.).

A fold is *rounded* if the angle of segments including the hinge do not differ greatly from other segments of similar length.

A fold is *isoclinal* if the limbs are approximately parallel. (G. *Isoklinalfalte*; D. *isoclinale ploo*i; F. *pli isoclinal*; R. *изоклиналильная*). Note that the term is not used where the parallelism is transient at the inflections. A significant length of limbs must be parallel (cf. Fleuty, 1964, p. 471).

A *fan-fold* has limbs convergent towards the axial surface. (G. *Fächerfalte*; D. *waaierploo*i; F. *pli en éventail*; R. *веерообразная*).

A *box-fold* is a composite fold and consists of two adjacent anticlines each approximately 90° without an intervening syncline, or a similar pair of synclines. (G. *Kofferfalte*; D. *Kofferploo*i; F. *pli coffré*; R. *коробчатая*).

Chevron folds are repeated angular folds with limbs of approximately equal length, and alternate limbs parallel. (F. *pli en chevron*; R. *у-образная* С.).

Zig-zag folds are repeated angular folds with adjacent limbs of unequal length and alternate limbs approximately equal and parallel. (G. *Zickzackfalte*; D. *zigzagploo*i; F. *pli en zigzag*)

Kink folds are very angular folds of small size (mesoscopic) with persistent planar axial surfaces.

A *kink band* is the common limb between two close parallel complementary kink folds the distal limbs being parallel.

Conjugate folds are a fold system consisting of two convergent sets of kink bands. (G. *zugeordneten Falten*; F. *plis conjugués*; R. *сопряженная* С.).

Relation of successive S-Surfaces

In *concentric folds* the orthogonal thickness of beds remains constant. (G. *parallele Faltung, konzentrische Faltung*; D. *concentrische ploo*ing; *evenivijdige ploo*ing, *parallele ploo*ing; F. *plissement parallèle*; R. *концентрическая, параллельная*).

The trace of s-surfaces on a dip section is a continuous curve made up of tangential circular arcs. In the limit, by taking segments short enough, any curve can be constructed from tangential circular arcs by continuously varying the radius of curvature. A normal to one s-surface is also normal to all other s-surfaces until a cusp is reached where the expanding arcs intersect another family of arcs of an adjacent part of the fold.

In *similar folds* the displacement of a folded s-surface in a definite direction causes it to coincide in turn with the other s-surfaces in succession. (G. *ähnliche Faltung, kongruente Faltung*; D. *gelijkformige plooing, kongruente plooing*; F. *plissement semblable, plissement similaire*; R. *подобная складка, конгруэнтная складка*). The folded s-surfaces are thus all similar in form. The direction of displacement is called the *diretrix* (Hills, 1951). The thickness of any bed or interval between s-surfaces remains constant if measured in the direction of the diretrix, but not if measured orthogonally. The line normal to the diretrix in the plane tangential to the shear surface is the axis of shear (E), σ_2 , null vector).

Concentric and similar folds are ideal limiting forms, and real folds may approximate to either or both. The physical and genetic conditions related to these forms will be discussed later.

The terms concentric and similar folding were introduced by van Hise (1895). He also used parallel folding as a synonym for concentric folding in the sense that in such folding a normal to any stratum is normal to other strata above and below it. Hence the normals see all beds as parallels. This usage has crossed directly into French (Goguel, 1952, p. 40). However Stoces and White (1935, figs. 203 and 205) misquote van Hise and use parallel folding as a synonym for similar folding, the idea being that if one folded stratum is displaced parallel to itself in the direction of shear it will coincide with the next stratum. In view of this contradictory usage, and as van Hise defined concentric and similar folding unambiguously and merely added parallel folding as a synonym it would be best to drop the term parallel folding. More recently, the terms *flexure* folding and *shear* folding have been substituted for concentric and similar folding respectively and these terms have gained wide currency. However as both types of folding involve shear to a comparative degree, and as both types of folds are flexures etymologically and in ordinary English, these substitutes should be dropped on grounds both of priority and precision. Flexure was defined by Powell (1876, p. 10-11) for bends caused primarily by vertical movement in contrast to folds due to horizontal pressure. This usage was followed by Bailey Willis (1934, p. 77). Nevin (1949, Chapter III)

uses flexure in a quite general sense with its ordinary English meaning. If the term flexure is used at all it should be used in this sense.

Bedding-plane slip (G. *Gleitung der Schichten langs der Schichtflächen*; F. *glissement dans les plans des couches*).

A fold is *carinate* (L. *carina*, keel) if one bed or member closes isoclinally on itself so that the next bed fails to enter the pinched fold, which then forms a keel or carina. (Р. килевидная. складка).

A *carinate* fold may contain a *detached core* which is separated from the rest of the formation and completely surrounded by the continuous formation. Such tear-drop-shaped detached cores are more common in *carinate* synclines than in anticlines. (G. *abgeschnurter Kern*, *abgequetschter Kern*, D. *abgesnuerde kern*; F. *noyau étranglé*).

Ptygmatic folds (Gr. *πτυγμα*, contorted) are a specific type of disharmonic fold found in quartzofeldspathic veins in migmatitic environments. They are small-scale (mesoscopic), rounded, lobate, continuous, commonly cylindroidal but usually lack cognate penetrative tectonic surfaces.

Folds are *disharmonic* when one part of the fold is deformed independently of a succeeding bed separated from it by a weak bed which has deformed substantially more freely. (Р. дисгармоничная). Salt and quickstones are commonly the weak formation.

Disjunctive folds are produced when relatively brittle thin beds are separated by relatively fluid layers, so that the former break up into tablet-like blocks following the general arrangement of the fold. Such folds belong usually to the sedimentation cycle, and the fluid layers are commonly quickstones.

Intraformational folding (G. *synsedimentäre Faltung*; F. *contournement intraformationnel*). Folding confined to a stratum between two non-folded strata.

Convolute folds literally are those with convolute axial surfaces. (G. *Gekrösestruktur*; D. *kronkelstructuur*; F. *structure convolute*) The term is continuously used for small-scale, often disharmonic folds confined to a single bed with strongly curved hinges, and involuted, whorled or branching axial surfaces. The folds tend towards concentric cylindroidal and die out towards top and bottom of the bed.

A *supratenuous* (L. *supra*, above *tenuis*, thin) fold shows thinning of beds over arches and thickening in the troughs, due to

rising of the arches during sedimentation, or to the differential compaction of sediments over buried ridges in the basement. This term was introduced by Nevin (1931). (Р. складка упиютения).

Drape folding is a synonym for supratenuous fold.

Bald-headed anticline: an anticline whose culmination has been deeply eroded prior to later deposition. (G. *Struktur mit fehlenden Dachschichten*; D. *structuur met ongedekte culminatie*; Р. размытая). *Scalped anticline* is almost synonymous, although supratenuous, baldheaded and scalped may be regarded as successive degrees. In the first there is noticeable thinning on top but all layers may be present. In the second one or more layers are absent. In the third the baring has been more severe!

Diapiric folds (Gr. $\delta\iota\alpha$ through, $\pi\epsilon\rho\sigma$ pierce) are piercing folds where a highly mobile formation breaks through higher strata towards the surface. (G. *Durchspiessungsfalte*, *diapire Falte*; D. *diapyrplooi*; F. *pli diapir*; Р. диапировая с, протыкающая). The piercing formation is commonly salt or quickstone.

Where a diapir increases its diameter upwards it is called a *mushroom fold*. (G. *Pilzfalte*; D. *paddestoelvormige kern*; F. *champignon*).

Diapirs are commonly surrounded partially or completely by a *rim syncline* (G. *Randmulde*; D. *randsynclinaal*; F. *synclinal bordier*).

Competent and incompetent.* These terms were first used to describe folded layers by Willis (1892, pp. 247-50). Willis defined *competent* layers as those layers which when bent into an anticlinal fold, are rigid enough to support the load of the overlying strata. (G. *kompetente Schicht*; D. *competente laag*; F. *couche compétente*; *assise rigide*; Р. конкурентный пласт). *Incompetent* layers are those which are incapable of transmitting such stresses to the adjacent strata. This concept is long outmoded, but the words *competent* and *incompetent* are well entrenched in the literature (e.g. Williams, 1961). I use the term *competent* to describe those layers which maintain, or tend to maintain their orthogonal thickness during folding, and the term *incompetent* to describe those layers which undergo large variations in orthogonal thickness during folding. *Competency* is a relative property, and a rock which is competent in one situation may be incompetent in another.

Mutual Relations of Folds

Folds may be grouped together to form larger folds, and the latter in turn may be part of a still larger fold. Where the sizes of folds in such composite folds fall into two or more sets, the folds are called first, second and third order folds, and so on, the first order being the greatest.

A *fold system* is a group of folds which occur together. (G. *Faltensystem*; D. *plooisysteem*; F. *système de plis*). A group of cognate folds is a *fold generation* (Turner and Weiss, 1963).

Congruous folds are major and minor folds in the same rocks, and which mutually conform in directions of axial surface and hinge. (Main fold: G. *Hauptfalte*; D. *hoofdplooi*; F. *pli principale*; Р. ГЛАВНАЯ). (Minor fold: G. *Nebenfalte*; D. *secundaire plooi*; F. *pli secondaire*; Р. ВТОРИЧНАЯ, ВТОРОСТЕПЕННАЯ). Where the folds do not conform they are *incongruous*. Care must be taken not to misread foreign texts in which this root (congruous) is usually applied to "congruent" folds in the sense of similar folds.

Crumpling (also called *puckering* or *plication*) refers to close small-scale folding which is usually penetrative and congruous. (G. *Faltelung*; D. *kreukeling*; F. *plissotement*; Р. МЕЛКАЯ, СКЛАДК, СМЯТИЯ).

The *faltenspiegel* is an enveloping surface which is tangential to successive antiformal or synformal hinges of a generation of folds. The *faltenspiegel* may form a higher-order fold.

Scale of Folds

Mesoscopic folding is a scale term introduced by Weiss (1959) to include folds which can be seen on the outcrop, including folds best studied with a hand lens. The term contrasts with *microscopic* on the one hand and *macroscopic* which includes all folds too big to be seen in single outcrop.

An *orocline* (Gr. *ορο*, mountain; *κλίνο*, bend) is a fold where the deformed unit is the orogen itself. Such folds are necessarily neutral folds.

Genetic Nomenclature

The following terms involve interpretation in respect to genesis of the folds or the controlling condition or mechanism.

Superposed folds are folds developed in rocks which have suffered prior folding (G. *zusammengesetzte Faltung*; D. *samengestelde plooing*; F. *plissement composé*).

Refolded fold: synonymous with superposed fold. (G. *wiedengefaltete Falte*; D. *herhaald geploide ploo*; F. *pli replissé*; R. *повторенная*).

Posthumous folding (L. *postumus* = last of all) almost synonymous with superposed folding, but some authors imply that the posthumous folding involves revival of the earlier stresses or constraints, which therefore relate the last folding to the earlier. (G. *Nachfaltung*, *posthume Faltung*; D. *naplooing*; F. *plissement tardif*, *plissement posthume*; R. *постумная складчатость*).

Flow folding is folding in which the rocks have behaved as fluids. (G. *Fliessfaltung*; D. *vloeiplooing*; F. *plissement fluidal*; R. *складка течения*).

Rheid folding (Gr. *ρην*, flow) is flow folding in which the rocks have remained solid or crystalline but have deformed as fluids because the duration of the loading was much longer than the relevant deformation time constant (i.e. the rheidity). It is characteristic of folds in salt, gypsum, ice, and (on appropriate time scales) of all crystalline rocks.

Shear folding results from penetrative minute displacements along closely spaced fractures or cleavage planes. (G. *Scherfaltung*; D. *schuifplooing*; F. *plissement cisailant*; R. *складка скалывания*).

Drag folds are congruous asymmetric minor folds on a major fold limb whose facings indicate the simple shear suffered by that limb. Drag fold is therefore a genetic term. (R. *складка волючения*).

Bedding-plane slip is the slippage of beds along bedding planes during folding. (G. *Gleiten der Schichten längs den Schichtflächen*; D. *glijding der lagen over de laagvlakken*; F. *glissement dans les plans des couches*).

Compressed fold (synonym appressed fold): fold whose axial width has been reduced by compression normal to the axial surface. (G. *Quetschfalte*, *komprimierte Falte*; D. *sammengedrukte ploo*; F. *pli comprimé*; R. *перезжатая с., сплюснутая с.*).

Cleavage *

Cleavage is the facility of a rock to split along definite, parallel, closely spaced surfaces, and it is caused either by mechanical fractures or parallel orientation of certain minerals. (G. *Schieferung*; D. *splijting*; *gesteentessplijting*; Fr. *clivage*; R. *слоистость*).

A cleavage is *penetrative* or *non-penetrative* on a certain scale depending on whether or not the rock will split into slices thinner than the given thickness. Cleavage penetrative to the scale of the constituent mineral grains is *flow* cleavage, whereas cleavage non-penetrative to the scale of grains is *fracture* cleavage. *Slaty* cleavage is a variety of flow cleavage produced by parallel orientation of mica flakes. However, there are so many definitions of slaty cleavage that depend to some degree on its mode of formation that I prefer to use the terms *slate-cleavage*, *sandstone-cleavage*, etc. to mean the cleavage *in the slate*, *sandstone*, etc. These terms are descriptive, and may embrace more than one genetic type.

REFERENCES

- BILLINGS, M.P.. 1942. *Structural Geology*. 1st ed. New York, Prentice-Hall.
- FLEUTY, M.J. 1964. The Description of Folds. *Proc. geol. Ass., Lond.*, 75, 461-492.
- GOGUEL, J. 1952. *Traité de Tectonique*. Paris, Masson.
- HILLS, E.S. 1951. *Outlines of Structural Geology*. 3rd. ed. London, Methuen.
- van HISE, C.R. 1894-5. Principles of North Americal Pre-Cambrian Geology. *U.S. geol. Surv.*, 16th Ann. Rept., Pt. 1, 581-843.
- LONGWELL, C.R. and R.F. FLINT. 1955. *Introduction to Physical Geology*. New York, Wiley.
- NEVIN, C.M. 1931 and 1949. *Principles of Structural Geology*. 1st and 4th ed. New York, Wiley.
- POWELL, J.W. 1876. Geology of the Uinta Mountains. *U.S. geog. and geol. Surv. of the Terr.* 10-11.
- STOCES, B. and C.H. WHITE. 1935. *Structural Geology*. London, Macmillan.

- TURNER, F.J. and L.E. WEISS. 1963. *Structural Analysis Of Metamorphic Tectonites*. New York, McGraw-Hill.
- WEISS, L.E. 1959. Structural Analysis of the Basement System at Turoka, Kenya. *Overseas Geology and Mineral Resources*. 7, No. 1, London. p. 10.
- WILLIAMS, E. 1961. The Deformation Of Confined, Incompetent Layers In Folding. *Geol. Mag.*, 98, 317-323.
- WILLIS, B. 1892. The Mechanics of Appalachian Structure. *U.S. geol. Surv.*, 13th Ann. Rept., Pt. 2, 213-281.
- WILLIS, B. and R. WILLIS. 1934. *Geologic Structures*. 3rd ed. New York, McGraw-Hill.
- WOOD, B.L. 1963. Structure of the Otago Schists. *N.Z. J Geol. Geophys.*, 6, 641-80.

APPENDIX 2

THE TERMS *SEDIMENTARY* AND *TECTONIC* AS APPLIED TO ROCK STRUCTURES

The terms *sedimentary* and *tectonic* are often used by geologists to describe structures. A *sediment* (the Shorter Oxford English Dictionary -- S.O.E.D.) is matter composed of particles which fall by gravity to the bottom of a liquid. In geology, *sedimentary* rocks are formed by the deposition of particles from the atmosphere and hydrosphere. *Tectonics* (S.O.E.D.) is the actual structure of the earth's crust, or general changes affecting it. In geology, there are a variety of ways in which the term *tectonics* is used and its definition is usually vague. *Structural geology* is the study of rock structures.

A brief survey of the literature shows that whereas there is reasonable agreement over the use of the term *sedimentary*, the term *tectonic* is used in many different, often conflicting ways. *Tectonic* is used variously to describe structures which may have formed:-

- (a) larger than a certain scale (Carey, 1962),

- (b) after lithification (Goguel, 1962), or
- (c) by the action of forces originating outside the deformed body (Belousov, 1962).

The confusion which results from the different usages of tectonic is well illustrated by Billings (1960) who writes (p.1),

"...tectonics and tectonic geology are terms that are synonymous with structural geology."

Yet on p. 226 he writes,

"...Folds as well as faults, are often classified as tectonic or nontectonic in origin. Those of tectonic origin result more or less directly from forces operating within the outer shell of the earth. Those of nontectonic origin are largely the result of movements under the influence of gravity near the surface of the earth, although the ultimate cause in many cases is tectonic."

Billings proliferates his confusion by writing,

"...the Jura Mountains, formerly believed to be tectonic, have been recently considered to be nontectonic."

De Sitter (1964, p. 3) introduces *tectonic* without definition, but in a sense which implies tectonics as the gross structure of the earth, i.e. as a scale term. De Sitter's book is concerned with structural geology and the word tectonics is not used, except in a vague way. Hills (1963, p. 3) states that,

"...traditionally the wider aspects of continental and oceanic, and eventually of global structures, are referred to as tectonics and geotectonics."

Hills uses the terms *diastrophic* and *non-diastrophic* to distinguish those structures which are formed by the action of deep-seated earth forces from those which are formed by gravitational forces. Both diastrophic and non-diastrophic structures can be tectonic if they are sufficiently large.

Goguel (1962, p.2) considers,

"...*Tectonics is concerned with the examination of ... deformations and with the study of deformed rock masses.*"

He regards (p. 101),

"...*non-tectonic displacements of beds may be produced either at the time of deposition or shortly thereafter.*"

The use of tectonic in this sense is based on the state of lithification of the sediment.

This brief summary shows clearly that at present there is no uniformity in the use of the term *tectonic*. In its literal sense, *tectonic* is synonymous with *Structural geology*, but literal usage makes the term *tectonic* redundant as applied to structures. Moreover, there is a tendency in the literature for *tectonic* to be attributive to the larger-scale structures so that a division of structures into *tectonic* and *non-tectonic* on the basis of scale should be acceptable.

Carey (1962, p. 98) has suggested that the realm of structural geology is a scale from 10 metres to 10 kilometres, and that of tectonics from 10 kilometres to 10,000 kilometres.

Strict subdivision in terms of scale is not entirely satisfactory as it is convenient to classify those small-scale structures that reflect, or are part of a large-scale structure, in the same category as the large-scale structure. Thus, if a small fold or a cleavage is genetically related to a structure large enough to be considered tectonic, it is convenient to call the fold or cleavage tectonic.

These considerations lead to the definition of a *tectonic structure* as any geologic structure that is larger than 10 kilometres, or that is genetically related to a geologic structure larger than 10 kilometres.

This arbitrary division of size at 10 kms. should not be regarded as inflexible. The size of structures should be related to a logarithmic, rather than a linear scale, so that a structure of 1 km. size bears the same relationship in scale to a structure of 10 kms. size, as the 10 kms. structure bears to a 100 kms. structure. A subsidiary problem is the definition of the "size" of a structure, and by this term I usually refer to its largest dimension. Thus, a fold 100 kms. long, 10 kms. wide and 1 km. deep is regarded as having a "size" of 100 kms. for the purpose of classification.

There is no implication of the causal force or the state of lithification in this definition; a structure can be both sedimentary and tectonic, as these are two different types of

classification. A division of structures according to the environment in which they have formed and their size is set out as follows:-

A *sedimentary structure* is a structure formed in a sediment at, or soon after the time of deposition. Sedimentary structures (sometimes referred to as *penecontemporaneous* structures) are *open-cast*, i.e. the structure has been formed before the next layers of sediment have been deposited. Open-cast structures are commonly recognized by erosional truncations of the uppermost layers. *Diagenetic structures* are formed after penecontemporaneous structures up to the time of final lithification. They are *closed-cast*, i.e. the uppermost layers of the structures are overlain by a variable thickness of sediment at the time of deformation. *Metamorphic structures* are structures formed when the rock is at temperatures and pressures indicated by characteristic metamorphic-mineral assemblages, and similarly *igneous structures* are formed when there is a silicate melt present.

Where one deformation simultaneously affects rocks in a range of environments, different parts of the structure are named according to the environment in which they are produced. Thus, in the case of a large-scale gravity slide involving partially molten basement in depth and submarine slumps on the sea floor (*cf.* Alpine nappes) all four classes of structure may

be developed, and they are named accordingly. As in petrology, the same problem exists of determining the onset and completion of diagenesis, and rather than fit structures into rigid categories they should be classified in a flexible fashion, e.g. early - and late - diagenetic, or high- and low-grade metamorphic. There is an anomaly in that a rock which is "finally lithified" may be deformed and yet not have reached a significant metamorphic grade. I have tried to cover this gap by extending diagenesis and metamorphism, and I have used terms such as *late-diagenetic* and *very low-grade metamorphic*. I am not satisfied with this usage, and it may be better to define a completely different new term. Table 1 outlines the classification of structures I have used in this thesis, and a few, general examples are given.

CLASSIFICATION OF STRUCTURES

ENVIRONMENT	SCALE		TECTONIC
	NON-TECTONIC	TECTONIC	
	Less than 10 kms.	10 kms.	Greater than 10 kms.
Deposition SEDIMENTARY (Perecontemporaneous or Open-cast)	Bedding perturbations, primary bedding structures, convolute folds, flow folds, ice-push folds submarine slumps.		Sedimentary formations, flysch, molasse, gravity slides.
DIAGENETIC (Closed-cast)	Supratenuous and compaction folds, closed-cast slumps, flame structures, load casts, quickstone slides and folds, shale diapirs, clastic dykes and sills		Some types of cleavage, large salt domes, some nappes.
Lithification METAMORPHIC	Folds and faults in contact aureoles, sheet jointing, collapse structures, local rheid folds in high-grade metamorphic terrains, some tension faults.		Most types of cleavage, nappes, thrust sheets, most folds and faults, granitization, oroclines, megashears.
Presence of a silicate melt IGNEOUS	Platy mineral orientation, volcanic pipes, dykes, necks, veins, columnar jointing, small diapiric plutons, ptygmatic folds.		Batholiths, layered basic intrusions, cone sheets, axial orogenic intrusions.

REFERENCES

- BELOUSSOV, V.V. 1962. *Basic Problems in Geotectonics*. New York, McGraw-Hill.
- BILLINGS, M.P. 1960. *Structural Geology*. 2nd ed. New York, Prentice-Hall.
- CAREY, S.W. 1962. Scale of geotectonic phenomena. *J. geol. Soc. India*, 3, 97-105.
- GOGUEL, J. 1962. *Tectonics*. San Francisco, Freeman.
- HILLS, E.S. 1963. *Elements of Structural Geology*. London, Methuen.
- de SITTER, L.U. 1964. *Structural Geology*. New York, McGraw-Hill.

APPENDIX 3

CRITIQUE OF SOME ASPECTS OF MODERN STRUCTURAL ANALYSIS

1. PREFERRED ORIENTATION OF FOLD-HINGES

An assumption sometimes made about soft-sediment slumping is that the fold-hinges are randomly oriented (Bryan and Jones, 1962, p. 230). The orientation of the fold-hinges in the syntaphral slumping at Paga Point is certainly not random, and the concentration is as dense as many recorded in metamorphic rocks. I have been unable to find any published data which support the contention of random fold-hinges in soft-sediment slumps, and there is no philisophical reason to expect fold-hinges to be random. Perhaps the geologists who have looked at soft-sediment deformations have been impressed by the complicated polyclinal nature of the axial surfaces, and it is true that the axial surfaces of metamorphic folds are more planar.

2. HETEROGENEITY AND HOMOGENEITY

One of the basic methods of analysing deformed rocks is to divide the whole area, which is usually heterogeneous, into homogeneous sub-areas. All that this method does, in fact, is to find a scale on which a series of measurements of a particular structural element can be divided into reasonably homogeneous domains. The same structural element may be heterogeneous on either a larger or smaller scale. Although structural geomericians do not state so explicitly, there is an underlying implication in many of the analyses that structural elements measured over a region can always be divided into homogeneous domains, and that these domains remain homogeneous on successively smaller scales. This concept is unsound, as such domains are homogeneous only on the scale for which they have been determined, and then only for the particular element involved.

At Sulphur Creek, Gee (1967, *pers. comm.*) has shown that the P1 deformation is homogeneous when mapped on the scale of $1:10^4$. When this deformation is mapped on scales of $1:10^2$ or $1:10^3$, the orientation of fold-hinges is homogeneous, but the axial surfaces are quite variable in attitude.

Structures and events deduced on one scale may not persist on larger scales. Means (1963) recognized this problem with the two sets of folds, F_1 and F_2 , in the Otago schists. The relationship between the two sets is uncertain, for although

in most places F_1 is overfolded by F_2 , in some places F_1 folds F_2 . As Means noted, no unique conclusions can be made about the order of development of the major structures from these minor structures. It may well be that the two sets of folds are essentially contemporaneous, although developed in different order from place to place. There is a parallel case in palaeontology where valid time correlations between widely spaced areas can be made on the basis of species and subgenera, yet correlations based on finer subdivisions of the taxonomy may give conflicting answers.

3. NON-CONTEMPORANEITY OF PARALLEL STRUCTURES

One of the most pervasive assumptions of structural geologists is that if a structure develops parallel to the axial surface of a fold, the folding and the development of the structure are contemporaneous. Justification of this assumption is sought in Occam's razor, and a classical example of the dilemma which this concept occasions is the controversy between Fourmarier (1956) and Rutten (1955 and 1956) on the relationship of slaty cleavage to folding in the Carboniferous of the Rhenic Massif and the Ardennes.

Fourmarier, presenting the conventional ideas on cleavage formation, contended that since in most cases slaty cleavage is parallel to the fold axial surface, the few examples in which the

cleavage transects the fold cores can be disregarded as local divergences. Rutten disagreed with this reasoning, maintaining that the parallelism of the cleavage and fold axial surfaces was incidental, and that the few disoriented folds show that there is no genetic relationship between the cleavage and the folding. Fourmarier claimed that cleavage and fold formation were synchronous, whereas Rutten concluded that the cleavage may have formed considerably later than the folds. I have mapped a comparable set of folds at Sulphur Creek, and it is clear that the cleavage, though related in a general way to the P1 deformation, is not genetically related to the formation of individual folds. In fact, the cleavage appears to have developed after most of the folding was accomplished.

Parallelism of structures does not prove contemporaneity, and any correlation which uses this criterion may be invalid. For example, parallelism or similarity of cleavage or schistosity from different areas is often used to correlate "phases" of folding. Thus, if at area A the fold X has a cleavage parallel to its axial surface, and the same cleavage is thought to occur at area B, there is a tendency to draw conclusions about the time relations between a fold Y in area B, and the fold X. In particular, if the cleavage in area B transects the fold core Y, the conclusion is reached that X is younger than Y. This is not valid reasoning, for the fold X may be younger, older or the same age as the fold Y, and the cleavage may be later than them both.

4. THE IMPLICATION OF FOLD-STYLE VARIATION IN METAMORPHISM

If the conclusion is valid that variation in pore pressure is an important cause of the diversity of fold style in metamorphic rocks, there are some interesting implications about metamorphic processes. One of the assumptions usually made in considerations of metamorphic reactions is that the pore pressure (in most cases the water pressure) equals the confining pressure. Yoder (1955), outlining the role of water in metamorphism, pointed out that there is no valid reason to justify this assumption, and the variation in fold style supports his criticism. Where intergranular movement is the dominant mode of deformation, concentric folding indicates pore pressures significantly lower than the confining pressures, whereas similar or "flow" folding implies pore pressures approximately equal to the confining pressures.

The diversity of fold styles in diagenetic and low-grade metamorphic rocks may indicate that there has been a large range of pore pressures. In particular, the common occurrence of concentric folds in such locales signifies that the pore pressure during most of the deformation, and perhaps metamorphism, was considerably less than the confining pressure. Rocks deformed at higher grades tend to have been mechanically more isotropic, and this could be interpreted as either that the pore pressure was approximately equal to the lithostatic load, or that the deformation was intragranular. Thus it appears that at least in diagenetic

and low-grade metamorphic environments, pore pressure as well as temperature and confining pressure, may have controlled the mineral facies developed.

5. ROTATIONAL AND IRROTATIONAL ELEMENTS IN KINEMATIC ANALYSIS

In any set of geometric data of a deformation, there are some elements which have undergone rotation, and others which have maintained a constant orientation during the movement. There is no problem in assigning the geometric relationships of the irrotational elements at the time of their formation to the postulated stress or strain field, but with the rotational elements it is necessary to determine:-

- (1) at what stage of the deformation they formed, and
- (2) what their geometry was at that time.

An element which forms early in a deformation may be distorted or rotated by the continuing deformation, and the determination of its true relationship to the principal axes of stress, strain or movement involves careful reconstruction.

This problem of reconstruction, simple enough in theory, is nonetheless commonly neglected in practice. Kinematic analyses of folds are usually presented in the form of a sketch of the fold and the various structural elements, together with

the generalized directions of inferred movement or stress., Little or no account is taken of whether the elements have rotated during the deformation, and rarely is the deformed body reconstructed stage by stage back to the undeformed state. Thus Badgley (1965, p. 68, Fig. 3 - 23), considering possible hypotheses for the deformation of oolites in the South Mountain area, Maryland, U.S.A., proposes three alternative hypotheses but neglects to consider the effect of the changing orientation of the oolites in the external stress field as the fold limbs are rotated towards the axial surface.

I have attempted to treat the problem of rotation in the structural reconstructions in this thesis. In particular, I have sought to explain the origin of the cleavage fans in the sandstone layers at Tullochgorum and Sulphur Creek in terms of rotation of the fold limbs after a planar cleavage has been formed throughout the rocks at a certain stage in the deformation. This explanation of cleavage fans is simpler than any which appeals to inherent properties of the rock, because the angle of divergence of the cleavage fans is quite variable from fold to fold and bears no recognizable relationship to variations in the rock type. Williams (1965) has attempted to explain the cleavage in the sandstone as caused by granular rearrangements within the sandstone layers during bending. In his hypothesis, the angle between the bedding and cleavage should show some consistent geometric relationship

both within any particular fold, and also from one fold to another. My measurements have shown that neither of these conditions prevail.

6. INFLUENCE OF PRE-EXISTING MECHANICAL SURFACES ON THE DEVELOPMENT OF FOLD-SURFACES

The most common type of analysis of a deformed region involves plotting all the structural elements, including fractures, on a point diagram such as a stereographic projection, recognizing the overall symmetry, and finally postulating the relationships with inferred movement or stress directions. No account is taken of the areal distribution of the particular elements, or the possible interrelations between subsets of the whole population. The problem at hand is whether the orientation of a fracture is controlled by the orientation of pre-existing mechanical surfaces, or whether its orientation is influenced only by the external forces. In the former case the deformed body is regarded as heterogeneous; in the latter it is homogeneous. As Whitten (1966) pointed out, the spatial distribution of the orientation of the elements is equally as important as their statistical orientation.

When this concept is applied to individual folds, the picture is not clear. Donath (1961) has shown how the orientation of shear fractures formed during experimental deformation of the Martinsburg Slate is strongly regulated by the orientation of

the cleavage. It appears that once a mechanical surface has developed, as long as the shear strength across the surface is different from the shear strength of the unaltered rock, the surface will influence the orientation of any fracture developing adjacent to it. Furthermore, if the orientation of the early surface is changed with respect to the external movement or stress field by progressive deformation, the early surface may assume different characters. In this way, en echelon, sigmoidal, tension joints commonly develop as en echelon shear joints inclined at a low angle to the main zone of movement. The portion of each shear joint in the movement zone is rotated during the deformation so that it finally becomes oriented in the tension direction, thereby producing a sigmoidal fracture.

In general, surfaces forming in the plane of maximum elongation will not be affected by pre-existing mechanical surfaces unless these surfaces re-orient the principal stress directions. Nevertheless, shear, and perhaps tension fractures are susceptible to disorientation. Thus, in any hypothesis of fold formation where fractures purported to be shear surfaces develop, cognizance must be taken of the pre-existing mechanical surfaces.

REFERENCES

- BADGLEY, P.C. 1965. *Structural And Tectonic Principles*.
New York, Harper and Row.
- BRYAN, W.H., and O.A. Jones. 1962. The bedded cherts of the
Neranleigh-Fernvale group of south-eastern
Queensland. *Proc. R. Soc. Qd.*, 73, 17-36.
- DONATH, F.A. 1961. Experimental study of shear failure in
anisotropic rocks. *Bull. geol. Soc. Am.*, 72,
985-99.
- FOURMARIER, P. 1956. Remarques au sujet de la schistosité en
général avec application aux terrains paléozoïques
de l'Ardenne et du massif schisteux Rhénan. *Geologie*.
Mijnb., 18, 47-56.
- GEE, R.D. 1967. *The tectonic evolution of the Rocky Cape*
geanticline in northwest Tasmania. Unpub. Ph.D.
thesis, Univ. of Tasm., 351 p.
- MEANS, W.D. 1963. Mesoscopic structures and multiple deformation
in the Otago schist. *N. Z. Jl. Geol. Geophys.*, 6,
801-816.
- RUTTEN, M.G. 1955. Schistosity in the Rhenic massif and the
Ardennes. *Geologie Mijnb.*, 17, 104-110.
- RUTTEN, M.G. 1956. Note on schistosity. *Geologie Mijnb.*, 18,
57-58.
- WHITTEN, E.H.T. 1966. Sequential multivariate regression methods
and scalars in the study of fold-geometry variability.
J. Geol., 74, 744-763.

- WILLIAMS, E. 1965. The deformation of competent granular layers in folding. *Am. J. Sci.*, 263, 229-237.
- YODER, H.S. 1955. Role of water in metamorphism. *Spec. Pap. geol. Soc. Am.*, 62, 505-524.